

รายงานวิจัยฉบับสมบูรณ์

โครงการ

เครือข่ายการควบคุมของซิกม่า-เอสและซิกม่า-เอ็น2 ในการทำให้เกิด การหลอมรวมของเซลล์เจ้าบ้านและการเกิดไบโอฟิล์มของเชื้อ

Burkholderia pseudomallei

โดย

ศาสตราจารย์ ดร.สุมาลี ตั้งประดับกุล และ คณะ

รายงานวิจัยฉบับสมบูรณ์

เครือข่ายการควบคุมของชิกม่า-เอสและชิกม่า-เอ็น2 ในการทำให้เกิดการ หลอมรวมของเซลล์เจ้าบ้านและการเกิดไบโอฟิล์มของเชื้อ Burkholderia pseudomallei

	คณะผู้วิจัย	สังกัด
1.	ศ.ดร.สุมาลี ตั้งประดับกุล	ภาควิชาชีวเคมี คณะวิทยาศาสตร์
2.	Mrs.Duong Thin Diep	ภาควิชาชีวเคมี คณะวิทยาศาสตร์
3.	นางสาวสุฑามาส นิยมพาณิชย์	ภาควิชาชีวเคมี คณะวิทยาศาสตร์
4.	นางสาวรุ่งรวี มงคลรบ	ภาควิชาชีวเคมี คณะวิทยาศาสตร์
5.	นางสาวกิติมา ศรีสง่า	ภาควิชาชีวเคมี คณะวิทยาศาสตร์

สหับสนุนโดยสำหักงานกองทุนสหับสนุนการวิจัย

(ความเห็นของรายงานนี้เป็นของผู้วิจัย สกว.ไม่จำเป็นต้องเห็นด้วยเสมอไป)

Abstract

A human severe infectious disease with high mortality rate in many Tropical countries, melioidosis, is caused by highly versatile pathogen Burkholderia pseudomallei. The function of the B. pseudomallei sigma S (RpoS) transcription factor in survival during stationary growth phase and conditions of oxidative stress is well documented. Besides rpoS, bioinformatics analysis of B. pseudomallei genome showed the existence of two rpoN genes, rpoN1 and rpoN2. To access the function of RpoN, both rpoN1 and rpoN2 were inactivated, unfortunately only the rpoN2 mutant ($\Delta rpoN2$) strain was successfully constructed and characterized. In this study the functions of the rpoN2 were analyzed for bacteria survival via biofilm formation and pathogenesis of bacterial intracellular survival via Multinucleated Giant Cell (MNGC) formation. The involvement of B. pseudomallei RpoS and RpoN2 in invasion, intracellular survival leading to the reduction in Multinucleated Giant Cell (MNGC) formation of RAW264.7 cell line was illustrated. Our result also demonstrated that MNGC formation in RAW264.7 cell line depended on a certain number of intracellular bacteria (at least 10⁴) and that both RpoS and RpoN2 are not directly involved in MNGC formation judging by the same 15% MNGC formation observed in RAW264.7 cells infected with either B. pseudomallei wild type MOI 2 or RpoN2 mutant ($\Delta rpoN2$) MOI 10 or RpoS mutant ($\Delta rpoS$) MOI 100. Moreover, the role of B. pseudomallei RpoS and RpoN2 in regulation of biofilm formation was studied. The biofilm formation is believed to be one of the possible relapse causes because of the ability to increase drug resistance. Extracellular polymeric substance (EPS) in biofilm has been reported to be related to limitation of antibiotic penetration in B. pseudomallei. However, the mechanisms through which that biofilm creates a restricting diffusion to antibiotics remains unclear. The result of CLSM revealed a reduction of the exopolyscharide production and disability of the micro-colony formation in B. pseudomallei mutants, which paralleled the antibiotic resistance. Different ratios of carbohydrate contents in exopolysaccharide of the mutants was detected, although they had the same components; glucose, galactose, mannose, and rhamnose with no detectable peak found in bpsI mutant. These results indicated that the correlation between these phenomenal in B. pseudomallei biofilm at least resulted from exopolysaccharide which may have been under the regulation of rpoN2 or rpoS genes.

Keywords: *Burkholderia pseudomallei*, Biofilm formation, Multinucleated Giant Cell (MNGC) formation, Sigma N2 factor (*rpo*N2), Sigma S factor (*rpo*S)

บทคัดย่อ

Burkholderia pseudomallei เป็นแบคทีเรียอันเป็นสาเหตุของโรคเมลิออยโคสิส โรคติดเชื้อในมนุษย์ที่ ร้ายแรง ระบาดในประเทศเขตร้อน หน้าที่ในการควบคุมการแสดงออกของยืนต่างๆในสภาวะแบคทีเรียเจริญ หรือเครียดจากออกซิเดทีฟ และการขาดอาหารอยู่ภายใต้การควบคุมด้วยซิกม่าเอส สารสนเทศทางยีโนมของแบคที่เรียดังกล่าวนี้พบว่ามียืนกลุ่มซิกม่าเอ็น และพบรหัสของยืนซิกม่าเอ็นใน 2 โครโมโซม เรียกว่า เอ็น1 และ เอ็น2 ทั้งนี้ซิกม่าเอ็นที่พบนี้ยังไม่มีการศึกษาบทบาทหน้าการควบคุมการ แสดงออกของยืนกลุ่มนี้มาก่อน การศึกษานี้จึงต้องการศึกษาบทบาทหน้าที่ของซิกม่าเอ็นเทียบกับซิกม่าเอส โดยการสร้างแบคที่เรียที่เกิดการผ่าเหล่าของยืนซิกม่าอื่น1 และเอ็น2 แต่เนื่องจากสามารถสร้างแบคที่เรียที่ผ่า เหล่าได้เฉพาะยืนเอ็น2 เท่านั้น ในการศึกษานี้จึงทำการศึกษาบทบาทหน้าที่ของยืนซิกม่าเอ็น2 เทียบกับซิกม่เอ สในการอยู่รอดของแบคทีเรียที่ภาวการณ์สร้างใบโอฟิล์ม และการที่แบคทีเรียอยู่รอคภายในเซลล์เจ้าบ้านที่ก่อ เกิดพยาธิสภาพการหลอมรวมตัวของเซลล์เจ้าบ้าน ผลจากการศึกษาการหลอมรวมตัวของเซลล์เจ้าบ้านพบว่า ซิกม่าเอส และซิกม่าเอ็น2 เกี่ยวข้องกับความสามารถในการเจาะเข้าเซลล์เจ้าบ้านส่งผลให้จำนวนเชื้อที่เข้า เซลล์เจ้าได้รับลดประสิทธิภาพเมื่อแบคทีเรียงาคยีนทั้งซิกม่าเอสและเอ็น2 แต่เมื่อเพิ่มจำนวนแบคทีเรียให้มี จำนวนเชื้อเข้าส่เซลล์เจ้าบ้านได้เพิ่มขึ้นจนมีจำนวนแบกทีเรียในระดับ 10⁴ แบกทีเรียต่อ 1 เซลล์เจ้าบ้าน พบว่า ปรากฏการณ์การหลอมรวมตัวของเซลล์เจ้าบ้านมีจำนวนและคุณลักษณ์เหมือนกันของแบคทีเรียปกติ เทียบกับ แบคทีเรียที่ผ่าเหล่าซิกม่าเอส และซิกม่าเอ็น2 แสดงว่าปรากฏการณ์หลอมรวมตัวของเซลล์เจ้าบ้าน ้เกี่ยวข้องกับหน้าที่ซิกม่าเอสและเอ็น2 โดยตรง นอกจากนี้การศึกษาบทบาทหน้าที่ของซิกม่าเอสและเอ็น2 ที่ ้เกี่ยวข้องกับการสร้างใบโอฟิล์ม พบว่าการขาดยืนซิกม่าเอสและเอ็น2 มีผลต่อโครงสร้างของใบโอฟิล์ม ที่ กระทบต่อสัดส่วนของคาร์โบไฮเดรท ได้แก่ กลูโคส กาแลคโตส แมนโนส และแรมโนส โดยส่งผลต่อการดึง ยาของเชื้อเมื่อเข้าสู่ภาวการณ์สร้างใบโอฟิล์ม

คำหลัก : เชื้อเมลิออยโคสิส, ใบโอฟิล์ม, การหลอมรวมตัวของเซลล์เจ้าบ้าน, ซิกม่า-เอส, ซิกม่า-เอ็น2

หน้าสรุปโครงการ (Executive Summary) ทุนวิจัยองค์ความรู้ใหม่ที่เป็นพื้นฐานต่อการพัฒนา

ชื่อโครงการ(ภาษาไทย) เครือข่ายการควบคุมของซิกม่า-เอสและซิกม่า-เอ็น2 ในการทำให้เกิดการหลอม

รวมของเซลล์เจ้าบ้านและการเกิดใบโอฟิล์มของเชื้อ Burkholderia pseudomallei

(ภาษาอังกฤษ) Network regulation of the two sigma families, sigma S and sigma N2, in

modulating multinucleated giant cells and biofilm formation of Burkholderia

pseudomallei

หัวหน้าโครงการ ศ.ดร.สุมาถี ตั้งประดับกุล ภาควิชาชีวเคมี คณะวิทยาศาสตร์ มหาวิทยาลัยมหิดล

ถนนพระราม 6 กรุงเทพฯ 10400 โทรศัพท์ 02 2015376 โทรสาร 02 354 7174

e-mail: sumalee.tan@mahidol.ac.th

Status, progression, information, knowledge and research which has been carried out relevant to the proposed topic

Melioidosis is caused by *Burkholderia pseudomallei*, an environmental gram-negative motile bacillus that is also an intracellular pathogen [1]. Following invasion into host cells, *B. pseudomallei* can survive and replicate intracellularly in both phagocytic and non-phagocytic cells [2]. The presence of the invading bacteria leads to host cell-to-cell fusion, resulting in the formation of multinucleated giant cells (MNGC) [3-5]. This unique feature of *B. pseudomallei* infection may be related to its pathogenesis, since granulomas and MNGCs have been found in the tissue of melioidosis patients [6]. The precise mechanism leading to development of MNGCs is not clear; however, it is reduced in the host cell model infected with the *B. pseudomallei* lacking type III secretion system cluster 3 (TTSS-3) gene *bipB* [7]. In addition, *B. pseudomallei* RpoS has been proposed to promote MNGC formation, a mediator of cell to cell spreading of bacteria [8]. How RpoS is controlling these processes in infected host cells remains to be elucidated.

Many reports have shown that a failure to properly diagnose this disease can lead to adverse outcomes, including death [9-11]. The treatment of melioidosis requires a prolonged course of the appropriate antibiotics, such as ceftazidime (CAZ) and meropenem (MRP), lasting for at least 20 weeks due to the inherent resistance of *B. pseudomallei* to many types of antibiotics, including penicillin, gentamicin, ampicillin, first-generation cephalosporin and second-generation cephalosporin as well as other commonly used antibiotics. Even when the recommended 20-week intensive antibiotic treatment is followed, the mortality rate from melioidosis remains high (40–50%), and relapse is common in endemic areas [12]. The biofilm is a glycocalyx polysaccharide matrix encasing the bacterial population as a barrier to support many functions for the survival of the species, and it may be the cause of disease recurrence [13]. The *B. pseudomallei* biofilm was reported to be a barrier to the diffusion of some antimicrobial agents thus limiting the activity and diffusion of the antibiotics [14], but this

ability has not been correlated with bacterial virulence [15]. Although the limitation of antibiotic penetration by the *B. pseudomallei* biofilm has been demonstrated, there remains a need to investigate how the biofilm creates the ability to retard the penetration of antibiotics.

The function of the *B. pseudomallei* sigma S (RpoS) transcription factor in survival during stationary growth phase and conditions of oxidative stress is well documented [16]. Besides rpoS, bioinformatics analysis of *B. pseudomallei* genome showed the existence of two rpoN genes, rpoN1 and rpoN2. To access the function of RpoN, both rpoN1 and rpoN2 were inactivated, unfortunately only the rpoN2 mutant ($\Delta rpoN2$) strain was successfully constructed and characterized [17]. In this study the functions of the rpoN2 were analyzed comparing with the rpoS for bacteria survival via biofilm formation and pathogenesis of bacterial intracellular survival via Multinucleated Giant Cell (MNGC) formation.

Objectives:

- 1. To study the biofilm and multinucleated giant cell formation between *B. pseudomallei rpoS* mutant and *rpoN2* mutant strains with its wild type.
- 2. To identify proteins involved in biofilm and multinucleated giant cell formation between *B. pseudomallei rpoS* mutant and *rpoN2* mutant strains with its wild type

Schedule for the entire project and expected outputs

Activities				Mo	nth				Expected outputs
	6	12		18	24		30	36	
1. Comparative analysis of biofilm formation between <i>B. pseudomallei rpoS</i> mutant and <i>rpoN2</i> mutant strains with its wild type using crystal violet staining and confocal analysis.	↓ ↓		*						1. Demonstrate the pathogenesis on biofilm formation between the two mutant strains.
2. Comparative analysis of multi- nucleated giant cell formation between <i>B. pseudomallei rpoS</i> mutant and <i>rpoN2</i> mutant strains with its wild type.		4		→					2. Demonstrate the pathogenesis on multinucleated giant cell formation between the two mutant strains.
3. Comparative proteomic profiles between between <i>B. pseudomallei rpoS</i> mutant and <i>rpoN2</i> mutant strains using both 2D-Gel and LC-MS/MS methods to identify proteins involved in both regulations.		4				>			3.Demonstration the intersection proteins that under regulation by both sigma S and sigma N2 4.Publish our results
4. Computational analysis of sigma S and sigma N regulons				4	◀			→	5. Extend more data and prediction of other proteins involved in both regulon and that will be able to design new drug target.6. Publish our results

Expected benefits

The knowledge gain from our study will provide basic information of host-bacterial interaction leading to a development of drug and therapeutic method in the future.

Apart from the three expected international publications, this work is also graduated the least 3 Ph.D. students and 2 M.Sc. students.

Connections with other experts within and outside Thailand

1. International collaborators:

• Dr. Mark Thomas and Dr. Jonathan G. Shaw at Medical School, Sheffield University, UK.

2. National collaborators:

- Prof. Stitaya Sirisinha at Dept. of Microbiology, Mahidol University, Bangkok
- Prof. Ducan Smith at Institute of Molecular Genetics and Genetic Engineering, Mahidol University, Salaya
- Dr. Pongsak Utaisincharoen at Dept. of Microbiology, Mahidol University, Bangkok
- Dr. Surasakdi Wongratanachewin at Dept of Microbiology, Medicine, Khon Khan University, Khon Khan
- Mrs. Wannaporn Wutiakanun at Welcome Unit, Faculty of Tropical Medicine, Mahidol University, Bangkok

Out puts:

I. Five International publications

- 1. Niyompanich S., Jaresitthikunchai J., Srisanga K., Roytrakul S., **Tungpradabkul S**. (2014) Source-identifying biomarker ions between environmental and clinical *Burkholderia pseudomallei* using whole-cell matrix-assisted laser desorption/ionization time-of-flight mass spectrometry (MALDI-TOF MS). PLoS One. 9: e99160. (IF=4.53)
- 2. Diep D., Phuong N.T., Hlaing M.M., Srimanote P., **Tungpradabkul S.** (2015) Role of *Burkholderia pseudomallei* sigma N2 in amino acids utilization and in regulation of catalase E expression at the transcriptional level. Inter. J. Bacteriol. ID 623967.(IF=)
- 3. Mongkolrob R., Taweechaisupapong S., **Tungpradabkul S.** (2015) Correlation between biofilm production, antibiotic susceptibility and exopolysaccharide composition in *Burkholderia pseudomallei bps*I, *ppk*, and *rpo*S mutant strains. Microbiol Immunol.59, 653-663.(IF = 1.4)
- 4. Niyompanich S., Srisanga K., Jaresitthikunchai J., Roytrakul S., **Tungpradabkul S.** (20015) Utilization of Whole-Cell MALDI-TOF Mass Spectrometry to Differentiate Burkholderia pseudomallei Wild-Type and Constructed Mutants. PLoS One. 14: e0144128. (IF = 4.53)
- 5. Sanongkiet S., Ponnikorn S., Udomsangpetch R., **Tungpradabkul S.** (2016) *Burkholderia pseudomallei rpoS* mediates iNOS suppression in human hepatocyte (HC04) cells. FEMS Microbiol Letters, 363: doi:10.1093. (IF = 1.858)

II. Internagtional Presentations

- 1. Kitima Srisanga¹, Suthamat Niyompanich¹, Sittiruk Roytrakul², Sumalee Tungpradabkul¹ (2014) Potential biomarkers between *Burkholderia pseudomallei* wild type and its *rpo*N2 mutant strain using MALDI-TOF Mass Spectrometry application. 13th Human Proteome Organization World Congress. October 5 8, 2014 Madrid, Spain.
- 2. Suthamat Niyompanich¹, Kitima Srisanga¹, Sittiruk Roytrakul², Sumalee Tungpradabkul¹ (2014) Relationship between biomarker discovery and colony morphology of *Burkholderia pseudomallei* by whole-cell matrix-assisted laser desorption ionization time-of-flight mass spectrometry (MALDI-TOF MS). 13th Human Proteome Organization World Congress. October 5 8, 2014 Madrid, Spain.

III. Human Resources Development 4 Ph.D. Students

- 1. Dr. Suthamas Niyompanich
- 2. Dr.Rungrawee Mongkolrop
- 3. Dr. Duong Thi Hong Diep
- 4. Dr. Sucharat Sanongkiet

Contents

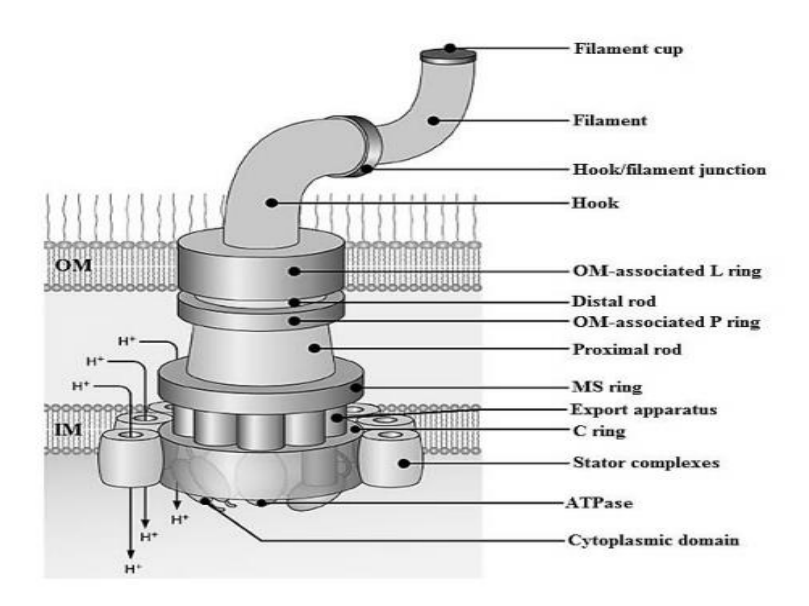
Abstract	I
Executive Summary	III
 Objectives 	IV
 Schedule for the entire project and expected outputs 	IV
 Expected benefits 	V
 Connections with other experts within and outside Thailand 	V
Out puts	V
Introduction	1
 Objectives 	1
Research Methods	4
 Construction of Burkholderia pseudomallei rpoN2 mutant and its role 	4
• Comparative analysis of multinucleated giant cell formation between <i>B</i> . <i>pseudomallei rpoS</i> mutant and <i>rpoN2</i> mutant strains with its wild type.	5
• Comparative analysis of biofilm formation between <i>B. pseudomallei rpoS</i> mutant and <i>rpoN2</i> mutant strains with its wild type using crystal violet staining and confocal analysis	6
• Comparative proteomic profiles between between <i>B. pseudomallei rpoS</i> mutant and <i>rpoN2</i> mutant strains with its wild type using both 2D-Gel and LC-MS/MS methods.	10
• Identification of proteins involved in both regulations, sigma S and sigma N2.	11
Results	12
• Construction of <i>B. pseudomallei rpoN2</i> and its role	12
• Comparative analysis of multinucleated giant cell formation between <i>B.</i> pseudomallei rpoS mutant and rpoN2 mutant strains with its wild type.	15
• Comparative analysis of biofilm formation between <i>B. pseudomallei rpoS</i> mutant and <i>rpoN2</i> mutant strains with its wild type using crystal violet staining and confocal analysis	20
• Comparative proteomic profiles between between <i>B. pseudomallei rpoS</i> mutant and <i>rpoN2</i> mutant strains with its wild type using both LCMS-MS and 2D-Gel Methods	27
• Identification of proteins involved in both regulations, sigma S and sigma N2	34
Discussion and Conclusion	37
References	44
Appendices	47
• Publication 1 (10 pages)	57
• Publication 2 (9 pages)	66
• Publication 3 (11 pages)	77
• Publication 4 (15 pages)	92
• Publication 5 (8 pages)	100

List of Figures

Figure 1	Model of the flagellar T3SS	1
Figure 2	Five steps of biofilm development	2
Figure 3	The differences of transcription initiations by the RNAP- σ^{70} and RNAP- σ^{54} holoenzymes	3
Figure 4	Drop plate technique for bacterial CFUs (colony forming units) counting	6
Figure 5	Flow chart of an antibiotic susceptibility test	8
Figure 6	Time course study on multinucleated giant cell (MNGC) formation in mouse macrophage cell line and intracellular survival of <i>B. pseudomallei</i>	16
Figure 7	The invasiveness of $\Delta rpoN2$ in comparison with <i>B. pseudomallei</i> wild type and $\Delta rpoS$	18
Figure 8	MNGC formation in RAW 264.7cells infected either with Bp WT MOI 2 or $\Delta rpoS$ MOI 100 or $\Delta rpoN2$ MOI 10 at PI 8h and 16h	20
Figure 9	Representation of <i>B. pseudomallei</i> biofilm by CLSM	21
Figure 10	Visualization of biofilm production and thickness in <i>B. pseudomallei</i>	23
Figure 11	The biofilm exopolysaccharide production of <i>B. pseudomallei</i>	24
Figure 12	Exopolysaccharide productions from CLSM and antibiotic resistance (IC50) of CAZ-and MRP-treated biofilm	25
Figure 13	Subtracted carbohydrate contents in the exopolysaccharides of all <i>B. pseudomallei</i> strains	26
Figure 14	Cluster analysis of <i>B. pseudomallei</i> wild-type and mutants.	28
Figure 15	The box and whiskers plot of candidate biomarkers in <i>B. pseudomallei</i> mutants	30
Figure 16	Summary the identification of the differences mutated strains of <i>B. pseudomallei</i>	31
Figure 17	2D-gel electrophoresis of <i>B. pseudomallei</i> wild-type (A) and <i>rpoS</i> mutant (B)	32
Figure 18	2D-gel electrophoresis of B. pseudomallei wild-type	33
Figure 19	Cysteine and methionine metabolisms	34
Figure 20	Histidine metabolism	35
Figure 21	Postulated biosynthetic pathways of the nucleotide sugar precursors for the biofilm exopolysaccharides	36
	List of Tables	
Table 1	Bacterial strains and plasmids used in this study	12
Table 2	Nitrogen and amino acid utilization of <i>B. pseudomallei</i> wild type 844 and <i>E. coli</i> derivatives	14
Table 3	Invasion of either <i>B. pseudomallei</i> wild type (WT), $\Delta rpoS$ or $\Delta rpoN2$ strain into RAW 264.7 cell line, as measured by the kanamycin protection assay	17
Table 4	MNGC formation in RAW 264.7 cells infected with either <i>B. pseudomallei</i> WT MOI 2 or $\Delta rpoS$ MOI 100 or $\Delta rpoN2$ MOI10 at PI 8h	19

Introduction

Melioidosis is caused by *Burkholderia pseudomallei*, an environmental gram-negative motile bacillus that is also an intracellular pathogen [1]. Following invasion into host cells, *B. pseudomallei* can survive and replicate intracellularly in both phagocytic and non-phagocytic cells [2]. The presence of the invading bacteria leads to host cell-to-cell fusion, resulting in the formation of multinucleated giant cells (MNGC) [3-5]. This unique feature of *B. pseudomallei* infection may be related to its pathogenesis, since granulomas and MNGCs have been found in the tissue of melioidosis patients [6]. The precise mechanism leading to development of MNGCs is not clear; however, it is reduced in the host cell model infected with the *B. pseudomallei* lacking type III secretion system cluster 3 (TTSS-3) gene *bipB* [7]. In addition, *B. pseudomallei* RpoS has been proposed to promote MNGC formation, a mediator of cell to cell spreading of bacteria [8]. How RpoS is controlling these processes in infected host cells remains to be elucidated.



<u>Fig. 1</u> Model of the flagellar T3SS. The components are filament structure, the hook-basal body, the cytoplasmic C ring, the ATPase and the export apparatus. There are 8-11 stator complexes containing proton-conducting channels which are responsible for converting the energy of the proton flux into a mechanical force, hence, driving flagellum rotation. The flagella T3SS-associated ATPase is involved in providing the energy required for the secretion, especially the initial process. The export apparatus and cytoplasmic domain play a key role in docking flagella-associated proteins and chaperones during the secretion process

Many reports have shown that a failure to properly diagnose this disease can lead to adverse outcomes, including death [9-11]. The treatment of melioidosis requires a prolonged

course of the appropriate antibiotics, such as ceftazidime (CAZ) and meropenem (MRP), lasting for at least 20 weeks due to the inherent resistance of *B. pseudomallei* to many types of antibiotics, including penicillin, gentamicin, ampicillin, first-generation cephalosporin and second-generation cephalosporin as well as other commonly used antibiotics. Even when the recommended 20-week intensive antibiotic treatment is followed, the mortality rate from melioidosis remains high (40–50%), and relapse is common in endemic areas [12]. The biofilm is a glycocalyx polysaccharide matrix encasing the bacterial population as a barrier to support many functions for the survival of the species, and it may be the cause of disease recurrence [13]. The *B. pseudomallei* biofilm was reported to be a barrier to the diffusion of some antimicrobial agents thus limiting the activity and diffusion of the antibiotics [14], but this ability has not been correlated with bacterial virulence [15]. Although the limitation of antibiotic penetration by the *B. pseudomallei* biofilm has been demonstrated, there remains a need to investigate how the biofilm creates the ability to retard the penetration of antibiotics.

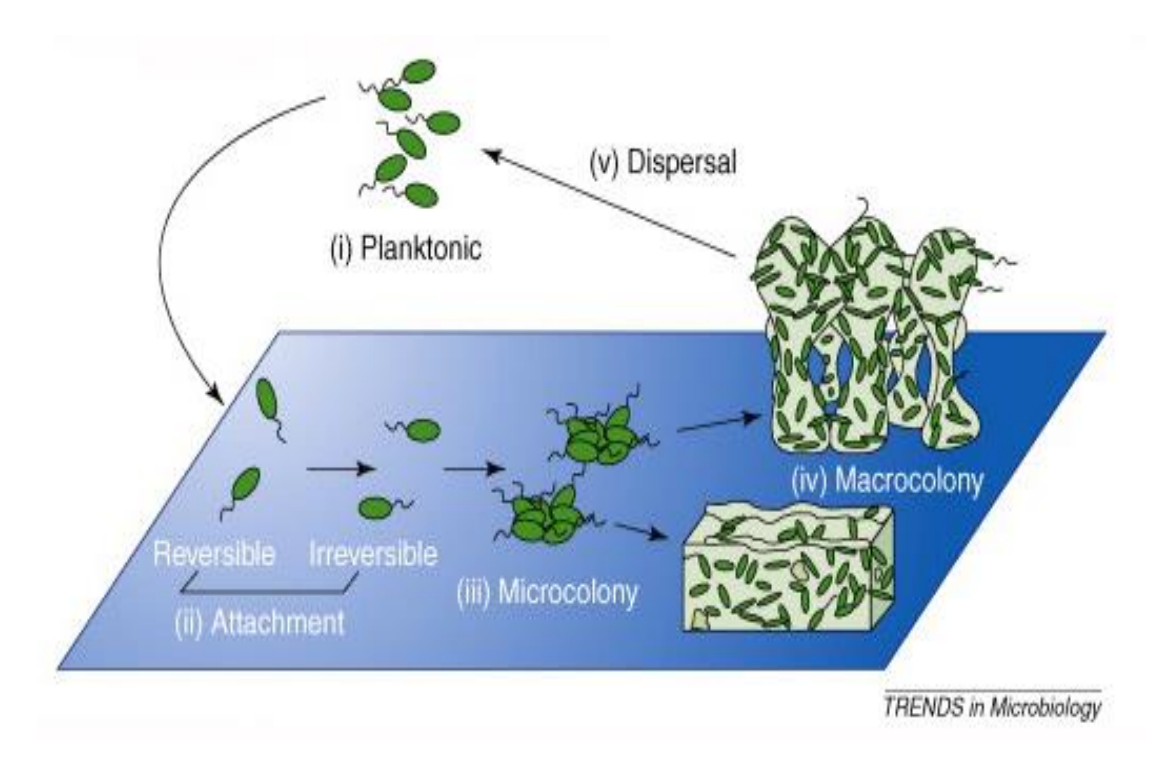
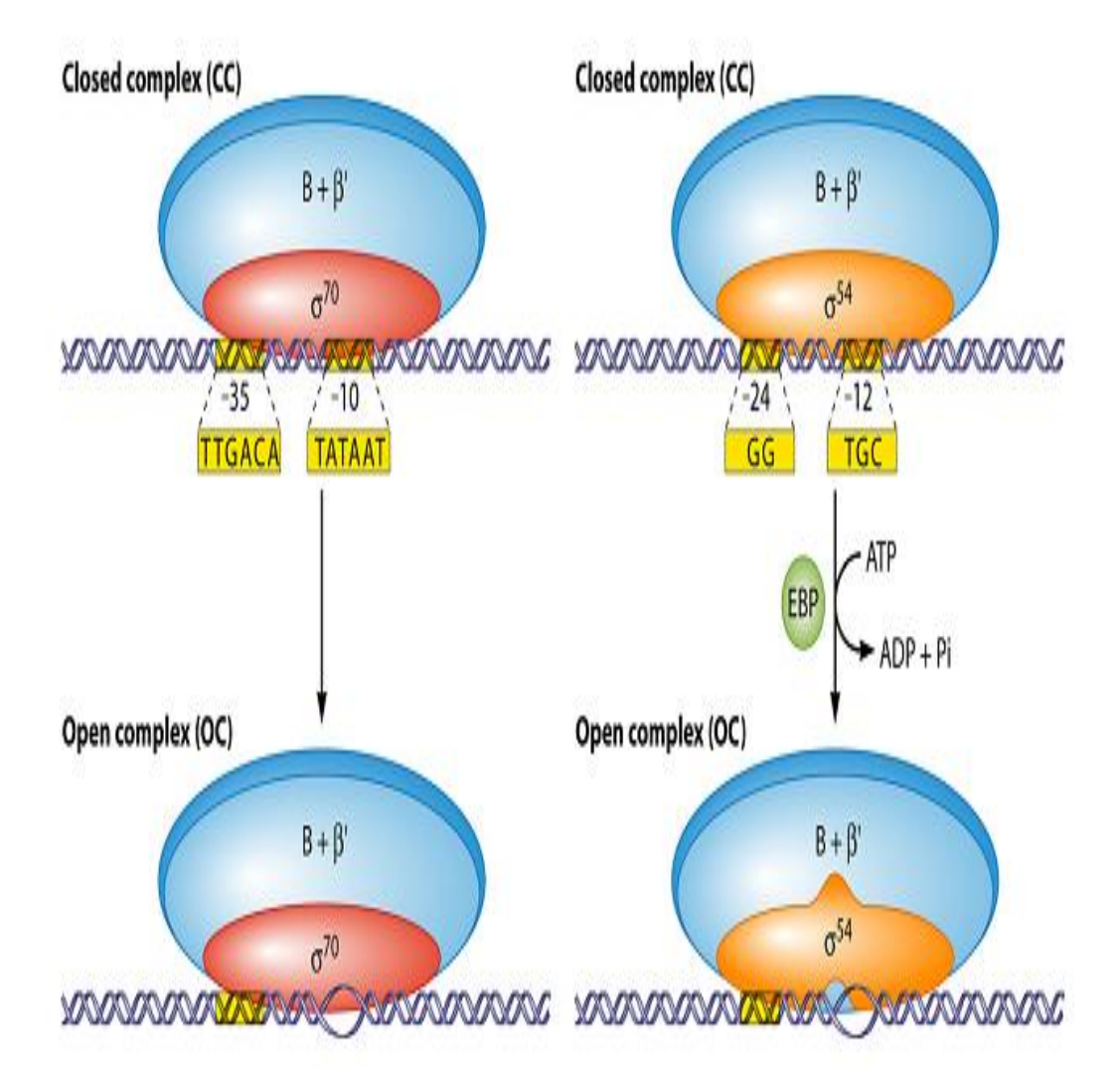


Fig. 2 Five steps of biofilm development

The function of the *B. pseudomallei* sigma S (RpoS) transcription factor in survival during stationary growth phase and conditions of oxidative stress is well documented [16]. Besides *rpoS*, bioinformatics analysis of *B. pseudomallei* genome showed the existence of two *rpoN* genes, *rpoN1* and *rpoN2*. To access the function of RpoN, both *rpoN1* and *rpoN2* were

inactivated, unfortunately only the rpoN2 mutant ($\Delta rpoN2$) strain was successfully constructed and characterized [17]. In this study the functions of the rpoN2 were analyzed comparing with the rpoS for bacteria survival via biofilm formation and pathogenesis of bacterial intracellular survival via Multinucleated Giant Cell (MNGC) formation.



 $\underline{Fig.~3}$ The differences of transcription initiations by the RNAP- σ^{70} and RNAP- σ^{54} holoenzymes.

Objectives:

- 1. To study the biofilm and multinucleated giant cell formation between *B. pseudomallei rpoS* mutant and *rpoN2* mutant strains with its wild type.
- 2. To identify proteins involved in biofilm and multinucleated giant cell formation between *B. pseudomallei rpoS* mutant and *rpoN2* mutant strains with its wild type

Research Methods

Based on objective 1

- 1.1 Construction of rpoN2 mutant Burkholderia pseudomallei
- 1.2 Comparative analysis of multinucleated giant cell formation between *B. pseudomallei rpoS* mutant and *rpoN2* mutant strains with its wild type.
- 1.3 Comparative analysis of biofilm formation between *B. pseudomallei rpoS* mutant and *rpoN2* mutant strains with its wild type using crystal violet staining and confocal analysis.

1.1 Construction of Burkholderia pseudomallei rpoN2 mutant and its role

An *rpoN2* knockout mutant (Table 1) was created to be pKRpoN2 according to a previously described procedure [16]. The pKRpoN2 was constructed by transferring the 363-bp partial digested *PstI* fragment from genomic DNA of *B. pseudomallei* into the mobilizable suicide vector pKNOCK-Tc [16]. A constructed *B. pseudomallei rpoN2* mutant was analyzed by Southern blot analysis and PCR as described elsewhere. To confirm that all changes in phenotypes were caused by the disruption of *rpoN2* and were not due to polar effects on downstream genes, a plasmid (pBSDRpoN2) containing the complete full-length *rpoN2* coding sequence under control of the *lacZ* and *cat* promoters was constructed and transferred into the *B. pseudomallei* mutant strains for complementation analysis. Likewise, pTOPO::*rpoN2*_{Bp} and pTOPO::*rpoN2*_{Bp799} were constructed and used to complement into JKD 184 *E. coli rpoN* negative mutant.

Nitrogen and amino acids utilization tests were performed in MM9 salts minimal agar containing either 20 mM ammonium chloride (NH₄Cl) or with other alternative nitrogen source such as arginine, glutamine, glycine, histidine, lysine, methionine, phenylalanine, tryptophan and valine at 5 mM concentration. Ten μ l of overnight growth of the desired bacterial strains (A₆₀₀ = 1) were inoculated onto the above agar medium and incubated at 37°C. Growths of the bacterial colony were observed daily for five consecutive days.

Statistical measurements of the all assays were carried out in three separate times. The results were expressed as the mean \pm standard deviation of days of growth. The significance of differences in nitrogen and amino acids utilization of bacterial strains were analyzed by Student's paired t-test (2-tailed) using SPSS statistical software program.

1.2 Comparative analysis of multinucleated giant cell formation between B. pseudomallei rpoS mutant and rpoN2 mutant strains with its wild type.

Infection assay: WT or $\Delta rpoS$ to the monolayer RAW 264.7 cells in 12-well plates with MOI (multiplicity of infection) 2, 10 or 20 bacteria per one mouse macrophage cell then shaking briefly to equally distribute the bacteria. Thereafter 2h incubation at 37°C with 5%CO₂ to allow bacteria enter the host cells, the monolayer RAW264.7 was washed twice with pre-warmed PBS and further incubated for 2h more in 2ml completed DMEM/high Glucose containing 250 µg/ml Kanamycin (Gibco Labs) to eliminate remaining extra cellular bacteria. To prevent the extracellular bacteria growth and maintaining infected monolayer RAW264.7 until the desired post infection (PI) time point for the collection, 2ml fresh DMEM/high Glucose media containing 50µg/ml Kanamycin was replenished after washing monolayer twice with PBS followed by removing old media. It should be mention that, the RAW264.7 cells were maintained in inactive stage with good round shape before using for all infection experiments in this study. To control the cross contamination after infection as well as the effect of Kanamycin 250µg/ml in killing extracellular bacteria, 10µl of cell culture media containing Kanamycin in each well of this infection assay was collected and plated on TSA for bacterial CFUs checking. At each indicated PI time point, the media was removed, the monolayer was washed twice with PBS and lysed by adding 200µl 0.1% Triton X-100(Sigma Chemicals, Co.) to liberate all the bacteria entered into RAW264.7 cells. To evaluate the invasiveness of B. pseudomallei WT and $\Delta rpoS$, cell lyses at PI 0h of infection assay with MOI 2, MOI 10 and MOI 20 were subjected to the serial dilution then plated onto the TSA (tryptic soy agar) for counting bacterial CFUs (colony forming units) after 48h incubation at 37°C.

Intracellular survival assay: The infection assay with MOI2. The infection assay was performed by the antibiotic (Kanamycin) protection method described before with some modifications. Briefly, 5.8 x 10⁴ RAW 264.7 cells were seeded in 12-well sterile non-pyrogenic cultured plates (SPL life sciences) overnight in 37°C humidified incubator with 5% CO₂ atmosphere. In the day of infection, the monolayer mouse macrophage was washed twice with PBS (phosphate buffered saline) pH7.4 before adding 2 ml fresh completed DMEM/high Glucose media for each well and one well was subjected to counting the number of cells by Trypan Blue Exclusion method. The healthy bacterial cells were collected from the 0.1% inoculated bacterial cultures in 5ml TSB by centrifugation 7000 x g. The bacterial cell pellets were then washed twice by PBS and re-suspended in completed DMEM/high Glucose cell

culture media and adjusted to 10^7 bacterial CFUs/ml by measuring OD $_{650}$ =0.1(DMEM media has a red color). It should be noted that, after measuring the OD $_{650}$ and adjustment to the desired number, the bacterial cells suspension in DMEM/high Glucose was subjected in serial dilution and plated on TSA (Tryptic soy agar) for CFU counting after 48h incubation at 37° C to confirm again the correlation between CFU/ml and OD $_{650}$. The infection assay was started by adding of ready prepared either *B. pseudomallei* bacteria per one RAW 264.7 cell) as described above was used for intracellular survival experiment. At each post infection (PI) time point (4h, 6h, 8h, 12h, 16h and 20h) the infected RAW264.7 cells were collected. The serial dilutions of cell lyses were plated onto the TSA by drop plate technique (Fig.4). After 48h incubation at 37° C for bacterial colony growth, the number of intracellular bacteria was evaluated by the CFUs counting in TSA plates.

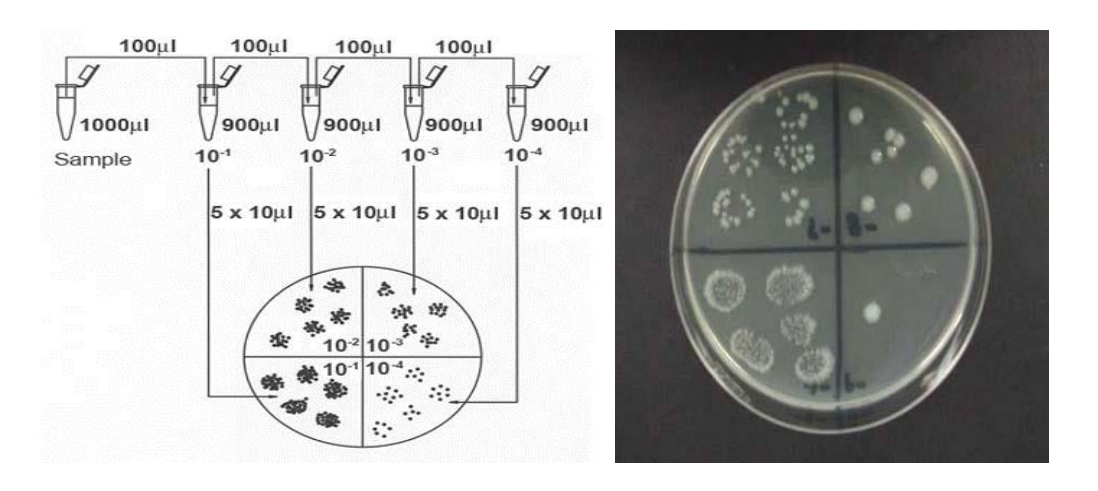


Fig. 4 Drop plate technique for bacterial CFUs (colony forming units) counting

1.3 Comparative analysis of biofilm formation between B. pseudomallei rpoS mutant and rpoN2 mutant strains with its wild type using crystal violet staining and confocal analysis.

Biofilm Visualization using confocal laser scanning microscopy (CLSM): A single colony of cultured bacteria was inoculated in 5 ml of MVBM and grown overnight at 37°C in a 200 rpm shaker incubator (Labcon, Laboratory Marketing Services, Johannesburg, South Africa). The overnight bacterial suspension was measured OD₆₀₀ and diluted into 0.1-0.15 (10⁷ CFU/ml). These diluted suspension was further 10-fold diluted and 1 ml of this final dilution was loaded into 24-well microtiter plate having a plastic cover slip underneath and statically incubated at 37°C for 24 hours. The visualization of biofilm forming bacteria using CLSM was carried out as previously described with slight modifications. Briefly, surface-attached cells were washed two times with 0.15 M PBS pH 7.0 and fixed by 2.5% v/v

glutaraldehyde in PBS pH 7.0 at 4°C for 3 hours. After three washes with PBS, the fixed-died bacterial biofilm was stained with fluorescein isothiocyanate-concanavalin A in distilled water (FITC-ConA; 50µg/ml), which reacts to exopolysaccharide of the biofilm, at room temperature for 15 min. After three times washing, , the bacterial biofilm was stained with propidium iodide (PI) in distilled water 8 µM at room temperature for 45 min. FITC-ConA fluorescein contains a lectin-chain (concanavalin A) that will conjugate to the exopolysaccharide matrixes secreted by the bacteria while PI penetrates only cells with damaged membranes and binds to DNA. Cells were mounted with 5 µl of Prolong Gold Antifade reagent (Invitrogen, Carlsbad, CA 92008, USA) and visualized, using a FluoView FV10i-DOC confocal microscope (OLYMPUS AMERICA, Melville, NY, USA). Fluorescent probes were excited as follows: FITC-ConA at 488 nm and PI at 535 nm. Two independent experiments were performed and each B. pseudomallei strain was captured with five different fields. All confocal images were digitized and analyzed with FV10-ASW 3.0 Viewer software to obtain biofilm thickness, biofilm integrated fluorescent intensity, bacterial density, and other parameters. Biofilm thickness and exopolysaccharide integrated fluorescent intensity were statistically transformed into logarithm and tested by One-Way ANOVA. All pairwise was tested further by the Fisher LSD method at alpha 0.05.

Antibiotic resistance analysis: Bacterial biofilms were formed on each peg by culturing cells in MVBM with specific conditions at an initial bacterial concentration of 10' CFU/ml. The final volume (150 µl) of each bacterial suspension was placed in the 96-well microtiter plate. Rows of the plate were arranged with three replicates for each strain, with one row containing only media to serve as a negative control. The plates were incubated with shaking at 100 rpm at 37°C, for 24 hours. Ceftazidime and meropenem were separately serial diluted in MHB medium in a new 96-well microtiter plate from 1024 µg/ml to 1 µg/ml with the final test volume of 200 µl per well. Antibiotic-free MHB medium were added into one column to serve as the growth control. Biofilm-bacteria present in the biofilm-lid were challenged with ceftazidime and meropenem at 37°C, 24 hours. Following the challenge step, the peg lid was washed using 0.9% NaCl to remove any residual antimicrobial agents. The turbidity of the challenge plates was checked by using the microtiter plate reader (Thermo Electron Corporation, MA, USA) at 620 nm to determine survival of planktonic bacteria. The peg lids were then placed over a new 96-well microtiter plate containing fresh MHB medium. The peg-attaching biofilm was removed by sonication for 5 minutes. After incubation for an additional 24 hours at 37°C, the presence of viable bacterial biofilm was determined by monitoring turbidity at 620 nm.

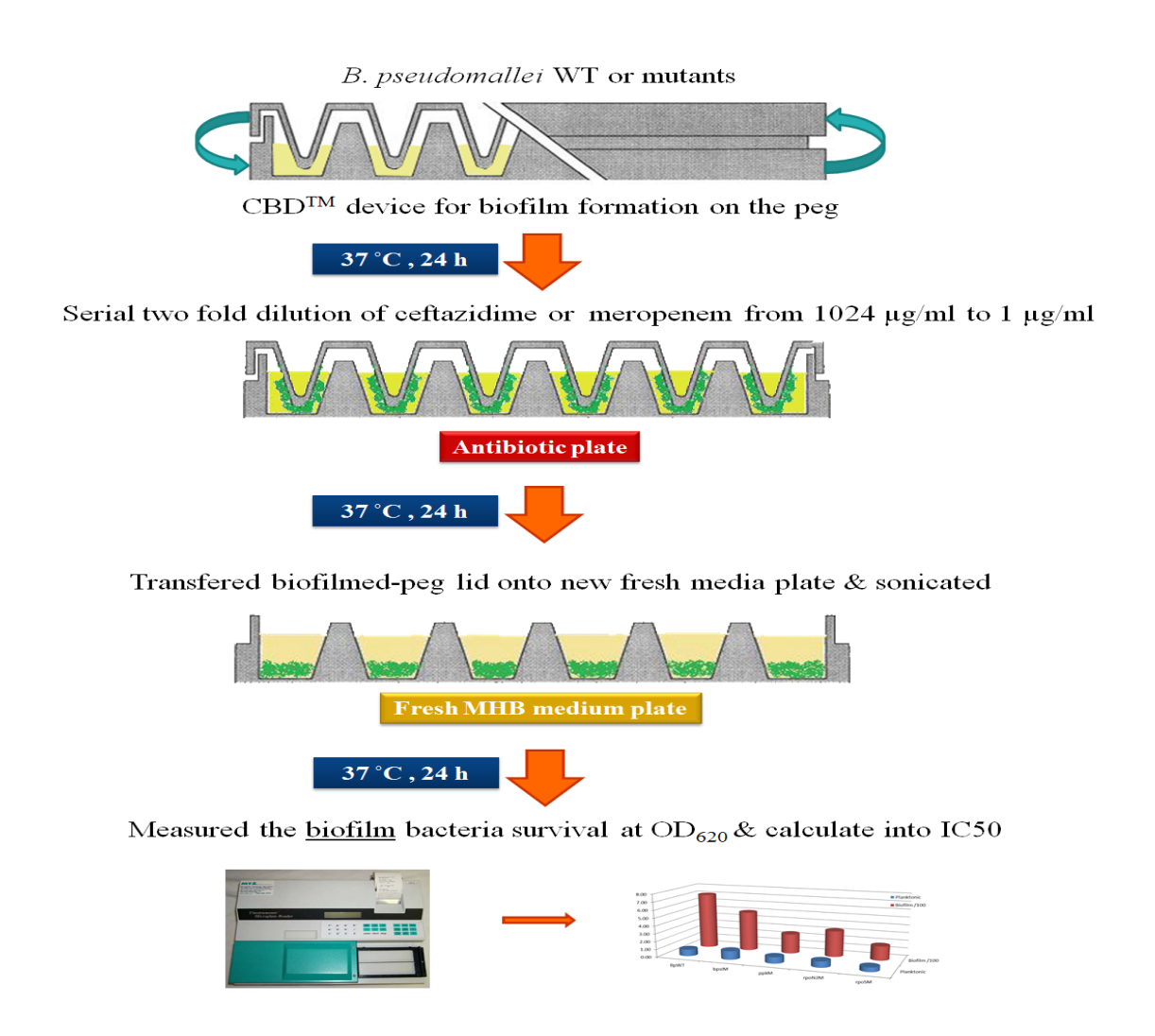


Fig. 5 Flow chart of an antibiotic susceptibility test

Exopolysaccharide composition analysis: Glycoconjugate composition analysis of exopolysaccharide in extracellular matrix extracted from *B. pseudomallei* was performed using gas chromatography-mass spectrometry (GC-MS). Trimethylsilyl (TMS) derivatives of the monosaccharide methyl glycosides were generated from the glycoconjugates by acid methanolysis prior to analysis as previously described [18] with slight modification. The exopolysaccharide samples, containing 0.5 mg of exopolysaccharide, from each *B. pseudomallei* strain were drying in 13 x 100 mm Teflon-Lined screw caps. Standard Mixtures of monosaccharaides expected to be in the exopolysaccharide were concurrently prepared with an interested sample. Before drying by lyophilization, 20 μg of *myo*-inositol as an internal standard is added into each sample and the standard mixture. The standard mixture was actualized through the whole procedure in parallel with all samples to be analyzed. After lyophilization the

dried sample and standard mixture were added with 500 µl of 1 M metanolic HCl for methanolysis at 85°C for 20 hours in heating block (Thermo Scientific, MA, US). Each of the sample caps must be tightly sealed due to the leakage of methanol or introduction of water into the vessels can lead to incompleteness of the hydrolysis reactions. After complete methanolysis, the methanolic HCl was evaporated at 45°C under a hot air by using Speed Vacuum Concentrator (Thermo Electron Corporation, MA, US) to remove the exceeded methanolic HCl. The methanolyzed samples were washed with 250 µl of methanol, followed by the evaporation at 45°C until the samples were completely dried. The washing and evaporating steps were repeated for one more time. The samples were then N-acetylated by the addition of 40 µl of pyridine and 40 µl of acetic anhydride in 200 µl of methanol and incubated at room temperature overnight to re-acetylated N-acetyl group of amino sugars. The remaining solvent and excess acetylating reagents of N-acetylation were evaporated under air at 45°C. To silylate the methylglycosides generated from methanolysis, 180 µl of the silylating reagent, Tri-Sil[®] reagent composed of hexamethyldisilazane (HMDS) and trimrthylchlorosilane (TMCS) in pyridine solvent (Pierce, Rockford, IL), was added to each of the dried samples. The volume of Tri-Sil reagent used in each sample must over exceed to the amount of the dried samples in order to the completeness of the silvlation. All sample tubes sealed with the screw cap were incubated at 85°C for 30 min. The excess Tri-Sil reagent was evaporated under air at room temperature, which should be carried out with a limited time because they are volatile after the silylation. After evaporation, TMS methylglycosides were rinsed with 1 ml of hexane by vortexing to dissolve the methylglycosides from the pellet, followed by centrifugation at 1,000 g for 3 min at room temperature to alleviate settling of insoluble salts. The supernatant hexane was transferred to 1.5 ml fresh vial glass tubes and evaporated under air at room temperature just until dry. The TMS methylglycosides were ready for GC-MS analysis and then were resuspended with 100 µl of hexane. One micro litter of TMS methylglycosides in hexane was automatically injected (split at 1:50) onto a Agilent Hewlett Packard Gas Chromatograph with auto sampler interfaced with a 5973N MSD (Agilent Technologies, CA, US) using a HP-1 fused silica capillary column (25m x 0.32 mm x 0.17 µm). Identification of the monosaccharide components was based on comparison of the retention times with those of the standard monosaccharides mixture [18]. All samples were analyzed in triplicated independent experiments.

Based on objective 2

- 2.1 Comparative proteomic profiles between between *B. pseudomallei rpoS* mutant and *rpoN*2 mutant strains with its wild type using both 2D-Gel and LC-MS/MS methods.
- 2.2 Identification of proteins involved in both regulations, sigma S and sigma N2.
- 2.1 Comparative proteomic profiles between between B. pseudomallei rpoS mutant and rpoN2 mutant strains with its wild type using both 2D-Gel and LC-MS/MS methods.

Protein extraction and two dimensional gel electrophoresis (2DE): Bacterial cultures were grown until early stationary phase. Proteins were extracted using 500 µl lysis buffer (8 M urea, 4% w/v CHAPS, 2 mM TBP, 1% v/v IPG buffer pH 4-7 (Amersham Biosciences, Upsala, Sweden) and 1% v/v protease inhibitor cocktail set II (CalBiochem, La Jolla, CA). The supernatant after cells lysis was transferred into clean microcentrifuge tubes and stored at -80°C until use. Protein concentrations were determined using RC DC protein assay kit (Bio-Rad, Hercules, CA) as previously described [19]. For 2DE, the first dimensional isoelectric focusing (IEF) was carried out using 500 µg protein samples with the rehydration buffer (8 M urea, 2% w/v CHAPS, 20 mM DTT and 1% v/v IPG buffer pH 4-7) adjusted to 350 µl total volume. Precast 18-cm Immobiline DryStrip with a linear pH 4-7 was used with the IPGphor II system (Amersham Biosciences) to perform IEF. The strips were rehydrated with the protein samples for 12 h at 20°C following with three voltage steps as previously described. All profiles were controlled at the current 50 µA/strip. The IPG strips were then equilibrated and transferred to the second dimensional SDS-PAGE using 12.5% polyacrylamide gel. SDS-PAGE was performed at 4°C with the constant electrical current at a 10 mA/gel. Protein spots were visualized by Coomassie Brilliant Blue G-250 (CBBG-250) staining and gels were scanned with an ImageMaster Scanner (Amersham Biosciences). Image analysis was performed using PDQuest software version 7.1 (Bio-Rad). Images from three independent cultures were compared. A master gel used for spot matching process was created from a wild-type 2D gel. The master gel was then used for matching of the corresponding protein spots between 2D gels. The relative intensity of each protein spots was determined by normalizing to the total intensity of the gel. Protein expression with intensity representing at least 3-fold different with p < 0.05 was considered in this analysis.

MALDI-TOF sample preparation: The microbial samples for MALDI-TOF analysis were prepared using previously described method. In brief, the colonies which were grown on Ashdown's agar plate were transferred into 900 μL of water and then deactivated with 300 μL of ethanol. The pellet was collected by centrifugation and mixed with a matrix solution containing 10 mg sinapinic acid in 1 mL of 50 % acetonitrile with 2.5 % trifluoroacetic acid. 2 μL of bacterial extract, with concentration approximately 0.3-0.5 μg/μL, were spotted on a MALDI steel target plate (MTP 384 ground steel plate, Bruker Daltonik, GmbH, Bremen, Germany) and were dried at room temperature. The *Escherichia coli* DH5α BRL was used as a positive control and the matrix solution without bacterial cells was used as a negative control. Twenty-four spots (n=24) from each sample were deposited on a target plate for determination of experimental reproducibility, thus each isolate was repeatedly examined twenty-four times. After drying, the target plate was subjected to analysis in the MALDI-TOF instrument.

MS instrumentation: MALDI-TOF analysis was carried out in an Ultraflex III TOF/TOF mass spectrometer utilized with a 337 nm N₂ laser and was operated by flexControl software (Bruker Daltonik, GmbH, Bremen, Germany). The machine was run in the linear positive mode and mass spectra in the range of 2-20 kDa were collected. The following instrumental parameters were used: acceleration voltages of 25.00 and 23.45 kV for ion source 1 and ion source 2, respectively, with a lens voltage of 6.0 kV. External calibration was performed to determine mass peak accuracy using a ProteoMassTM peptide & protein MALDI-MS calibration kit (Sigma Aldrich, St. Louis, MO, United States) consisting of human ACTH fragment 18-39 (m/z 2465), bovine insulin oxidized B chain (m/z 3465), bovine insulin (m/z 5731), equine cytochrome c (m/z 12362), and equine apomyoglobin (m/z 16952). Each spectrum was compiled from 500 laser shots, with a 50 Hz laser.

2.2 Identification of proteins involved in both regulations, sigma S and sigma N2.

The biosynthesis pathways such as cysteine synthesis, histidine synthesis, purine metabolism and pentose phosphate pathway were performed by using KEGG database.

Results

Construction of B. pseudomallei rpoN2 and its role

In order to determine a constructed *rpoN2* mutant whether RpoN2 is an essential for the *B. pseudomallei* growth in the absence of amino acid supplementation, we compared the growth of the wild-type, *rpoN2* isogenic mutant and the *rpoN2* mutant carrying *rpoN2*-complementing plasmid. No differences in growth were observed among the strains (Table 1). These results indicating that *rpoN2* may be either not necessary or lacked of the functions for amino acid utilization phenotypes.

 Table 1
 Bacterial strains and plasmids used in this study

Strain or plasmid	Genotype or relevant characteristic	Source (Ref.)
Bacteriastrains		·
PP844	Wild type, clinical isolate from blood	This study
E .coli SM10 λpir	λpir (thi thr leu tonA lacY supE recA::RP4-2- Tc::Mu Km) used for transformation of recombinant plasmid pKNOCK::rpoN2 _{Bp}	[20]
E. coli JKD 814	rpoN::tet®	[21]
Plasmids		
pKNOCK-Tc	Mobilizable suicide vector carrytig Tet ^R gene	[22]
pKRpoN2	pKNOCK-Tc containing a 363-bp internal segment of <i>B. Pseudomallei rpoN2</i> gene	This study
pBBR1MCS	Broad-host-range cloning vector, Cm ^r	[23]
pBSDRpoN2	pBR1MCS containing full-length rpoN2 gene	This study
pCR [®] 2.1-TOPO	Cloning vector for PCR product, Kanamycin and Ampicillin resistance	Invitrogen, California, USA
pTOPO::rpoN2 _{Bp799}	pCR [®] 2.1-TOPO vector containing 799-bp fragment of truncated <i>rpoN2</i> gene from <i>B. pseudomallei</i> strain 844, Kanamycin and Ampicillin resistance	This study
pTOPO::rpoN _{Ec}	pCR [®] 2.1-TOPO vector containing full-lenght <i>rpoN</i> gene from <i>E. coli</i> , Kanamycin and Ampicillin resistance	This study

To determine whether the rpoN2 is not necessary or is lacked of the functions in amino acid utilization in B. pseudomallei. We performed the complementation assay by transforming a full-length B. pseudomallei rpoN2 (TOPO::rpoN2Bp plasmid DNA) and a 799-fragment rpoN2 (TOPO::rpoN2Bp799 plasmid DNA) into E. coli JKD 814 which is lacked of rpoN and compared with E. coli JKD 814 complemented with TOPO::rpoN_{Ec} plasmid DNA). A 10 μL (A₆₀₀=1) of bacterial culture was inoculated on M9 minimal agar containing each amino acid and incubated at 37°C for 5 days. E. coli rpoN mutant JKD 814 and E. coli wild type JM 109 were negative and positive controls, respectively. The experiments were carried out in three biological replicates. The differences in utilization of each amino acid for each construct were compared to that of JKD 814 and analyzed using Student's paired t-test. B. pseudomallei wild type strain 844 showed the similar colony growth rate to E. coli wild type in the utilization of histidine as sole nitrogen source. Like E. coli wild type, B. pseudomallei also grew on M9 munimal agar supplemented with NH₄Cl, lysine and tryptophan but the growths were approximately one day delay (Table 2). Although, the growth of B. pseudomallei could be investigated on arginine and valine sole nitrogen source, the colonies were not observed until after day four of incubation. On the other hand, B. pseudomallei wild type utilized glutamine and phenylalanine faster than that of E. coli wild type. However, unlike E. coli wild type, B. pseudomallei could not utilize glycine as a growth substrate. The rpoN mutant E. coli JKD 814 and JKD 814 harboring either pCR® 2.1-TOPO vector alone or plasmid containing only partial ORF of rpoN2 (TOPO::rpoN2Bp799 [799-bp]) exhibited no growth on minimal media supplemented with all nitrogen sources tested in this study after 5- day of incubation (Table 2).

Although the delay in growth were demonstrated, when TOPO:: $rpoN_{Ec}$ recombinant plasmid which contained entire ORF of *E. coli rpoN* was complemented into JKD 814 *E. coli rpoN* mutant, they were able to restore their growth phenotype on all tested amino acids except methionine and valine (Table 2). In contrast, the mutant JKD 814 complemented TOPO:: $rpoN_{Ec}$ strain exhibited the faster growing on the simple nitrogenous compound NH₄Cl compared to the *E. coli* wild type. The similar growth patterns were also observed in the mutant JKD 814 complemented with TOPO:: $rpoN2_{Bp}$ with the exception of methionine. Moreover, in minimal media supplemented with sole lysine, the mutant JKD 814 complemented with TOPO:: $rpoN2_{Bp}$ appeared to grow slower than that of the mutant complemented with TOPO:: $rpoNE_{Cc}$ and the *E. coli* wild type.

Compared to *B. pseudomallei* wild type strain 844, *rpoN* mutant JKD 814 complemented with TOPO::*rpoN2*_{Bp} grew slightly faster on M9 minimal media supplemented with NH₄Cl,

arginine and tryptophan while it grew slower in glutamine, histidine and phenylalanine. No difference in growth rate was inspected when lysine was used as a sole nitrogen source. Moreover, the valine utilization could not be restored in the $rpoN2_{Bp}$ complemented strain. Surprisingly, the rpoN mutant JKD 814 complemented with TOPO:: $rpoN2_{Bp}$ were able to grow on media supplemented with glycine and methionine which were the characteristic of E. coli wild type and not of B. pseudomallei wild type strain 844 phenotype (Table 2).

The overall results suggested that any difference in nitrogen utilization observed in this study were mediated by RpoN from either *E. coli* or *B. pseudomallei*. Therefore we have demonstrated that the *B. pseudomallei rpoN2* has fully functions in regulation of nitrogen and amino acids utilization.

Table 2 Nitrogen and amino acid utilization of B. pseudomallei wild type 844 and E. coli derivatives.

Day of growth appearance (mean ± SD)				SD) ^a			
Nitrogen Source	E. coli JM 109	JKD 814 rpoN mutant	JKD 814 harboring pTOPO vector	JKD 814 harboring TOPO:: rpoN _{Ec}	JKD 814 harboring TOPO:: rpoN2Bp	JKD 814 harboring TOPO:: rpoN2 _{Bp799}	B. pseudomallei wild type 844
NH ₄ Cl	3.7±0.6*	±	±	2.7 ± 0.6*	2 ±1	NG	4.7 ± 0.6*
Arginine	1.3±0.6*	±	±	3.3 ± 0.6*	3.3 ± 0.6*	±	4.7 ± 0.6*
Glutamine	2.7±0.6*	NG	NG	4.6 ± 0.6*	3.7 ± 0.6*	NG	1.3 ± 0.6*
Glycine	2.7 ± 0.6 *	±	±	2.3 ± 0.6 *	2.7 ±0.6*	±	±
Histidine	1.3 ± 0.6*	NG	NG	4 ± 1*	2.3 ± 0.6*	NG	1.3 ± 0.6*
Lysine	3.3 ± 0.6*	NG	NG	3.7 ± 0.6*	4.3 ± 1.2*	NG	4.7 ± 0.6*
Methionine	4.7 ± 0.6*	NG	NG	NG	4.7 ± 0.6*	NG	±
Phenylalanine	4.7 ± 0.6*	NG	±	4.7 ± 0.6*	$3.7 \pm 0.6*$	±	1.3 ± 0.6*
Tryptophan	1.7 ± 0.6*	±	±	1.7 ± 0.6*	1.7 ± 0.6*	NG	2.7 ± 0.6 *
Valine	1.3 ± 0.6*	NG	NG	NG	NG	NG	4.7 ± 0.6*

^aData represent geometric mean (± standard error) from three independent experiment. NG indicates the absence of growth. ± indicates the very sparingly growth inspected on day 6. * Significant differences in amino acid utilization compared to E. coli rpoN mutant JKD 814 (p ≤ 0.05, Student's paired t-test)

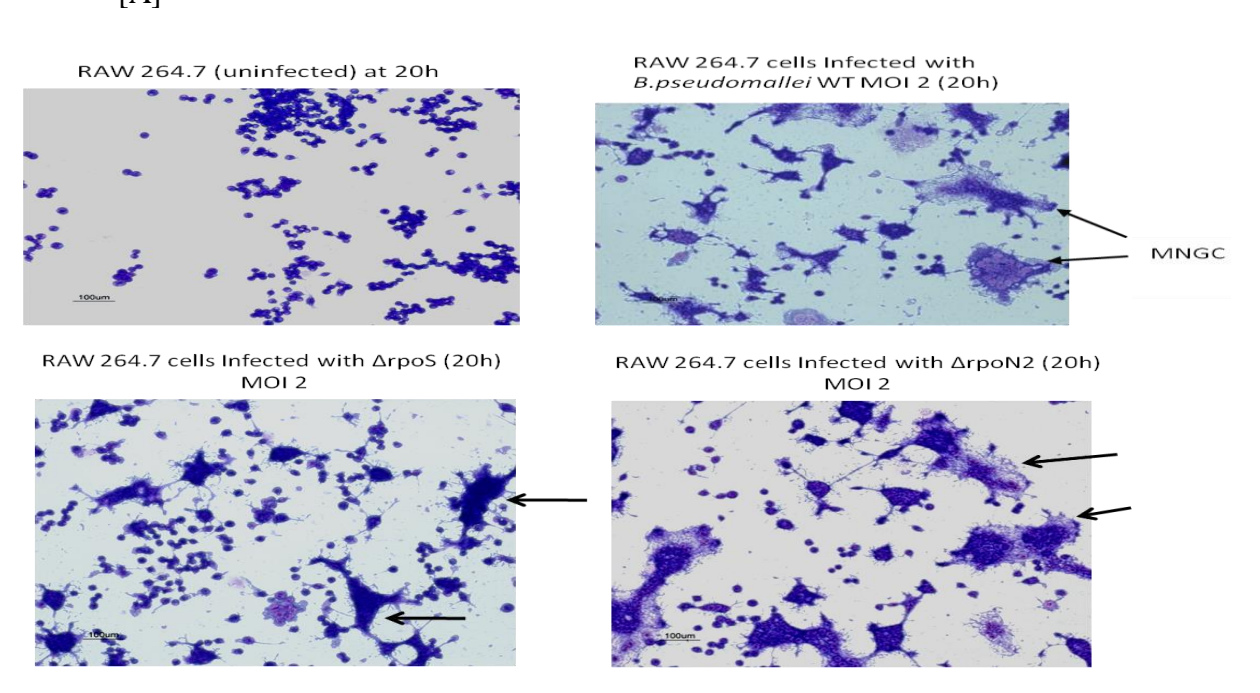
Comparative analysis of multinucleated giant cell formation between B. pseudomallei rpoS mutant and rpoN2 mutant strains with its wild type.

Correlation between multinucleated giant cell (MNGC) formation of infected mouse macrophage cells and intracellular survival of B. pseudomallei wild type, $\Delta rpoN2$ and $\Delta rpoS$

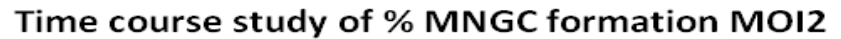
To study the potential involvement of *B. pseudomallei* RpoS and RpoN2 in bacterial intracellular life style especially in modulating MNGC formation of RAW 264.7 cells, the infection assays with MOI 2 were performed and the MNGC formation of infected RAW 264.7 cells with either WT, $\Delta rpoS$ and $\Delta rpoN2$ was examined. The MNGC formations are founded in all cases and its percentages are correlated with the intracellular bacterial number (Fig. 6).

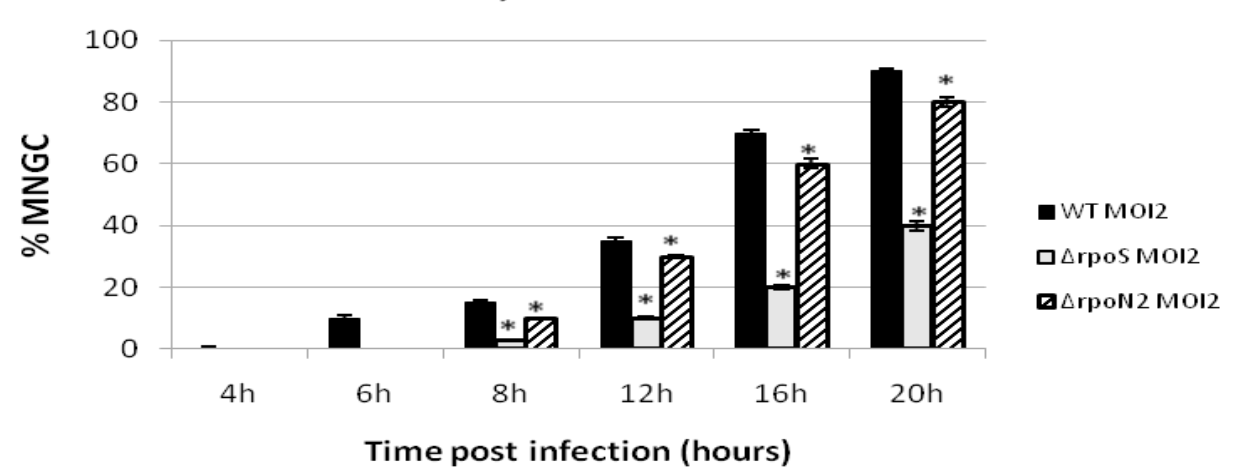
For the time course study on intracellular survival of *B. pseudomallei* and MNGC formation of infected RAW264.7 cells, two separate infection experiments with MOI 2 (two bacteria per one host cell) were performed in parallel. The infection assay was carried out as described in material and method. At each indicated PI (post infection) time point, the infected RAW264.7 cells were lysed with 0.1% Triton X100 and drop plate culture following the serial dilution of the lyses for intracellular bacteria counting or fixed with absolute cold methanol (or para-formaldehyde 1%) for Giemsa staining in the parallel experiment to count host cell MNGCs.





[B]





[C]

Intracellular survival of B. pseudomallei WT and mutants

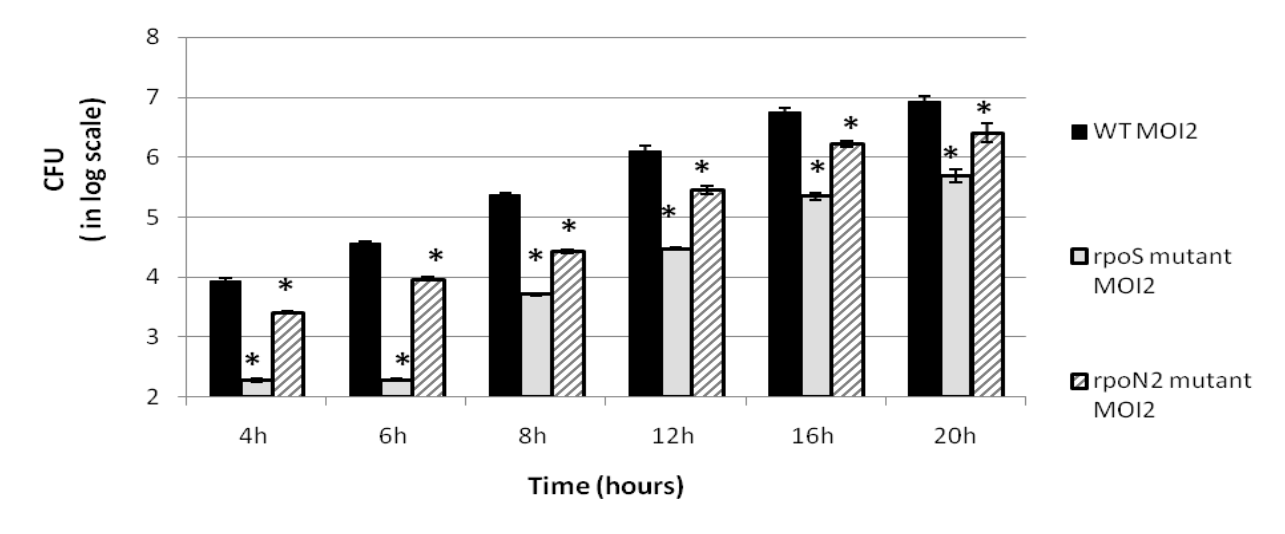


Fig. 6 Time course study on multinucleated giant cell (MNGC) formation in mouse macrophage cell line and intracellular survival of *B. pseudomallei* wild type, ΔrpoN2 and ΔrpoS. 10⁵ RAW 264.7 cells were exposured to either *B. pseudomallei* wild type or ΔrpoSor ΔrpoN2 strain with MOI 2 (two bacteria per one RAW cell) and the Kanamycin protection assay was performed. (A) Giemsa staining for observation MNGC formation of RAW 264.7 infected with either *B. pseudomallei* WT or ΔrpoN2or ΔrpoS at 20h; (B) Time course study on % MNGC formation in RAW 264.7 cells. The infected cells were fixed, stained with Giemsa, then the pictures were taken under Inverted Microscope (Nikon, TE2000U) and counted by ImageJ program. The graph was plotted base on the mean of 3 separated experiments, each was performed in duplicate, * P <0.01 by Students' t-test. (C) At different post infection (PI) time points 4h, 6h, 8h, 12h, 16h, 20h, the infected RAW cells were collected and lysed with 0.1% Triton X-100.

RpoN2 and RpoS involve in invasion of *B. pseudomallei* into mouse macrophage cell line (RAW 264.7)

To verify the involvement of RpoS and RpoN2 in invasiveness and whether the MOI (Multiplicity of infection) is affected to MNGC formation or not, *B. pseudomallei* wild type, rpoS mutant ($\Delta rpoS$) and rpoN2 mutant ($\Delta rpoN2$) strains were infected in to mouse macrophage cell line (RAW 264.7) with multiplicity of infection (MOI) either 2 or 10 or 20 bacteria per single host cell. The number of intracellular bacteria was analyzed by standard antibiotic protection assay. All three strains *B. pseudomallei* wild type, $\Delta rpoS$ and $\Delta rpoN2$ were able to enter the RAW 264.7 cell line (Table 3) with about 4.8%, 0.1% and 1.2% respectively in comparison with the starting innoculum size. In all cases, the *B. pseudomallei* $\Delta rpoS$ was less invasive than $\Delta rpoN2$ and $\Delta rpoN2$ was less invasive than wild type. The results presented in Fig. 7 confirmed that $\Delta rpoS$ and $\Delta rpoN2$ appeared to have significantly lower invasiveness than wild-type, judging from the number of intracellular bacteria recovered 4 h after the infection.

Table 3 Invasion of either *B. pseudomallei* wild type (WT), $\Delta rpoS$ or $\Delta rpoN2$ strain into RAW 264.7 cell line, as measured by the kanamycin protection assay.

Bacterial strain	Innoculum size a	Mean no. of intracellular	% internalization
	(CFU)	bacteria after 4h incubation ^b	
		(CFU)	
WT MOI2	1.89×10^{5}	$8.63 \times 10^3 \pm 6.01 \times 10^2$	4.57
WTMOI10	8.20×10^5	$3.86 \times 10^4 \pm 2.05 \times 10^2$	4.71
WT MOI 20	2.00×10^6	$9.69 \times 10^4 \pm 1.80 \times 10^3$	4.84
ΔrpoS MOI2	1.97×10^5	$1.91 \times 10^2 \pm 6.25 \times 10^0$	0.10
$\Delta rpoS$ MOI 10	9.30×10^5	$8.83 \times 10^2 \pm 6.47 \times 10^1$	0.09
$\Delta rpoSMOI~20$	1.89×10^6	$1.64 \times 10^3 \pm 6.95 \times 10^1$	0.09
ΔrpoN2 MOI 2	2.10×10^5	$2.58 \times 10^{3} \pm 8.47 \times 10^{1}$	1.23
ΔrpoN2 MOI 10	9.71×10^5	$1.23 \times 10^4 \pm 8.26 \times 10^2$	1.27
ΔrpoN2 MOI 20	2.21×10^6	$3.05 \times 10^4 \pm 2.19 \times 10^3$	1.38

a. Innoculum size = number of bacteria was added into 10^5 RAW 264.7 host cells and the mixtures were incubated for 4h.

b. Number CFU of liberated intracellular bacteria after 4h incubation \pm standard error of the mean (SEM) from three separated experiments, each carry out duplicate.

Invasion of *B. pseudomallei* WT, ΔrpoS and ΔrpoN2 strain into RAW 264.7 cell line

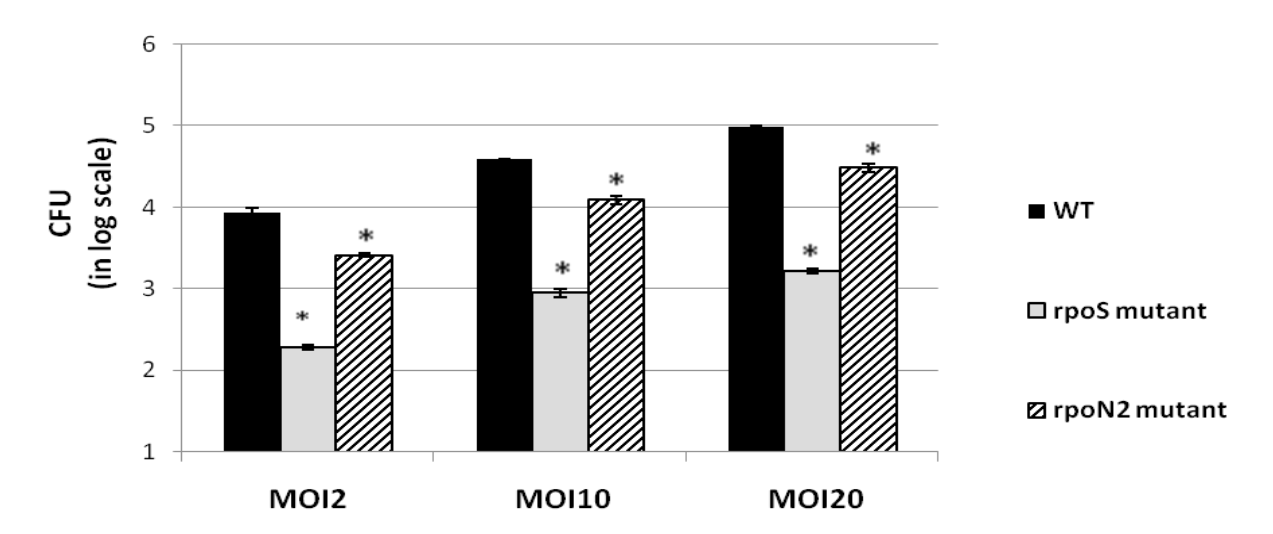


Fig. 7 The invasiveness of $\Delta rpoN2$ in comparison with *B. pseudomallei* wild type and $\Delta rpoS$. 1x10⁵ RAW 264.7 cells/well in 12well-plates were infected with either bacteria WT (wild type), rpoS mutant ($\Delta rpoS$) or rpoN2 mutant ($\Delta rpoN2$) with MOI2, MOI10 and MOI20. After incubation 2h for bacterial entering to the host cell, the media was removed, each well was washed 2 time with PBS, thereafter the infected RAW264.7 cells were further incubate 2h in fresh medium containing250μg/ml Kanamycin to kill extracellular bacteria. RAW 264.7 cells were then lysed with 0.1%Triton X-100 and intracellular bacteria were quantitated by plating serial dilutions of the lysate. Data are expressed as the mean and standard error of the mean (SEM) for three separated experiments, each carriout triplicate. * P < 0.001 by Students's t-test.

<u>Percentage of MNGC formation in RAW 264.7 cell line is depend on certain number</u> of bacteria inside the host cell.

In order to verify for the observation that % MNGC formation of infected RAW264.7 cells is depended on intracellular bacterial number of either WT, $\Delta rpoS$ or $\Delta rpoN2$, time course study on intracellular survival of bacteria as well as %MNGC formation of infected host cells was examined. In this experiment, the same number bacteria of either *B. pseudomallei* WT or $\Delta rpoN2$ or $\Delta rpoS$ strain was forced to enter the RAW 264.7 cells. Data in Table 3 showed that the invasiveness of *B. pseudomallei* WT was 50 times higher than $\Delta rpoS$ and about 5 times higher than $\Delta rpoN2$, so the infection assay with MOI2 for wild type and MOI 100 for $\Delta rpoS$ or MOI 10 for $\Delta rpoN2$ was designed and carried out (Fig. 8).

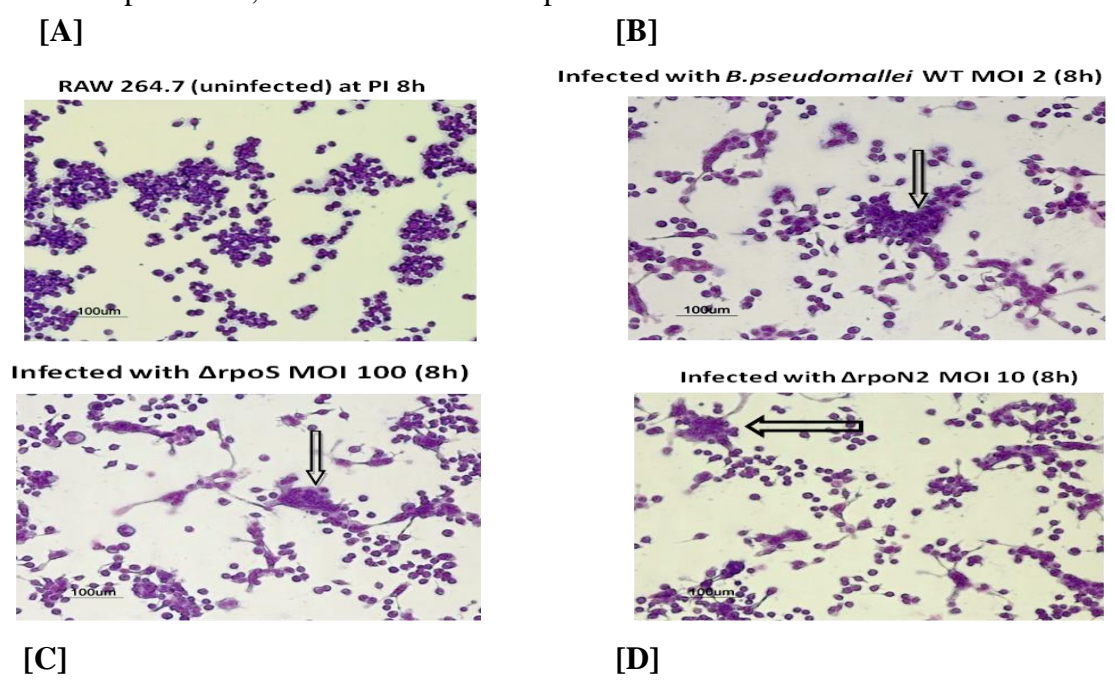
At PI 8h the same intracellular number of WT or $\Delta rpoN2$ or $\Delta rpoS$ was found by CFU counting

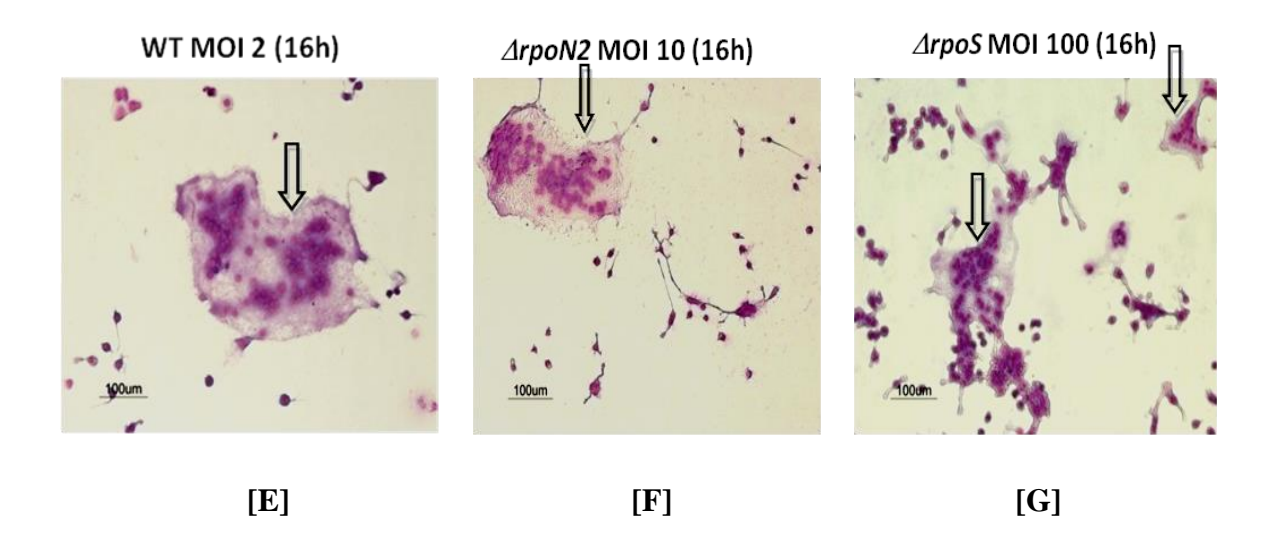
(about 10^5 bacteria) (Table 3). It is correlated with the same percentage of MNGC formation (15%) in the RAW 264.7 infected with either WT or $\Delta rpoN2$ or $\Delta rpoS$ (Table 4), suggesting the certain number of intracellular bacteria (at least 5×10^4) is required to cause the morphological changes of RAW264.7 cells and *B. pseudomallei* RpoS and RpoN2 may not directly involved in the MNGC formation of the host.

Table 4 MNGC formation in RAW 264.7 cells infected with either *B. pseudomallei* WT MOI 2 or $\Delta rpoS$ MOI 100 or $\Delta rpoN2$ MOI10 at PI 8h

Bacterial strain	Innoculum size ^a (CFU)	No. of intracellular bacteria at PI 8h ^b (CFU)	MNGC formation ^c in RAW 264.7 cells infected
			with bacteria at PI 8h (%)
WT MOI2	1.93E+05	$1.42 \times 10^5 \pm 4.73 \times 10^3$	15.32 ± 0.73^{d}
ΔrpoS MOI100	1.27E+07	$1.58 \times 10^5 \pm 1.04 \times 10^4$	15.87 ± 0.22^{d}
ΔrpoN2 MOI 10	9.72E+05	$1.68 \times 10^5 \pm 1.04 \times 10^4$	16.12 ± 0.13^{d}

- a. Innoculum size = number of indicated *B. pseudomallei* was added into 10^5 RAW 264.7 host cells.
- b. Number CFU (Mean) of intracellular bacteria at post infection 8h (PI 8h) \pm standard error of the mean (SEM) from three separated experiments, each carried out in duplicate.
- c. %MNGC = (number of nuclei within multinucleated giant cells/total number counted) x 100
- d. Percentages were determined at 8h after RAW 264.7 cells infected with indicated strains of B. pseudomallei. Data are Means \pm SEMs from at least three independent experiments, each carried out in duplicate.





<u>Fig. 8</u> MNGC formation in RAW 264.7cells infected either with Bp WT MOI 2 or $\Delta rpoS$ MOI 100 or $\Delta rpoN2$ MOI 10 at PI 8h and 16h. Infection assay was performed as described in material and method. At PI 8h the RAW 264.7 cells were fixed with absolute cold methanol (or para-formaldehyde) for 15min and stained with Giemsa. Uninfected RAW 264.7 at PI 8h were in inactivated stage with good round shape (A), whereas the same %MNGC formation (15%) of RAW cells infected with either Bp WT MOI2 (B) or $\Delta rpoS$ MOI 100 (C) or $\Delta rpoN2$ was found. The arrows indicated the MNGC formation in infected RAW cells. (E), (F), (G) are the pictures showing the enlargement of MNGCs induced by *B. pseudomallei* WT, $\Delta rpoN2$ and $\Delta rpoS$ at PI 16h.

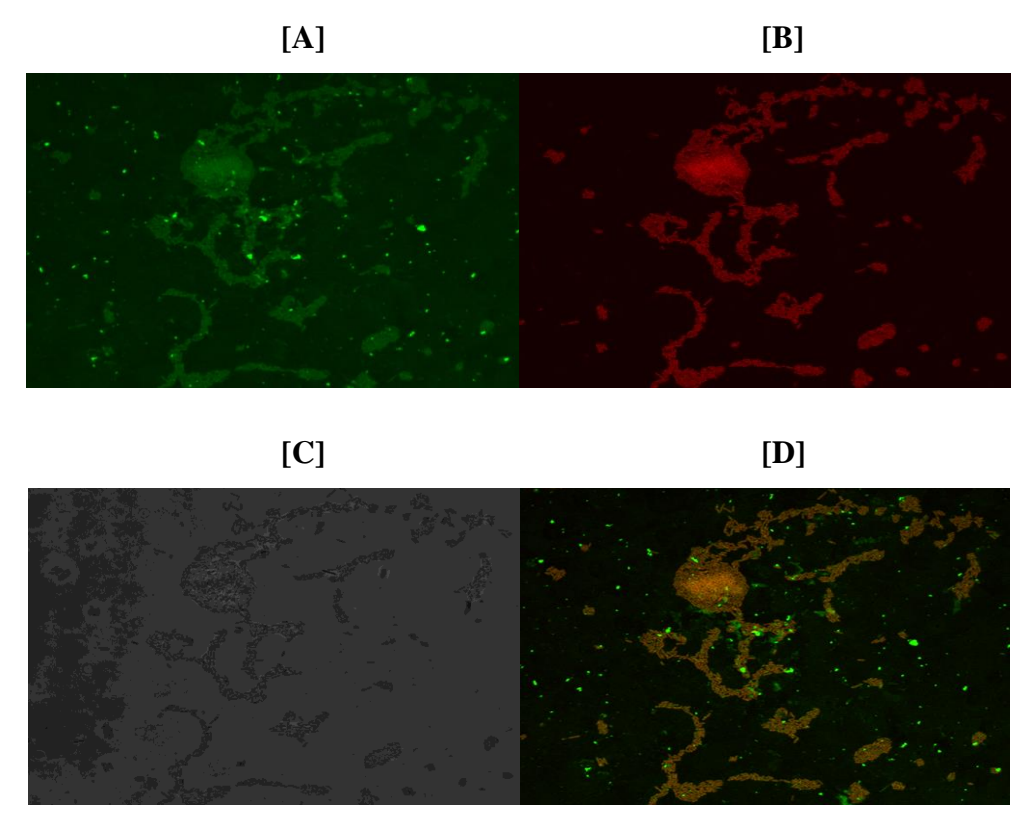
Comparative analysis of biofilm formation between B. pseudomallei rpoS mutant and rpoN2 mutant strains with its wild type using crystal violet staining and confocal analysis

Visualization of biofilm structure using confocal laser scanning microscope (CLSM)

To investigate characteristic of biofilm formation among bpsI, ppk, rpoN2 and rpoS B. pseudomallei mutant strains in more details, CLSM was used to visualize biofilm architecture, micro-colony formation, thickness and exopolysaccharide production in each of the B. pseudomallei strains between LB and MVBM media. It is apparent that all B. pseudomallei mutants had distinct defectiveness on an ability of biofilm formation in both media. The fixed-death bacteria were stained with FITC-ConA fluorescein which has lectin-chain of isothiocyanate-concanavalinA that will be conjugate to exopolysaccharide matrix of the bacteria. After washing of exceed FITC-conA, the bacteria were continuously stained with Propidium iodide (PI) that will penetrate into the death cells and bind to bacterial DNA. Five different fields for each B. pseudomallei strain were captured in Z-axis direction and used for determination of biofilm thickness and exopolysaccharide integrated fluorescent intensity.

FITC-ConA was excited with blue laser at wavelength 490 nm and emitted green

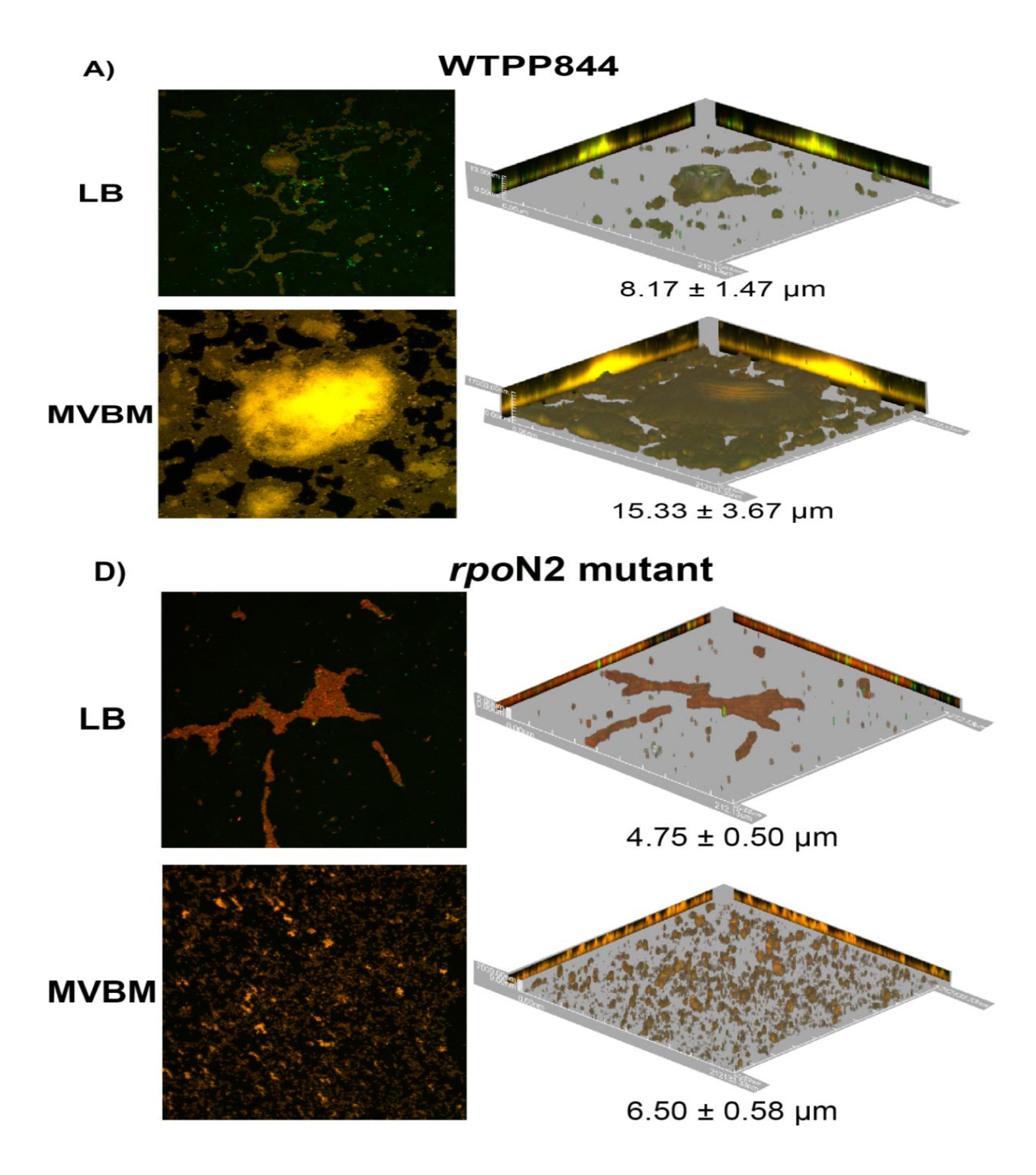
laser at wavelength 525 nm and PI was excited with dark red laser at wavelength 535 nm and emitted the light red laser at wavelength 617 nm (Figure 9). Therefore, the exopolysaccharide matrix was represented with green color (Figure 9A) and the bacterial cells were shown in red color (Figure 9B). CLSM can present a photo merging between each fluorescein dye thus yellow color was representation of the bacteria cells having their exopolysaccharide matrix around them (Figure 9D). The light microscope image of the bacteria was also shown in Figure 9C for comparison with the fluorescent images.

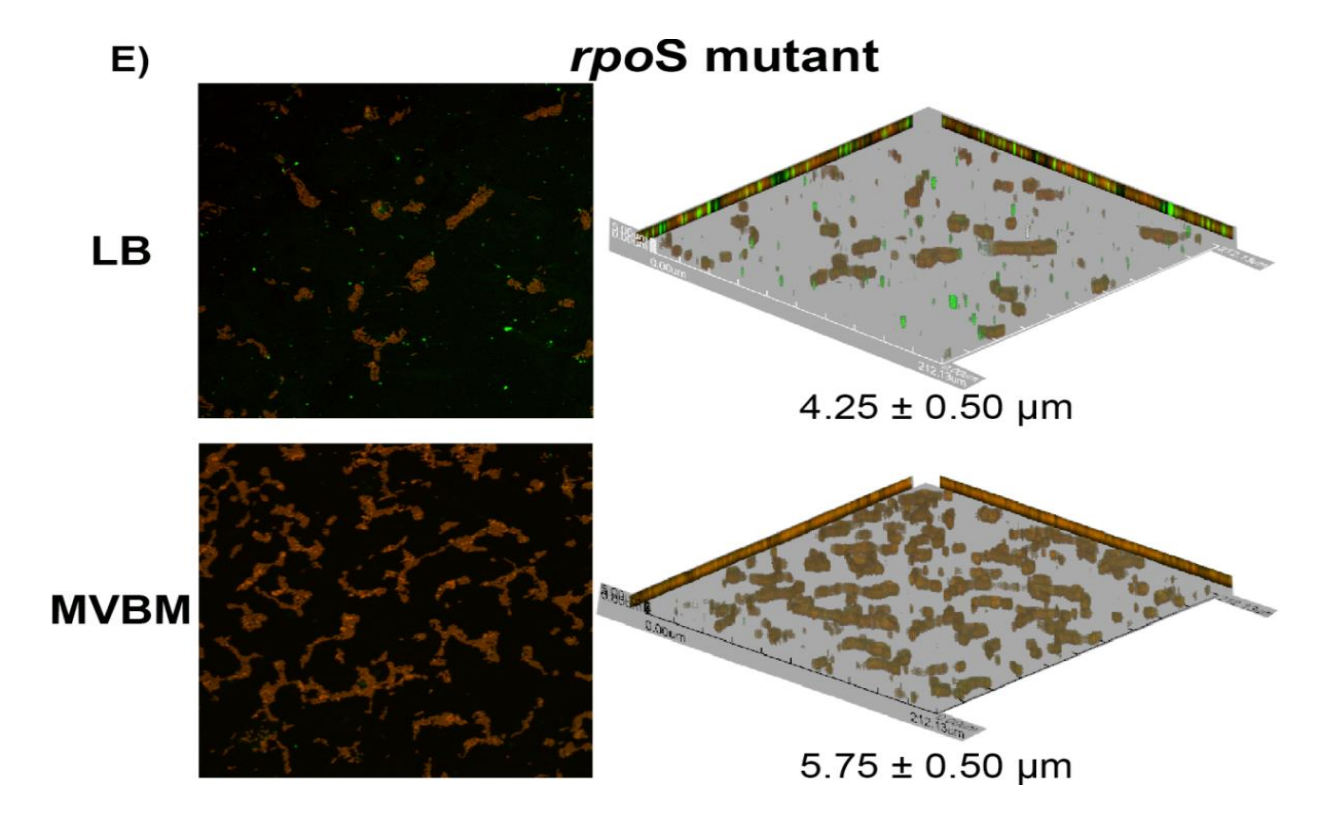


<u>Fig. 9</u> Representation of *B. pseudomallei* biofilm by CLSM. The CLSM images of *B. pseudomallei* wild type which also represent micro-colony formation. A) Exopolysacchride matrix was stained with FITC-ConA. B) Bacteria cells which their DNA were stained by PI. C) Bacteria cells from light microscope and D) The merged image between A and B; yellow color represents for bacteria cells having exopolysaccharide matrix.

The CLSM images have elucidated micro-colony formation and thickness of *B. pseudomallei* in Figure 5.3. Five fields for each *B. pseudomallei* strain were captured and biofilm thickness was calculated from the number of pictures taken in every 1 µm form the top along the depth (Z-axis). It is obvious that micro-colonies of *B. pseudomallei* wild type was formed in both LB and MVBM (Fig. 10A), which is the overlapping of a group of bacterial cells, scattered throughout the slide. Apparently, MVBM can induce micro-colonies formation more

than LB media, in terms of size and thickness. Micro-colony thickness of the wild type biofilm in LB was illustrated at 8.17 ± 1.47 µm which is about two-fold less than the thickness in MVBM (18.77 ± 3.67 µm). Moreover, MVBM can obviously induce more bacterial attachment and spreading onto the surface which should be suitable for the initial step of biofilm formation.

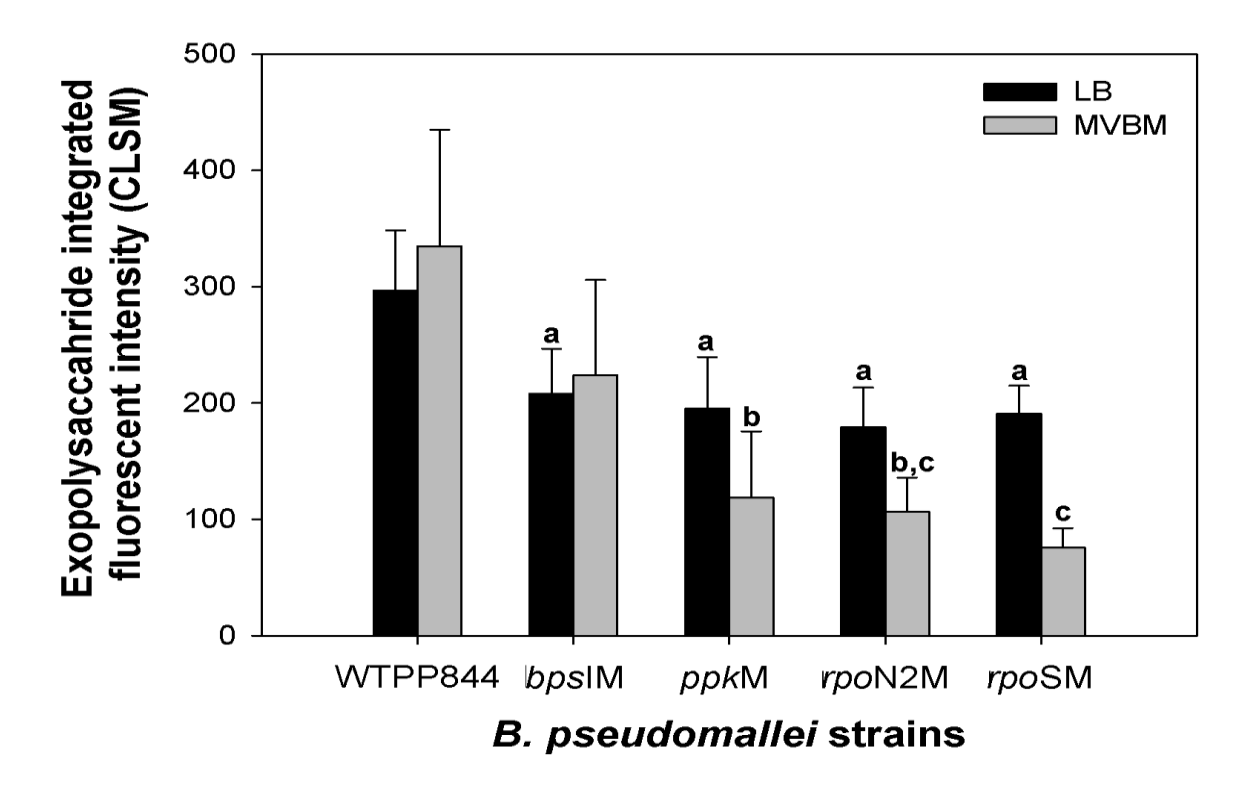




<u>Fig. 10</u> Visualization of biofilm production and thickness in *B. pseudomallei* A) wild type PP844, D) *rpo*N2, and E) *rpo*S mutant strains in both LB and MVBM using CLSM

The biofilm exopolysaccharide integrated fluorescent intensity was calculated from five-observed fields using FV10-ASW 3.0 Viewer software and averaged into Figure 10. The results demonstrate that each of the *B. pseudomallei* mutant strain produced biofilm exopolysaccharide significantly lower than the wild type both in LB and MVBM. However, there is no significant difference between each mutants cultured in LB medium while distinct exopolysaccharide production among the mutants was observed in MVBM, which the *bps*I mutant had higher exopolysaccharide production than the *ppk* mutant followed by the *rpo*N2 and *rpo*S mutants (p=<0.001) suggesting that they do have specific effects on the ability of biofilm formation

It is evident that exopolysaccharide production results obtained here (Fig. 11) are in good agreement with previous micro-colony formation and biofilm thickness which are apparently shown that MVBM have particular effects on biofilm formation of *B. pseudomallei* more than LB. These finding support our postulation that MVBM is more suitable for biofilm study than LB media as it can induce biofilm phenotype clearer than the other. Furthermore, as biofilm characters in MVBM showed specific ability of each mutant, it indicates that our genes of interest have specific influences on biofilm formation in *B. pseudomallei*.



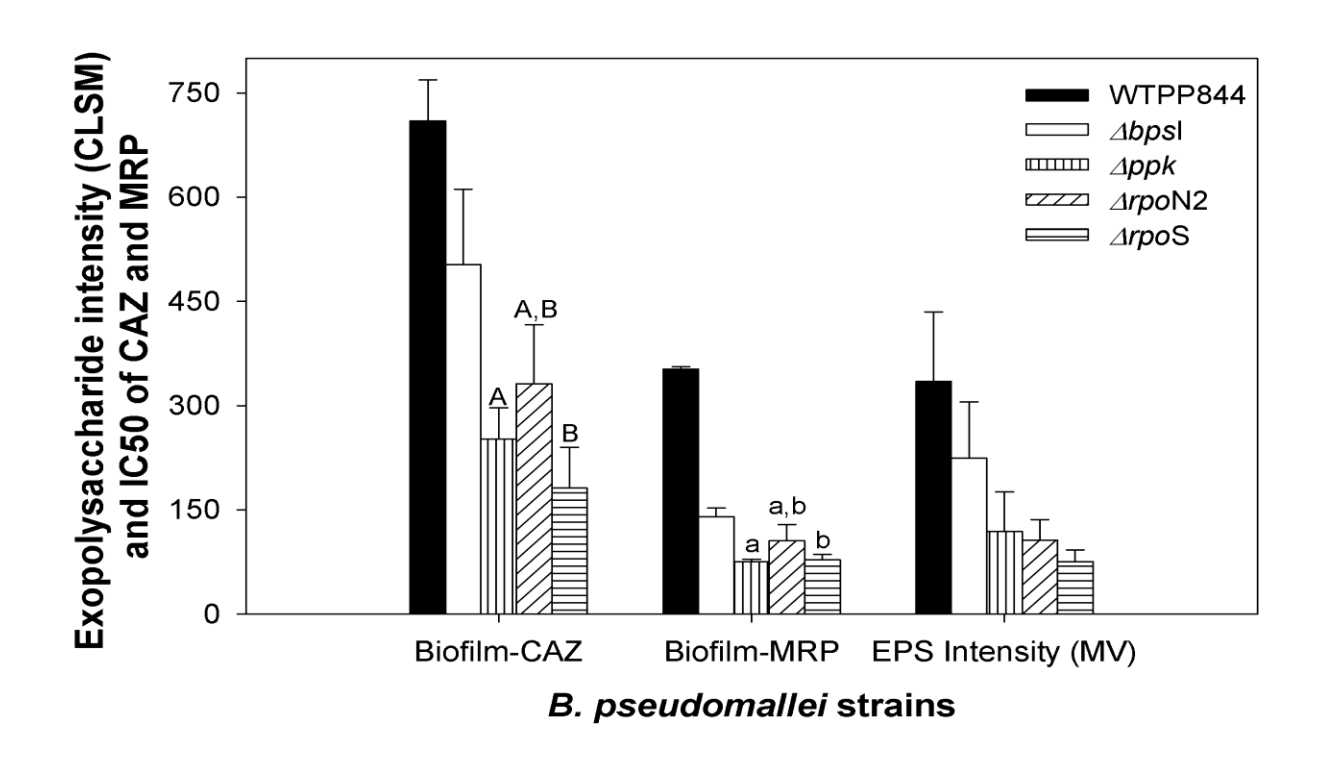
<u>Fig. 11</u> The biofilm exopolysaccharide production of *B. pseudomallei*. The averaged exopolysaccharide integrated fluorescent intensity of *B. pseudomallei* biofilms in LB and MVBM media calculated from CLSM. Same alphabet represents for the same group with no significant difference.

Correlation between the exopolysaccharide production and the antibiotic resistance in the *B. pseudomallei* biofilms

The IC50 of biofilm-treated with CAZ shows a substantial difference among biofilm *B. pseudomallei* mutant strains in contrast to the IC50s of biofilm-treated with MRP that are similar to each other. The difference between CAZ IC50s among *B. pseudomallei* mutants suggests that each mutated gene has the different effect on biofilm formation. While the MRP IC50s between the mutants were observed, it may be implied that the smaller structure of MRP is not affected for the diffusion through the altered biofilm extracellular matrix. The *bps*I mutant displayed higher antibiotic resistance than any other mutants in both CAZ and MRP treatment (P=<0.001), indicating that lack of the *bps*I gene was not greatly altered its biofilm formation. The mutants that showed the greatest effect on biofilm mediated antibiotic resistance are *ppk* and *rpo*S as they exhibit the lowest IC50 values for both CAZ and MRP with mutation of the *rpo*S gene displaying the lowest antibiotic resistance. The *rpo*N2 mutant showed an intermediate defect in biofilm mediated resistance with 53% and 70% reductions in IC50 for CAZ and MRP,

respectively, even there was no significant different with *ppk* mutant in CAZ treatment and with *bps*I mutant in MRP treatment. Thus, *rpo*N2 appears to have a limited regulatory role in biofilm formation which should be different from *rpo*S gene.

Comparison between the exopolysaccharide production by CLSM and IC 50 values of CAZ and MRP treatments has revealed a similar trend between these two phenomenal. Therefore, it may be implied that there is a possible link between these two phenomenal which may be under the regulation of our investigated genes in *B. pseudomallei* biofilm. Although there is no significant difference between the capability of antibiotic resistance in biofilm *ppk*, *rpo*N2 and *rpo*S mutants for both antibiotics, they still have particular biofilm formation ability as illustrated in Fig. 12. This suggests that these four genes cause specific influences on biofilm production which greatly affect the biofilm structure resulting in the reciprocal decrease of antibiotic resistance.



<u>Fig. 12</u> Exopolysaccharide productions from CLSM and antibiotic resistance (IC50) of CAZ-and MRP-treated biofilm. Comparisons between exopolysaccharide integrated fluorescent intensity and IC50 of CAZ and MRP treatments in biofilm condition of *B. pseudomallei* wild type and four mutant strains were shown. The same alphabets on the bar graphs are represented within the same group indicating no significant difference. (P = <0.001).

Quantitation of monosaccharide components of analyzed exopolysaccharides

To quantitate the amount of monosaccharides in unknown sample, the standard mixture of the relevant particular glycoconjugate, consisting of rhamnose, xylose, mannose, galactose and glucose, was subjected to parallel derivatization with the sample and further analyzed in GC-MS. The amount (milligrams) of each sugar in the standard mixture is a function of the number of sugars that were mixed together. The ratio of the peak area of an internal standard, added to the mixture, to that of each standard sugar in the mixture was determined as detector response factor (dRF) are determined as mentioned above and used to calculate the amount of each component of the sample being analyzed. The total ion chromatogram of each biofilm exopolysaccharide from 0.5 mg of purified biofilm exopolysaccharide material of all *B. pseudomallei* strains revealed the identification of monosaccharide types and percent peak areas which were further used for the weight calculation. After the identification of multiple peaks in the analyzed sample using a comparison of the retention times, weight of identified sugar in unknown (mg) was calculated according to the following formula as mentioned earlier.

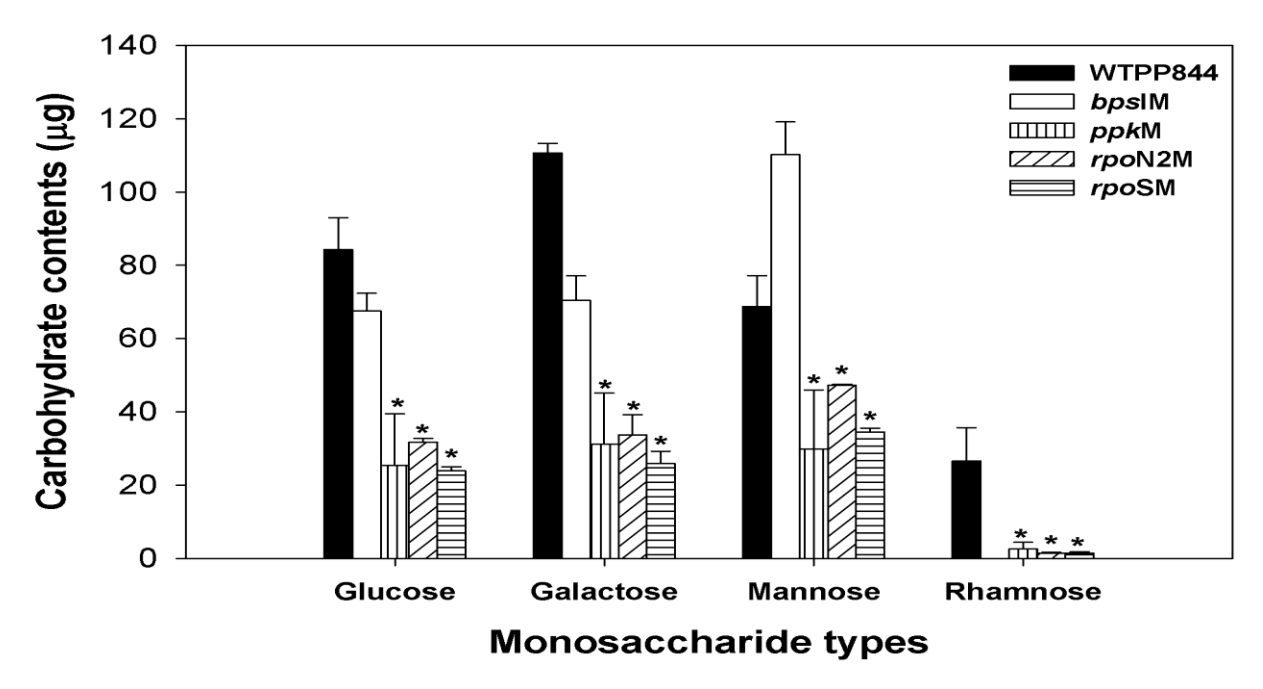


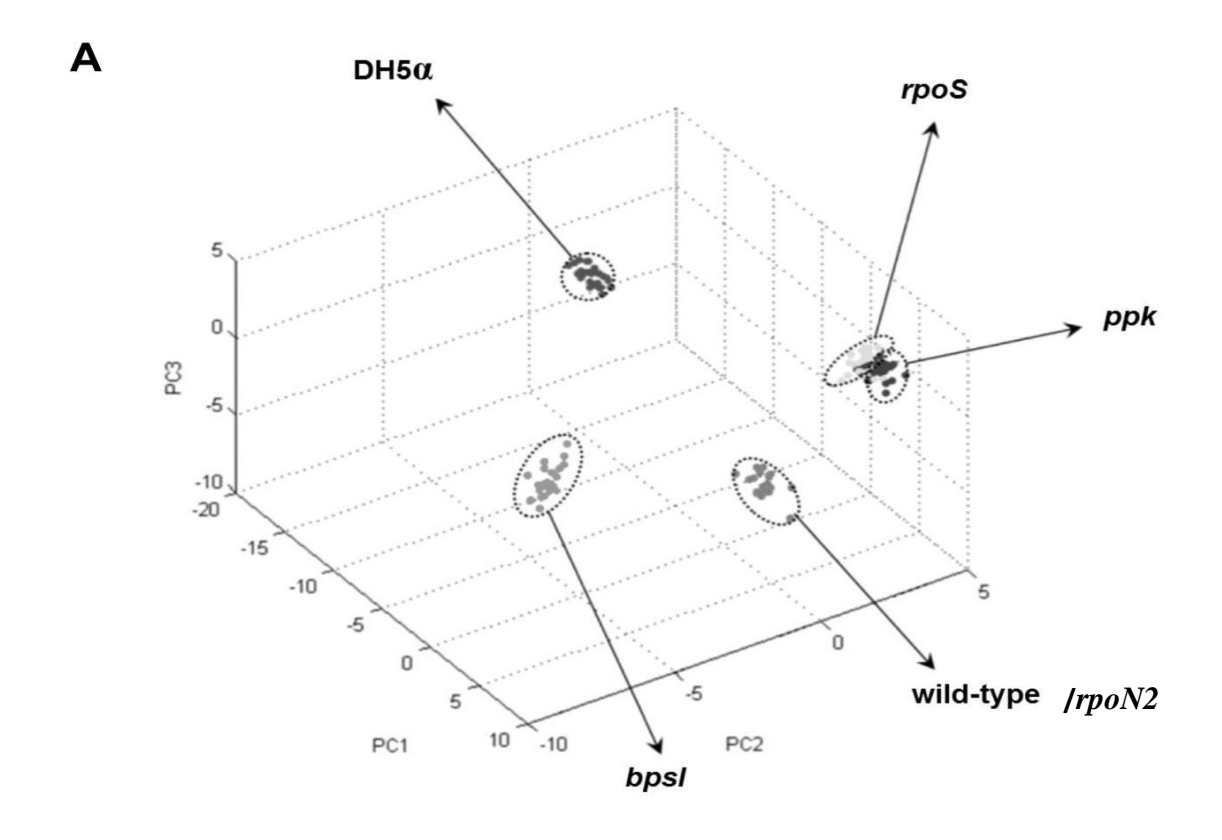
Fig. 13 Subtracted carbohydrate contents in the exopolysaccharides of all *B. pseudomallei* strains. The carbohydrate contents of the exopolysaccharides produced by *B. pseudomallei* wild type and mutant strains after subtraction from the biofilm production capacity determined by CLSM were compared to each other; $\blacksquare = BpWT$, $\square = bpsIM$, $\square = ppkM$, $\square = rpoN2M$ and $\square = rpoSM$. Asterisks indicate that there is no significant difference between those strains within a monosaccharide type.

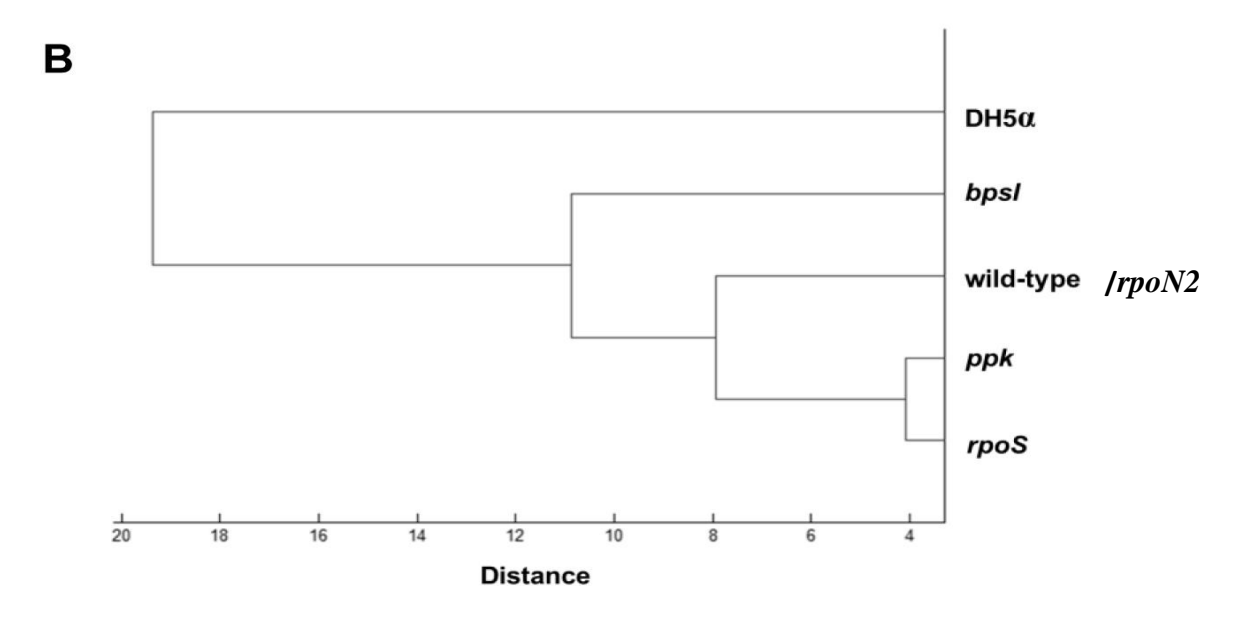
In addition, this carbohydrate composition analysis of the exopolysaccharides was studied from equal amounts of purified carbohydrate material; nevertheless, each *B. pseudomallei* strain has a unique capacity for biofilm formation as previously reported. Thus, to obtain a more precise view of the effects of these genes on the biofilm production capacity, recalculation of the carbohydrate contents was performed according to the biofilm capacity. The specific biofilm capacity factors were calculated from each exopolysaccharide integrated fluorescent intensity by CLSM, for which the wild type strain was designed as the positive control, and used to subtract all of the carbohydrate contents as found in this study. The subtracted carbohydrate contents among *B. pseudomallei* strains were compared in Figure 13. It can be clearly seen in Figure 13 that there are shifts in the carbohydrate ratios and deprecated production of the monosaccharide types.

Comparative proteomic profiles between between B. pseudomallei rpoS mutant and rpoN2 mutant strains with its wild type using both LCMS-MS and 2D-Gel Methods

MALDI-TOF Analysis: Cluster analysis

To determine whether MALDI profiles of each mutant with a single gene mutation were distributed in a distinct cluster, the total of single MALDI spectra of PP844, *rpoS*, *ppk*, and *bpsI* isolates were subjected to PCA and unsupervised hierarchical clustering analyses using ClinProTools. *E. coli* DH5α was used as an outgroup species in analyses. All isolates exhibited distinctly separate distribution, as illustrated by results of PCA score plot (Fig 14A). The unsupervised hierarchical clustering analysis derived from the PCA scores, resulting in a dendrogram (Fig 14B), revealed that PP844, *rpoS*, and *ppk* clustered in the same clade. In addition, the *rpoS* and *ppk* isolates were grouped closer and displayed the shortest distance among all the bacterial isolates tested. This indicated a high similarity in MALDI profiles between *rpoS* and *ppk*. It was observed that a clade of *bpsI* isolate showed a greater_distribution from the others. Hence, based on this study, the whole-cell MALDI-TOF MS technique could be used to distinguish *B. pseudomallei* mutants containing single gene disruptions from the wild-type PP844.





<u>Fig. 14</u> Cluster analysis of *B. pseudomallei* wild-type and mutants. (A) PCA score plot representing clusters of each isolate (dashed circles) illustrated separately distribution with the *rpoS* and *ppk* isolates producing a much closer cluster. (B) Dendrogram derived from PCA scores demonstrates that *B. pseudomallei* PP844, *rpoS*, and *ppk* clustered on the same clade, while a clade of *bpsI* showed a greater distance than others

Candidate biomarkers

Comparison between MALDI spectra of PP844, rpoS, ppk, and bpsI isolates revealed visually slight, but significant changes in mass intensities. To determine the biomarkers specific to each strain observed from the whole-cell MALDI-TOF MS analysis, the average mass spectrum of each of the three mutants was individually compared against that of the PP844 wild-type (pair test) using ClinProTools. We employed the statistical approach incorporated with ClinProTools to provide the average mass peak list of each pair test (signal to noise threshold of 5.00 in the mass range of 2-20 kDa). Subsequently all peaks were evaluated referring to fold differences of average peak intensities and the pvalue from W/KW statistical calculation. The average peak intensity was calculated from peak intensity of the respective mutant isolate divided by that of the wild-type. As displayed in Fig 15, the specific biomarkers for each mutant displayed significant differences (p < 0.001) and > 2-fold differences in average peak intensity. With these analyses, the mass peaks at m/z 2721 and 2748 Da were identified for the rpoS isolate, while the peaks at m/z 3150, 3378, and 7994 Da were specific for ppk. A total of seven mass peaks were defined for bpsI isolate, with a mass ranging from m/z 3000-6000, including m/z 3420, 3520, 3587, 3688, 4623, 4708, and 5450 Da. Moreover, Quick Classifier (QC) model, a univariate sorting algorithm that statistically calculates individual peak area, was used to evaluate cross validation of all data sets. A value of 100% was obtained, indicating high reliability of the model prediction and thus accurate classification of test isolates. In addition, the area under the ROC curve (AUC) value of individual mass peaks was determined, with each mass peak showed the AUC value of 1, indicating 100% sensitivity (all true positives were found) and 100% specificity (no false positives were found). All together these mass peaks, unique to each isolate, could be potential biomarkers in order to facilitate the differentiation of the corresponding *B. pseudomallei* wild-type and mutants.

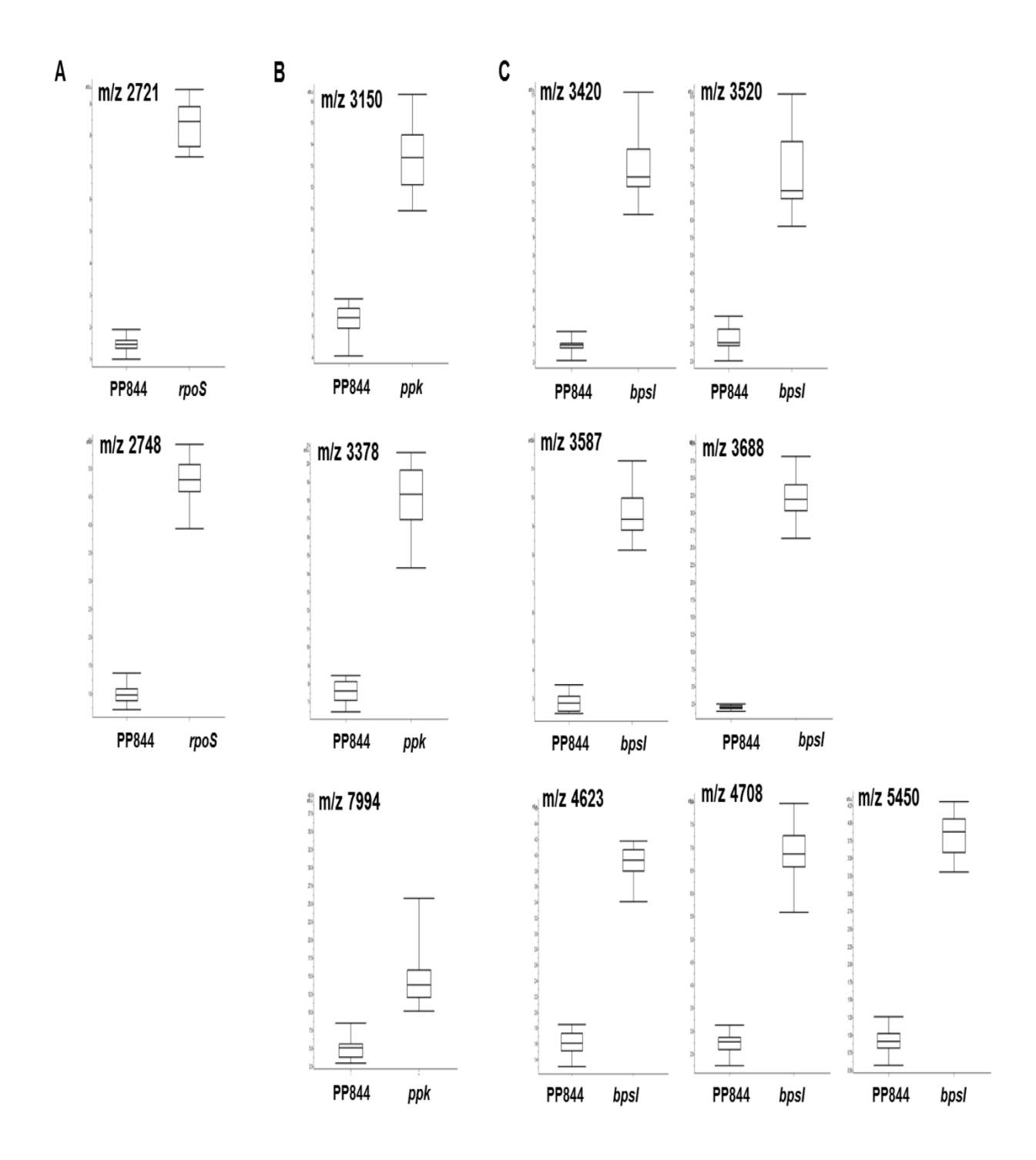


Fig. 15 The box and whiskers plot of candidate biomarkers in *B. pseudomallei* mutants. All of the candidate biomarkers were selected from ClinProTools analysis on the basis of W/KW statistics with significance at p < 0.001 and exhibiting average peak intensity differences > 2-fold. The biomarkers at m/z 2721 and 2748 Da were identified for rpoS (A), m/z 3150, 3378, and 7994 Da for ppk (B), and m/z 3420, 3520, 3587, 3688, 4623, 4708, and 5450 Da for bpsI (C). The top and bottom whiskers indicate the maxima and minima values of mass peak intensity, respectively. The intersection line represents the median. In the box, a range below and upper the intersection line displays the 25%-quartiles and 75%-quartiles, respectively.

Morphotype and phenotypic identification

All isolates used in this study were confirmed as *B. pseudomallei* by the identification scores obtained from BioTyper analysis and the existence of the five *B. pseudomallei*-specific biomarkers presented in our MALDI average. However, the observed bacterial morphology of all isolates cultured on Ashdown's selective agar illustrated distinct colony phenotypes (Fig 16), their components of ionized cell surface represented more reliable taxonomic identification as *B. pseudomallei* species based on whole-cell MALDI-TOF MS analysis.

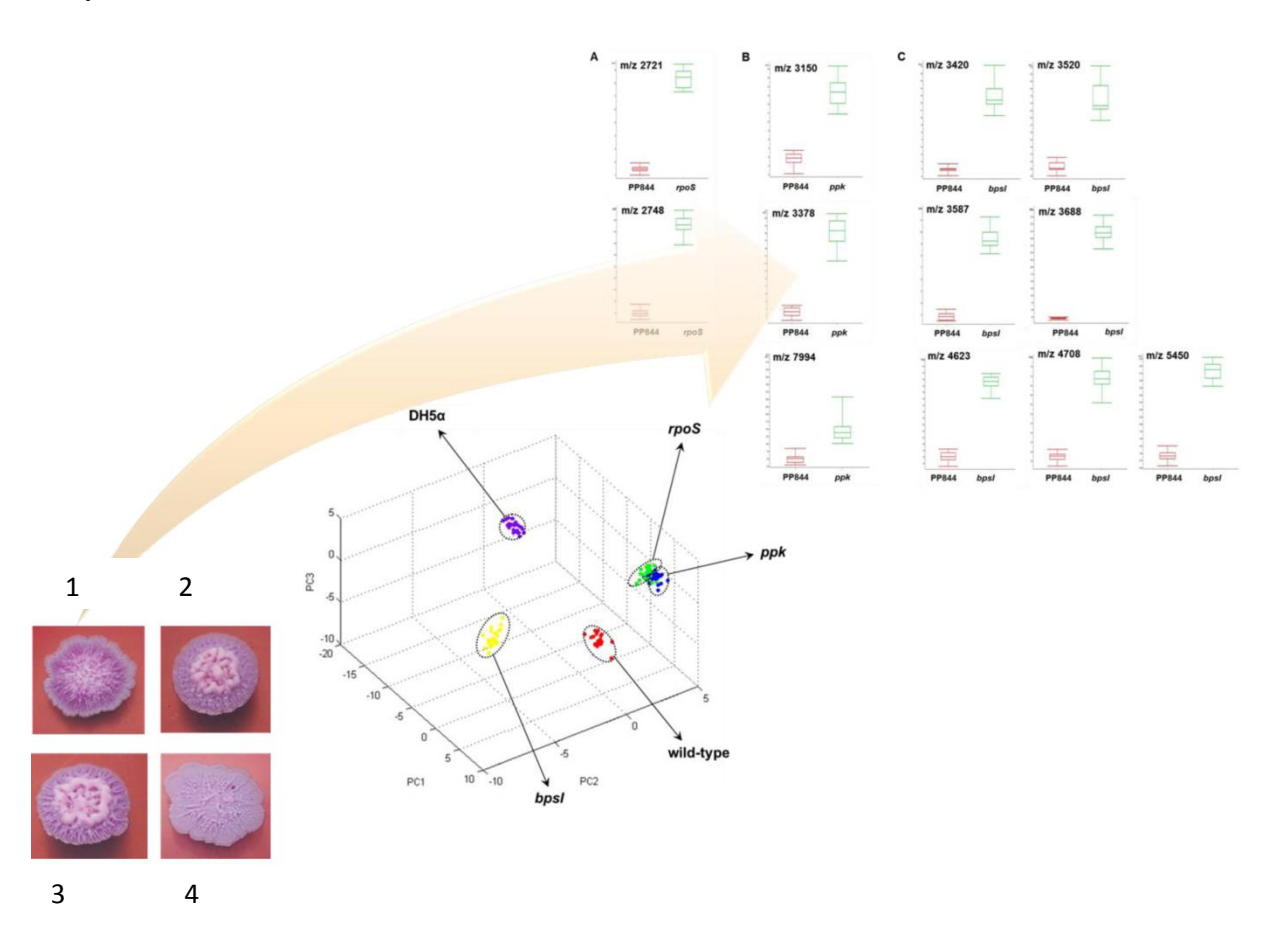


Fig. 16 Summary the identification of the differences mutated strains of *B. pseudomallei* started from morphology (1 is WT/ rpoN2, 2 is rpoS, 3 is ppk and 4 is bpsI) to cluster analysis and ended with biomarkers identification

Proteomic analysis of B. pseudomallei

A proteomic expression in wild-type and *rpoS* mutant strains of *B. pseudomallei* were analyzed as shown in Fig. 17.

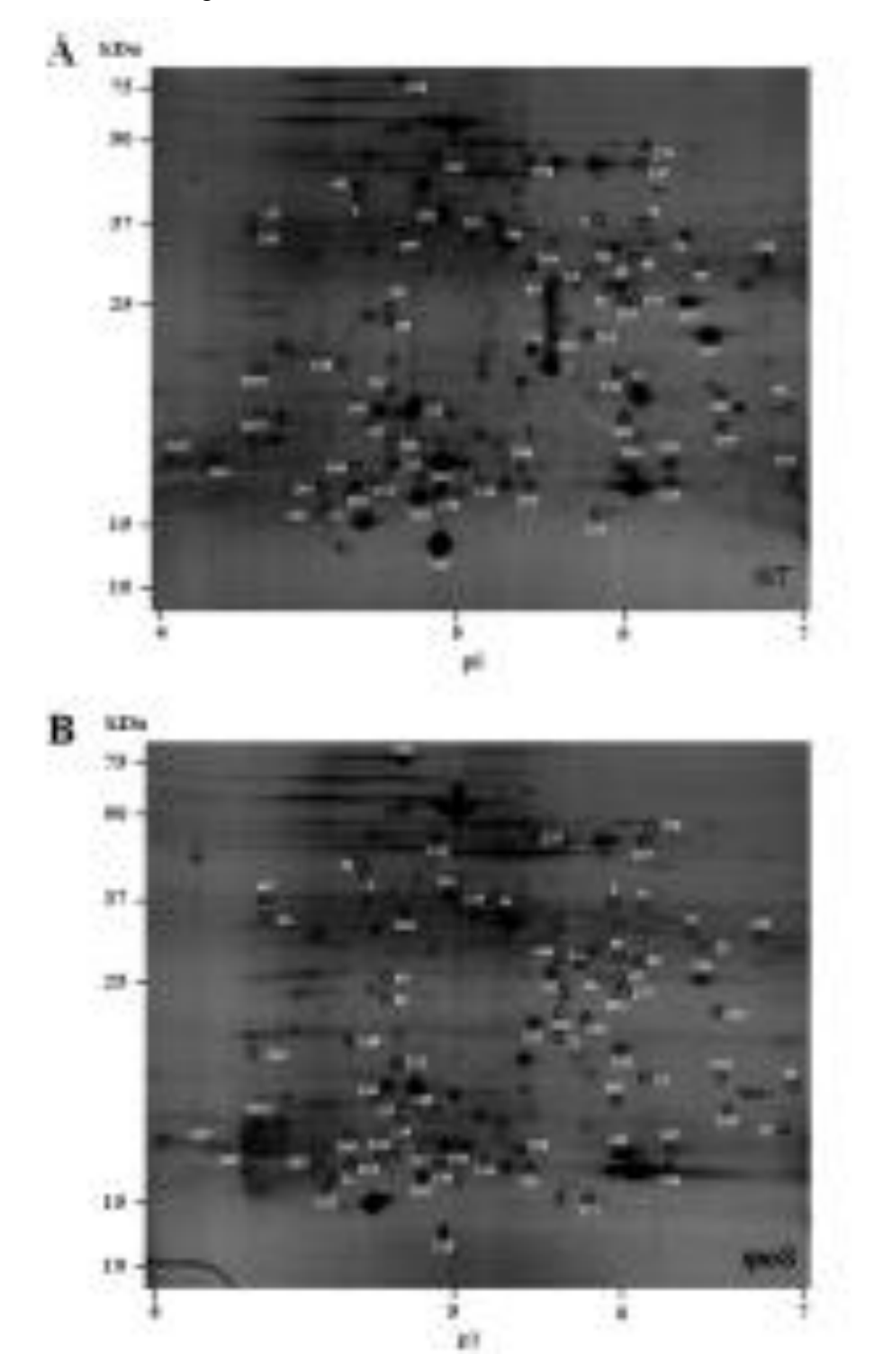
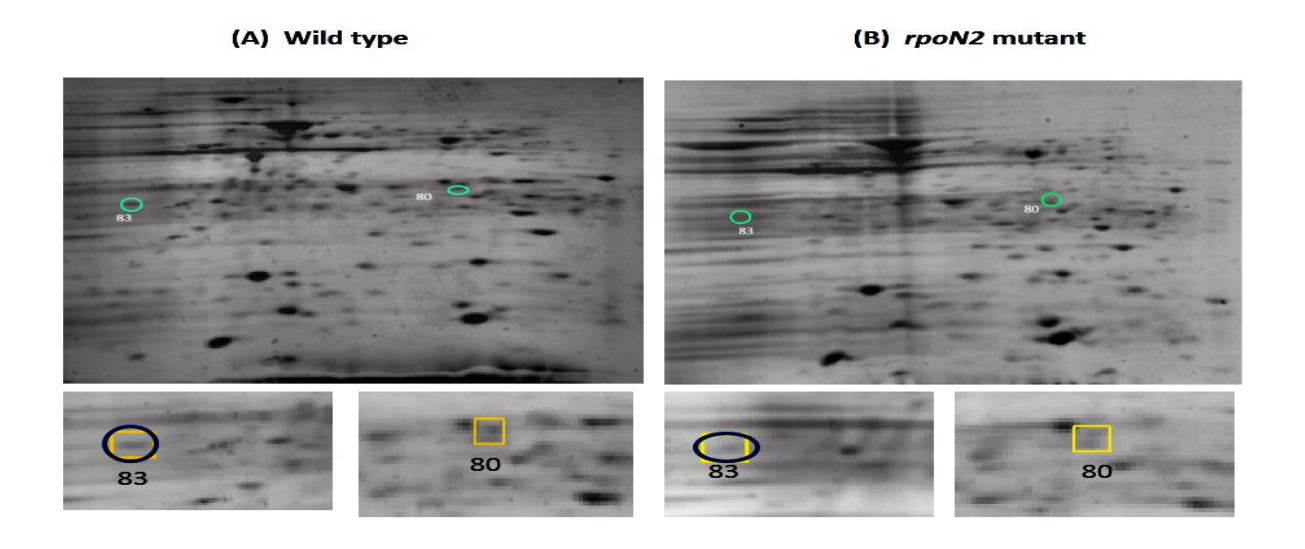


Fig. 17 2D-gel electrophoresis of B. pseudomallei wild-type (A) and rpoS mutant (B).

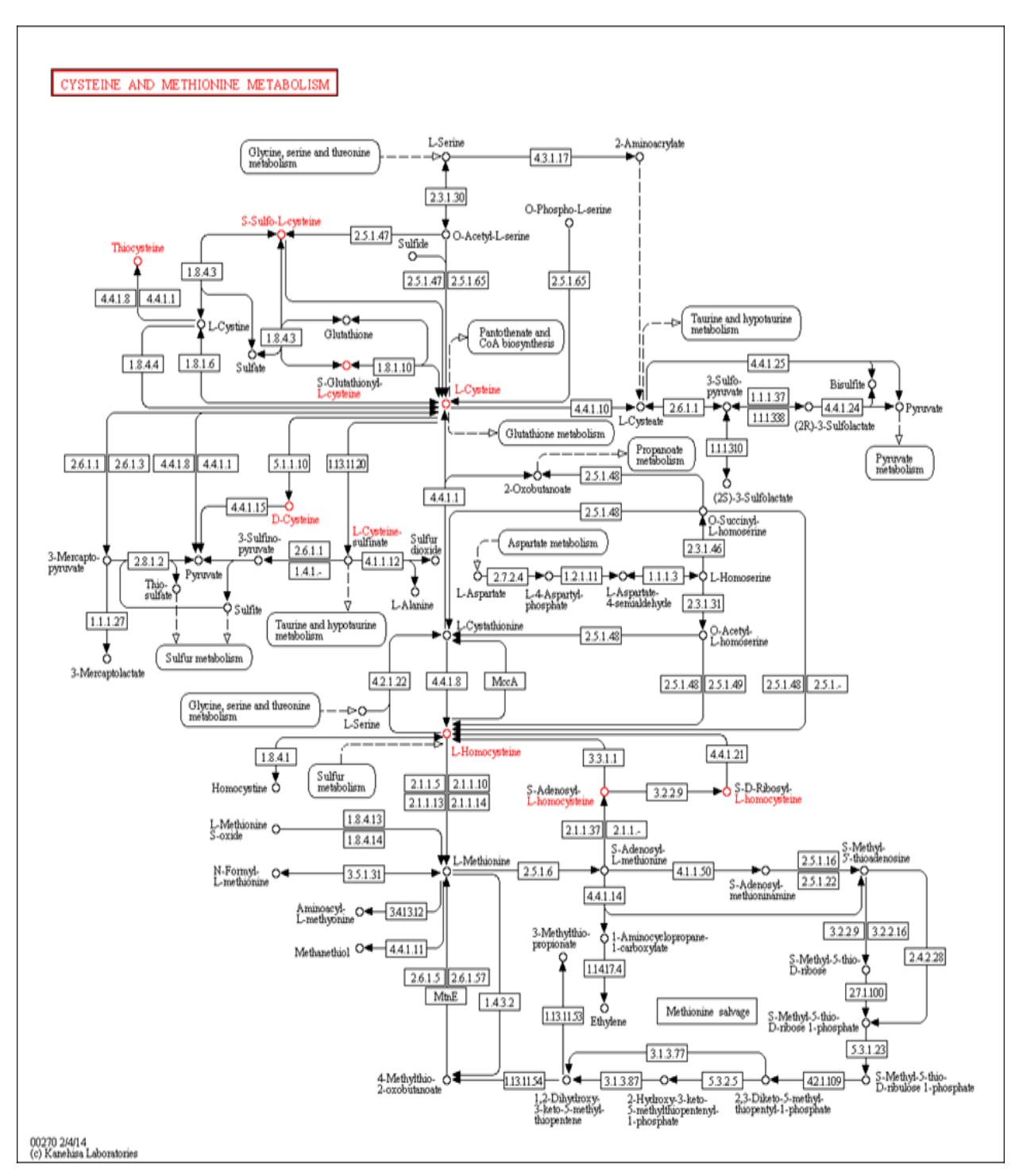
A comparison of proteomic expressions in wild-type and rpoN2 mutant strains of B. pseudomallei was set the cutoff to be a three folds difference between the wild-type and rpoN2 mutant. The results for proteins located between pH 4.5 to 7 and molecular weight of 20-75kDa are shown in Fig 18. The identity of proteins was determined using the reference map from the wild-type analysis [19]. Total of 21 spots were identified. The up-regulated proteins in the rpoN2 mutant strain included 14 proteins and the down-regulated proteins in rpoN2 mutant included 7 proteins as indicated in Fig 18A and 18B. The numbers of each spot are from the wild-type reference map which was used to study the RpoS-regulon of B. pseudomallei [24]. The 7 proteins are down-regulated in *rpoN2* mutant including proteins involved in energy metabolism, lipid metabolism, transcription and several hypothetical proteins of unknown function. In addition, 14 proteins appeared to be up-regulated in rpoN2 mutant, the majority of which are involved in carbohydrate metabolism, post-translation modification, cell envelope biogenesis and outer membrane formation. In order to identify the enzymes responsible for nitrogen utilization, amino acid synthesis and uptake, we found phosphotibosyl formimino-5aminomidazole carboxaminde ribonucleotide isomerase (HisA) (spot number 83) and Cysteine synthase (CysM) (spot number 80) that are involved in histidine and cysteine synthesis respectively (Fig 18A, 18B).



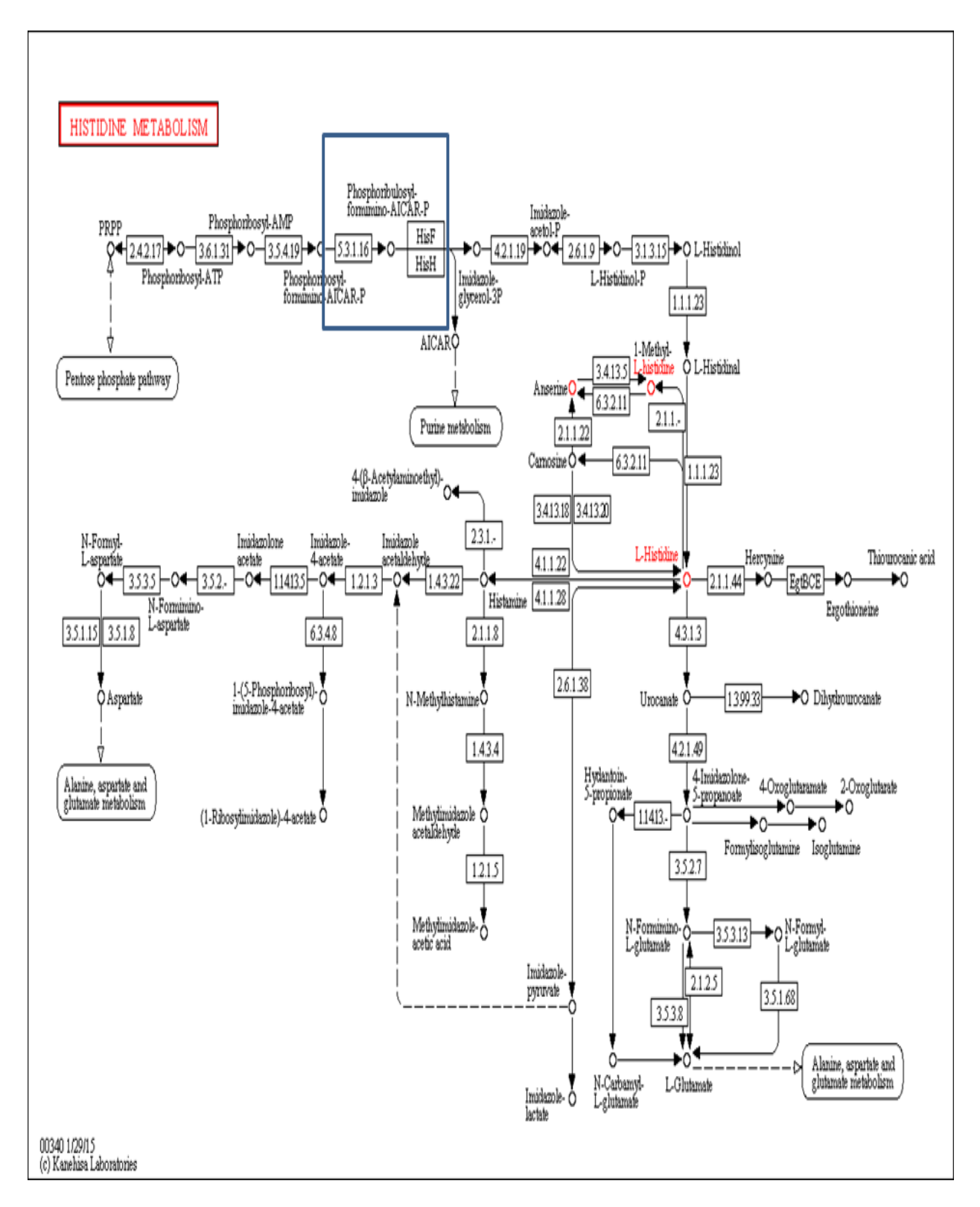
<u>Fig. 18</u> 2D-gel electrophoresis of *B. pseudomallei* wild-type (A) and *rpoN2* mutant (B) obtain from stationary phase of growth. PDQuest program was used to analysis the group's sample of wild-type and mutant that compared with reference map of *B. pseudomallei*. The circles are indicated spot numbers 80 (CysM) and 83 (HisA) that are down-regulated in a *rpoN2* mutant strain.

Identification of proteins involved in both regulations, sigma S and sigma N2

The biosynthesis pathways such as cysteine synthesis, histidine synthesis, purine metabolism and pentose phosphate pathway were performed by using KEGG database as shown in Fig. 19 and 20.

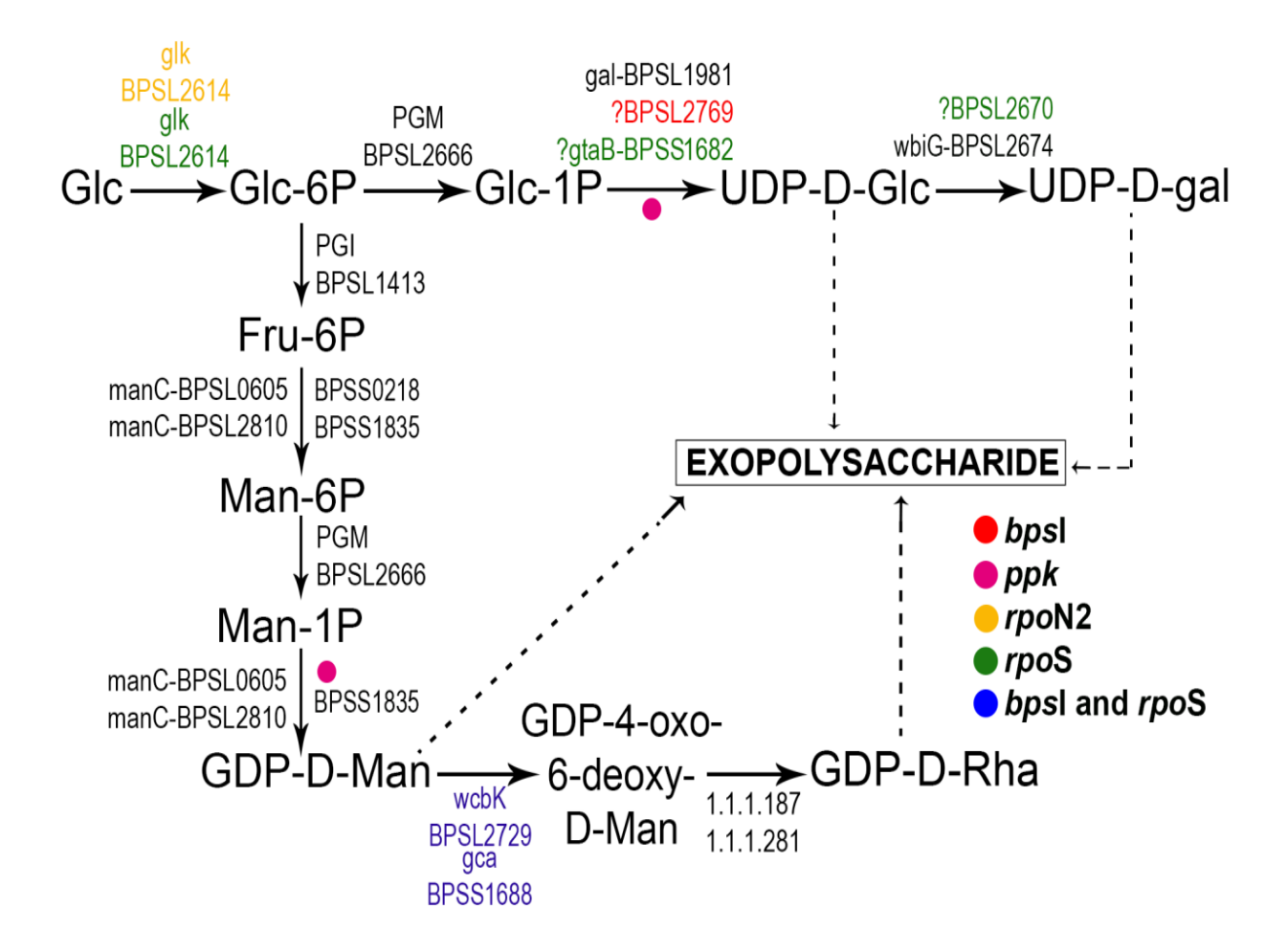


<u>Fig. 19</u> Cysteine and methionine metabolisms. The square is a pathway synthesis from glycine, serine and threonine metabolisms to L-cysteine. http://www.genome.jp/kegg



<u>Fig. 20</u> Histidine metabolism. The square is the phosphoribosyl formimino-5-aminoimidazole carboxamide ribonucleotide isomerase (HisA). http://www.genome.jp/kegg

The possible biosynthetic pathway of the nucleotide sugar precursors for biofilm exopolysaccharides production in *B. pseudomallei* according to the work of Richuo J.A. [25] is postulated with all of the annotated enzymes as shown in Figure 21. To verify whether our genes of interest may involve in regulations of these exopolysaccharide biosynthetic enzymes, 150 bps upstream regions of each enzyme were used to predict for *bps*I-, *rpo*N- and *rpo*S-dependent promoters by using the Hidden Markov Model (HMM) based method as previously described by Osiriphun, Y [24], with prediction training sets created from *bps*I- and *rpo*S-dependent genes in *B. pseudomallei* [24, 27], while the *rpo*N training set was created from σ54-dependent promoter sequences of *E. coli* [27].



<u>Fig. 21</u> Postulated biosynthetic pathways of the nucleotide sugar precursors for the biofilm exopolysaccharides. Enzymes predicted to be under *bps*I regulation (red abbreviations), *rpo*N2 regulation (yellow abbreviations), *rpo*S regulation (green abbreviations) and both *bps*I and *rpo*S regulation (blue abbreviation) are indicated. The steps postulated to be involved with *ppk* function are illustrated with pink spots.

Discussion

B. pseudomallei rpoN2 gene organization in chromosome II was inspected to find the RpoN2-dependent gene cluster. In bacteria having more than one copy of rpoN gene, the RpoN-dependent gene transcription is regulated normally by the rpoN organization gene cluster, means that specific rpoN gene is located nearby its regulon. The gene clusters adjacent to B. pseudomalleirpoN2 are uncharacterized, but one katE gene was found (Nychayapun thesis, 2005). Previously, it has been reported that B. pseudomallei catalase II (encode by katE) activity was absent in $\Delta rpoN2$ mutant during earlier to late stationary phase (12h to 72h) of growth by zymography of catalase activity, suggesting that RpoN2 is involve in the katE expression at translational level (Phuong thesis, 2010). In this study, the involvement of RpoN2 in katE expression at transcriptional level is confirmed by qRT-PCR result in relative quantitation of katE expression in $\Delta rpoN2$ and WT strain [17]. In each time point of stationary and late-stationary phase the expression of katE in $\Delta rpoN2$ and $\Delta rpoS$ strains is significant lower than in WT, suggesting the involvement of both sigma factors in katE expression regulation. Thus the evidences that B. pseudomallei RpoN2 plays a specific function like virulence regulation rather than core functions for normal growth in enrich media.

The involvement of *B. pseudomallei* RpoS and RpoN2 in bacterial invasion, intracellular survival and MNGC formation in mouse macrophage RAW 264.7 cell lines were performed. Prior work has documented the involvement of *B. pseudomallei* RpoS in modulating MNGC formation in RAW 264.7 mouse macrophage cells. Utainsincharoen and co-workers [8] were the first to demonstrate that *B. pseudomallei* null mutant rpoS ($\Delta rpoS$) strain failed to induce MNGC formation in the infected host cells at 8h post infection [8], however the study focused on a single post infection time point. In this study, the expansion was carried out with modified invasion assays to allow for investigation of MNGC formation in infected host RAW264.7 cells up to 20h post infection. My results suggest that *B. pseudomallei* RpoS and RpoN2 is indeed involved in the entry and intracellular survival of bacteria and therefore the subsequent MNGC formation of infected host cells. The number of $\Delta rpoS$ bacteria that successfully infect RAW264.7 cells is lower than $\Delta rpoN2$ and $\Delta rpoN2$ is lower than wild type, leading to a reduction in MNGC formation in macrophage cells infected with mutant strains at every post infection time point monitored. In addition, the results in Tab. 4.2 extend our finding, confirming that the %MNGC formation in RAW264.7 cells is dependent on the bacterial number inside the

host cells (at least 5 x 10^4 bacteria). Our analysis indicates a strong correlation between intracellular survival of bacteria and MNGC formation in infected host cells which was not obvious in the previous study that monitored a single post-infection time point.

Correlation between antibiotic resistance of the biofilm stage and exopolysaccharide composition in B. pseudomallei biofilm were studied. As the major component of extracellular polymeric substance (EPS) of the biofilm is exopolysacharides and EPS has been reported as a diffusion barrier of the biofilm, the decreased antibiotic resistance of B. pseudomallei mutants may result from an aberration in the exopolysaccharide structure. In this study, GC-MS analysis of the purified biofilm exopolysaccharides revealed that the mutated genes obviously affect the ratio of carbohydrate composition. The exopolysaccharide matrix of the B. pseudomallei wild type biofilm consisted of glucose, galactose, mannose, and rhamnose in the ratio 1.00:1.31:0.82:0.30, which galactose appears to be a major component (P = < 0.001). Previous studies have demonstrated that B. pseudomallei produce an acidic, water-soluble exopolysaccharide, with the structure, [-->3)-beta-D-Galp2Ac-(1-->4)-alpha-D-Galp-(1-->3)beta-D-Galp-(1- ->5)-beta-Kdo-(2-->]n, that can be recognized by the IgG 1 monoclonal antibody 3015. However, this exopolysaccharide was identified as capsular polysaccharide as its repeating unit contains Kdo, a major component of the capsular polysaccharide (141, 142). Our carbohydrate compositions analysis indicates some similarity to the previously described triplebranched heptasaccharide repeating unit of the capsule polysaccharide (CP2) in B. pseudomallei, composed of glucose, galactose, mannose, rhamnose, and glucuronic acid. However, the proportion of carbohydrate residues presented in the biofilm exopolysaccharide we identified (glucose, galactose, and mannose) were not similar to the major component of CP2 (glucose, galactose, and rhamnose) [28]. Therefore, it is evident that the expolysaccharide identified in this study may not be the capsular polysaccharide, nevertheless, this capsule CP2 may act as the core polysaccharide needed for structural maturation in the biofilm extracellular matrix. Consistent with our observations that the exopolysaccharide produced by Burkholderia cepacia are composed of galactose (major component), rhamnose, mannose, glucose, and glucuronic acid [29].

The same carbohydrate contents were found in all of the *B. pseudomallei* mutant biofilms with the different ratios and the major component. Dramatic reductions in rhamnose production were evidently showed in the biofilm exopolysaccharide matrix of all mutants, especially in the *bpsI* mutant in which rhamnose cannot be detected. As the defective drug

resistance in all of the biofilm mutants was previously illustrated, it may be conceivable that the disruption of the biofilm matrix results from the loss of rhamnose leading to the partial disability of the diffusion barrier of the biofilm. Remarkably, the carbohydrate contents of the bpsI mutant contains negligible reduction when compared to the wild type, whereas the mannose production is dramatically increased, suggesting that the lack of this mutated gene slightly causes the perturbation of the matrix structure resulting in an moderate impact on the dysfunction of the biofilm antibiotic resistance, which may come from the slight reduction of glucose and galactose together with the absence of rhamnose. Moreover, the dramatic accumulation of mannose found in this mutant cannot help recover the ability of antibiotic resistance, suggesting that glucose, galactose and rhamnose should be the major components of exopolysaccharide in EPS of B. pseudomallei biofilm instead of mannose. While the measurable influence of the bpsI mutation on the biofilm exopolysaccharide compositions led in the intermediate disability of the drug resistance, the ppk, rpoN2 and rpoS genes caused significant effects on all of the carbohydrate compositions, corresponding to particular extenuations in their antibiotic resistant abilities. From the data gained in this study, it can be implied that the exopolysaccharide composition of the biofilm matrix is a major structural content important for restricting antibiotic diffusion.

Apparently, the exopolysaccharide matrix from the bpsI, rpoN2 and rpoS mutants revealed significant increases in mannose and loss of rhamnose production, indicating that there could be a correlation between the mannose and rhamnose biosynthetic pathways. From the literature reviews, Richuo, J.A. et al [25] has demonstrated the biosynthesis pathways of biofilm exopolysaccharide in Burkholderia cepacia IST408. This bacteria has previously been reported its exopolysaccharide was consisted of glucose, galactose, mannose, rhamnose and glucoronic acid, which similar to our finding in B. pseudomallei, and required the nucleotide activated sugar as precursors for the synthesis [25]. Interestingly, from the synthesis of nucleotide sugar precursors for the exopolysaccharide pathway of B. cepacia IST408, it was reported that UDPgalactose is synthesised from UDP-glucose and that GDP-mannose is a precursor for GDPrhamnose synthesis. Comparative analysis of possible exopolysaccharide biosynthesis enzymes annotated in each step of B. cepacia in B. pseudomallei was performed by database searching, according to the annotated information of the enzymes in metabolic pathways of B. pseudomallei, to determine whether the enzymes involved in activated sugar precursor formation were presented. As expected, all of the enzymes needed for the synthesis of activated sugar precursors for the exopolysaccharide biosynthesis were identified in *B. pseudomallei*.

The possible biosynthetic pathway of the nucleotide sugar precursors for biofilm

exopolysaccharides production in B. pseudomallei according to the work of Richuo J.A. [25] is postulated with all of the annotated enzymes. To verify whether our genes of interest may involve in regulations of these exopolysaccharide biosynthetic enzymes, 150 bps upstream regions of each enzyme Hidden Markov Model (HMM) based method as previously described by Osiriphun, Y [24], with prediction training sets created from bpsI- and rpoS-dependent genes in B. pseudomallei [24, 27], while the rpoN training set was created from σ54-dependent promoter sequences of E. coli. BPSL2769 and wcbK-BPSL2729 or gca-BPSS1688, which is GDP (GCP) -mannose-4,6-dehydratase, were predicted to be under bpsI regulation because all of them were predictably found to have a lux box-like promoter of the bpsI gene. BPSL2769 or UTP glucose-1-phosphate uridylyltransferase (EC 2.7.7.9) is responsible for converting glucose-1-phosphate into UDP-D-glucose. While the other two enzymes, wcbK-BPSL2729 and gca-BPSS1688 (GDP-mannose-4,6-dehydratase (EC 4.2.1.47)), are responsible for converting GDPmannose into GDP-4-oxo-6-deoxy-D-mannose, which is further converted into GDP-rhamnose by GDP-4-dehydro-6-deoxy-D-mannose reductase (EC 1.1.1.281). Corresponding to our observation, the carbohydrate contents found in the bpsI mutant demonstrated that glucose and galactose contents were slightly reduced and mannose was accumulated. As the two predicted enzymes were found in front of glucose and galactose synthesis, the lack of bpsI may result in the reduction of these two sugars. Moreover, wcbK- BPSL2729 and gca-BPSS1688 are responsible for converting UDP-mannose into UDP-rhamnose, thus the mannose accumulation may result from dysfunction of this gene. This finding suggests that these two enzymes might be under bpsI regulation.

There are only three enzymes among all of the postulated enzymes having a chance to be under *bps*I control. However, many of these enzymes, including glucokinase (glk-BPSL2614), UDP-glucose-1-phosphate uridylyltransferase (gtaB-BPSS1682), UDP-glucose 4-epimerase (BPSL2670) and GDP-mannose-4,6-dehydratase (BPSL2729) (Appendix C), were predictably identified the *rpo*S-dependent promoter in front of their starting site, which all of them are involved in either the conversion of UDP-glucose into UPD-galactose or the conversion of GDP-mannose into GDP-rhamnose, especially glucokinase (glk), which functions in the first step of the pathway (Figure 6.1). Both BPSL2769 and gtaB-BPSL1682 predicting to be under *rpo*S control involve in the conversion of glucose-1-phosphate into UDP-glucose. Remarkably, wcbK-BPSL2729 and gca-BPSS1688 were previously predicted to be under *bps*I regulation, they were predictably found to have *rpo*S promoters in front of lux box-like promoters as well. As previously mentioned, *rpo*S has the positive regulation on *bpsI* expression

in *B. pseudomallei*, thus this supports the assumption that *rpoS* has the superior impact on exopolysaccharide synthesis than *bpsI*.

The carbohydrate components of the *rpo*N2 and *rpo*S mutant biofilm are similar in quantities and types. From the promoter prediction of *rpo*N-dependent promoter retrieved from *E. coli*, there is only one enzyme predicted to have the *rpo*N-dependent promoter, which is glucokinase (glk-BPSL2614). This possible promoter was found in front of the *rpo*S-dependent promoter previously identified. As the carbohydrate contents of *rpo*N2 and *rpo*S mutant biofilms show reciprocal ratios, but the *rpo*N2 mutant contains little higher quantity than the *rpo*S mutant. This result corresponds well with the promoter prediction of *rpo*N2- and *rpo*S-dependent promoters found that *rpo*S predictably regulates many enzymes than *rpo*N2 resulting in the higher effects on exopolysaccharide production of the biofilm.

This observation of bpsI-, rpoN2- and rpoS-dependent promoters supports our results that bpsI, rpoN2 and rpoS may control the transcription of some biosynthetic enzymes essential to the production of activated sugar precursors for exopolysaccharide biosynthesis, especially rpoS, which should be involved in every carbohydrate synthesis, resulting in the significant decreases in all of the carbohydrate contents. Although rpoN2 has shown a strong impact on the exopolysaccharide contents as well, it would rather have less effect on this mechanism than rpoS which may due to the only one possible regulated enzyme. Meanwhile, bpsI has specific regulation only on glucose, galactose and rhamnose, which has resulted in the moderate production of biofilm exopolysaccharide. Interestingly, a correlation between quorum sensing and rhamnose synthesis, which is an important polysaccharide in biofilm formation and found to be disappeared in the bpsI mutant, has been reported and have shown that P. aeruginosa uses acyl-homoserine lactone signals during cell-cell communication to coordinate the expression of genes responsible for the production of polysaccharides in the biofilm as well as other virulent factors. In agreement with our observation, this finding confirms that bpsI is not only involved in quorum sensing but also in the control of polysaccharide synthesis, especially in rhamnose production. In addition, Gamage has described the function of the bpsI gene in cellcell communication for micro-colony formation and determination of the ultimate threedimensional architecture of the mature biofilm. There are some evidences showing that rpoN2 and rpoS genes have positive regulations on exopolysaccharide biosynthesis of V. anguillarum and Agrobacterium, nevertheless, the correlation between these two genes and the synthesis of biofilm exopolysaccharide was not been elucidated in B. pseudomallei. From our knowledge, this is the first report in which rpoN2 and rpoS genes have potentialities in particular functions on exopolysaccharide biosynthesis through the regulation of enzymes important for the production of activated sugar precursors.

The carbohydrate content ratio found in the ppk mutant biofilm evidently showed significant reduction. Since Tunpiboonsak, S., has postulated the ppk functions in supplementing energy for all of the biofilm formation processes, including biofilm formation, maturation and extracellular matrix accumulation [30], this explicit alteration of the exopolysaccharide content ratio supports the assumption of ppk function in biofilm stages that ppk gene should have particular roles in activation of the sugar precursors at the specific steps (pink spots). Polyphosphate kinase is an enzyme responsible for synthesis of inorganic polyphosphate from ATP, which is further used as precursors for synthesis of the activated sugars; thus it is possible that the mutation of this gene may result in the un-activated sugars. From this reason, the exopolysaccharide framework could not be formed and would cause a further dramatic impact on antibiotic resistance of the mutant. Interestingly, the *P. aeruginosa ppk* mutant has also been shown to be deficient in rhamnolipid production and formation and differentiation of biofilm as well as displaying aberrant quorum sensing. This evidence supports our assumption that ppk gene should involve in the formation of activated sugar precursors of exopolysaccharide production in the biofilm stage of B. pseudomallei. In summary, the exopolysaccharides of the biofilm matrix in B. pseudomallei are composed of following three major carbohydrate types: glucose, galactose and mannose, which could be controlled by the investigated genes, including bpsI, ppk, rpoN2 and rpoS genes.

For the better understand the role of RpoN2 in amino acid utilization, we used 2-dimension polyacrylamide gels to identify proteins with altered levels in the *rpoN2* mutant since RpoN2 may regulate these proteins. Cells have many ways to obtain amino acids such as transport form environment, *de novo* synthesis or synthesis from other amino acids and we speculated that RpoN2 might be involved in the regulation of some proteins involved in these processes. Analysis of soluble extracts using 2D-gels and PDQest software package to identify the proteins with altered abundance, we found that cysteine synthase (CysM) and phosphoribosyl formimino-5-aminoimidazole carboxamide ribonucleotide isomerase (HisA) were both down-regulated in the *rpoN2* mutant. While the levels of CysM and HisA were decreased in the *rpoN2* mutant, it was able to synthesize/uptake sufficient cysteine and histidine to grow on MM9 medium. It is possible that both cysteine and histidine could be produced using intermediates from other pathways or other amino acids as precursors. Investigating the

connections between cysteine synthesis and other biosynthetic pathway using http://www.genome.jp/kegg revealed that in addition to the de novo pathway for cysteine synthesis it is possible to produce cysteine from glycine, serine and threonine. The connection between cysteine synthesis and the production of other amino acids may explain why the rpoN2 mutant, that should not be able to produce cysteine from the de novo pathway utilizing CysM, can grow on MM9 medium. As was seen with cysteine synthesis, histidine can also be synthesized from several precursors. HisA is a protein in amino acid metabolism specific to histidine biosynthesis and function in the synthesis L-histidinol-P and purine metabolism from the pentose phosphate pathway as shown in Fig 3 (http://www.genome.jp/kegg). This protein was decreased in rpoN2 mutant indicating that it is regulated by RpoN2, however alternative pathways are present that can compensate for loss of HisA dependent histidine production. Our study is the first to identify and demonstrate a role of RpoN2 in B. pseudomallei and that would be further identified other RpoN2 regulons.

References

- [1] Cheng, A.C. and B.J. Currie, *Melioidosis: epidemiology, pathophysiology, and management*. Clin Microbiol Rev, 2005. **18**(2): p. 383-416.
- [2] Lazar Adler, N.R., et al., *The molecular and cellular basis of pathogenesis in melioidosis:* how does Burkholderia pseudomallei cause disease? FEMS Microbiol Rev, 2009. **33**(6): p. 1079-99.
- [3] Jones AL, Beveridge TJ, Woods DE. Intracellular survival of Burkholderia pseudomallei. *Infect Immun* 1996; **64**: 782-90.
- [4] Kespichayawattana W, Rattanachetkul S, Wanun T *et al.* Burkholderia pseudomallei induces cell fusion and actin-associated membrane protrusion: a possible mechanism for cell-to-cell spreading. *Infect Immun* 2000; **68**: 5377-84.
- [5] Pruksachartvuthi S, Aswapokee N, Thankerngpol K. Survival of Pseudomonas pseudomallei in human phagocytes. *Journal of medical microbiology* 1990; 31: 109-14.
- [6] Wong KT, Puthucheary SD, Vadivelu J. The histopathology of human melioidosis. *Histopathology* 1995; **26**: 51-5.
- [7] Suparak S, Kespichayawattana W, Haque A *et al.* Multinucleated giant cell formation and apoptosis in infected host cells is mediated by Burkholderia pseudomallei type III secretion protein BipB. *J Bacteriol* 2005; **187**: 6556-60.
- [8] Utaisincharoen P, Arjcharoen S, Limposuwan K *et al.* Burkholderia pseudomallei RpoS regulates multinucleated giant cell formation and inducible nitric oxide synthase expression in mouse macrophage cell line (RAW 264.7). *Microb Pathog* 2006; **40**: 184-9.
- [9] Brent, A.J., et al., *Misdiagnosing melioidosis*. Emerg Infect Dis, 2007. **13**(2): p. 349-51.
- [10] Dance, D.A., Melioidosis: the tip of the iceberg? Clin Microbiol Rev, 1991. 4(1): p. 52-60.
- [11] Ulrich, R.L., et al., Role of quorum sensing in the pathogenicity of Burkholderia pseudomallei. J Med Microbiol, 2004. **53**(Pt 11): p. 1053-64.
- [12] Patel, N., et al., Development of vaccines against Burkholderia pseudomallei. Front Microbiol, 2011. 2: p. 198.
- [13] Sawasdidoln, C., et al., Growing Burkholderia pseudomallei in biofilm stimulating conditions significantly induces antimicrobial resistance. PLoS One, 2010. **5**(2): p. e9196.

- [14] Pibalpakdee, P., et al., *Diffusion and activity of antibiotics against Burkholderia* pseudomallei biofilms. Int J Antimicrob Agents, 2012. **39**(4): p. 356-9.
- [15] Taweechaisupapong, S., et al., *Virulence of Burkholderia pseudomallei does not correlate with biofilm formation*. Microb Pathog, 2005. **39**(3): p. 77-85.
- [16] Subsin B, Thomas MS, Katzenmeier G *et al*. Role of the stationary growth phase sigma factor RpoS of Burkholderia pseudomallei in response to physiological stress conditions. *J Bacteriol* 2003; **185**: 7008-14.
- [17] Diep D, Phuong NTT, Hlaing MM, Srimanote P, Tungpradabkul S. Role of *Burkholderia* pseudomallei sigma N2 in amino acids utilization and in regulation of catalase E expression at the transcriptional level. *Int. J. Bacteriol* 2015; ID 623967, 6 pages.
- [18] Merkle, R.K. and I. Poppe, *Carbohydrate composition analysis of glycoconjugates by gasliquid chromatography/mass spectrometry. Methods Enzymol*, 1994. **230**: p. 1-15.
- [19] Wongtrakoongate P., Roytrakul S., Yasothornsrikul S., Tungpradabkul S. A proteome reference map of the causative agent of melioidosis *Burkholderia pseudomallei*. *J Biomed Biotechnol* 2011; ID 530926, 5 pages.
- [20] Donnenberg M. S., Kaper J. B. Construction of an eae deletion mutant of enteropathogenic *Escherichia coli* by using a positive-selection suicide vector. *Infect Immun* 1991; **59**: 4310-17.
- [21] Reitzer L, Scheider B. Metabolic context and possible physiological themes of sigma 54-dependent genes in *Escherichia coli*. *Microbiol Mol Biol Rev* 2001; **65**, 422–444.
- [22] Alexeyev M. The pKNOCK series of broad-host-range mobilizable suicide vectors for gene knockout and targeted DNA insertion into the chromosome of gram-negative bacteria. *BioTechniques*.1999; **26**, 824–828.
- [23] Kovach M. E., Phillips R. W., Elzer P. H., 2ndRoop R. M., Peterson K. M. pBBR1MCS: A broad-host-range cloning vector. *BioTechniques* 1994; **16**: 800-2.
- [24] Osiriphun Y, Wongtrakoongate P, Sanongkiet S *et al.* Identification and characterization of RpoS regulon and RpoS-dependent promoters in Burkholderia pseudomallei. *Journal of proteome research* 2009; **8**: 3118-31.
- [25] Richau, J.A., J.H. Leitao, and I. Sa-Correia, Enzymes leading to the nucleotide sugar precursors for exopolysaccharide synthesis in Burkholderia cepacia. Biochem Biophys Res Commun, 2000; **276**(1): p. 71-6.
- [26] Kiratisin, P. and S. Sanmee, *Roles and interactions of Burkholderia pseudomallei BpsIR quorum-sensing system determinants*. J Bacteriol, 2008. **190**(21): p. 7291-7.

- [27] Zhao, K., M. Liu, and R.R. Burgess, *Promoter and regulon analysis of nitrogen assimilation factor, sigma54, reveal alternative strategy for E. coli MG1655 flagellar biosynthesis.* Nucleic Acids Res, 2010. **38**(4): p. 1273-83.
- [28] Kawahara, K., S. Dejsirilert, and T. Ezaki, *Characterization of three capsular polysacharides produced by Burkholderia pseudomallei*. FEMS Microbiol Lett, 1998. **169**(2): p. 283-7.
- [29] Cescutti, P., et al., *Structural study of the exopolysaccharide produced by a clinical isolate of Burkholderia cepacia*. Biochem Biophys Res Commun, 2000; **273**(3): p. 1088-94.
- [30] Tunpiboonsak, S., et al., Role of a Burkholderia pseudomallei polyphosphate kinase in an oxidative stress response, motilities, and biofilm formation. J Microbiol, 2010. **48**(1): p. 63-70.



Source-Identifying Biomarker Ions between Environmental and Clinical *Burkholderia pseudomallei* Using Whole-Cell Matrix-Assisted Laser Desorption/ Ionization Time-of-Flight Mass Spectrometry (MALDI-TOF MS)



Suthamat Niyompanich^{1,9}, Janthima Jaresitthikunchai^{2,9}, Kitima Srisanga¹, Sittiruk Roytrakul², Sumalee Tungpradabkul^{1,8}

1 Department of Biochemistry, Faculty of Science, Mahidol University, Bangkok, Thailand, 2 National Center for Genetic Engineering and Biotechnology, Pathumthani, Thailand

Abstract

Burkholderia pseudomallei is the causative agent of melioidosis, which is an endemic disease in Northeast Thailand and Northern Australia. Environmental reservoirs, including wet soils and muddy water, serve as the major sources for contributing bacterial infection to both humans and animals. The whole-cell matrix-assisted laser desorption/ionization time-of-flight mass spectrometry (whole-cell MALDI-TOF MS) has recently been applied as a rapid, accurate, and high-throughput tool for clinical diagnosis and microbiological research. In this present study, we employed a whole-cell MALDI-TOF MS approach for assessing its potency in clustering a total of 11 different *B. pseudomallei* isolates (consisting of 5 environmental and 6 clinical isolates) with respect to their origins and to further investigate the source-identifying biomarker ions belonging to each bacterial group. The cluster analysis demonstrated that six out of eleven isolates were grouped correctly to their sources. Our results revealed a total of ten source-identifying biomarker ions, which exhibited statistically significant differences in peak intensity between average environmental and clinical mass spectra using ClinProTools software. Six out of ten mass ions were assigned as environmental-identifying biomarker ions (EIBIs), including, m/z 4,056, 4,214, 5,814, 7,545, 7,895, and 8,112, whereas the remaining four mass ions were defined as clinical-identifying biomarker ions (CIBIs) consisting of m/z 3,658, 6,322, 7,035, and 7,984. Hence, our findings represented, for the first time, the source-specific biomarkers of environmental and clinical *B. pseudomallei*.

Citation: Niyompanich S, Jaresitthikunchai J, Srisanga K, Roytrakul S, Tungpradabkul S (2014) Source-Identifying Biomarker Ions between Environmental and Clinical *Burkholderia pseudomallei* Using Whole-Cell Matrix-Assisted Laser Desorption/Ionization Time-of-Flight Mass Spectrometry (MALDI-TOF MS). PLoS ONE 9(6): e99160. doi:10.1371/journal.pone.0099160

Editor: Fatah Kashanchi, George Mason University, United States of America

Received January 11, 2014; Accepted May 12, 2014; Published June 10, 2014

Copyright: © 2014 Niyompanich et al. This is an open-access article distributed under the terms of the Creative Commons Attribution License, which permits unrestricted use, distribution, and reproduction in any medium, provided the original author and source are credited.

Funding: This work was supported by the Thailand Research Fund and Faculty of Science Mahidol University. S. Niyompanich received the Ph.D. scholarship from RGJ (the Royal Golden Jubilee) No. PHD/0341/2551. The funders had no role in study design, data collection and analysis, decision to publish, or preparation of the manuscript.

1

Competing Interests: The authors have declared that no competing interests exist.

- * E-mail: sumalee.tan@mahidol.ac.th
- 9 These authors contributed equally to this work.

Introduction

Melioidosis is a serious, often fatal, human disease which is caused by a motile, Gram-negative bacillus namely, *Burkholderia pseudomallei*. This disease is widely prevalent in tropical zones between latitudes 20°N and 20°S, which are commonly reported in Southeast Asia and Northern Australia [1]. These endemic areas have been illustrated with high mortality rates of about 40% [2]. *B. pseudomallei* is an environmental saprophyte which is normally found in wet soils and muddy waters contributing bacterial infection into humans and animals [3]. People who are directly in contact with soil and water contaminated with *B. pseudomallei* are affected by this disease [1,4]. Cases of disease transmission among humans are rarely reported [3]. Clinical signs, representing in patients with melioidosis, vary from asymptomatic,

localized acute or chronic pneumonia, and septicemia forms, which require antibiotic treatment for long periods [1,5]. Currently, there are no vaccines available against this disease [2].

The epidemiological data of melioidosis in Thailand has revealed significantly higher infection rates in patients from northeastern regions than those in other parts of Thailand, in agreement with several reports from other countries including in Laos and Taiwan, regarding the relationship between occurrence of the disease and environmental exposure to *B. pseudomallei* [6–9]. Hence, melioidosis is considered as an environmental disease [10], owing to soil and water being observed to be important reservoirs for this organism. Isolates of *B. pseudomallei* from environmental and clinical sources are markedly diverse but some isolates from either group can be categorized into the identical molecular type [11]. Evidence from the studies by Haase et al have demonstrated

that soil isolates mostly show less cytolethality compared to isolates from patients [12]. In contrast, Liew et al have investigated the enzyme profiling of environmental and clinical *B. pseudomallei* using the APIZYM system. The results have shown that bacteria from two sources secrete similar enzymes and the environmental isolates display higher protease activity than clinical isolates [13]. However, the association of virulence levels, according to their respective sources, is controversial and has yet been elucidated. Therefore, the source-identification of *B. pseudomallei* is essential not only for an implementing epidemiological strategy but also for surveillance, prevention and control of melioidosis.

Many studies have attempted to differentiate *B. pseudomallei* isolates from distinct origins by using various molecular typing tools including, ribotyping, pulsed-field gel electrophoresis (PFGE), restriction fragment length polymorphism (RFLP), randomly amplified polymorphic DNA (RAPD), multilocus enzyme electrophoresis (MEE), and multilocus sequence typing (MLST) [14–20]. In addition, a recent study by Bartpho et al has investigated the genomic islands (GIs) for use as the potential marker for distinguishing environmental and clinical isolates of *B. pseudomallei* on the basis of the microarray-based comparative genome hybridization (CGH) method [21]. But the limitations of these molecular approaches are that they are time-consuming, labourand cost-intensive and require several steps to accomplish in the identification and typing of microorganisms. Thus, new analytical tools are needed to provide a better analysis [22].

In recent years, matrix-assisted laser desorption/ionization time-of-flight mass spectrometry (MALDI-TOF MS) is a wellestablished instrument used in routine clinical diagnosis and in various fields of microbiological research, including microbial systematics, environmental microbiology, and epidemiology [23,24]. This is because it provides an ideal identification system and has more advantages over conventional methods, such as offering rapid, accurate, economical, and high throughput analysis [25,26]. In principle, MALDI-TOF MS generates a unique mass spectrum as a fingerprint from whole-cell bacteria or crude extract. Obtained spectra can further be compared to the reference spectra in a database, resulting in the scores for identification at both the genus and species levels [22,26,27]. This technique also allows the identification at subspecies or strain level [28,29] and can produce biomarkers calculated from particular algorithms which are specific for those species of interest [25]. MALDI-TOF MS has been used to identify and discriminate a wide range of microorganisms, including Escherichia [30], Staphylococcus [31], Salmonella [32], Enterococcus [33], Candida [34], Lactococcus [35], Aeromonas [36], Vibrio [37], and Erwinia [38]. Moreover, it is being introduced to utilize in biodefense applications by identifying the presence of biomarker mass ions in biological weapons (BW), comprising microorganisms and biotoxins [39]. The Centers for Disease Control (CDC) has designated B. pseudomallei as a category B agent due to its potential as a bioterrorism weapon [40]. The rapid and robust identification of B. pseudomallei based on MALDI-TOF is therefore required for early-warning and medical prevention of melioidosis. The recent study has applied whole-cell MALDI-TOF MS for identification and differentiation of B. mallei and B. pseudomallei [41]. However, there are no reports of anyone using whole-cell MALDI-TOF MS to discriminate between environmental and clinical isolates of B. pseudomallei. In this study, we have employed the whole-cell MALDI-TOF MS approach to examine its ability to group B. pseudomallei isolates according to their respective sources and investigate the source-specific biomarkers for distinguishing these isolates of different origins.

Results

Identification of Burkholderia pseudomallei isolates

To determine whether all environmental and clinical isolates were B. pseudomallei based on whole-cell MALDI-TOF MS method, we performed pattern matching and considered obtaining scores for identification using BioTyper 2.0 software. Generally, identification scores based on pattern matching imply reliable identification at the genus or species levels for any tested microorganism. Scores are obtained by comparison of tested mass fingerprints with the main spectral projections (MSPs) resulting in logarithmic scores between 0 (unrelated) to 3 (identical) [41]. Criteria for microorganism identification that are suggested by manufacturer are: (1) unreliable identification has a score < 1.7, (2) genus identification has a score between 1.7–1.9, and (3) species identification has a score ≥ 1.9 [42]. Since MSPs of B. pseudomallei were not available in our MALDI BioTyper library, we generated B. pseudomallei K96243 mass spectra as an in-house reference spectrum, by using BioTyper 2.0 to confirm identification of other tested isolates. All of the mass spectra queries collected from FlexAnalysis were matched against K96243 reference spectrum giving a score for each isolate as summarized in Table 1. The identification scores obtained were between 1.90-2.48, thus all samples in this study were confirmed, at species level, as B. pseudomallei. The average spectrum of each B. pseudomallei strain was generated by a combination of raw twenty mass spectra using the ClinProTools software (Figure 1). It could be observed that the mass patterns were similar among both environmental and clinical isolates. The recent study from Karger et al has shown the unique biomarkers for identifying B. pseudomallei and B. mallei using the intact cell MALDI-TOF method [41]. As the results from Karger et al show, the specific mass ions at 4,410, 5,794, 6,551, 7,553, and 9,713 are used as taxon-specific biomarkers in all B. mallei and B. pseudomallei samples. Mass peak at m/z 4,410 is commonly found in all nine Burkholderia species (B. mallei, B. pseudomallei, B. thailandensis, B. ambifaria, B. cenocepacia, B. dolosa, B. glathe, B. multivorans, and B. stabilis). Another important biomarker is m/z 9,713 which is used for differentiating the Pseudomonas group, including B. mallei, B. pseudomallei, and B. thailandensis, from the other Burkholderia species. The effective mass that can discriminate between B. mallei/B. pseudomallei group and B. thailandensis is m/z 6,551. Due to the close relationship between the species of B. mallei and B. pseudomallei, they have suggested that these two strains differ significantly, based on the mass peak intensity at m/z 5,794 and 7,553 by using ClinProTools software. As expected, the MALDI-TOF average mass spectra of all tested strains, in our study, contained the prominent biomarkers (m/z 4,410, 5,794, 6,551, 7,553, and 9,713) as shown in vertical dashed lines in Figure 1. It indicates that these mass ions are conserved as species-specific biomarkers among B. pseudomallei strains based on the whole-cell MALDI-TOF method.

Cluster analysis of B. pseudomallei isolates

In this study, a total of eleven isolates of *B. pseudomallei* came from two major sources, environmental and clinical sources. To determine whether the ability of whole-cell MALDI-TOF MS method could group isolates according to their respective sources, raw mass spectra of all *B. pseudomallei* isolates, obtained from FlexAnalysis, were then analyzed using ClinProTools software to generate a principal component analysis (PCA) and a dendrogram. PCA demonstrated that environmental and clinical isolates intermixed together and did not form distinct groups according to their own origins (Figure 2A). Dendrogram calculated from the PCA scores, on the basis of a scored-based algorithm, illustrated

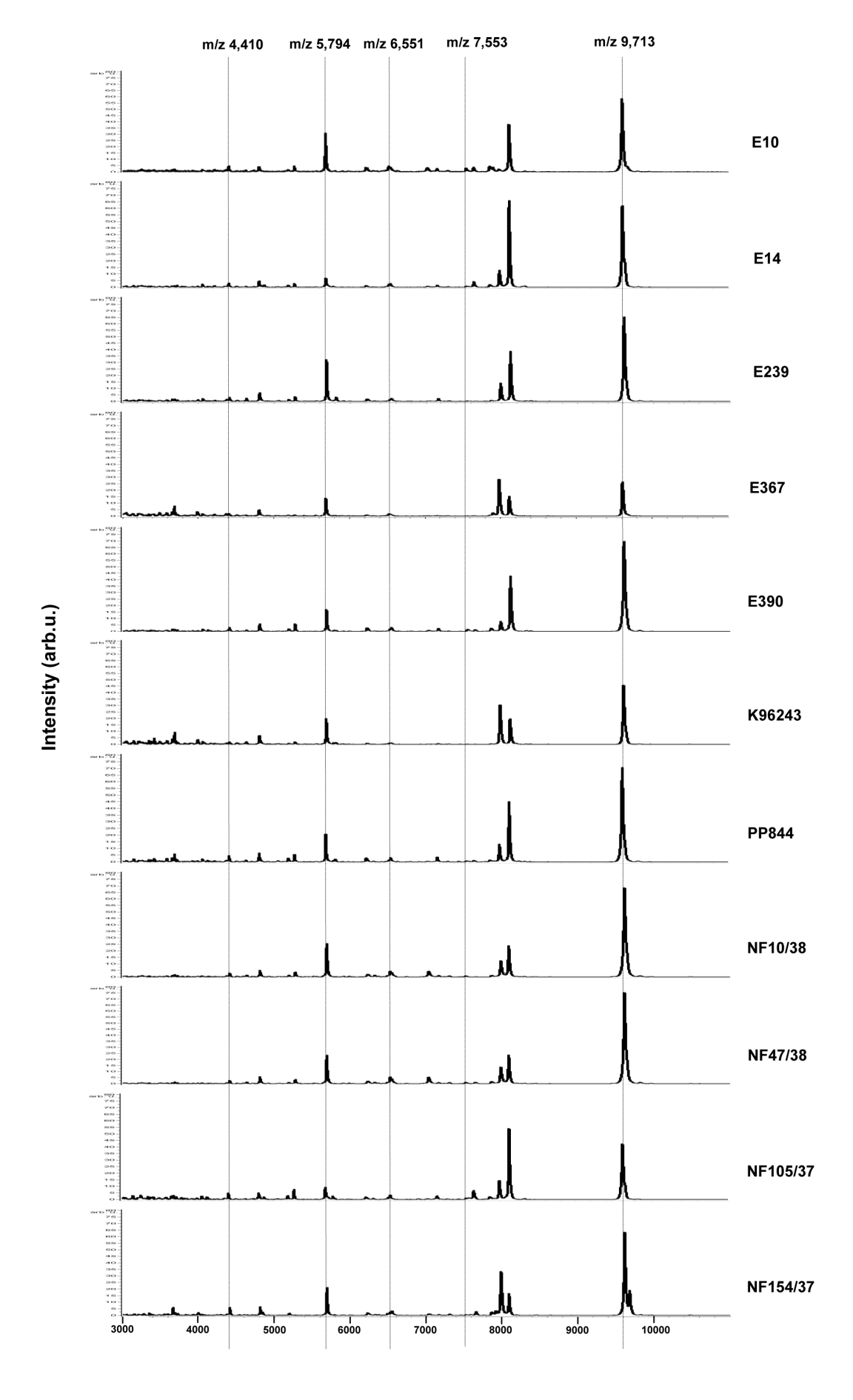


Figure 1. Average MALDI-TOF mass spectra of each *B. pseudomallei* **isolates.** Environmental (E10-E390) and clinical *B. pseudomallei* (K96243-NF154/37) samples displayed very similar peak patterns. All prominent biomarkers proposed by Karger et al for the identification of *B. pseudomallei* at m/z 4,410, 5,794, 6,551, 7,553, and 9,713 were detected in all mass spectra of tested strains in this study (vertical dashed lines). doi:10.1371/journal.pone.0099160.q001

that three of the six environmental isolates; E239, E390, and E14, were grouped on their own cluster, the same as the three clinical isolates; NF154/37, NF47/38, and NF10/38. Two of the clinical isolates; NF105/37 and PP844 were grouped with the environmental clade. The E10, from the environmental source, was grouped with the clinical cluster. In addition, K96243 and E367 isolates were dispersed and formed their own cluster (Figure 2B). Even though all of *B. pseudomallei* isolates were not clustered by their sources, most of them (6 out of 11 isolates) could be differentiated according to their respective source groups using the whole-cell MALDI-TOF MS method.

Biomarkers for discrimination of environmental and clinical *B. pseudomallei* isolates

An average mass spectrum of environmental set was constructed from a set of 5 environmental average spectra (E10-E390) (Figure 3A). Similarly, an average mass spectrum of clinical set was generated from a combination of 6 clinical average spectra (K96243-NF154/37) as displayed in Figure 3B. The two average mass spectra of these two groups demonstrated a high similarity in peak patterns but differed in peak intensities. To investigate the source-specific biomarkers for discrimination of B. pseudomallei corresponding to their origins (environmental and clinical sources), we analyzed these two source-representative mass spectra by using the Quick Classifier (QC) algorithm in the ClinProTools software which subsequently provided the candidate peak lists between the two sample groups based on statistical calculations, Wilcoxon/ Kruskal-Wallis statistics. The potential source-specific biomarker peaks were evaluated in the mass range of m/z 2,000-20,000. ClinProTools analysis totally revealed 23 biomarkers that demonstrated significant differences in peak intensity between environmental and clinical groups (data not shown). We stringently examined further on differential peak signals between the two sets and calculated as fold differences of the individual biomarker. Peak intensity values and fold differences were summarized in Table 2. Fold difference of each biomarker was individually calculated using peak intensity of environmental divided by that of clinical group. Biomarkers that exhibited > 1.5 fold and < 0.67 fold were

Table 1. Identification scores of all B. pseudomallei isolates.

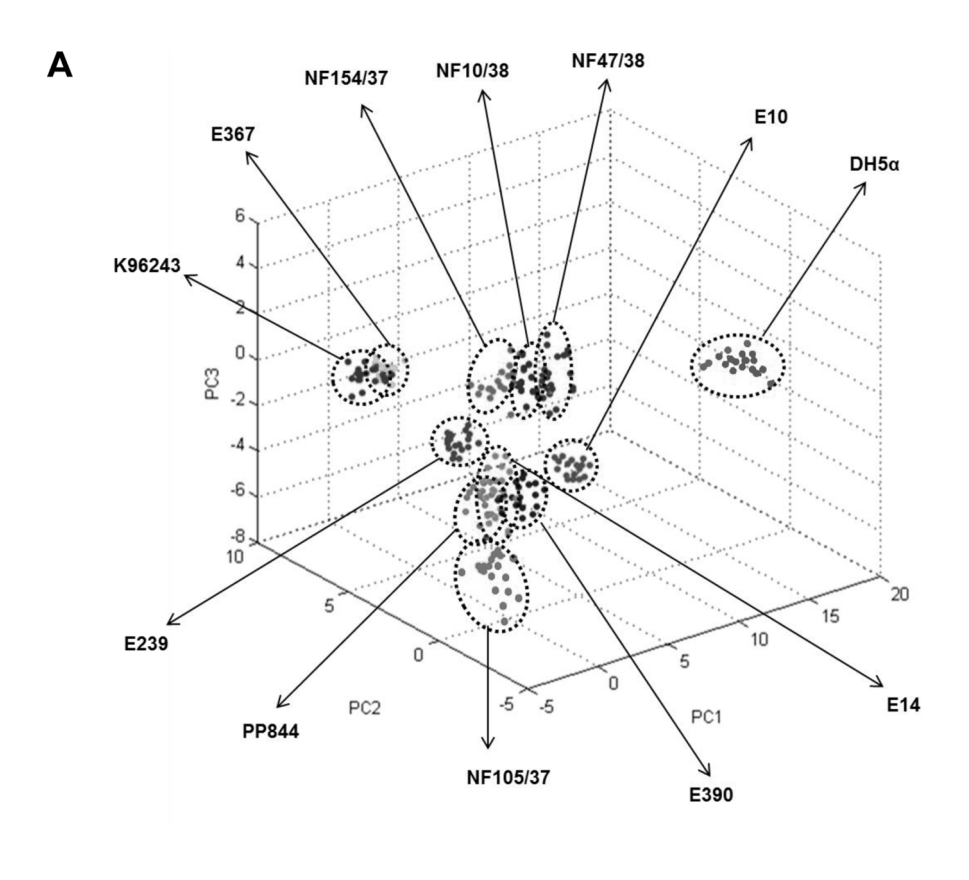
Idoutification come
Identification score
1.90
2.17
2.26
2.18
2.29
2.48
2.28
1.94
1.90
2.22
1.99

doi:10.1371/journal.pone.0099160.t001

chosen and classified as environmental-specific and clinical-specific mass ions, respectively. A total of 10 effective source-specific biomarkers was therefore selected. Six out of the ten biomarkers were defined as environmental-identifying biomarker ions (EIBIs), consisting of m/z 4,056, 4,214, 5,814, 7,545, 7,895, and 8,112 (doubly charge of 4,056), which were shown as E1-E6, respectively (see the vertical dashed lines in Figure 3). While the remaining 4 biomarkers were assigned as clinical-identifying biomarker ions (CIBIs), which showed significantly higher intensities than that of the environmental set, containing m/z 3,658, 6,322, 7,035, and 7,984, which were marked as C1-C4, respectively (see the vertical solid lines in Figure 3). Hence, these mass ions could be used as the potential source-specific biomarkers to discriminate *B. pseudomallei* in relation to their source groups.

Discussion

Whole-cell MALDI-TOF MS has been demonstrated as a useful tool for rapid identification and classification of a variety species of microorganisms. It could be observed that most of the resultant mass peaks, as shown in B. pseudomallei mass fingerprints (Figure 1), were in the range of m/z 2,000-11,000 Da, which are typically reported to be adequate for species discrimination and are similar to the results of Salmonella and Vibrio sp. [32,37]. Each average mass spectrum, belonging to each strain, exhibited very similar peak patterns but distinctive peak intensities (Figure 1). Due to our MALDI BioTyper database not containing the main spectral projections (MSPs) of B. pseudomallei, we had to construct an in-house B. pseudomallei strain K96243 as a reference spectrum for performing pattern matching and further identifying the tested samples at both genus and species levels. According to criteria for species identification, the score must be \geq 1.90. As per the results in Table 1, the scores of a total of eleven tested isolates, obtained from BioTyper analysis, varied from 1.90-2.48, indicating that all the isolates in this study were confirmed as B. pseudomallei. The range of identification scores extensively varied suggesting a variation at the subspecies level of B. pseudomallei, in agreement with Karger's study, as they reported a large score ranging between 2.25-2.89 [41]. The results revealed lower identification scores than which of Karger's, owing to in this study we constructed only K96243 as a reference spectrum and all mass spectra (from a total of 11 B. pseudomallei strains) were queried to perform pattern matching against the K96243 reference spectrum. It was notably observed that K96243 had the highest score value because of the existing of K96243 reference spectrum in our inhouse MSPs database. However, the obtained identification scores were still sufficient for confirmation procedure of all B.pseudomallei isolates based on MALDI-TOF. Not only availability of MSPs databases but also the influences of culture media and incubation times might have caused the lower identification scores. Our study used different medium and incubation time for bacterial cultivation, such as using Ashdown's selective agar for 7 days according to Chantratita et al [43] because it is a selective medium that is commonly used for isolating and culturing B. pseudomallei, which differed from Karger's study, which used a nutrient blood agar and incubated for 48 hours. The standard protocols for whole-cell MALDI-TOF must be maintained for reducing the data variation between laboratories. Nevertheless, the mass ions, defined as taxon-specific biomarkers for B. pseudomallei identification, were



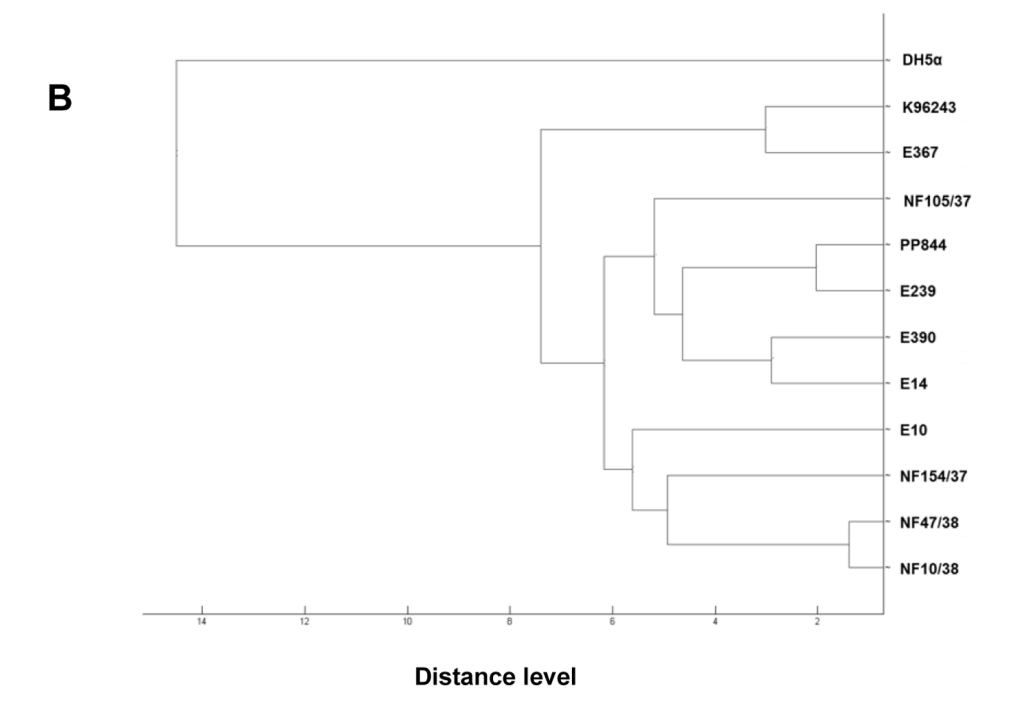


Figure 2. Principal component analysis (PCA) and cluster analysis of *B. pseudomallei* **isolates.** A) PCA analysis analyzed from total mass spectra showed intermixture and widely spreaded of all isolates from two source groups. **B**) Dendrogram constructed from the scores of PCA demonstrated that three of six environmental isolates; E239, E390, and E14 were grouped on their own cluster. Similarly, three clinical isolates, consisting of NF154/37, NF47/38, and NF10/38, were clustered together. *E. coli* DH5α was used as an outgroup taxon. Numbers shown in x-axis revealed distance level of tested isolates. doi:10.1371/journal.pone.0099160.g002

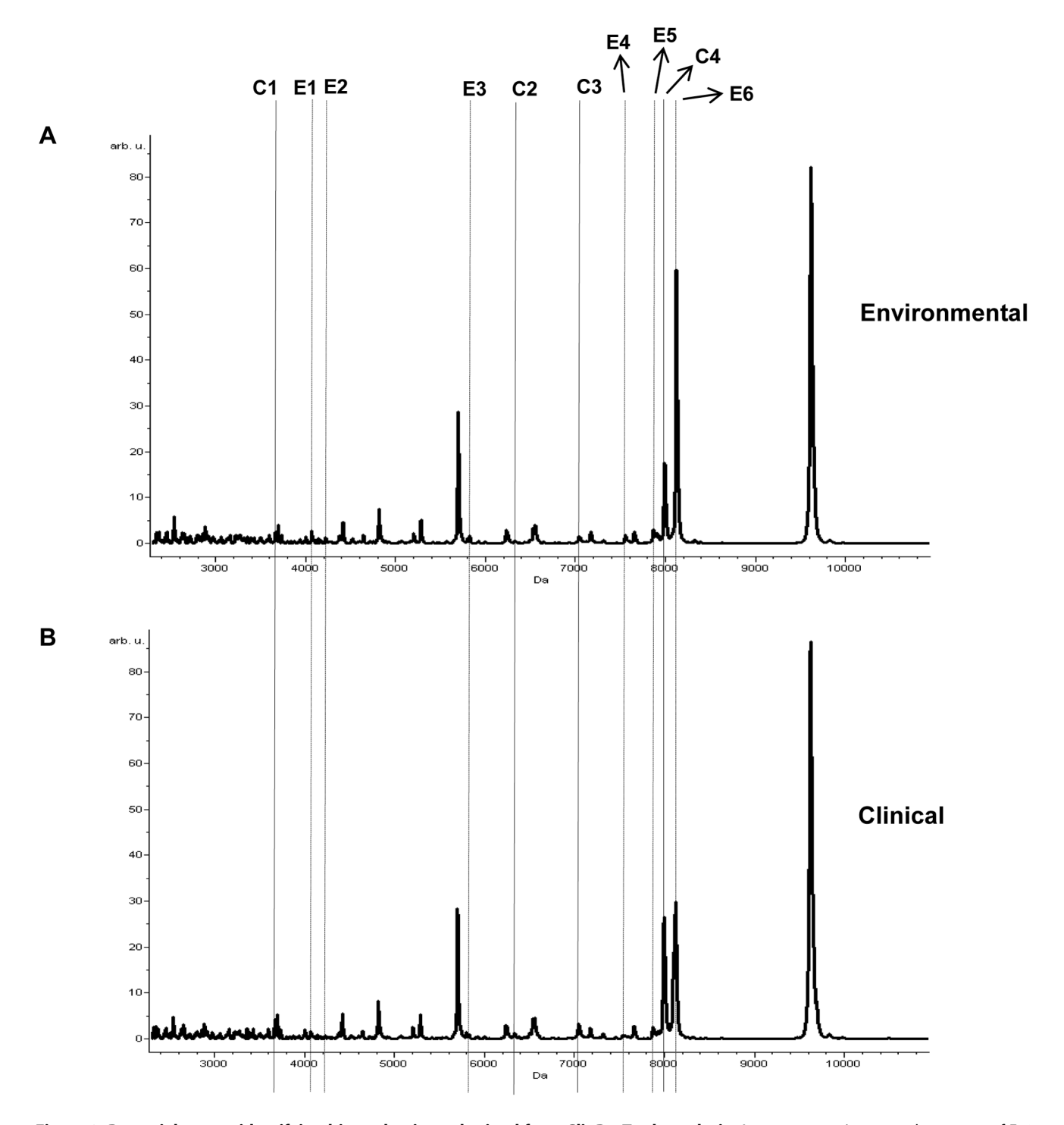


Figure 3. Potential source-identifying biomarker ions obtained from ClinProTools analysis. An average environmental spectrum of E10-E390 strains (**A**) had a very similar pattern as in a clinical set of K96243-NF154/37 (**B**) but peak intensity was different. The vertical dashed lines, E1-E6, indicated as environmental-identifying biomarker ions (ElBIs), consisting of m/z 4,056, 4,214, 5,814, 7,545, 7,895, and 8,112 whereas the vertical solid lines marked as C1-C4 displayed clinical-identifying biomarker ions (ClBIs), containing m/z 3,658, 6,322, 7,035, and 7,984. doi:10.1371/journal.pone.0099160.g003

detected in our findings; including, m/z at 4,410, 5,794, 6,551, 7,553, and 9,713 [41]. In detail, the *Burkholderia* species must contain m/z 4,410 since it regards as a faithful biomarker among *Burkholderia* spp. The mass ion at m/z 9,713 is specific for the *Pseudomonas* group, including *B. mallei*, *B. pseudomallei*, and *B. thailandensis*. The mass peak at m/z 6,551 is an effective mass ion

that is used for dividing *B. thailandensis* from the *B. mallei/B. pseudoma*llei group. As study from Lau et al, these taxon-specific biomarkers can also be found in MALDI-TOF MS mass spectrum of *B. pseudomallei* [44]. Hence, these five biomarkers are common and conserved as species-specific biomarkers among *B. pseudomallei* strains. At m/z 5,794 and 7,553, Karger et al have also suggested

Table 2. Peak intensity values and fold differences of all source-identifying biomarker ions of *B. pseudomallei*.

Biomarker ion	m/z value	Peak intensity (arb.u.)		Fold difference*
		environmental	clinical	
E1	4,056	2.7	1.7	1.59
E2	4,214	1.2	0.7	1.71
E3	5,814	1.7	1.0	1.70
E4	7,545	1.8	0.8	2.25
E5	7,895	2.25	0.98	2.30
E6	8,112	59	29	2.03
C1	3,658	2.375	4.125	0.58
C2	6,322	0.6	1.325	0.45
C3	7,035	1.5	3.4	0.44
C4	7,984	16.5	26.3	0.63

All ten source-identifying biomarker ions were selected on the basis of Wilcoxon/Krustal-Wallis statistics which were significantly different at p < 0.01. *Fold difference of each biomarker ion was calculated using peak intensity of environmental divided by that of clinical group. doi:10.1371/journal.pone.0099160.t002

the consideration of peak intensity at these two m/z peaks for differentiating *B. mallei* and *B. pseudomallei*, because these two species are closely related. We observed likely mass ions at m/z 5,794 resulting in the higher peak intensity than the m/z 7,553 in our tested *B. pseudomallei* samples. Therefore, it could be inferred that the whole-cell, or intact cell, method should be able to be used to analyze the samples under different experimental conditions and generate the stable mass ions for bacterial identification analysis, as previously described in several studies [26,45].

Our principal component analysis (PCA) demonstrated that all tested B. pseudomallei isolates were intermixed, thus they were not grouped in accordance with their origins (Figure 2A). The PCA scores were then used to generate a dendrogram in order to examine the ability of MALDI-TOF MS in grouping analysis of samples from different sources. From a total of 11 strains, overall six strains were grouped correctly to their sources (Figure 2B). In this study, whole-cell MALDI-TOF MS seems likely to possess low ability of categorization with B. pseudomallei samples. However, the MALDI-TOF MS application for cluster analysis by source is widely used with other bacterial species, such as E. coli [30], and Entercoccus spp. [33]. In those studies, the rates of overall correct classification of E. coli and Enterococcus spp. by MALDI-TOF MS are 73% and 67%, respectively. Those authors have further suggested that grouping analysis on the basis of the MALDI-TOF approach does not classify all of isolates correctly with respect to their own sources (for example, it does not succeed in the grouping of E. coli and Enterococcus isolated from humans), however, MALDI-TOF still represents an effective ability in grouping analysis when compared to other molecular typing methods, such as rep-PCR [30,33]. Therefore, examination in terms of source categorization by MALDI-TOF could be altered, depending on a variety of tested bacterial species. In our results, the imprecise cluster analysis on the basis of the mass fingerprint-based approach between these two source groups of B. pseudomallei strains might indicate the relatedness of clonality between environmental and clinical isolates as suggested by Haase et al and Currie et al [11,46]. In addition, there is a chance that the occurrence of invasive B. pseudomallei strains from clinical specimens, such as fecal, urine, sputum, and pus of infected humans or animals can contaminate the environment, followed by infection in humans and animals, that are exposed to contaminated soil and water [47]. These events could lead to the misclassification of B. pseudomallei from differential source groups. The small number of samples in this study might also provide less information for strain categorization using MALDI-TOF analysis. A collection from *B. pseudomallei* of each source should be added and other experimental factors that affect the quality of mass spectra have to be considered and examined in future experiments in order to obtain sufficient peak ions for use in cluster analysis.

Several publications have previously illustrated the use of various molecular typing methods for both the identification and differentiation of B. pseudomallei strains according to their different sources [14-20,48]. Bartpho et al have recently applied the microarray-based comparative genome hybridization (CGH) method to discover different genomic islands (GIs) in environmental and clinical samples and have found that clinical B. pseudomallei isolates contain GI8.1, 8.2, and 15, which cannot be detected in environmental isolates [21]. But the limitations of these techniques are that they are time-consuming, labour- and costintensive and require several steps to accomplish in the process of the identification and typing of microorganisms. To our knowledge, this study is the first to describe the use of whole-cell MALDI-TOF MS to identify the source-identifying biomarker ions of environmental and clinical B. pseudomallei isolates at the proteomic profiling level. Average environmental and clinical mass spectra which were source representatives demonstrating a high level of peak pattern similarity but differed in peak intensity were further analyzed by ClinProTools software to discover the potential source-specific biomarkers in the mass range of 2,000-20,000 Da. We exhibited a total of ten mass ions corresponding to source-identifying biomarkers that showed significant differences of peak intensity between environmental and clinical B. pseudomallei groups (Table 2). Six environmental-identifying biomarker ions (EIBIs) including, m/z 4,056, 4,214, 5,814, 7,545, 7,895, and 8,112 (doubly charge of 4,056), showed an obvious higher peak intensity than those in the clinical set. While four clinicalidentifying biomarker ions (CIBIs), consisted of m/z 3,658, 6,322, 7,035, and 7,984, explicitly contained higher mass intensity over that of the environmental set (Figure 3). For obtaining sufficient peak profiles, suitable protocols for whole-cell MALDI-TOF analysis and other important factors, including bacterial culture conditions, matrix types, sample preparation methods, and variabilities in crystal formation, which influence the mass fingerprints in respect to peak quality and quantity, have to be

investigated for an improvement on capability to distinguish closely-related species at the strain level. Typically, several researchers have shown that the protein biomarkers for identification at genus- and species-level correspond to abundant proteins inside the cells, such as ribosomal proteins and DNA or RNA binding proteins [23,28,35]. Dieckmann et al have additionally found that mass peak ions, which are subspecies-specific biomarkers in Salmonella spp., also contain putative uncharacterized proteins, thus the means of strain identification of bacteria requires the consideration of the extent of all those proteins in addition to ribosomal proteins [32]. Our study has yet to assign all EIBIs and CIBIs of B. bseudomallei to that of known expressed proteins. Further mass peak identification based on a bioinformatics-enabled approach could provide more information of differentially expressed proteins among environmental and clinical isolates under certain conditions.

Materials and Methods

Bacterial isolates and culture conditions

All bacterial isolates were cultured under the BSL3 conditions, which are approved by the committee from Faculty of Science, Mahidol University. The bacteria were provided by the authorities via personal permission. Environmental B. pseudomallei samples were isolated from soil in various areas of northeast Thailand and clinical samples were obtained from melioidosis patients which were stored in 80% glycerol stock at -80°C. Isolation sources of all B. pseudomallei samples were shown in Table 3. Each bacterial sample from glycerol stock was cultured in Luria-Bertani (LB) broth medium for 16 hours at 37°C with shaking at 180 rpm. Subsequently, the bacteria were subcultured into a new LB broth medium with 0.1% inoculum and incubated for 3 hours with shaking. To obtain colonies for MALDI-TOF MS analysis; after incubation the bacterial culture was serially diluted with LB medium, spread plated on Ashdown's selective agar and incubated at 37°C for 7 days as previously described in [43].

Sample preparation for MALDI-TOF MS analysis

The bacterial colonies on Ashdown's agar were picked into 900 µl of water and suspended with 300 µl of ethanol. Bacterial

cells were harvested by centrifugation. The cell pellets were then resuspended and vigorously mixed with MALDI matrix solution consisting of 10 mg sinapinic acid in 1 ml of 50% acetonitrile containing 2.5% trifluoroacetic acid. A 2- μ L of the mixture was directly spotted onto a MALDI target plate (MTP 384 ground steel plate, Bruker Daltonik, GmbH, Bremen, Germany) and allowed to air dry. Twenty replicates (n = 20) of each bacterial lysate were spotted onto the target plate in the same mass spectrometer run in order to examine data reproducibility.

MALDI-TOF MS instrument and data analysis

A Ultraflex III TOF/TOF mass spectrometer (Bruker Daltonik GmbH, Bremen, Germany) was employed for sample analysis. The instrument was externally calibrated using a ProteoMass peptide & protein MALDI-MS calibration kit (Sigma-Aldrich, St. Louise, MO) which includes human ACTH fragment 18-39 (m/z = 2,465), bovine insulin oxidized B chain (m/z = 3,465), bovine insulin (m/z = 5,731), equine cytochrome c (m/z = 12,362), and equine apomyoglobin (m/z = 16,952). MALDI-TOF MS operated in linear positive mode within the mass range of 2,000-20,000 m/z. Five hundred shots were accumulated, with a 50 Hz laser, for each sample. Parameters in flexControl were carried out according to the manufacturer's instructions (Bruker Daltonik GmbH, Bremen, Germany) using acceleration voltage of 25.00 kV (ion source 1) and 23.45 kV (ion source 2) and lens voltage of 6.0 kV. On account of our BioTyper database not containing B. pseudomallei reference spectra, we therefore constructed mass spectra of strain K96243 as an in-house reference spectrum, because this strain is well-known and is the first of the established genome sequences [49]. The reference spectrum of K96243 was generated from twenty single spectra. Total mass spectra of each bacterial sample acquired from FlexAnalysis version 3.0 (Build 92) were used to perform pattern matching against the reference spectrum of the K96243 strain using the MALDI BioTyper 2.0 software package. The calculation of matching peaks between the tested spectra and the reference spectra in the database provides the identification score for any given sample. Average spectrum for each B. pseudomallei strain was constructed from a set of twenty replicate spectra. For identifying the biomarkers to discriminate between environmental and clinical

Table 3. All Burkholderia pseudomallei strains used in this study.

Source	Isolate	Isolation source	Reference
Environmental	E10 ^a	Ubon Ratchathani	[51]
	E14 ^a	Ubon Ratchathani	[51]
	E239 ^a	Yasothon	this study
	E367 ^a	Si Sa Ket	this study
	E390 ^a	Ubon Ratchathani	this study
Clinical	K96243 ^b	Pus	[49]
	PP844 ^c	Blood	[53]
	NF10/38 ^d	Blood	[52]
	NF47/38 ^d	Blood	[52]
	NF105/37 ^d	Pus	[52]
	NF154/37 ^d	Pus	[52]

^aE10-E390 were received from Dr. Vanaporn Wuthiekanun, Wellcome Trust Unit, Faculty of Tropical Medicine, Mahidol University, Bangkok, Thailand.
^bK96423 was received from Assoc. Dr. Surasakdi Wongratanacheewin, Melioidosis Research Center, Faculty of Medicine, Khon Kaen University, Khon Kaen, Thailand.
^cPP844 was received from Prof. Dr. Stitaya Sirisinha, Department of Microbiology, Faculty of Science, Mahidol University, Bangkok, Thailand.
^cMr10/38-NF154/37 were received from National Institute of Health of Thailand, Ministry of Public Health, Nonthaburi, Thailand.
^cdoi:10.1371/journal.pone.0099160.t003

stains, the two average mass spectra of these two groups were further analyzed using ClinProTools version 2.2 (Build 78) [50]. Parameter settings for spectra preparation in the ClinProTools software were: top hat baseline subtraction, a resolution of 800 ppm, and a mass range of 2,000–20,000 m/z. Peak picking was based on total average spectrum, using a signal to noise ratio threshold of 5. The sort mode for peak selection was based on Wilcoxon/Kruskal-Wallis statistics at p-value < 0.01. Principal component analysis (PCA) and dendrogram for cluster analysis were automatically conducted with the integrated tool in the ClinProTools, MATLAB algorithm.

Conclusions

Whole-cell MALDI-TOF MS is a worthy and rapid tool which can be employed to analyze bacterial isolates under different experimental conditions and generate the stable mass ions for reliable bacterial identification analysis. PCA and cluster analysis demonstrated that environmental and clinical isolates of *B. pseudomallei* intermixed together and could not completely group all isolates in accordance to their sources. Future experiments should comprise a large number of *B. pseudomallei* from each source group to obtain more mass spectra information for the improvement of source categorization analysis. Notably, our study has shed light on the efficacy of whole-cell MALDI-TOF analysis for identifying the source-specific biomarkers for facilitating the

References

- Cheng AC, Currie BJ (2005) Melioidosis: epidemiology, pathophysiology, and management. Clinical microbiology reviews 18: 383-416.
- Wiersinga WJ, Currie BJ, Peacock SJ (2012) Melioidosis. The New England journal of medicine 367: 1035–1044.
- Galyov EE, Brett PJ, DeShazer D (2010) Molecular insights into Burkholderia pseudomallei and Burkholderia mallei pathogenesis. Annual review of microbiology 64: 495–517.
- Wiersinga WJ, van der Poll T, White NJ, Day NP, Peacock SJ (2006) Melioidosis: insights into the pathogenicity of Burkholderia pseudomallei. Nature reviews Microbiology 4: 272–282.
- Jenney AW, Lum G, Fisher DA, Currie BJ (2001) Antibiotic susceptibility of Burkholderia pseudomallei from tropical northern Australia and implications for therapy of melioidosis. International journal of antimicrobial agents 17: 109– 113.
- Vuddhakul V, Tharavichitkul P, Na-Ngam N, Jitsurong S, Kunthawa B, et al. (1999) Epidemiology of Burkholderia pseudomallei in Thailand. The American journal of tropical medicine and hygiene 60: 458–461.
- Trakulsomboon S, Vuddhakul V, Tharavichitkul P, Na-Gnam N, Suputtamongkol Y, et al. (1999) Epidemiology of arabinose assimilation in Burkholderia pseudomallei isolated from patients and soil in Thailand. The Southeast Asian journal of tropical medicine and public health 30: 756–759.
- Rattanavong S, Wuthiekanun V, Langla S, Amornchai P, Sirisouk J, et al. (2011) Randomized soil survey of the distribution of Burkholderia pseudomallei in rice fields in Laos. Applied and environmental microbiology 77: 532–536.
- Chen Y-S, Lin H-H, Mu J-J, Chiang C-S, Chen C-H, et al. (2010) Distribution
 of melioidosis cases and viable Burkholderia pseudomallei in soil: evidence for
 emerging melioidosis in Taiwan. Journal of clinical microbiology 48: 1432–1434.
- Ulett GC, Currie BJ, Clair TW, Mayo M, Ketheesan N, et al. (2001) Burkholderia pseudomallei virulence: definition, stability and association with clonality. Microbes and infection/Institut Pasteur 3: 621–631.
- Haase A, Smith-Vaughan H, Melder A, Wood Y, Janmaat A, et al. (1995) Subdivision of Burkholderia pseudomallei ribotypes into multiple types by random amplified polymorphic DNA analysis provides new insights into epidemiology. Journal of clinical microbiology 33: 1687–1690.
- Haase A, Janzen J, Barrett S, Currie B (1997) Toxin production by Burkholderia pseudomallei strains and correlation with severity of melioidosis. Journal of Medical Microbiology 46: 557–563.
- Liew SM, Tay ST, Wongratanacheewin S, Puthucheary SD (2012) Enzymatic profiling of clinical and environmental isolates of Burkholderia pseudomallei. Tropical biomedicine 29: 160–168.
- Sernswan RW, Wongratanacheewin S, Trakulsomboon S, Thamlikitkul V (2001) Ribotyping of Burkholderia pseudomallei from clinical and soil isolates in Thailand. Acta Tropica 80: 237–244.
- Inglis TJ, Garrow SC, Henderson M, Clair A, Sampson J, et al. (2000) Burkholderia pseudomallei traced to water treatment plant in Australia. Emerging infectious diseases 6: 56–59.

discrimination of environmental and clinical *B. pseudomallei* isolates. The rapid typing of *B. pseudomallei* from various sources, using the MALDI-TOF approach, could enable the tracking of *B. pseudomallei* during outbreaks and provide benefits with regards to medical prevention and the treatment of melioidosis. To the future aspects, a bioinformatics-based approach should be applied for investigating protein assignment and providing powerful identification and differentiation procedures of microorganisms at the strain level.

Acknowledgments

We are very grateful to Dr. Vanaporn Wuthiekanun (Wellcome Trust Unit, Faculty of Tropical Medicine, Mahidol University), Prof. Dr. Stitaya Sirisinha (Department of Microbiology, Faculty of Science, Mahidol University), Assoc. Dr. Surasakdi Wongratanacheewin (Melioidosis Research Center, Faculty of Medicine, Khon Kaen University), and NIH of Thailand for providing all bacterial isolates. We would like to thank Mr. Kevin John Kirk (Faculty of Graduate Studies, Mahidol University) for proofreading the manuscript.

Author Contributions

Conceived and designed the experiments: ST SR. Performed the experiments: SN JJ KS. Analyzed the data: JJ SR. Contributed reagents/materials/analysis tools: SR ST. Wrote the paper: SN ST.

- Winstanley C, Hales BA, Corkill JE, Gallagher MJ, Hart CA (1998) Flagellin gene variation between clinical and environmental isolates of Burkholderia pseudomallei contrasts with the invariance among clinical isolates. Journal of medical microbiology 47: 689–694.
- Leelayuwat C, Romphruk A, Lulitanond A, Trakulsomboon S, Thamlikitkul V (2000) Genotype analysis of Burkholderia pseudomallei using randomly amplified polymorphic DNA (RAPD): indicative of genetic differences amongst environmental and clinical isolates. Acta tropica 77: 229–237.
- Norton R, Roberts B, Freeman M, Wilson M, Ashhurst-Smith C, et al. (1998) Characterisation and molecular typing of Burkholderia pseudomallei: are disease presentations of melioidosis clonally related? FEMS immunology and medical microbiology 20: 37–44.
- Cheng AC, Godoy D, Mayo M, Gal D, Spratt BG, et al. (2004) Isolates of Burkholderia pseudomallei from Northern Australia are distinct by multilocus sequence typing, but strain types do not correlate with clinical presentation. Journal of clinical microbiology 42: 5477–5483.
- Vesaratchavest M, Tumapa S, Day NPJ, Wuthiekanun V, Chierakul W, et al. (2006) Nonrandom distribution of Burkholderia pseudomallei clones in relation to geographical location and virulence. Journal of clinical microbiology 44: 2533–2557.
- Bartpho T, Wongsurawat T, Wongratanacheewin S, Talaat AM, Karoonuthaisiri N, et al. (2012) Genomic islands as a marker to differentiate between clinical and environmental Burkholderia pseudomallei. PLoS ONE 7: e0037762.
- Sauer S, Kliem M (2010) Mass spectrometry tools for the classification and identification of bacteria. Nature reviews Microbiology 8: 74–82.
- Welker M, Moore ERB (2011) Applications of whole-cell matrix-assisted laserdesorption/ionization time-of-flight mass spectrometry in systematic microbiology. Systematic and applied microbiology 34: 2–11.
- Murray PR (2010) Matrix-assisted laser desorption ionization time-of-flight mass spectrometry: usefulness for taxonomy and epidemiology. Clinical Microbiology and Infection 16: 1626–1630.
- Krásný L, Hynek R, Hochel I (2013) Identification of bacteria using mass spectrometry techniques. International Journal of Mass Spectrometry 353: 67– 70
- Carbonnelle E, Mesquita C, Bille E, Day N, Dauphin B, et al. (2011) MALDI-TOF mass spectrometry tools for bacterial identification in clinical microbiology laboratory. Clinical Biochemistry 44: 104–109.
- Intelicato-Young J, Fox A (2013) Mass spectrometry and tandem mass spectrometry characterization of protein patterns, protein markers and whole proteomes for pathogenic bacteria. Journal of microbiological methods 92: 381– 396.
- Sandrin TR, Goldstein JE, Schumaker S (2013) MALDI TOF MS profiling of bacteria at the strain level: a review. Mass spectrometry reviews 32: 188–217.
- Wolters M, Rohde H, Maier T, Belmar-Campos C, Franke G, et al. (2011) MALDI-TOF MS fingerprinting allows for discrimination of major methicillinresistant Staphylococcus aureus lineages. International journal of medical microbiology: IJMM 301: 64–68.

- Siegrist TJ, Anderson PD, Huen WH, Kleinheinz GT, McDermott CM, et al. (2007) Discrimination and characterization of environmental strains of Escherichia coli by matrix-assisted laser desorption/ionization time-of-flight mass spectrometry (MALDI-TOF-MS). Journal of microbiological methods 68: 554–562.
- Rajakaruna L, Hallas G, Molenaar L, Dare D, Sutton H, et al. (2009) High throughput identification of clinical isolates of Staphylococcus aureus using MALDI-TOF-MS of intact cells. Infection, genetics and evolution: journal of molecular epidemiology and evolutionary genetics in infectious diseases 9: 507– 513.
- Dieckmann R, Helmuth R, Erhard M, Malorny B (2008) Rapid classification and identification of Salmonellae at the species and subspecies levels by wholecell matrix-assisted laser desorption ionization-time of flight mass spectrometry. Applied and environmental microbiology 74: 7767–7778.
- Giebel RA, Fredenberg W, Sandrin TR (2008) Characterization of environmental isolates of Enterococcus spp. by matrix-assisted laser desorption/ionization time-of-flight mass spectrometry. Water research 42: 931–940.
 Marklein G, Josten M, Klanke U, Müller E, Horré R, et al. (2009) Matrix-
- Marklein G, Josten M, Klanke U, Müller E, Horré R, et al. (2009) Matrixassisted laser desorption ionization-time of flight mass spectrometry for fast and reliable identification of clinical yeast isolates. Journal of Clinical Microbiology 47: 2912–2917.
- Tanigawa K, Kawabata H, Watanabe K (2010) Identification and typing of Lactococcus lactis by matrix-assisted laser desorption ionization-time of flight mass spectrometry. Applied and environmental microbiology 76: 4055–4062.
- 36. Donohue MJ, Smallwood AW, Pfaller S, Rodgers M, Shoemaker JA (2006) The development of a matrix-assisted laser desorption/ionization mass spectrometry-based method for the protein fingerprinting and identification of Aeromonas species using whole cells. Journal of microbiological methods 65: 380–389.
- Éddabra Ř, Prévost Ğ, Scheftel J-M (2012) Rapid discrimination of environmental Vibrio by matrix-assisted laser desorption ionization time-offlight mass spectrometry. Microbiological research 167: 226–230.
- Sauer S, Freiwald A, Maier T, Kube M, Reinhardt R, et al. (2008) Classification and identification of bacteria by mass spectrometry and computational analysis. PloS one 3: e0002843.
- Demirev PA, Fenselau C (2008) Mass spectrometry in biodefense. Journal of mass spectrometry: JMS 43: 1441–1457.
- Rotz LD (2002) Public health assessment of potential biological terrorism agents. Emerging Infectious Diseases 8: 225–230.
- Karger A, Stock R, Ziller M, Elschner MC, Bettin B, et al. (2012) Rapid identification of Burkholderia mallei and Burkholderia pseudomallei by intact cell Matrix-assisted Laser Desorption/Ionisation mass spectrometric typing. BMC Microbiology 12.
- Seng P, Drancourt M, Gouriet F, La Scola B, Fournier P-E, et al. (2009) Ongoing revolution in bacteriology: routine identification of bacteria by matrix-

- assisted laser desorption ionization time-of-flight mass spectrometry. Clinical infectious diseases: an official publication of the Infectious Diseases Society of America 49:543-551.
- Chantratita N, Wuthiekanun V, Boonbumrung K, Tiyawisutsri R, Vesaratchavest M, et al. (2007) Biological relevance of colony morphology and phenotypic switching by Burkholderia pseudomallei. Journal of bacteriology 189: 807–817.
- 44. Lau SKP, Tang BSF, Curreem SOT, Chan T-M, Martelli P, et al. (2012) Matrix-assisted laser desorption ionization-time of flight mass spectrometry for rapid identification of Burkholderia pseudomallei: importance of expanding databases with pathogens endemic to different localities. Journal of Clinical Microbiology 50: 3142–3143.
- Valentine N, Wunschel S, Wunschel D, Petersen C, Wahl K (2005) Effect of culture conditions on microorganism identification by matrix-assisted laser desorption ionization mass spectrometry. Applied and Environmental Microbiology 71: 58–64.
- Currie B, Smith-Vaughan H, Golledge C, Buller N, Sriprakash KS, et al. (1994) Pseudomonas pseudomallei isolates collected over 25 years from a non-tropical endemic focus show clonality on the basis of ribotyping. Epidemiology and infection 113: 307–312.
- 47. Dance DA (2000) Ecology of Burkholderia pseudomallei and the interactions between environmental Burkholderia spp. and human-animal hosts. Acta tropica 74: 159–168.
- Baker A, Mayo M, Owens L, Burgess G, Norton R, et al. (2013) Biogeography of Burkholderia pseudomallei in the Torres Strait Islands of Northern Australia. Journal of Clinical Microbiology.
- Holden MTG, Titball RW, Peacock SJ, Cerdeño-Tárraga AM, Atkins T, et al. (2004) Genomic plasticity of the causative agent of melioidosis, Burkholderia pseudomallei. Proceedings of the National Academy of Sciences of the United States of America 101: 14240–14245.
- Ketterlinus R, Hsieh S-Y, Teng S-H, Lee H, Pusch W (2005) Fishing for biomarkers: analyzing mass spectrometry data with the new ClinProTools software. BioTechniques Suppl: 37–40.
- Niumsup P, Wuthiekanun V (2002) Cloning of the class D beta-lactamase gene from Burkholderia pseudomallei and studies on its expression in ceftazidimesusceptible and -resistant strains. The Journal of antimicrobial chemotherapy 50: 445–455
- Tungpradabkul S, Wajanarogana S, Tunpiboonsak S, Panyim S (1999) PCR-RFLP analysis of the flagellin sequences for identification of Burkholderia pseudomallei and Burkholderia cepacia from clinical isolates. Molecular and cellular probes 13: 99–105.
- Subsin B, Thomas MS, Katzenmeier G, Shaw JG, Tungpradabkul S, et al. (2003) Role of the stationary growth phase sigma factor RpoS of Burkholderia pseudomallei in response to physiological stress conditions. J Bacteriol 185: 7008–7014.

Hindawi Publishing Corporation International Journal of Bacteriology Volume 2015, Article ID 623967, 10 pages http://dx.doi.org/10.1155/2015/623967



Research Article

Role of *Burkholderia pseudomallei* Sigma N2 in Amino Acids Utilization and in Regulation of Catalase Expression at the Transcriptional Level

Duong Thi Hong Diep, ¹ Nguyen Thi Thanh Phuong, ¹ Mya Myintzu Hlaing, ² Potjanee Srimanote, ^{2,3} and Sumalee Tungpradabkul ¹

¹Department of Biochemistry, Faculty of Science, Mahidol University, Bangkok 10400, Thailand

Correspondence should be addressed to Sumalee Tungpradabkul; pexcotung@gmail.com

Received 7 August 2015; Revised 29 October 2015; Accepted 2 November 2015

Academic Editor: Gary Dykes

Copyright © 2015 Duong Thi Hong Diep et al. This is an open access article distributed under the Creative Commons Attribution License, which permits unrestricted use, distribution, and reproduction in any medium, provided the original work is properly cited.

Burkholderia pseudomallei is the causative agent of melioidosis. The complete genome sequences of this pathogen have been revealed, which explain some pathogenic mechanisms. In various hostile conditions, for example, during nitrogen and amino acid starvation, bacteria can utilize alternative sigma factors such as RpoS and RpoN to modulate genes expression for their adaptation and survival. In this study, we demonstrate that mutagenesis of rpoN2, which lies on chromosome 2 of B. pseudomallei and encodes a homologue of the sigma factor RpoN, did not alter nitrogen and amino acid utilization of the bacterium. However, introduction of B. pseudomallei rpoN2 into E. coli strain deficient for rpoN restored the ability to utilize amino acids. Moreover, comparative partial proteomic analysis of the B. pseudomallei wild type and its rpoN2 isogenic mutant was performed to elucidate its amino acids utilization property which was comparable to its function found in the complementation assay. By contrast, the rpoN2 mutant exhibited decreased katE expression at the transcriptional and translational levels. Our finding indicates that B. pseudomallei RpoN2 is involved in a specific function in the regulation of catalase E expression.

1. Introduction

Melioidosis is an endemic disease in Southeast Asia and northern Australia. The causative agent of melioidosis in humans is *Burkholderia pseudomallei* which is a facultative intracellular pathogen. This organism is a polar flagellated Gram negative bacterium that can infect both humans and animals [1–3]. The mechanism by which *B. pseudomallei* causes melioidosis and its virulence is partly understood. The major regulatory control mechanisms for the expression of genes including virulent genes are the sigma factors. There are two major families of sigma factors which are sigma 70 (RpoD) and sigma 54 (RpoN) [4]. Sigma 54 is required only for a specific metabolic pathway such as nitrogen utilization and amino acids synthesis [5]. Moreover, sigma 54 regulates

the transcription of virulence associated genes including pili, flagella, and alginate biosynthesis operons in *Pseudomonas aeruginosa* and *Vibrio* species [6–8].

The analysis of *B. pseudomallei* genome has been identified in two copies of *rpoN* genes in two genomic locations, *rpoN1* on chromosome 1 and *rpoN2* on chromosome 2. To date, nothing is known at the molecular level regarding the function of sigma 54 (RpoN) in *B. pseudomallei*. Therefore, it was of interest to determine whether *B. pseudomallei* RpoN1 or RpoN2 is involved in nitrogen and amino acids utilization. To investigate this, the defined *B. pseudomallei* strain 844 *rpoN1* and *rpoN2* knockout mutants were constructed. However, only *rpoN2* knockout mutant was successfully constructed. The role of RpoN2 in nitrogen and amino acids utilization was examined and compared to that

²Department of Clinical Microbiology, Faculty of Medical Technology, Mahidol University, Salaya 73170, Thailand

³Graduate Programme in Biomedical Sciences, Faculty of Allied Health Science, Thammasat University, Rungsit 12121, Thailand

Strain or plasmid	Genotype or relevant characteristic	Source (reference)
Bacteria strains		
PP844	Wild type, clinical isolate from blood	This study
E. coli SM10 λpir	λpir (thi thr leu tonA lacY supE recA::RP4-2-Tc::Mu Km) used for transformation of recombinant plasmid pKNOCK::rpoN2 _{Bp}	[15]
E. coli JKD 814	rpoN::tet	[16]
Plasmids		
pKNOCK-Tc	Mobilizable suicide vector carrying Tet ^R gene	[10]
pKRpoN2	pKNOCK-Tc containing 363 bp internal segment of <i>B. pseudomallei rpoN2</i> gene	This study
pBBR1MCS	Broad-host-range cloning vector, Cm ^r	[17]
pBSDRpoN2	pBR1MCS containing full-length rpoN2 gene	This study
pCR 2.1-TOPO	Cloning vector for PCR product, Kanamycin and Ampicillin resistance	Invitrogen, California, USA
pTOPO::rpoN2 _{Bp799}	pCR 2.1-TOPO vector containing 799 bp fragment of truncated <i>rpoN2</i> gene from <i>B. pseudomallei</i> strain 844, Kanamycin and Ampicillin resistance	This study
pTOPO:: $rpoN_{Ec}$	pCR 2.1-TOPO vector containing full-length <i>rpoN</i> gene from <i>E. coli</i> , Kanamycin and Ampicillin resistance	This study

TABLE 1: Bacterial strains and plasmids used in this study.

of *E. coli* lacking RpoN by complementation assay in *rpoN* mutant derivative *E. coli* JKD 814. A comparative proteomic analysis of the *B. pseudomallei* wild type and its *rpoN2* isogenic mutant was performed to elucidate its amino acids utilization property. Moreover, we have identified RpoN2 specific function and found that it is involved in regulation of catalase E expression both at the transcriptional and at the translational levels.

2. Materials and Methods

- 2.1. Bacterial Strain and Growth Conditions. The bacterial strains used are listed in Table 1. B. pseudomallei is routinely maintained in Luria-Bertani (LB) medium. Pseudomonas agar base supplemented with SR103E (Cetrimide, Fucidin, and Cephaloridine) from Oxoid was used after conjugation as selective medium to inhibit growth of E. coli. Ashdown agar plate was also used for B. pseudomallei specific selective medium. All cultures were grown at 37°C in an aerobic condition with 250 rpm shaking. Tetracycline (60 μ g/mL) and chloramphenicol (40 μ g/mL) were added to media when required.
- 2.2. Construction of B. pseudomallei rpoN2 Mutant and Its Complemented Strain. rpoN2 knockout mutant (Table 1) was created to be pKRpoN2 according to a previously described procedure [9]. pKRpoN2 was constructed by transferring the 363 bp partial digested PstI fragment from genomic DNA of B. pseudomallei into the mobilizable suicide vector pKNOCK-Tc [10]. The constructed B. pseudomallei rpoN2 mutant was analyzed by Southern blot analysis and PCR as described elsewhere [11]. To confirm that all changes in phenotypes were caused by the disruption of rpoN2 and were not due to polar effects on downstream genes, a plasmid

(pBSDRpoN2) containing the complete full-length *rpoN2* coding sequence under control of the *lacZ* and *cat* promoters was constructed and transferred into the *B. pseudoma-llei* mutant strains for complementation analysis. Likewise, pTOPO::*rpoN2*_{Bp} and pTOPO::*rpoN2*_{Bp799} were constructed and used to complement into JKD 814 *E. coli rpoN* negative mutant. All plasmids constructed are listed in Table 1.

2.3. Nitrogen and Amino Acids Utilization Tests. Nitrogen and amino acids utilization tests were performed in MM9 salts minimal agar containing either 20 mM ammonium chloride (NH₄Cl) or other alternative nitrogen sources such as arginine, glutamine, glycine, histidine, lysine, methionine, phenylalanine, tryptophan, and valine at 5 mM concentration. $10~\mu L$ of overnight growth of the desired bacterial strains ($A_{600}=1$) was inoculated onto the above agar medium and incubated at 37°C. Growths of the bacterial colony were observed daily for five consecutive days.

Statistical measurements of all assays were carried out in three separate times. The results were expressed as the mean \pm standard deviation of days of growth. The significance of differences in nitrogen and amino acids utilization of bacterial strains was analyzed by Student's paired t-test (2-tailed) using SPSS statistical software program.

2.4. Protein Extraction and Two-Dimensional Gel Electrophoresis (2DE). Bacterial cultures were grown until early stationary phase. Proteins were extracted using $500~\mu L$ lysis buffer (8 M urea, 4% w/v CHAPS, 2 mM TBP, 1% v/v IPG buffer, pH 4–7) (Amersham Biosciences, Uppsala, Sweden) and 1% v/v protease inhibitor cocktail set II (Calbiochem, La Jolla, CA). The supernatant after cells lysis was transferred into clean microcentrifuge tubes and stored at $-80^{\circ} C$ until use. Protein concentrations were determined using RC DC

protein assay kit (Bio-Rad, Hercules, CA) as previously described [12]. For 2DE, the first-dimensional isoelectric focusing (IEF) was carried out using 500 μg protein samples with the rehydration buffer (8 M urea, 2% w/v CHAPS, 20 mM DTT, and 1% v/v IPG buffer, pH 4-7) adjusted to 350 µL total volume. Precast 18-cm Immobiline DryStrip with a linear pH 4-7 was used with the IPGphor II system (Amersham Biosciences) to perform IEF. The strips were rehydrated with the protein samples for 12 h at 20°C following three voltage steps as previously described [12]. All profiles were controlled at the current 50 μ A/strip. The IPG strips were then equilibrated and transferred to the second-dimensional SDS-PAGE using 12.5% polyacrylamide gel. SDS-PAGE was performed at 4°C with the constant electrical current at 10 mA/gel. Protein spots were visualized by Coomassie Brilliant Blue G-250 (CBBG-250) staining and gels were scanned with an ImageMaster Scanner (Amersham Biosciences). Image analysis was performed using PDQuest software version 7.1 (Bio-Rad). Images from three independent cultures were compared. A master gel used for spot matching process was created from a wild type 2D gel. The master gel was then used for matching of the corresponding protein spots between 2D gels. The relative intensity of each protein spot was determined by normalizing to the total intensity of the gel. Protein expression with intensity representing at least 3-fold difference with P < 0.05 was considered in this analysis. The biosynthesis pathways such as cysteine synthesis, histidine synthesis, purine metabolism, and pentose phosphate pathway were performed by using KEGG database [13].

2.5. Protein Extraction and Activity Staining for Catalase. Bacterial cultures were grown in various growth phase (12, 24, 48, and 72 hours) conditions. The bacterial pellets were lysed on ice by sonication in one-tenth of the original culture volume of phosphate buffer (5 mM potassium phosphate, pH 7.0, 5 mM EDTA, 10% glycerol, and 25 mM phenylmethylsulfonyl fluoride). Proteins were extracted as previously described [14]. The total protein concentration in each sample was determined with Bradford Reagent (Sigma Chemical, St. Louis, MO).

Catalase activities present in crude extracts of *B. pseudomallei* cells were determined by loading 20 µg of protein in 12% nondenaturing polyacrylamide gel. After polyacrylamide gel electrophoresis, the gels were washed three times with PBS (20 min each) to remove surface attached buffer ions as previously described [14]. Immediately, the gels were incubated with a solution of 2% (w/v) ferric chloride-potassium ferricyanide, until the gel was stained green.

2.6. RNA Isolation, cDNA Synthesis, and Relative Gene Expression Analysis. RNA extraction procedures were performed using TRIzol reagent (Invitrogen, USA). 1 mL of various growth phase cultures (24, 48, and 72 hours) was harvested and collected by centrifugation. RNA extraction was carried out following the manufacturer's instructions. Each RNA sample was treated with RQ1 RNase-free DNase (Promega, USA) and tested for DNA contamination as previously

described [11]. Measurement of RNA concentration was performed using Nanodrop 2000 (Thermo Fisher Scientific, USA). cDNA synthesis was performed using Superscript III Reverse Transcriptase First Strand cDNA synthesis kit (Invitrogen, USA) following the manufacturer's instructions.

Relative quantification real-time PCR for the katE gene was performed using Rotor-Gene 3000 (Corbett Research, Australia). Primers (katE-F primer 5'-TCT ACA CCG ACG AGG GCA AC-3' and katE-R primer 5'-TTC CTC CGG AAT CAG CTT GG-3') were designed using Primer3 software [19], and the reactions were quantified using SYBR GreenER qPCR SuperMix Universal (Invitrogen, USA). All reactions were programmed with dissociation curve analysis to prevent nonspecific and primer-dimer formation as previously described [20]. Gene encoding 23s rRNA was used as a reference control for normalization. The results were analyzed using the comparative Ct method or $\Delta\Delta$ Ct method (Applied Biosystems).

Statistical analysis of this study was performed from at least 3 independent experiments, each carried out in duplicate or triplicate. Values were presented as means \pm standard error. Statistical significance of differences between the two means was calculated using SigmaStat 3.5 software and evaluated by Student's t-test and P value < 0.01 was considered significant.

3. Results

3.1. Nitrogen and Amino Acids Utilization Tests in Escherichia coli. In order to determine a constructed rpoN2 mutant whether RpoN2 is essential for the B. pseudomallei growth in the absence of amino acid supplementation, we compared the growth of the wild type rpoN2 isogenic mutant and the rpoN2 mutant carrying rpoN2-complementing plasmid. No differences in growth were observed among the strains (data not shown). These results indicate that rpoN2 may be either not necessary or lacking the functions for amino acid utilization phenotypes.

To determine whether the *rpoN2* is not necessary or lacks the functions in amino acid utilization in B. pseudomallei, we performed the complementation assay by transforming full-length B. pseudomallei rpoN2 (TOPO::rpoN2_{Bp} plasmid DNA) and 799-fragment rpoN2 (TOPO::rpoN2.pos-plasmid DNA) into E. coli JKD 814 which lacks of rpoN and then compared with E. coli JKD 814 complemented with TOPO::rpoN_{Ec} plasmid DNA using as a positive control. $10 \,\mu\text{L} \, (A_{600} = 1)$ of bacterial culture was inoculated on M9 minimal agar containing each amino acid and incubated at 37°C for 5 days. E. coli rpoN mutant JKD 814 and E. coli wild type JM 109 were negative and positive controls, respectively. The experiments were carried out in three biological replicates. The differences in utilization of each amino acid for each construct were compared to that of JKD 814 and analyzed using Student's paired *t*-test. *B. pseudomallei* wild type strain 844 showed similar colony growth rate to E. coli wild type in the utilization of histidine as sole nitrogen source. Like E. coli wild type, B. pseudomallei also grew on M9 minimal agar supplemented with NH₄Cl, lysine,

			Day of	growth appearan	ce (mean ± SD) ^a		
Nitrogen source	E. coli JM 109	JKD 814 rpoN mutant	JKD 814 harboring pTOPO vector	JKD 814 harboring TOPO:: <i>rpoN</i> _{Ec}	JKD 814 harboring TOPO:: <i>rpoN2</i> _{Bp}	JKD 814 harboring TOPO:: <i>rpoN2</i> _{Bp799}	B. pseudomallei wild type 844
NH ₄ Cl	$3.7 \pm 0.6^*$	±	±	$2.7 \pm 0.6^*$	2 ± 1	NG	$4.7 \pm 0.6^*$
Arginine	$1.3 \pm 0.6^*$	±	±	$3.3 \pm 0.6^*$	$3.3 \pm 0.6^*$	±	$4.7 \pm 0.6^*$
Glutamine	$2.7 \pm 0.6^*$	NG	NG	$4.6 \pm 0.6^*$	$3.7 \pm 0.6^*$	NG	$1.3 \pm 0.6^*$
Glycine	$2.7 \pm 0.6^*$	±	±	$2.3 \pm 0.6^*$	$2.7 \pm 0.6^*$	±	±
Histidine	$1.3 \pm 0.6^*$	NG	NG	$4\pm1^*$	$2.3 \pm 0.6^*$	NG	$1.3 \pm 0.6^*$
Lysine	$3.3 \pm 0.6^*$	NG	NG	$3.7 \pm 0.6^*$	$4.3 \pm 1.2^*$	NG	$4.7 \pm 0.6^*$
Methionine	$4.7 \pm 0.6^*$	NG	NG	NG	$4.7 \pm 0.6^*$	NG	±
Phenylalanine	$4.7 \pm 0.6^*$	NG	±	$4.7 \pm 0.6^*$	$3.7 \pm 0.6^*$	±	$1.3 \pm 0.6^*$
Tryptophan	$1.7 \pm 0.6^*$	±	±	$1.7 \pm 0.6^*$	$1.7 \pm 0.6^*$	NG	$2.7 \pm 0.6^*$
Valine	$1.3 \pm 0.6^*$	NG	NG	NG	NG	NG	$4.7 \pm 0.6^*$

Table 2: Nitrogen and amino acid utilization of B. pseudomallei wild type 844 and E. coli derivatives.

and tryptophan but the growths were approximately one-day delay (Table 2). Although the growth of *B. pseudomallei* could be investigated on arginine and valine sole nitrogen source, the colonies were not observed until after day four of incubation. On the other hand, *B. pseudomallei* wild type utilized glutamine and phenylalanine faster than *E. coli* wild type. However, unlike *E. coli* wild type, *B. pseudomallei* could not utilize glycine as a growth substrate.

The *rpoN* mutant *E. coli* JKD 814 and JKD 814 harboring either pCR 2.1-TOPO vector alone or plasmid containing only partial ORF of *rpoN2* (TOPO::*rpoN2*_{Bp799} [799 bp]) exhibited no growth on minimal media supplemented with all nitrogen sources tested in this study after 5 days of incubation (Table 2).

Although the delay in growth was demonstrated, when TOPO:: $rpoN_{\rm Ec}$ recombinant plasmid which contained entire ORF of *E. coli rpoN* was complemented into JKD 814 *E. coli rpoN* mutant, the growth phenotypes were able to restore all tested amino acids except methionine and valine (Table 2). In contrast, the mutant JKD 814 complemented TOPO:: $rpoN_{\rm Ec}$ strain exhibited faster growing on the simple nitrogenous compound NH₄Cl compared to the *E. coli* wild type. Similar growth patterns were also observed in the mutant JKD 814 complemented with TOPO:: $rpoN2_{\rm Bp}$ with the exception of methionine. Moreover, in minimal media supplemented with sole lysine, the mutant JKD 814 complemented with TOPO:: $rpoN2_{\rm Bp}$ appeared to grow slower than the mutant complemented with TOPO:: $rpoN2_{\rm Bp}$ appeared to grow slower than the mutant complemented with TOPO:: $rpoN2_{\rm Ec}$ and the *E. coli* wild type.

Compared to *B. pseudomallei* wild type strain 844, rpoN mutant JKD 814 complemented with TOPO:: $rpoN2_{\rm Bp}$ grew slightly faster on M9 minimal media supplemented with NH₄Cl, arginine, and tryptophan while it grew slower in glutamine, histidine, and phenylalanine. No difference in growth rate was inspected when lysine was used as a sole nitrogen source. Moreover, the valine utilization could not be restored in the $rpoN2_{\rm Bp}$ complemented strain. Surprisingly, the rpoN mutant JKD 814 complemented with TOPO:: $rpoN2_{\rm Bp}$ was able to grow on media supplemented with glycine and

methionine which were the characteristic of *E. coli* wild type and not of *B. pseudomallei* wild type strain 844 phenotype (Table 2).

The overall results suggested that any difference in nitrogen utilization observed in this study was mediated by RpoN from either *E. coli* or *B. pseudomallei*. Therefore, we have demonstrated that *B. pseudomallei rpoN2* has full functions in regulation of nitrogen and amino acids utilization.

3.2. Partial Proteomic Analysis of B. pseudomallei rpoN2 Mutant Compared with Its Wild Type. A comparison of proteomic expressions in wild type and *rpoN2* mutant strains of B. pseudomallei was set as the cutoff to be a threefold difference between the wild type and rpoN2 mutant. The results for proteins located in pH range 4.5 to 7 and molecular weight 20-75 kDa are shown in Figure 1. The identity of proteins was determined using the reference map from the wild type analysis [18]. A total of 21 spots were identified. The upregulated proteins in the *rpoN2* mutant strain included 14 proteins and the downregulated proteins in rpoN2 mutant included 7 proteins as indicated in Figures 1(a) and 1(b). The numbers of each spot are referred to the same numbers as mentioned in the B. pseudomallei wild-type proteome reference map [18] which was used to study the RpoS regulon of B. pseudomallei [21]. The 7 proteins are downregulated in rpoN2 mutant including proteins involved in energy metabolism, lipid metabolism, transcription, and several hypothetical proteins of unknown function. In addition, 14 proteins appeared to be upregulated in rpoN2 mutant, the majority of which are involved in carbohydrate metabolism, posttranslation modification, cell envelope biogenesis, and outer membrane formation as summarized in Table 3. In order to identify the enzymes responsible for nitrogen utilization and amino acid synthesis and uptake, we found phosphoribosyl formimino-5-aminoimidazole carboxamide ribotide isomerase (HisA) (spot number 83) and cysteine synthase (CysM) (spot number 80) that are involved in histidine and cysteine synthesis, respectively (Figures 1(a) and 1(b)).

^aData represent geometric mean (\pm standard error) from three independent experiments. NG indicates the absence of growth. \pm indicates the very sparing growth inspected on day 6. *Significant differences in amino acid utilization compared to *E. coli rpoN* mutant JKD 814 ($P \le 0.05$, Student's paired t-test).

TABLE 3: Comparative partial proteomic analysis of rpoN2 mutant compared to wild type of B. pseudomallei. The spot numbers assigned in this study are identical to the number of spots in B. pseudomallei 2DE reference map [18].

(1) Cell envelope biogenesis and outer membrane Acetyltransferase (GAT) family protein UDP-N-acetyluntamy pertapeptide synthase UDP-N-acetyluntamy pertapeptide synthase (UDP-N-acetyluntamy pertapeptide synthase (UDP-N-acetyluntamy pertapeptide synthase (UDP-N-acetyluntamy pertapeptide synthase (Daylo	↑830			1 - I
amily (Ppk2) lelta subunit lelta subunit lelta subunit sun hate dehydrogenase (GapA) -sugar epimerases -2-enyl diphosphate reductase (IspH) Ino-5-aminoimidazole carboxamide ribotide isomerase (HisA) f, ArsR family I isomerase B laterafficking, and secretion Bipip cone LcrH/SycD Independence of the supplies of the suppl			1	
amily (Ppk2) letta subunit latta (GapA) latta (Ga		4.9	7T.0c	λ .
imily (Ppk2) letta subunit letta subunit (NAD) family protein In hate dehydrogenase (GapA) sugar epimerases -2-enyl diphosphate reductase (IspH) I depeptide/polyketide synthase (CmaB) In no-5-aminoimidazole carboxamide ribotide isomerase (HisA) In carboxylase f. ArsR family I isomerase B isomerase B lat rafficking, and secretion lat rafficking, and secretion I bip. In the family I In the family	↑ 5.02		41.55	2
amily (Ppk2) letta subunit letta subunit sm hate dehydrogenase (GapA) -sugar epimerases -2-enyl diphosphate reductase (IspH) l peptide/polyketide synthase (CmaB) lno-5-aminoimidazole carboxamide ribotide isomerase (HisA) l) lecarboxylase t, ArsR family 1 lication lisomerase B lear trafficking, and secretion BipD rone LcrH/SycD l left amily libitanily 1 libitanily 2 libitanily 3 libitanily 3 libitanily 4 libitanily 6 libitanily 7 libitanily 7 libitanily 8 libitanily 8 libitanily 9				
letha subunit (NAD) family protein 1 (NAD) family protein 1 1 1 1 1 1 1 1 1 1 1 1 1	↑3.17	•	44.26	40
lefta subunit sm sm sm hate dehydrogenase (GapA) -sugar epimerases -2-enyl diphosphate reductase (IspH) 1 d peptide/polyketide synthase (CmaB) 1 no-5-aminoimidazole carboxamide ribotide isomerase (HisA) 1 fl. fl. f. ArsR family 1 ication siomerase B e lar trafficking, and secretion BipD rone LcrH/SycD 1 lefamily	↑3.40	4.97	53.93	15
sm hate dehydrogenase (GapA) -sugar epimerases -sugar epimerases -2-enyl diphosphate reductase (IspH) d peptide/polyketide synthase (CmaB) 1 no-5-aminoimidazole carboxamide ribotide isomerase (HisA) 1 1 1 1 1 1 1 1 1 1 1 1 1 1 1 1 1 1 1	0.17 \	5.34 3	36.59	26
hate dehydrogenase (GapA) hate dehydrogenase (GapA) -sugar epimerases -sugar epimerases -sugar epimerases -sugar epimerases -sugar epimerases -sugar epimerase (IspH) 12-enyl diphosphate reductase (IspH) 12-enyl diphosphate reductase (IspH) 1	0.19 ↓		55.39	24
hate dehydrogenase (GapA) -sugar epimerases -sugar epimerases -sugar epimerases -sugar epimerases 1:-2-enyl diphosphate reductase (IspH) 1-1-2-enyl diphosphate reductase (LispH) 1-2-enyl diphosphate reductase (LispH) 1-3-enyl diphosphate reductase (HisA) 1-3-				
-sugar epimerases -sugar epimerases -sugar epimerases -sugar pimerase (IspH) d peptide/polyketide synthase (CmaB) 1 Ino-5-aminoimidazole carboxamide ribotide isomerase (HisA) 1) decarboxylase decarboxylase 1 1 1 1 1 1 1 1 1 1 1 1 1 1 1 1 1 1	↑3.38		20.88	48
d peptide/polyketide synthase (CmaB) In o-5-aminoimidazole carboxamide ribotide isomerase (HisA) In o-5-aminoimidazole carboxamide ribotide isomerase (HisA) It is a secretion It is and secretion It is and secretion It is and secretion It is a secretion	↑ 12.58	5.21	27.78	26
d peptide/polyketide synthase (CmaB) In o-5-aminoimidazole carboxamide ribotide isomerase (HisA) In no-5-aminoimidazole carboxamide ribotide isomerase (HisA) It accarboxylase It accarboxyl				
hecarboxylase t, ArsR family 1 isomerase B isomerase B isomerase B isomerase B isomeraticking, and secretion BipD rone LcrH/SycD Index family Branily	↑5.07 0.21 l	5.94 6.19	40.81 3719	71
Ino-5-aminoimidazole carboxamide ribotide isomerase (HisA) decarboxylase 1 3 r, ArsR family 1 ication isomerase B isomerase B isomerase B it and secretion BipD rone LcrH/SycD 1 1 1 1 1 1 1 1 1 1 1 1 1	→ 1			
1) decarboxylase	0.20 ↓	4.42	31	83
decarboxylase 3 5, ArsR family 1 ication isomerase B e alar trafficking, and secretion BipD rone LcrH/SycD 1 1 1 1 1 1 1 1 1 1 1 1 1	0.33 ↓	5.75	36.11	80
-phosphate decarboxylase al protein L3 nn regulator, ArsR family 1 ional modification lyl cis-trans isomerase B S-transferase ty, intracellular trafficking, and secretion ctor protein BipD etion chaperone LcrH/SycD nnses 1 1 1 1 1 1 1 1 1 1 1 1 1				
al protein L3 on nal regulator, ArsR family 1 ional modification lyl cis-trans isomerase B S-transferase ty, intracellular trafficking, and secretion ctor protein BipD etion chaperone LcrH/SycD onses l protein Corp. OprB family 1 1 1 1 1 1 1 1 1 1 1 1 1	↑ 6.42	4.99	32.79	88
	↑3.49	4.14	27.8	150
	0.20↓	4.92	37.92	124
	↑3.37	5.97	16.15	179
1 1 1	↑ 22.15	6.05	66.61	174
	↑ 3.05	6.5	22	176
erone LcrH/SycD prB family	↑5.04	4.38	34.37	194
prB family	↑ 6.23		18.52	190
prB family				
	↑3.16	5.01	38.71	233
(12) hyponetical protein				
1	↑3.15		16.53	253
Hypothetical protein BPSS0931 0.03 U	0.03 ↓	4.64	23.63	274

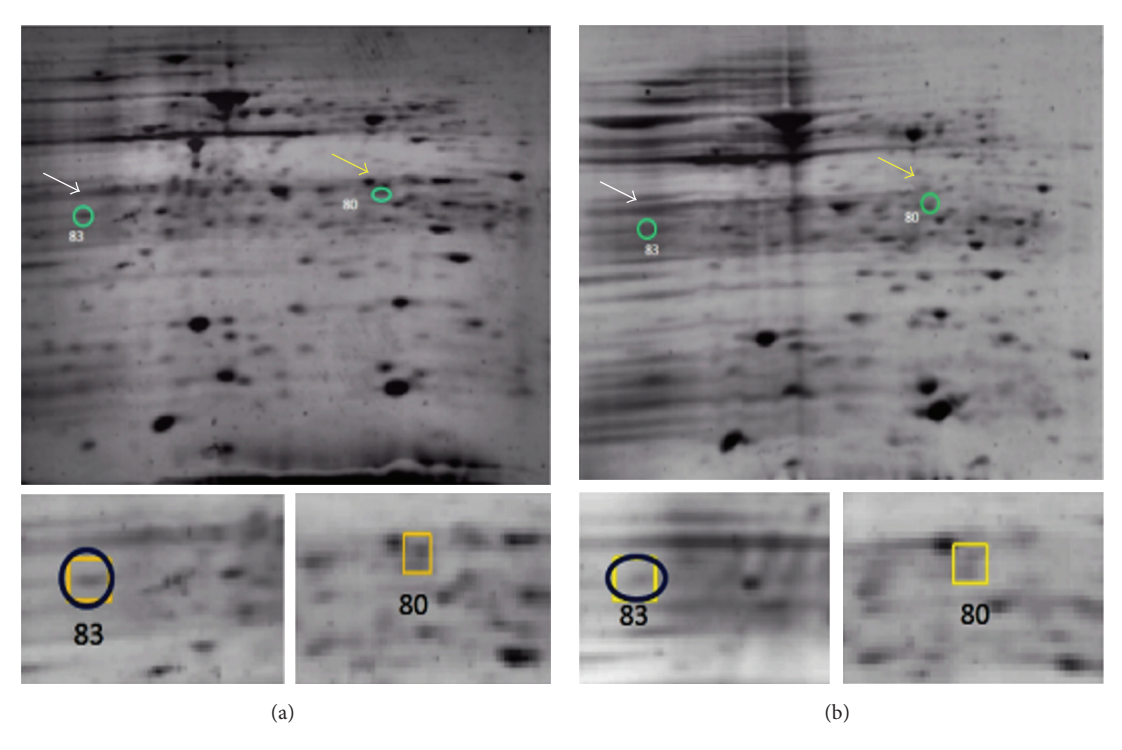


FIGURE 1: 2D-gel electrophoresis of *B. pseudomallei* wild type (a) and *rpoN2* mutant (b) obtained from stationary phase of growth. PDQuest program was used for analysis of the group's sample of wild type and mutant compared with reference map of *B. pseudomallei*. The circles indicate spot numbers 80 (CysM) and 83 (HisA) that are downregulated in *rpoN2* mutant strain.

However, both histidine and cysteine biosynthetic pathway can produce these amino acids from several starting points using both *de novo* synthesis and the intermediates in other biosynthetic pathways (Figures 2 and 3) [13]. Therefore, *B. pseudomallei* HisA and CysM are not essential for production of histidine and cysteine. Our partial proteomic analysis supported the function of RpoN2 that is not essential for nitrogen and amino acids utilization.

3.3. Positive Regulation of RpoN2 on katE in B. pseudomallei. Using bioinformatics prediction for chromosome 2, a potential RpoN box [4] was identified in front of the katE gene. An activity staining assay for catalase [14] was performed for the wild type rpoN2 isogenic mutant and the rpoN2 mutant carrying the rpoN2-complementing plasmid. The results suggest that catalase E or KatE activity is regulated by RpoN2 as shown in Figure 4(a). In particular, the rpoN2 complemented strain fully restores the KatE activity as shown in Figure 4(a). To demonstrate that catalase E activity is regulated at the transcriptional level, qRT-PCR was performed as shown in Figure 4(b). katE expression in the wild type was detected from 48 hours to 72 hours of bacterial growth, whereas no katE expression was detected in the rpoN2 mutant.

4. Discussion

In several bacterial pathogens, RpoN (δ^{54}) is known to be involved in pathogenesis and virulence such as nitrogen

utilization and amino acid assimilation; capsular polysaccharide and lipopolysaccharide synthesis; flagella and pili biosynthesis; type III secretion; and biofilm formation [5-8, 22–24]. Rhizobium etli has two copies of the rpoN gene and experiments with the mutant strains revealed that rpoN1 and rpoN2 genes are both active but under different physiological conditions [25]. The rpoN1 gene is essential during the growth phase while *rpoN2* is required for metabolism [25]. In *B*. pseudomallei, each chromosome contains a member of the sigma 54 family (RpoN1 and RpoN2) which are known to be involved in amino acid utilization and some virulence factors but the function of each RpoN is still unclear. In this study, construction of both rpoN1 and rpoN2 knockout mutants was performed but, unfortunately, the *rpoN1* mutant could not be obtained. We therefore focused on the role of B. pseudomallei δ^{54} (RpoN2) in comparison with the wild type strain PP844, rpoN2 mutant, and complemented rpoN2. MM9 culture medium containing only inorganic salts, a carbon source, and water was used for testing whether RpoN2 was necessary for growth in the absence of amino acid supplementation. The wild type and the complemented *rpoN2* contain all the genes needed for survival and as predicted both of these strains can grow in the absence of the addition of exogenous amino acids (MM9). However, the *rpoN2* mutant is missing RpoN2 activity that has been proposed to regulate the transcription of some proteins involved in amino acid biosynthesis. If RpoN2 has a major role in amino acid utilization, the rpoN2 negative mutant would be unable to grow in the absence of amino acid supplementation. Our results show that the B. pseudomallei rpoN2 mutant strain

Cysteine and methionine metabolism

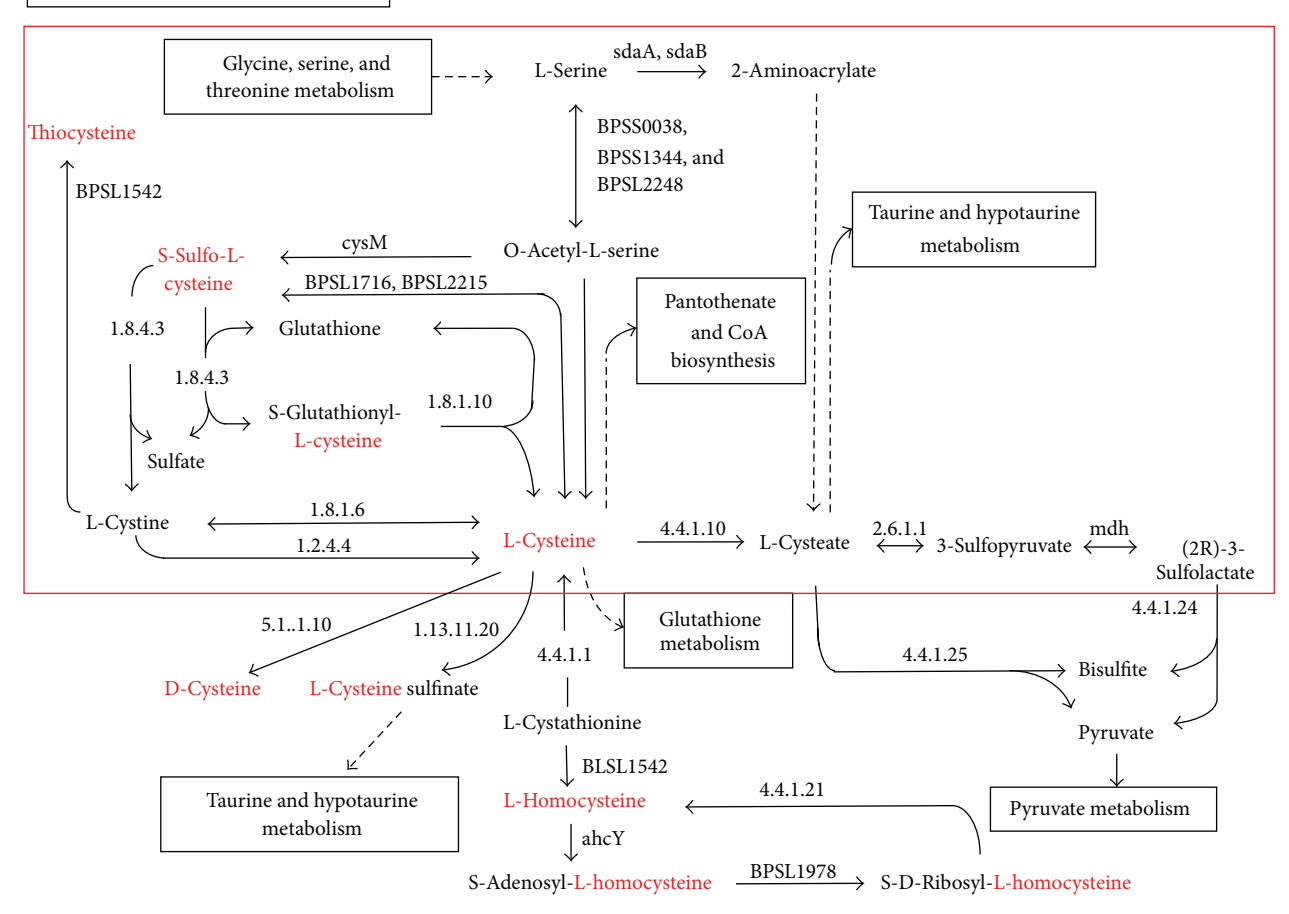


FIGURE 2: Cysteine and methionine metabolisms. The square is a pathway synthesis from glycine, serine, and threonine metabolisms to L-cysteine. http://www.genome.jp/kegg.

was able to grow in MM9 medium indicating that RpoN2 is not essential in regulating amino acid utilization. However, the possibility that these phenotypes might be compensated by another *rpoN* gene product on chromosome 1 of *B. pseudomallei* could not be excluded.

In order to demonstrate the ability of *B. pseudomallei rpoN2* gene product to have a function in regulation of amino acid utilization, a complementation assay by restoration growth of *E. coli rpoN* mutant in minimal media supplemented with various amino acids (Table 2) was performed. Indeed, the ability to grow in the presence of glycine and methionine was the characteristic of *E. coli* wild type. Moreover, the ability to utilize glycine and methionine as sole nitrogen source in *E. coli* (Table 2) was previously shown to be regulated by RpoN [16, 23–27]. Due to the fact that all of the RpoN_{Bp} functional domains are almost identical to that of RpoN_{Ec}, therefore, it is possible that RpoN_{Bp} is able to induce the transcription of the heterologous glycine and methionine utilization genes in *E. coli* JKD 814 in similar fashion to the *E. coli* RpoN.

In phenylalanine and glutamine utilization test, slower growth rate of JKD harboring TOPO:: $rpoN2_{Bp}$ compared to *B. pseudomallei* wild type was demonstrated (Table 2). It has

been previously reported that the decrement in gene transcription by RpoN regulon is likely to be the consequence of the differences in the nucleotide sequence around the RpoNconserved recognition sites 12 and 24 located upstream of the target genes [28]. Thus, it is possible that RpoN_{Bp} may prefer to recognize and induce the promoter sequence upstream of the genes required for phenylalanine and glutamine utilization in B. pseudomallei wild type more than that of E. coli JKD 814. However, it is also possible that phenylalanine and glutamine utilization system in B. pseudomallei wild type and E. coli may differ or operate differently. This hypothesis is also underscored by the data presented in Table 2 that E. coli wild type usually utilized phenylalanine and glutamine at least one day slower than B. pseudomallei wild type. Currently, the phenylalanine and glutamine utilization mechanisms in B. pseudomallei have not yet been elucidated. In addition, due to the difference in their native habitats, the discrepancy in the range of RpoN-controlled nitrogen utilization genes between E. coli and B. pseudomallei is also probably due to the specific control circuits to achieve the optimal adaptation to the different environments. The transport of nitrate across the membrane or the production of nitrate reductase and lysine decarboxylase in B. pseudomallei is not under

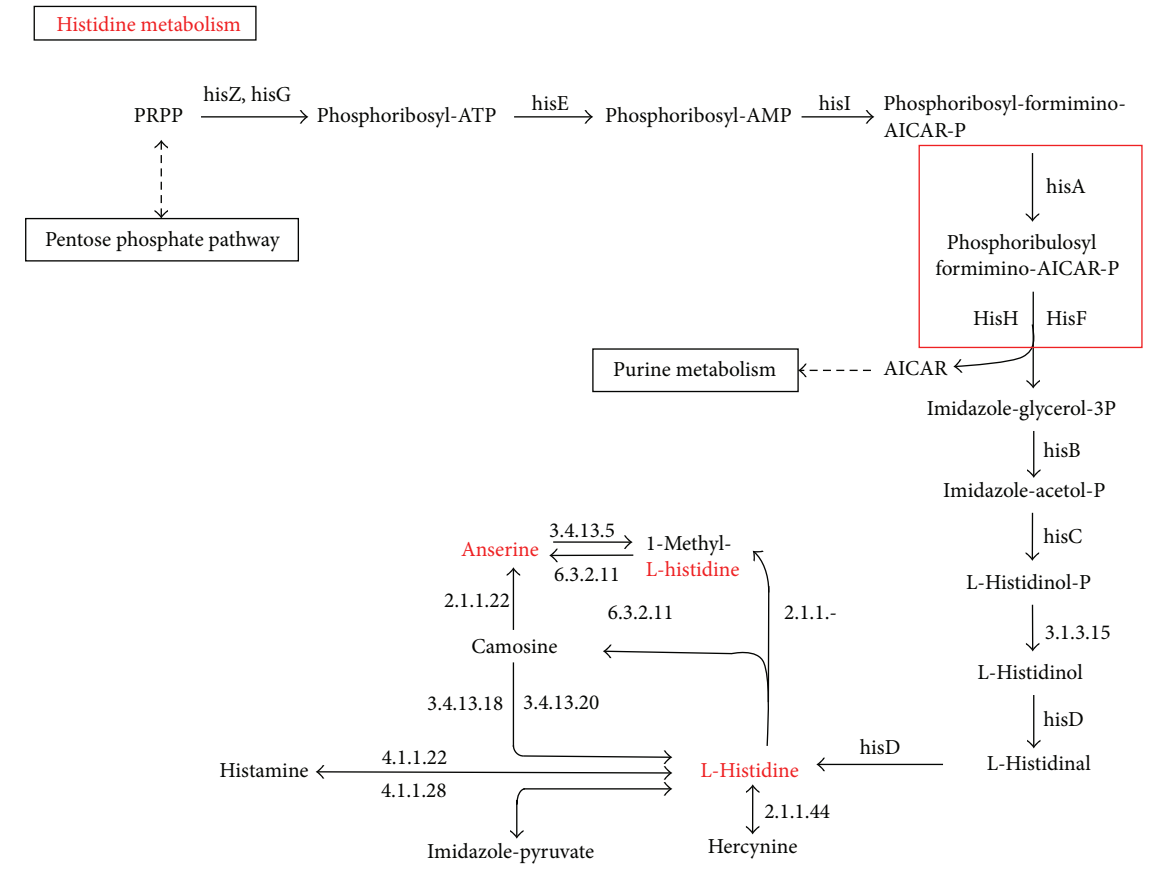


FIGURE 3: Histidine metabolism. The square is the phosphoribosyl formimino-5-aminoimidazole carboxamide ribotide isomerase (HisA). http://www.genome.jp/kegg.

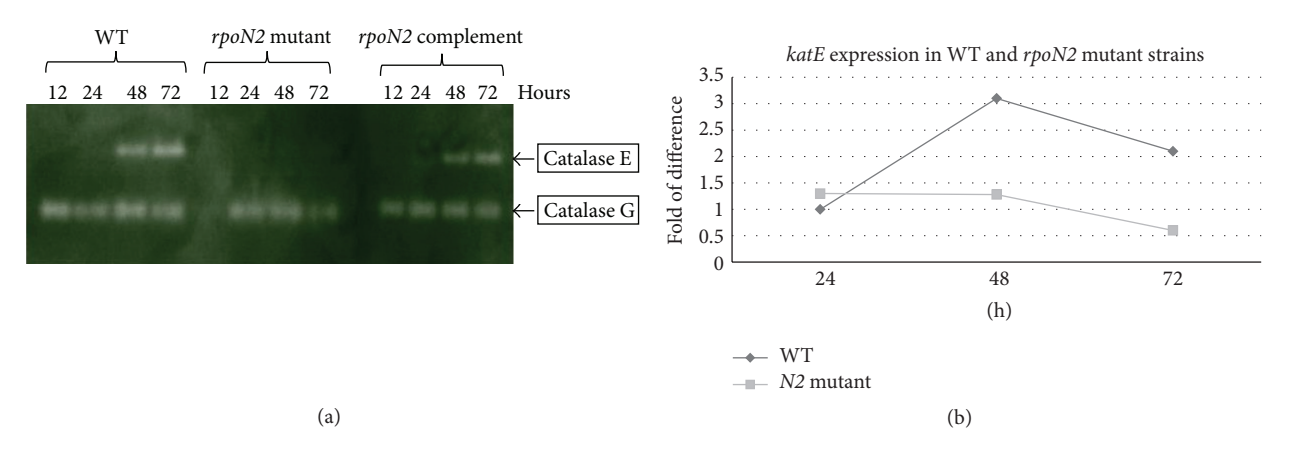


FIGURE 4: (a) Zymography of catalase activities during various stages. *B. pseudomallei* PP844 wild type (WT), the *rpoN2* isogenic mutant (*rpoN2* mutant), and the *rpoN2* mutant carrying the *rpoN2*-complementing plasmid (*rpoN2* complement) were grown aerobically in LB medium for 12, 24, 48, and 72 hours. The extracted cells (15 µg of protein) were prepared for electrophoresis in 10% nondenaturing polyacrylamide gel and stained for catalase activity in a solution of 2% (w/v) ferric chloride-potassium ferric cyanide. (b) Relative quantification real-time RT-PCR (qRT-PCR) for *B. pseudomallei katE* expression was compared between the *rpoN2* isogenic mutant (*N2* mutant) and the wild type PP844 (WT) at various stages (24, 48, and 72 hours) of growth. The *katE* gene primers were designed using Primer3 software. All fold difference values were normalized with 23s rRNA expression and the values are the mean standard deviations; analysis is performed in triplicate.

the control of RpoN2_{Bp} as there was no different result observed among E. coli wild type, E. coli JKD 814, and JKD 814 derivatives. In E. coli and other Gram negative bacteria, lysine is metabolized by two major pathways, the lysine oxygenase and the pipecolate route [29, 30]. In the former route, L-lysine is oxidatively decarboxylated by lysine oxygenase to form 5aminovaleramide, whereas in the latter, L-lysine is converted to D-lysine, which is then oxidatively deaminated, cyclized, and finally reduced to L-pipecolate [29, 30]. Moreover, E. coli can also utilize lysine as a sole carbon source and this ability is also under the control of σ^{54} (RpoN) [29]. In contrast, Pseudomonas putida, the B. pseudomallei related species, was able to utilize lysine only as a nitrogen source and this ability was also under the control of σ^{54} (RpoN) [15]. However, our results are not able to draw conclusion that the growth on minimal medium supplemented with lysine of B. pseudomallei and JKD 814 harboring TOPO::rpoN2Bp is due to either the utilization of carbon or nitrogen source.

For better understanding the role of RpoN2 in amino acid utilization, we used 2-dimension polyacrylamide gels to identify proteins with altered levels in the rpoN2 mutant since RpoN2 may regulate these proteins. Cells have many ways to obtain amino acids such as transport from environment, de novo synthesis, or synthesis from other amino acids and we speculated that RpoN2 might be involved in the regulation of some proteins involved in these processes. By analysis of soluble extracts using 2D gels and PDQuest software package to identify the proteins with altered abundance, we found that cysteine synthase (CysM) and phosphoribosyl formimino-5-aminoimidazole carboxamide ribotide isomerase (HisA) were both downregulated in the rpoN2 mutant. While the levels of CysM and HisA were decreased in the rpoN2 mutant, it was able to synthesize/take up sufficient cysteine and histidine to grow on MM9 medium. It is possible that both cysteine and histidine could be produced using intermediates from other pathways or other amino acids as precursors. Investigating the connections between cysteine synthesis and other biosynthetic pathways using http://www.genome.jp/kegg [13] revealed that in addition to the de novo pathway for cysteine synthesis it is possible to produce cysteine from glycine, serine, and threonine (Figure 2). The connection between cysteine synthesis and the production of other amino acids may explain why the *rpoN2* mutant, which should not be able to produce cysteine from the *de novo* pathway utilizing CysM, can grow on MM9 medium. As was seen with cysteine synthesis, histidine can also be synthesized from several precursors. HisA is a protein in amino acid metabolism specific to histidine biosynthesis and function in the synthesis of L-histidinol-P and purine metabolism from the pentose phosphate pathway as shown in Figure 3 (http://www.genome.jp/kegg) [13]. This protein was decreased in rpoN2 mutant indicating that it is regulated by RpoN2; however alternative pathways are present that can compensate for loss of HisA dependent histidine production. Our study is the first to identify and demonstrate a role of RpoN2 in *B. pseudomallei*.

In contrast to the similarity of amino acid utilization between the *rpoN2* mutant and the wild type, the *rpoN2*

mutant exhibited decreases in katE expression, both at the transcriptional and at the translational levels. Catalase is ubiquitous, well-studied enzyme that catalyzes the decomposition of hydrogen peroxide. It is an important enzyme for the survival of facultative aerobic organisms exposed to oxidative stress conditions. Using bioinformatics prediction for chromosome 2, a potential RpoN box [4] was identified in front of the katE gene. An activity staining assay for catalase [14] was performed. The results suggest that catalase E or KatE activity is regulated by RpoN2. In particular, the rpoN2 complemented strain fully restores the KatE activity indicating that it is not due to polar effects on downstream genes. To demonstrate that the catalase E activity is regulated at the transcriptional level, qRT-PCR [11, 19, 20] was performed and the result is comparable to the KatE activity detecting from 48 hours to 72 hours of bacterial wild type growth. Interestingly, it has been reported that B. pseudomallei KatE activity [14] may be controlled by RpoS. In that study, the authors demonstrated the catalase activities at the translational level in which the catalase E activity was assessed only by activity staining assay. The contradictory results found in this study are more reliable because we determined that an RpoN box is in front of a katE gene and also because the katE gene expression was detected by qRT-PCR. We therefore hypothesized a possibility of cross communication between these two sigma families, RpoS and RpoN2, via KatE regulation, and that is currently under our investigation.

In conclusion, we report a novel finding that *B. pseudomallei* has 2 copies of RpoN and that RpoN2 is located on chromosome 2. *rpoN2* does not directly function in amino acid utilization in *B. pseudomallei* but it can restore this function in *E. coli*. The constructed *B. pseudomallei rpoN2* mutant lacking KatE activity is demonstrated by activity staining assay and qRT-PCR. In contrast to RpoN1, RpoN2 is therefore involved in a specific function for the regulation of catalase E expression both at the transcriptional and at the translational levels.

Abbreviations

B. pseudomallei: Burkholderia pseudomallei

2DE: Two-dimensional gel electrophoresis

KatE: Catalase E

qRT-PCR: Quantitative Reverse

Transcriptase-Polymerase Chain

Reaction.

Conflict of Interests

The authors declare that their financial supports do not have any conflict of interests regarding the publication of this paper and the grants were only for academic study.

Acknowledgments

The research project was supported by the National Science and Technology Development Agency, Pathum Thani, Thailand, and the Thailand Research Fund. Duong Thi Hong Diep

was supported by the TRIG project from the University of Medicine and Pharmacy at Ho Chi Minh City.

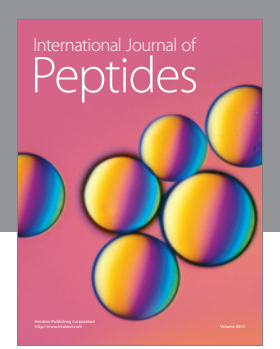
References

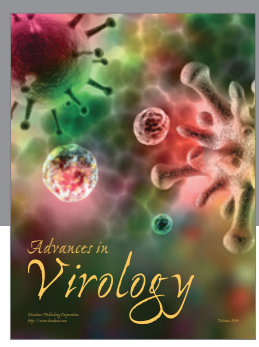
- [1] C. Howe, A. Sampath, and M. Spotnitz, "The *Burkholderia pseudomallei* group: a review," *Journal of Infectious Diseases*, vol. 124, pp. 598–606, 1997.
- [2] J. Sanford and J. R. Douglas, Principles and Practice of Infectious Diseases, Churchill Livingstone Press, New York, NY, USA, 1990
- [3] A. Leelarasamee and S. Bovornkiti, "Melioidosis: review and update," *Reviews of Infectious Diseases*, vol. 11, no. 3, pp. 413–425, 1989
- [4] M. M. S. M. Wösten, "Eubacterial sigma-factors," FEMS Microbiology Reviews, vol. 22, no. 3, pp. 127–150, 1998.
- [5] E. L. Hendrickson, J. Plotnikova, S. Mahajan-Miklos, L. G. Rahme, and F. M. Ausubel, "Differential roles of the *Pseudomonas aeruginosa PA14 rpoN* gene in pathogenicity in plants, nematodes, insects, and mice," *Journal of Bacteriology*, vol. 183, no. 24, pp. 7126–7134, 2001.
- [6] P. A. Totten, J. Cano Lara, and S. Lory, "The rpoN gene product of Pseudomonas aeruginosa is required for expression of diverse genes, including the flagellin gene," Journal of Bacteriology, vol. 172, no. 1, pp. 389–396, 1990.
- [7] K. S. Ishimoto and S. Lory, "Formation of pilin in *Pseudomonas aeruginosa* requires the alternative σ factor (RpoN) of RNA polymerase," *Proceedings of the National Academy of Sciences of the United States of America*, vol. 86, no. 6, pp. 1954–1957, 1989.
- [8] R. Ramphal, L. Koo, K. S. Ishimoto, P. A. Totten, J. C. Lara, and S. Lory, "Adhesion of *Pseudomonas aeruginosa* pilin-deficient mutants to mucin," *Infection and Immunity*, vol. 59, no. 4, pp. 1307–1311, 1991.
- [9] K. B. Low, "Conjugational methods for mapping with Hfr and F-Prime strains," *Methods in Enzymology*, vol. 204, pp. 43–62, 1991.
- [10] M. F. Alexeyev, "The pKNOCK series of broad-host-range mobilizable suicide vectors for gene knockout and targeted DNA insertion into the chromosome of gram-negative bacteria," *BioTechniques*, vol. 26, no. 5, pp. 824–828, 1999.
- [11] J. Sambrook and W. Russell, *Molecular Cloning: A Laboratory Manual*, Cold Spring Harbor Laboratory Press, Cold Spring Harbor, New York, NY, USA, 2001.
- [12] P. Wongtrakoongate, N. Mongkoldhumrongkul, S. Chaijan, S. Kamchonwongpaisan, and S. Tungpradabkul, "Comparative proteomic profiles and the potential markers between *Burkholderia pseudomallei* and *Burkholderia thailandensis*," *Molecular and Cellular Probes*, vol. 21, no. 2, pp. 81–91, 2007.
- [13] Kyoto Encyclopedia of Genes and Genomes (KEGG), "Pathways mapping for cysteine and histidine," 2015, http://www.genome.jp/kegg/pathway.html.
- [14] W. Jangiama, S. Lopraserf, and S. Tungpradabkula, "Role of *Burkholderia pseudomallei* rpoS in regulation of catalase activities under hydrogen peroxide induction," *ScienceAsia*, vol. 34, no. 1, pp. 23–29, 2008.
- [15] M. S. Donnenberg and J. B. Kaper, "Construction of an eae deletion mutant of enteropathogenic *Escherichia coli* by using a positive-selection suicide vector," *Infection and Immunity*, vol. 59, no. 12, pp. 4310–4317, 1991.
- [16] L. Reitzer and B. L. Schneider, "Metabolic context and possible physiological themes of sigma 54-dependent genes in

- Escherichia coli," Microbiology and Molecular Biology Reviews, vol. 65, no. 3, pp. 422–444, 2001.
- [17] M. E. Kovach, R. W. Phillips, P. H. Elzer, R. M. Roop II, and K. M. Peterson, "pBBR1MCS: a broad-host-range cloning vector," *BioTechniques*, vol. 16, no. 5, pp. 800–802, 1994.
- [18] P. Wongtrakoongate, S. Roytrakul, S. Yasothornsrikul, and S. Tungpradabkul, "A proteome reference map of the causative agent of melioidosis *Burkholderia pseudomallei*," *Journal of Biomedicine and Biotechnology*, vol. 2011, Article ID 530926, 5 pages, 2011.
- [19] S. Rozen and H. Skaletsky, "Primer3 on the WWW for general users and for biologist programmers," *Methods in Molecular Biology*, vol. 132, pp. 365–386, 2000.
- [20] P. Wongtrakoongate, S. Tumapa, and S. Tungpradabkul, "Regulation of a quorum sensing system by stationary phase sigma factor RpoS and their co-regulation of target genes in *Burkholderia pseudomallei*," *Microbiology and Immunology*, vol. 56, no. 5, pp. 281–294, 2012.
- [21] Y. Osiriphun, P. Wongtrakoongate, S. Sanongkiet, P. Suriyaphol, V. Thongboonkerd, and S. Tungpradabkul, "Identification and characterization of RpoS regulon and RpoS-dependent promoters in *Burkholderia pseudomallei*," *Journal of Proteome Research*, vol. 8, no. 6, pp. 3118–3131, 2009.
- [22] B. Magasanik, "The regulation of nitrogen utilization in enteric bacteria," *Journal of Cellular Biochemistry*, vol. 51, no. 1, pp. 34–40, 1993.
- [23] M. J. Merrick and R. A. Edwards, "Nitrogen control in bacteria," Microbiological Reviews, vol. 59, no. 4, pp. 604–622, 1995.
- [24] S. Kustu, E. Santero, J. Keener, D. Popham, and D. Weiss, "Expression of sigma 54 (*ntrA*)-dependent genes is probably united by a common mechanism," *Microbiological Reviews*, vol. 53, no. 3, pp. 367–376, 1989.
- [25] J. Michiels, M. Moris, B. Dombrecht, C. Verreth, and J. Vanderleyden, "Differential regulation of *Rhizobium etli rpoN2* gene expression during symbiosis and free-living growth," *Journal of Bacteriology*, vol. 180, no. 14, pp. 3620–3628, 1998.
- [26] D. P. Zimmer, E. Soupene, H. L. Lee et al., "Nitrogen regulatory protein C-controlled genes of *Escherichia coli*: scavenging as a defense against nitrogen limitation," *Proceedings of the National Academy of Sciences of the United States of America*, vol. 97, no. 26, pp. 14674–14679, 2000.
- [27] B. P. Rosen, "Basic amino acid transport in Escherichia coli," The Journal of Biological Chemistry, vol. 246, no. 11, pp. 3653–3662, 1971
- [28] H. Arai, M. Hayashi, A. Kuroi, M. Ishii, and Y. Igarashi, "Transcriptional regulation of the flavohemoglobin gene for aerobic nitric oxide detoxification by the second nitric oxideresponsive regulator of *Pseudomonas aeruginosa*," *Journal of Bacteriology*, vol. 187, no. 12, pp. 3960–3968, 2005.
- [29] T. Kohler, S. Harayama, J. Ramos, and K. Timmis, "Involvement of *Pseudomonas putida* RpoN σ factor in regulation of various metabolic functions," *Journal of Bacteriology*, vol. 171, no. 8, pp. 4326–4333, 1989.
- [30] Y. F. Chang and E. Adams, "D-Lysine catabolic pathway in Pseudomonas putida: interrelations with L-lysine catabolism," Journal of Bacteriology, vol. 117, no. 2, pp. 753–764, 1974.

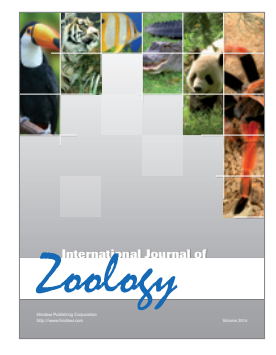








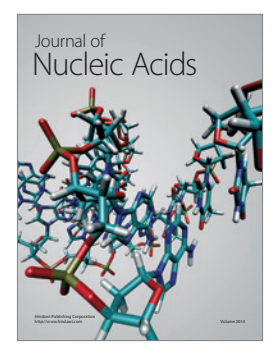




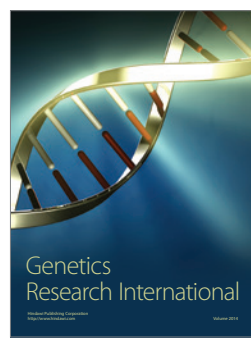




Submit your manuscripts at http://www.hindawi.com





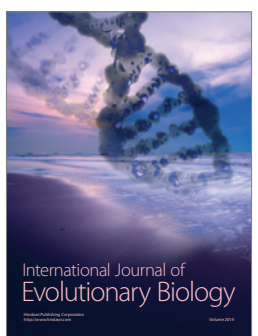


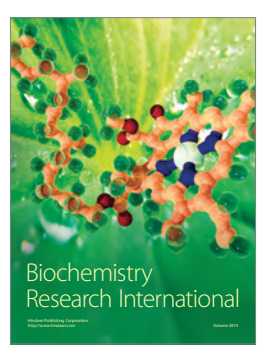
Archaea

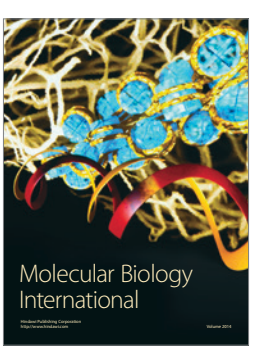


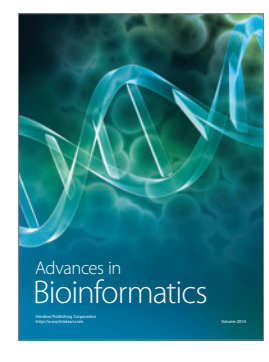
Reséarch

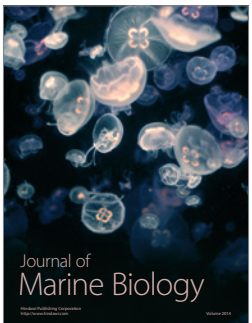












Microbiology and Immunology

Microbiol Immunol 2015; 59: 653–663 doi: 10.1111/1348-0421.12331

ORIGINAL ARTICLE

Correlation between biofilm production, antibiotic susceptibility and exopolysaccharide composition in *Burkholderia pseudomallei bps*I, *ppk*, and *rpo*S mutant strains

Rungrawee Mongkolrob¹, Suwimol Taweechaisupapong² and Sumalee Tungpradabkul¹

¹Biochemistry Department, Faculty of Science, Mahidol University, Rama VI Road, Bangkok 10400, Thailand and ²Melioidosis Research Center and Biofilm research group, Faculty of Dentistry, Khon Kaen University, Khon Kaen 40002, Thailand

ABSTRACT

Burkholderia pseudomallei is the cause of melioidosis, a fatal tropical infectious disease, which has been reported to have a high rate of recurrence, even when an intensive dose of antibiotics is used. Biofilm formation is believed to be one of the possible causes of relapse because of its ability to increase drug resistance. EPS in biofilms have been reported to be related to the limitation of antibiotic penetration in B. pseudomallei. However, the mechanisms by which biofilms restrict the diffusion of antibiotics remain unclear. The present study presents a correlation between exopolysaccharide production in biofilm matrix and antibiotic resistance in B. pseudomallei using bpsI, ppk, and rpoS mutant strains. CLSM revealed a reduction in exopolysaccharide production and disabled micro-colony formation in B. pseudomallei mutants, which paralleled the antibiotic resistance. Different ratios of carbohydrate contents in the exopolysaccharides of the mutants were detected, although they have the same components, including glucose, galactose, mannose, and rhamnose, with the exception being that no detectable rhamnose peak was observed in the bpsI mutant. These results indicate that the correlation between these phenomena in the B. pseudomallei biofilm at least results from the exopolysaccharide, which may be under the regulation of bpsI, ppk, or rpoS genes.

Key words antibiotic resistance, biofilm, exopolysaccharide, gas chromatography-mass spectrometry.

Burkholderia pseudomallei, a Gram-negative aerobic bacterium, is the causative agent of a life-threatening disease of humans known as melioidosis. Many reports have shown that a failure to properly diagnose this disease can lead to adverse outcomes, including death (1–3). As a result of the inherent resistance of B. pseudomallei to many types of antibiotics, a common treatment of melioidosis requires an initial period of intensive treatment, such as CAZ and MRP, for at least 10 days, continued by at least 3 months of prolonged

oral eradication therapy of the appropriate antibiotics such as TMP-SMX plus doxycycline (4). Even when the recommended 20-week intensive antibiotic treatment is followed, the mortality rate from melioidosis remains high (40–50%), and relapse is common in endemic areas (5). The biofilm is a glycocalyx polysaccharide matrix encasing the bacterial population as a barrier to support many functions for the survival of the species, and it may be the cause of disease recurrence (6).

Correspondence

Sumalee Tungpradabkul, Biochemistry Department, Faculty of Science, Mahidol University, Rama VI Road, Bangkok 10400, Thailand. Tel: +02-201-5376; fax: +02-354-7174; email: pexcotung@gmail.com, sumalee.tan@mahidol.ac.th

Received 29 July 2015; revised 12 October 2015; accepted 14 October 2015.

List of Abbreviations: AHL, N-acyl-homoserine lactone; CAZ, ceftazidime; CBD, Calgary Biofilm Device; CLSM, confocal laser scanning microscopy; CV, crystal violet; EPS, extracellular polymeric substances; FITC-conA, fluorescein isothiocyanate-concanavalin A; glk, glucokinase; IMP, imipenem; MRP, meropenem; PI, propidium iodide; TMP-SMX, trimethoprim/sulfamethoxazole; TMS, trimethylsilyl.

The EPS in biofilms are a variety of macromolecules including DNA, proteins, lipids and polysaccharides, the main structural component. The biofilm exopolysaccharides can be presented in many forms such as cell-bound capsular polysaccharides, unbound 'slime' or free exopolysaccharides, and an O-antigen component of lipopolysaccharides (7, 8). Many studies of characterization and structure of the carbohydrate types in biofilm of this bacterium have been reported (9-11). The 'slime' polysaccharides studied were found to consist of galactose, glucose, mannose, rhamnose and two unidentified carbohydrates (12). Moreover, a study of the exopolysaccharide contents in other Burkholderia species, such as Burkholderia cepacia, showed similar components in which the exopolysaccharides were composed of galactose, rhamnose, mannose, glucose, and glucuronic acid (13). Bacteria capable of forming biofilms display enhanced antibiotic resistance compared to their free-living planktonic counterparts. The B. pseudomallei biofilm was reported to be a barrier to the diffusion of some antimicrobial agents, thus limiting the activity and diffusion of the antibiotics (14), but this ability has not been correlated with bacterial virulence (15). Although limitation of antibiotic penetration by B. pseudomallei biofilm has been demonstrated, there remains a need to investigate how the biofilm creates the ability to retard the penetration of antibiotics.

Three *B. pseudomallei* mutants defective in the *bps*I, *rpo*S, and *ppk* genes were previously constructed and described by our laboratory (16–18). *B. pseudomallei bps*I encodes autoinducer synthase, which is important for the synthesis of the quorum-sensing signal molecule AHL (16). The alternative sigma factor S (sigma 38 or *rpo*S) is important for survival under conditions of stress (17). The polyphosphate kinase gene, *ppk*, encodes an enzyme responsible for the synthesis of inorganic polyphosphate from ATP, which has been reported to be relevant in biofilm formation (18). In addition, previous studies from other Gramnegative bacteria have shown that these regulatory genes have roles in biofilm antibiotic resistance (19–22).

In the present study, we carried out a correlation between exopolysaccharide production in the biofilm matrix and antibiotic resistance in *B. pseudomallei* by using *bps*I, *ppk*, and *rpo*S mutant strains. Similar reductions in exopolysaccharide production and antibiotic resistance, including different ratios of monosaccharide types in the exopolysaccharides of the biofilm, have been observed in the mutant strains, suggesting that our genes of interest have specific effects on exopolysaccharide production, leading to the

ineffective function of the biofilm matrix as an antibiotic barrier.

MATERIALS AND METHODS

Bacterial strains and culture conditions

Table 1 lists the strains of *B. pseudomallei* used in the present study. PP844 is a clinical isolate from the blood of a melioidosis patient (23, 24). The three *B. pseudomallei* mutant strains lacking the *bps*I, *ppk*, and *rpo*S genes were constructed as previously described (16–18). Bacteria were grown on LB agar and subcultured in Modified Vogel and Bonner's medium (MVBM), a specific medium used to promote the formation of biofilms (6). For the *B. pseudomallei* mutant strains, tetracycline was added to the media at a 60 μg/mL final concentration when required. All *B. pseudomallei* strains had similar growth rates in MVBM media until 36 hr (data not shown).

Biofilm visualization using CLSM

A single colony of bacteria cultured on a LB agar plate was inoculated in 5 mL MVBM at 37°C overnight. The precultures of each bacterial strain were adjusted to obtain an initial cell concentration of 10⁷ CFU/mL. A final volume (1 mL) of each inoculum was placed in each well of a 24-well plate having a plastic cover slip underneath, and the plates were statically incubated at 37°C for 24 hr. Visualization of the biofilm-forming bacteria using CLSM was carried out as previously described (18) with slight modifications. Briefly, surface-attached cells on a plastic cover slip were washed three times with $0.15 \,\mathrm{M}$ PBS (pH = 7.0) and fixed by 2.5% v/v glutaraldehyde in PBS with a pH of 7.0 at 4°C for 3 hr. After three washes with PBS, the fixed (dead) bacterial biofilm was stained with FITC-ConA (50 µg/mL), which reacts with the exopolysaccharides of the biofilm, at room temperature for 15 min. After washing, the bacterial biofilm was stained with 8 µM PI at room temperature for 45 min. The cover slips were mounted and visualized using a FluoView FV10i-DOC confocal microscope (Olympus, Tokyo, Japan). Two independent experiments were carried out and each B. pseudomallei strain was captured with five different fields. All confocal images were digitized and analyzed with FV10-ASW 3.0 Viewer software to obtain the thicknesses of the biofilms by z-axis scanning, the integrated fluorescent intensities of the biofilms and other parameters. Biofilm thickness and exopolysaccharide integrated fluorescent intensity were statistically transformed into logarithms and were tested by one-way anova. All

Table 1. Bacterial strains and plasmids used in the present study

Strain or plasmid	Genotype or relevant characteristic	Reference	
Burkholderia pseudomallei WTPP844 bpsIM	Prototroph, blood culture isolate from a patient at Khon Kaen University Hospital PP844:: pKBI	(23, 24) (16)	
ppkM	NF10/38:: pKPPK	(18)	
rpoSM	PP844:: pKBS1	(17)	
Plasmids			
pKBI	pKNOCK-Tc containing a 298-bp internal segment of the B. pseudomallei bpsl gene	(16)	
рКРРК	pKNOCK-Tc containing a 500-bp internal segment of the B. pseudomallei ppk gene	(18)	
pKBS1	pKNOCK-Tc containing a 600-bp internal segment of the <i>B. pseudomallei rpoS</i> gene	(17)	

pairwise comparisons were further tested by the Fisher least significance difference (LSD) method at an alpha level of 0.05.

Antibiotic resistance analysis of planktonic and biofilm conditions using CBD

The CBD is available through MBEC Biofilms Technology Ltd (Calgary, AB, Canada). Antibiotic susceptibility tests between planktonic- and biofilm-promoting conditions within the same strain were carried out as described by Ceri et al. (25) with slight modifications (6). The CDB is a 96-well microtiter plate with a lid containing 96 pegs sealed on the top. The pegs are designed to fit into the channels of a standard 96-well plate and canalize the flow of medium across the pegs to produce consistent shear force in each well, resulting in equivalent biofilm formation at each peg site (25). Bacterial biofilms were formed on each peg by culturing cells in MVBM with specific conditions at an initial bacterial concentration of 10⁷ CFU/mL. Each bacterial suspension (150 µL) was placed in the 96-well microtiter plate. Rows of the plate were arranged with three replicates for each strain, with one row containing only media to serve as a negative control. The plates were incubated with shaking at 100 r.p.m. at 37°C for 24 hr. CAZ and MRP were separately serially diluted in Mueller Hinton Broth (MHB) medium in a new 96-well microtiter plate from 1024 µg/mL to 1 µg/mL with a final test volume of 200 µL per well. Antibiotic-free MHB medium was added into one column to serve as the growth control. After the biofilms formed on the lids of the CBD, the remaining planktonic cells were removed by rinsing with normal saline. Bacteria present in the biofilm lid were challenged with CAZ and MRP at 37°C for 24 hr. Following the challenge step, the peg lid was washed to remove any residual antimicrobial agents. Turbidity of the challenge plates was checked by using a microtiter plate reader at 620 nm to determine survival of the planktonic bacteria. The peg lids were then placed over a new 96-well microtiter plate containing fresh MHB medium. The peg-attaching biofilm was removed by sonication for 5 min. After incubation for an additional 24 hr at 37°C, the presence of a viable bacterial biofilm was determined by monitoring the turbidity at 620 nm. The surviving planktonic and biofilm bacteria were reported as IC_{50} values of bacterial inhibition or half-maximal inhibitory concentration for comparison between the two antibiotic conditions. Results were statistically tested within the group by one-way anova. All pairwise comparisons were further tested by the Fisher LSD method at an alpha level of 0.05.

Isolation of the biofilm exopolysaccharides using ethanol precipitation

Overnight bacterial cultures were started with 1% v/v inoculums into 300-mL cultures of MVBM under specific conditions in a 500-mL flask. The bacteria were statically cultured at 37°C for 4-5 days. The biofilm-pellicle was gathered from the top of the culture using a 10-mL pipette with a final medium volume of <5 mL. Extracellular matrix isolation was carried out as previously described with slight modifications (26). Briefly, after washing with 10 mL of sterile distilled H₂O, the pellicle was treated with 25 mL of 1 M NaOH and vortexed for 30 min. The treated pellicle was centrifuged at 200,000 g in a SW70 Ti rotor of Optima LE80K ultracentrifuge (Beckman Coulter, CA, USA) for 1 hr at 4°C. A 0.2-μm sterile filter was used for purifying the supernatant prior to neutralization with 12 M HCl. The digested exopolysaccharide was precipitated by adding ethanol to a 70% final concentration, and then it was placed at -20°C overnight. The precipitant of the carbohydrate-bound salts was collected by centrifugation at 29,581 g in a Sorvall SLA-1000TC rotor of highspeed Refrigerated Centrifuge (Sorvall® RC-5C plus) (Thermo Fisher Scientific, MA, USA) for 45 min at 4°C. After washing with 70% ethanol and air-drying for 1 hr, the pellet was dissolved in water and lyophilized

overnight. The lyophilized product was resuspended in water, which was followed by dialysis against 4L water three times. The purified carbohydrates were lyophilized again before the analysis of carbohydrate composition by gas chromatography-mass spectrometry (GC-MS) (26).

Exopolysaccharide composition analysis

Exopolysaccharide composition analysis of the extracellular matrix extracted from B. pseudomallei was done using GC-MS as previously described (27). Prior to analysis, the exopolysaccharides were methanolysed to turn them into methyl glycosides, and then they were further derivatized using TMS reagents to become volatized TMS derivatives (26). Methyl glycosides were produced from 0.5 mg of dry sample by methanolysis in 1-M methanolic HCl at 80°C for 20 hr, followed by Nacetylation of acetic anhydride and pyridine in methanol overnight to re-acetylate the *N*-acetyl group of the amino sugars. The samples were then trimethylsilylated by treatment with excess Tri-Sil® reagent HMDS-TMCS in pyridine (Pierce, Rockford, IL) at 80°C for 30 min. After evaporation of the excess Tri-Sil reagent, TMS methyl glycosides were rinsed with 1 mL hexane, which was followed by repeated evaporation. The purified TMS derivatives were resuspended with 100 µL hexane. Standard monosaccharides were derivatized along with samples and myo-inositol was used as an internal standard (27). One microliter of TMS methyl glycosides in hexane was injected (split at 1:50) onto an Agilent Hewlett Packard gas chromatograph (Agilent Technologies, CA, USA) with an autosampler interfaced with a 5973N MSD (Agilent Technologies, CA, USA) using a HP-1 fused silica capillary column (Agilent Technologies, CA, USA) (25 m \times 0.32 mm \times 0.17 μ m). Identification of the monosaccharide components was based on comparison of the retention times with those of the standard monosaccharides, and the amount of each monosaccharide type was calculated as previously described (27). The ratio of the monosaccharide amounts in each strain was calculated and statistically tested by one-way anova followed by the Fisher LSD method at an alpha level of 0.05. Triplicate independent experiments were carried out.

As a result of the distinct capacity for biofilm formation in each *B. pseudomallei* strain, the amount of each monosaccharide in the exopolysaccharides formed in the purified carbohydrate may not have correctly represented the effects of mutated genes on biofilm production capacity. Therefore, the biofilm capacity factors in each strain were calculated from the exopolysaccharide integrated fluorescent intensity according to the following formula, for which the wild-

type strain was designed as the positive control and was used to subtract all of the carbohydrate contents:

 $Biofilm\ capacity\ factors = \frac{intensity\ of\ the\ mutant}{exopolysaccharide\ integrated\ fluorescent}$ $intensity\ of\ the\ wild\ type$

RESULTS

Characteristics of biofilm formation in *B.* pseudomallei mutants

In earlier studies, the relevant functions of the genes of interest for biofilm formation have been reported in many bacteria. To investigate characteristics of biofilm formation among bpsI, ppk, and rpoS B. pseudomallei mutant strains, CLSM was used to visualize the architecture, thickness and exopolysaccharide production in the biofilms of each of the *B. pseudomallei* strains. It is apparent that all B. pseudomallei mutants were defective in their abilities to form biofilms. Figure 1 illustrates the characteristics of the biofilms among the *B*. pseudomallei strains. The wild type obviously showed micro-colony formation with the highest thickness at $15.33 \pm 3.67 \,\mu\text{m}$, whereas mutant strains rarely formed a large micro-colony, as indicated in Figure 1. Although characteristics of cell aggregation can be observed in all of the mutants, especially in the bpsI mutant, these characteristics cannot imply that micro-colonies were formed because of the smaller thicknesses (approximately 6 µm). The exopolysaccharide integrated fluorescent intensity was calculated from five observed fields using FV1000 Viewer software as shown in Figure 2. The results demonstrate that each of the B. pseudomallei mutant strains had significantly lower exopolysaccharide production than the wild type. The bpsI mutant had higher exopolysaccharide production than the ppk mutant followed by the *rpoS* mutant ($P \le 0.001$). Based on the experimental data, it appears that our genes of interest have specific influences on biofilm formation in B. pseudomallei, which correspond to previous reports (21, 28-29). Although CLSM can provide more details on biofilm architecture, the ability for the enhancement of drug resistance, as a major biofilm capability, could provide greater understanding of the function of the biofilm.

Effect of different biofilm formation abilities on antibiotic resistance

Biofilm formation is known to alter antibiotic resistance in many bacteria (6). Thus, it is interesting to investigate whether the different biofilm formation abilities among

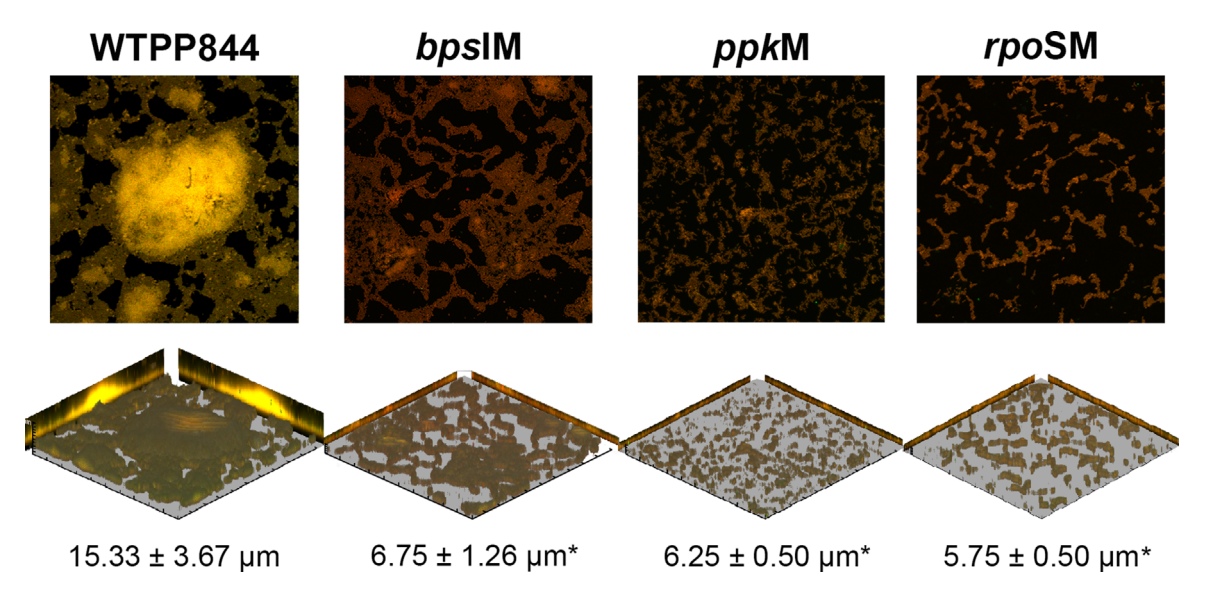


Fig. 1. Micro-colony characteristics and biofilm thickness of *Burkholderia pseudomallei* wild type as well as *bpsl*, *ppk*, and *rpoS* mutant strains using CLSM are represented in μ m \pm SD. Asterisks indicate that there is no significant difference within those strains.

the *B. pseudomallei* mutants can affect the antibiotic resistance function of the biofilm. The antibiotic resistances of the *B. pseudomallei* mutants were investigated using both planktonic- and biofilm-forming conditions by the CDB, a commercial device used for testing antibiotic susceptibility. All *B. pseudomallei* strains were tested simultaneously in 96-well microtiter plates with two independent biological replicates. CAZ and MRP were chosen because these drugs are currently used in the treatment of melioidosis. All of the *B. pseudomallei* strains under planktonic conditions displayed a similar IC₅₀ for CAZ and MRP, which was

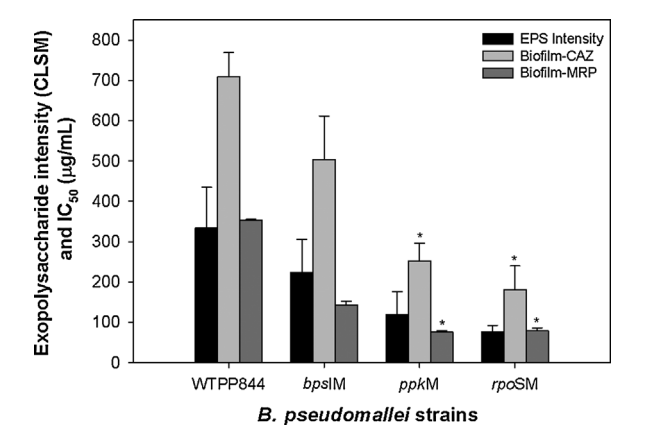


Fig. 2. Comparisons between exopolysaccharide integrated fluorescent intensity (EPS intensity) and the IC_{50} values of CAZ and MRP treatments (CAZ-treated biofilm; and CAZ-treated biofilm) in biofilms of *Burkholderia pseudomallei* wild type and the three mutant strains. Asterisks within the same group indicate no significant difference ($P \le 0.001$).

approximately 0.5–1 µg/mL (data not shown). Under biofilm-promoting conditions, the IC₅₀ values for both drugs were significantly increased 100–700-fold as shown in Figure 2. The IC₅₀ values of biofilm treated with CAZ in the *bps*I, *ppk*, and, *rpo*S strains were approximately 29%, 64% and 74% lower than for the *B. pseudomallei* wild type, respectively, whereas the IC₅₀ values of biofilm-treated with MRP for the mutant strains decreased by approximately 60%, 79% and 77%, respectively ($P \le 0.001$). Notably, IC₅₀ values for CAZ were roughly two- to three-fold greater than those observed for MRP, which is consistent with results obtained in the previous study (14).

The IC₅₀ values of biofilm treated with CAZ show differences among the B. pseudomallei biofilms from mutant strains in contrast to the IC₅₀ values of biofilm treated with MRP, which are similar to each other. The bpsI mutant displayed higher antibiotic resistance than any of the other mutants with both CAZ and MRP treatment ($P \le 0.001$), indicating that lack of the bpsI gene did not greatly alter its biofilm formation. Although there is no significant difference between the capability for antibiotic resistance in biofilm ppk and rpoS mutants, they still both have particular biofilm formation abilities. This suggests that these two genes cause specific influences on the production of the biofilm, which greatly affects the biofilm structure resulting in the reciprocal decrease in antibiotic resistance. As a similar trend between the exopolysaccharide production by CLSM and the IC50 values of CAZ and MRP treatments was observed, it may imply that there is a possible link between these two phenomena, which may be under the regulation of the *B. pseudomallei* biofilm genes investigated.

Exopolysaccharide composition in *B. pseudomallei* mutant strains

EPS of the biofilm are suggested as a major barrier in the protection of bacteria from a hostile environment and contain exopolysaccharides as the principal structural component (8). Thus, it is possible that reduction of the drug resistance capability in biofilm B. pseudomallei mutants may result from defects in the exopolysaccharide architecture. To investigate whether mutations of the bpsI, ppk, and rpoS genes result in alterations in the carbohydrate compositions of the biofilm, the exopolysaccharide matrix was isolated and ethanol-precipitated. TMS derivatives of the lyophilized biofilm glycoconjugates were further analyzed using GC-MS with triplicate independent samples. Table 2 illustrates the carbohydrate contents of 0.5 mg purified biofilm exopolysaccharide material of B. pseudomallei wild type and all of the mutant strains. The ratio of the carbohydrate contents in each strain was calculated by using glucose as a calibrator because this sugar is commonly found in other bacterial exopolysaccharide matrices (12, 13, 30). The carbohydrates in the exopolysaccharide matrix of the wild-type biofilm are glucose, galactose, mannose, and rhamnose in the ratio 1.00:1.31:0.82:0.30. Noticeably, glucose and mannose are the main components in equal amounts, whereas galactose also appears to be a major component ($P \le 0.001$), which is consistent with a previous report (13). The exopolysaccharide matrices of the B. pseudomallei mutant strains contain the same carbohydrate contents; however, shifts in the ratios of the contents can be observed. The bpsI mutant exhibits a different carbohydrate content ratio (1.00:1.04:1.63:ND), in which mannose becomes the major component instead of galactose as in the wild type. Interestingly, the monosaccharide content of this mutant is likely to be increased, whereas no detectable peak of rhamnose was observed, as shown in Table 2. Likewise, the ppk and rpoS mutants contain distinct carbohydrate content ratios of 1.00:1.23:1.18:0.10 and 1.00:1.08:1.44:0.06, respectively, in which no significant difference was found between the glucose, galactose and mannose in the ppk mutant (Table 2). Similar trends in the carbohydrate ratios were revealed between the bpsI and rpoS mutants, with mannose as the major component. Perceptibly, a remarkable reduction in the rhamnose content can be observed in all of the mutants, especially in the bpsI mutant. Therefore, it is possible that the genes of interest may be involved in the regulation of rhamnose biosynthesis. As the mannose contents were elevated

Table 2. Carbohydrate contents in the exopolysaccharide matrix of the Burkholderia pseudomallei biofilm

	Carbohyd	Carbohydrate contents $(\mu g \pm \text{SD})\!/0.5\text{mg}$ purified exopolysaccharides	mg purified exopolysacch	arides	Carbohydrat	Carbohydrate contents ($\mu g \pm SD)\!/biofilm$ production capacity))/biofilm productio	n capacity
B. pseudomallei strains	Glucose (Ratio)	Galactose (Ratio)	Mannose (Ratio)	Rhamnose (Ratio)	Glucose	Galactose	Mannose	Rhamnose
WTPP844	84.27 ± 8.71 (1.82)*	$100.91 \pm 7.19 (1.31)$	$68.75 \pm 8.41 \ (0.82)^*$	26.55 ± 9.09 (0.30) 84.27 ± 8.71	84.27 ± 8.71	110.61 ± 2.60	68.75 ± 8.41	26.55 ± 9.91
MIsdq	$100.91 \pm 7.19 (1.00)^*$	$105.14 \pm 10.02 \ (1.04)^*$	$164.61 \pm 13.39 (1.63)$	QN.	67.53 ± 4.81	70.36 ± 6.71	110.16 ± 8.96	ΔN
ppkM	$71.53 \pm 39.67 (1.00)^*$	$87.84 \pm 39.33 \ (1.23)^*$	84.24 ±45.32 (1.18)*	$7.03 \pm 5.24 (0.10)$	25.36 ± 14.06	31.14 ± 13.94	29.86 ± 16.07	2.49 ± 1.86
rpoSM	$105.78 \pm 4.67 \; (1.00)^*$	$114.50 \pm 14.86 \; (1.08)^*$	$152.45 \pm 4.92 \ (1.44)$	$6.06 \pm 1.59 \ (0.06)$ 23.89 ± 1.06	23.89 ± 1.06	25.86 ± 3.36	34.43 ± 1.11	1.37 ± 0.36

*No significant difference between these monosaccharide ratios ND, no detection of the carbohydrate peak. in both the *bpsI* and *rpoS* mutant strains, which also included rhamnose reductions, we speculated that a correlation between the mannose and rhamnose synthetic pathways should exist, which is modulated by these genes. In addition, this carbohydrate composition analysis of the exopolysaccharides was studied from equal amounts of purified carbohydrate material; nevertheless, each *B. pseudomallei* strain has a unique capacity for biofilm formation as previously reported. Thus, to obtain a more precise view of the effects of these genes on the biofilm production capacity, recalculation of the carbohydrate contents was done according to the biofilm capacity.

The specific biofilm capacity factors were calculated from each exopolysaccharide integrated fluorescent intensity by CLSM and used to subtract all of the carbohydrate contents as reported in Table 2. Figure 3 compares the subtracted carbohydrate contents among B. pseudomallei strains. It can be clearly seen in Figure 3 that there are shifts in the carbohydrate ratio and a modulated production of the monosaccharide types. Noticeably, the glucose and galactose contents were dramatically reduced in all of the mutants, especially in the ppk and rpoS mutants by approximately 70–72% and 72-77%, respectively. Although the bpsI mutant displayed reductions in the glucose and galactose contents, it showed only 20% and 36% lower contents compared to the wild type. Together with glucose and galactose production, all of the mutants also showed massive reductions in the rhamnose contents by 91-95% for the ppk and rpoS mutants, whereas no rhamnose production was detected in the bpsI mutant. Surprisingly, although

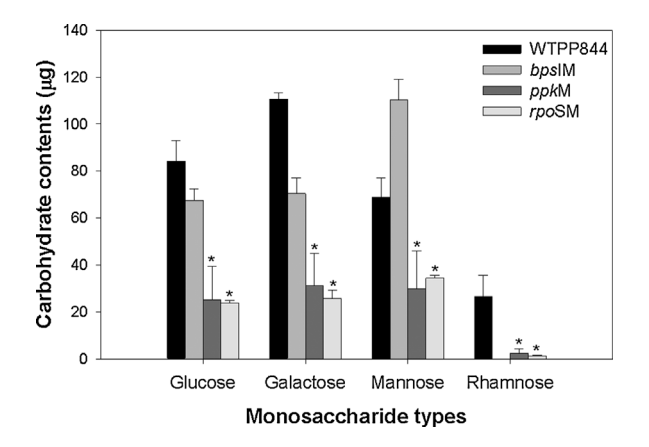


Fig. 3. Carbohydrate contents of the exopolysaccharides produced by *Burkholderia pseudomallei* wild-type and mutant strains after subtraction from the biofilm production capacity determined by CLSM were compared to each other;

BPWT; = bpsIM; = ppkM; = rpoSM.

Asterisks indicate no significant difference between those strains within a monosaccharide type.

mannose production in the *ppk* and *rpo*S mutants was reduced by 57% and 50%, respectively, the mannose content of the *bps*I mutant increased by up to 60% compared to the wild type. Consistent with the previous results, the *bps*I mutant has a lower effect on the biofilm exopolysaccharide composition than the other mutants because of its higher production of glucose, galactose and mannose. Therefore, these results suggest that the exopolysaccharide compositions of *B. pseudomallei* biofilms are modulated by *bps*I, *ppk*, and *rpo*S genes resulting in defects of the core biofilm polysaccharide structure, which may influence the antibiotic resistance.

DISCUSSION

Biofilm-forming bacteria are well known to be capable of enhancing antibiotic resistance compared to their planktonic counterparts. EPS in the biofilm have been reported to be the greatest barrier to diffusion for drug penetration into various bacteria (8). Previous studies from other Gram-negative bacteria have shown that drug resistance in the biofilm partly involves quorum-sensing communication and many regulatory genes, including *ppk* and *rpoS* genes (20–22). In *B. pseudo-mallei*, the biofilm was reported to be a diffusion barrier for some of the antimicrobial agents; however, how the biofilm has the ability to retard antibiotic penetration is still unrevealed.

Using B. pseudomallei mutants (bpsI, ppk, and rpoS) previously constructed and characterized by our group, we have demonstrated a correlation between biofilm production and antibiotic resistance under the regulation of these genes. The B. pseudomallei mutants displayed a significant defect in micro-colony formation, biofilm thickness, and exopolysaccharide production along with a reduction in the antibiotic resistance of the biofilm, suggesting that the loss of antibiotic resistance ability is a consequence of a defective biofilm as a result of the mutated gene. This finding extends those of Pibalpakdee et al. (14), confirming that the B. pseudomallei biofilm generates a restrictive diffusion barrier for some types of antimicrobial agent, such as CAZ and imipenem (IMP) (14), and our genes of interest may play an important role in this phenomenon. A substantial difference, which was almost two-fold, in the biofilmtreated IC50 values of B. pseudomallei wild type was observed between CAZ and MRP. As CAZ has a larger chemical structure than MRP, this suggests that the biofilm likely poses a diffusion barrier for larger antimicrobial agents. This corresponds well with previous studies suggesting that small molecules should not be limited by biofilms (31, 32). According to the intermediate reduction in the biofilm capability and

antibiotic resistance in the *bps*I mutant, it may be implied that this gene should have less involvement in biofilm resistance than the *ppk* and *rpo*S genes. Noticeably, positive regulation of *rpo*S on *bps*I expression and auto-inducer production on a stationary phase has been reported (33). Thus, this study supports the assumption that the *rpo*S gene has more effect on biofilm characteristics than does the *bps*I gene. Our finding therefore indicates that the *bps*I, *ppk*, and *rpo*S genes have specific roles in biofilm formation and in the antibiotic resistance of *B. pseudomallei*.

As EPS has been reported as the diffusion barrier of the biofilm, correlation with these phenomena of B. pseudomallei mutants may involve the production of the matrix. In the present study, GC-MS analysis of the biofilm exopolysaccharides revealed that the mutated genes apparently affect the carbohydrate composition ratio. The exopolysaccharide matrix of the B. pseudomallei wild-type biofilm is composed of glucose, galactose, mannose, and rhamnose in the ratio 1.00:1.31:0.82:0.30, with the major component being galactose. Our result is compatible with previous carbohydrate composition analysis of the biofilm exopolysaccharide matrix in Burkholderia cepacia, which is composed of glucose, galactose (the major component), mannose, rhamnose, and glucuronic acid (13). The carbohydrate contents found in all of the B. pseudomallei mutant biofilms contain the same components as the wild type, but the ratios and the major components are different. The mutants obviously showed a dramatic reduction in rhamnose production in the biofilm exopolysaccharide matrix, especially in the bpsI mutant in which rhamnose cannot be detected. Compared with the defective drug resistance in all of the mutants, it may be assumed that the loss of rhamnose can be considered to be the cause of the disruption to the biofilm matrix leading to the diffusion barrier of the biofilm being partially disabled. Remarkably, the carbohydrate contents of the bpsI mutant are negligibly reduced, and the mannose content is significantly increased, suggesting that the matrix structure of this mutant is slightly perturbed resulting in an intermediate effect on the reduction of the antibiotic resistance, which may come from the absence of rhamnose. Whereas the intermediate influence of the bpsI mutation on the exopolysaccharide composition resulted in moderately reduced drug resistance, the ppk and rpoS genes caused significant impacts on every carbohydrate composition, corresponding to significant decreases in their antibiotic-resistant abilities. From the data gained in this study, it can be suggested that the exopolysaccharide composition of the biofilm matrix is the major structural content important for blocking antibiotic diffusion.

The exopolysaccharide matrix from the bpsI and rpoS mutants revealed a significant increase in mannose and the loss of rhamnose production, indicating that there should be a correlation between the mannose and rhamnose biosynthetic pathways. From the nucleotide sugar precursors for the exopolysaccharide pathway of Burkholderia cepacia IST408, it was reported that UDPgalactose is synthesised from UDP-glucose and that GDP-mannose is the precursor for GDP-rhamnose synthesis (34). As the exopolysaccharide contents of B. cepacia have similar components to our finding (13), it may have similar exopolysaccharide biosynthetic pathways in B. pseudomallei biofilm. In order to find a possible model of exopolysaccharide production in B. pseudomallei biofilm which should be under the regulation of the investigated genes, comparative analysis of the exopolysaccharide biosynthetic enzymes annotated in each step of the pathway of B. cepacia was carried out by database searching in B. pseudomallei. As shown in Figure 4, all of the enzymes needed for the synthesis of activated sugar precursors for the exopolysaccharide biosynthetic in B. pseudomallei were identified. To verify how our interested genes may be involved in the regulation of these exopolysaccharide biosynthetic enzymes, upstream regions of each enzyme were used to predict for bpsI- and rpoS-dependent promoters by using the Hidden Markov Model (HMM) as previously described (35), with prediction training sets created from bpsI- and rpoS-dependent genes in B. pseudomallei (35, 36). As shown in Figure 4, BPSL2769 or UTP glucose-1-phosphate uridylyltransferase (EC 2.7.7.9) and wcbK-BPSL2729, which is GDP-mannose-4,6-dehydratase (EC 4.2.1.47), were predicted to be under bpsI regulation because both of them were predictably found the lux-box-like promoters of the bpsI gene in the upstream regions (data not shown). WcbK-BPSL2729 is responsible for converting UDPmannose into GDP-4-oxo-6-deoxy-D-mannose, which is further used as a precursor for UDP-rhamnose synthesis. Therefore, our observation supports that bpsI might regulate the production of glucose, galactose and rhamnose in exopolysaccharide biofilm via the biosynthetic enzymes. While bpsI has a chance to control two genes among all of the biosynthetic enzymes, the rpoS-dependent promoter was predictably identified in many enzymes, including glucokinase (glk-BPSL2614), UDP-glucose-1-phosphate uridylyltransferase (gtaB-BPSS1682), UDP-glucose 4-epimerase (BPSL2670) and GDP-mannose-4,6-dehydratase (BPSL2729) (data not shown). All of these enzymes are involved in either the conversion of UDP-glucose into UPD-galactose or in the conversion of GDP-mannose into GDP-rhamnose, especially glucokinase (glk), which functions in the first

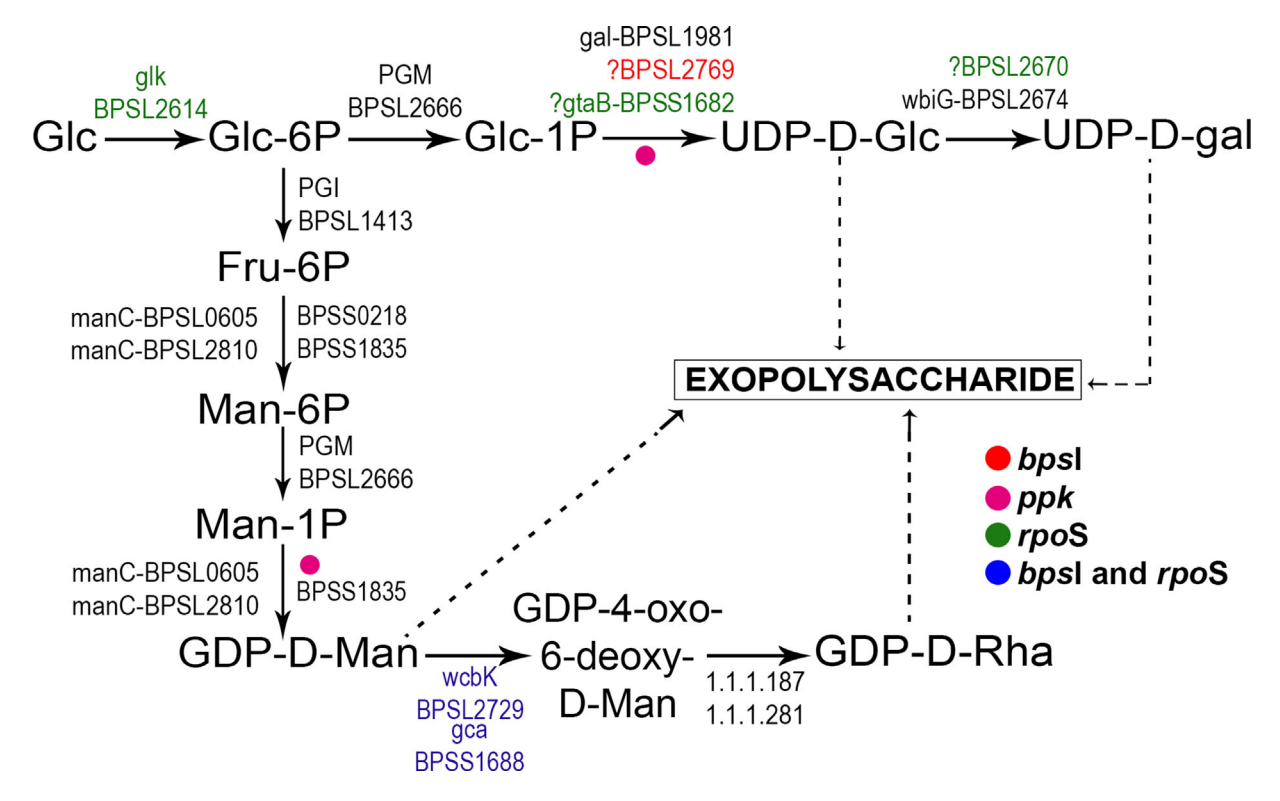


Fig. 4. Postulated biosynthetic pathway of the nucleotide sugar precursors for the biofilm exopolysaccharides. Enzymes predicted to be under *bps*I regulation (red abbreviations), *rpo*S regulation (green abbreviations) and both *bps*I and *rpo*S regulation (blue abbreviations) are indicated. The steps postulated to be involved with *ppk* function are illustrated with pink spots.

step of the pathway (Fig. 4). Notably, this observation supports our results that bpsI and rpoS might control the transcription of some biosynthetic enzymes important for production of activated sugar precursors for exopolysaccharide biosynthesis, especially rpoS, which should be involved in all of the carbohydrate synthesis, resulting in significant decreases in all of the carbohydrate contents. Interestingly, a correlation between quorum sensing and rhamnose synthesis, which is an important polysaccharide in biofilm formation, has been reported (37). It has been shown that Pseudomonas aeruginosa uses acyl-homoserine lactone signals during cell-cell communication to coordinate the expression of genes responsible for the production of polysaccharides in biofilm as well as in other virulence factors (37). Moreover, the function of the bpsI gene in cell-cell communication for micro-colony formation and the determination of the ultimate 3-D architecture of the mature biofilm have been described (29). In agreement with our observation, this finding confirms that bpsI is not only involved in quorum sensing but also in the control of polysaccharide synthesis, especially in rhamnose production. The explicit alteration of the carbohydrate content ratio found in the ppk mutant biofilm extends the understanding of ppk function in the biofilm stage as reported by Tunpiboonsuk *et al.*, who postulated that *ppk* is involved in supplementing energy for every step of biofilm formation (18). Activation of sugar precursors for exopolysaccharide synthesis requires inorganic polyphosphate produced from ATP by the *ppk* gene; thus, it is possible that a mutation of this gene may result in inactivated sugars. The exopolysaccharide framework therefore could not be formed and would cause a further dramatic impact on the antibiotic resistance of the mutant. In conclusion, the exopolysaccharides of the biofilm matrix in *B. pseudomallei* are composed of the following three major carbohydrate types: glucose, galactose and mannose, which could be controlled by the investigated genes.

Our results provide insight into a correlation between biofilm formation and antibiotic resistance in *B. pseudomallei*, in which the exopolysaccharides could be the main components in creating the diffusion barrier for the antibiotics, although other EPS components may collaborate thereby raising the antibiotic resistance in the biofilm. The exopolysaccharide production in the biofilm of *B. pseudomallei* remarkably showed a particular production ability reciprocal to drug resistance, in which the *bpsI* gene could play a specific function in rhamnose synthesis. Meanwhile, the *ppk* and

rpoS genes uniquely influence the synthesis of all of the carbohydrates, and the connection between the mannose and rhamnose biosynthetic pathways can be observed in all of the mutants, particularly for the bpsI gene mutant. Most notably, to our knowledge, this is the first study in which the rpoS gene displayed a particular function on exopolysaccharide biosynthesis in B. pseudomallei, which is relevant to drug resistance. However, the molecular perception of regulation of exopolysaccharide synthesis through these genes remains to be investigated. This knowledge may help the understanding of the antibiotic resistance mechanism in the biofilm of B. pseudomallei. Therefore, an important goal for future studies is to determine the molecular insight of such genes on exopolysaccharide production and the roles of other EPS components in the drug resistance of the biofilm.

ACKNOWLEDGMENTS

This work was supported by the Thailand Research Fund and a grant to R. Mongkolrob from the Office of the Higher Education Commission. We thank Dr Sakawrat Kanthawong, Faculty of Medicine, Khonkan University, for her assistance with the CDB device. CLSM was operated at the Bioimaging Center, Faculty of Science, Mahidol University. GC-MS was operated by Mr Sirichai Kositarat, Central Instrument Facility, Faculty of Science, Mahidol University.

DISCLOSURE

No authors have any conflicts of interest to declare.

REFERENCES

- Ulrich R.L., Deshazer D., Brueggemann E.E., Hines H.B., Oyston P.C., Jeddeloh J.A. (2004) Role of quorum sensing in the pathogenicity of Burkholderia pseudomallei. *J Med Microbiol* 53: 1053–64.
- 2. Dance D.A. (1991) Melioidosis: the tip of the iceberg? *Clin Microbiol Rev* 4: 52–60.
- Brent A.J., Matthews P.C., Dance D.A., Pitt T.L., Handy R. (2007) Misdiagnosing melioidosis. Emerg Infect Dis 13: 349–51.
- 4. Chetchotisakd P., Chierakul W., Chaowagul W., Anunnatsiri S., Phimda K., Mootsikapun P., Chaisuksant S., Pilaikul J., Thinkhamrop B., Phiphitaporn S., Susaengrat W., Toondee C., Wongrattanacheewin S., Wuthiekanun V., Chantratita N., Thaipadungpanit J., Day N.P., Limmathurotsakul D., Peacock S.J. (2014) Trimethoprim-sulfamethoxazole versus trimethoprim-sulfamethoxazole plus doxycycline as oral eradicative treatment for melioidosis (MERTH): a multicentre, double-blind, non-inferiority, randomised controlled trial. Lancet 383: 807–14.
- Patel N., Conejero L., De Reynal M., Easton A., Bancroft G.J., Titball R.W. (2011) Development of vaccines against Burkholderia pseudomallei. Front Microbiol 2: 198.

- Sawasdidoln C., Taweechaisupapong S., Sermswan R.W., Tattawasart U., Tungpradabkul S., Wongratanacheewin S. (2010) Growing Burkholderia pseudomallei in biofilm stimulating conditions significantly induces antimicrobial resistance. PLoS One 5:e9196.
- Bazaka K., Crawford R.J., Nazarenko E.L., Ivanova E.P. (2011)
 Bacterial extracellular polysaccharides. Adv Exp Med Biol 715:
 213–26
- Martin C., Low W.L., Gupta A., Amin M.C., Radecka I., Britland S.T., Raj P., Kenward K.M. (2014) Strategies for antimicrobial drug delivery to biofilm. *Current Pharm Design* 21: 43–66
- Steinmetz I., Rohde M., Brenneke B. (1995) Purification and characterization of an exopolysaccharide of Burkholderia (Pseudomonas) pseudomallei. *Infect Immun* 63: 3959–65.
- Nimtz M., Wray V., Domke T., Brenneke B., Haussler S., Steinmetz I. (1997) Structure of an acidic exopolysaccharide of Burkholderia pseudomallei. FEBS J 250: 608–16.
- Reckseidler-Zenteno S.L., Viteri D.F., Moore R., Wong E., Tuanyok A., Woods D.E. (2010) Characterization of the type III capsular polysaccharide produced by Burkholderia pseudomallei. *J Med Microbiol* 59: 1403–14.
- Denisov I. (1985) [The polysaccharide component of Pseudomonas pseudomallei slime]. Zh Mikrobiol Epidemiol Immunobiol 11: 23–6.
- Cescutti P., Bosco M., Picotti F., Impallomeni G., Leitao J.H., Richau J.A., Sa-Correia I. (2000) Structural study of the exopolysaccharide produced by a clinical isolate of Burkholderia cepacia. *Biochem Biophys Res Commun* 273: 1088–94.
- Pibalpakdee P., Wongratanacheewin S., Taweechaisupapong S., Niumsup P.R. (2012) Diffusion and activity of antibiotics against *Burkholderia pseudomallei* biofilms. *Int J Antimicrob Agents* 39: 356–9.
- Taweechaisupapong S., Kaewpa C., Arunyanart C., Kanla P., Homchampa P., Sirisinha S., Proungvitaya T., Wongratanacheewin S. (2005) Virulence of *Burkholderia* pseudomallei does not correlate with biofilm formation. *Microb* Pathog 39: 77–85.
- Lumjiaktase P., Diggle S.P., Loprasert S., Tungpradabkul S., Daykin M., Camara M., Williams P., Kunakorn M. (2006) Quorum sensing regulates dpsA and the oxidative stress response in *Burkholderia pseudomallei*. *Microbiology* 152: 3651–9.
- Subsin B., Thomas M.S., Katzenmeier G., Shaw J.G., Tungpradabkul S., Kunakorn M. (2003) Role of the stationary growth phase sigma factor RpoS of *Burkholderia pseudomallei* in response to physiological stress conditions. *J Bacteriol* 185: 7008–14.
- 18. Tunpiboonsak S., Mongkolrob R., Kitudomsub K., Thanwatanaying P., Kiettipirodom W., Tungboontina Y., Tungpradabkul S. (2010) Role of a *Burkholderia pseudomallei* polyphosphate kinase in an oxidative stress response, motilities, and biofilm formation. *J Microbiol* 48: 63–70.
- Cochran W.L., Suh S.J., Mcfeters G.A., Stewart P.S. (2000) Role of RpoS and AlgT in *Pseudomonas aeruginosa* biofilm resistance to hydrogen peroxide and monochloramine. *J Appl Microbiol* 88: 546–53.
- Ito A., Taniuchi A., May T., Kawata K., Okabe S. (2009) Increased antibiotic resistance of *Escherichia coli* in mature biofilms. *Appl Environ Microbiol* 75: 4093–100.
- 21. Drozd M., Gangaiah D., Liu Z., Rajashekara G. (2011) Contribution of TAT system translocated PhoX to

- Campylobacter jejuni phosphate metabolism and resilience to environmental stresses. *PLoS ONE* **6**:e26336.
- Taylor P.K., Yeung A.T., Hancock R.E. (2014) Antibiotic resistance in *Pseudomonas aeruginosa* biofilms: Towards the development of novel anti-biofilm therapies. *J Biotechnol* 191: 121–30
- Wuthiekanun V., Smith M.D., Dance D.A., Walsh A.L., Pitt T. L., White N.J. (1996) Biochemical characteristics of clinical and environmental isolates of *Burkholderia pseudomallei*. J Med Microbiol 45: 408–12.
- Anuntagool N., Intachote P., Wuthiekanun V., White N.J., Sirisinha S. (1998) Lipopolysaccharide from nonvirulent Ara+ Burkholderia pseudomallei isolates is immunologically indistinguishable from lipopolysaccharide from virulent Araclinical isolates. Clin Diagn Lab Immunol 5: 225–9.
- Ceri H., Olson M.E., Stremick C., Read R.R., Morck D., Buret A. (1999) The Calgary Biofilm Device: new technology for rapid determination of antibiotic susceptibilities of bacterial biofilms. *J Clin Microbiol* 37: 1771–6.
- Friedman L., Kolter R. (2004) Two genetic loci produce distinct carbohydrate-rich structural components of the *Pseudomonas* aeruginosa biofilm matrix. *J Bacteriol* 186: 4457–65.
- Merkle R.K., Poppe I. (1994) Carbohydrate composition analysis of glycoconjugates by gas-liquid chromatography/mass spectrometry. *Methods Enzymol* 230: 1–15.
- Irie Y., Starkey M., Edwards A.N., Wozniak D.J., Romeo T., Parsek M.R. (2010) *Pseudomonas aeruginosa* biofilm matrix polysaccharide Psl is regulated transcriptionally by RpoS and post-transcriptionally by RsmA. *Mol Microbiol* 78: 158–72.
- Gamage A.M., Shui G., Wenk M.R., Chua K.L. (2011) N-Octanoylhomoserine lactone signalling mediated by the BpsI-BpsR quorum sensing system plays a major role in biofilm

- formation of *Burkholderia pseudomallei*. *Microbiology* **157**: 1176–86
- Friedman L., Kolter R. (2004) Genes involved in matrix formation in *Pseudomonas aeruginosa* PA14 biofilms. *Mol Microbiol* 51: 675–90.
- Rodriguez-Martinez J.M., Ballesta S., Pascual A. (2007) Activity and penetration of fosfomycin, ciprofloxacin, amoxicillin/ clavulanic acid and co-trimoxazole in *Escherichia coli* and *Pseudomonas aeruginosa* biofilms. *Int J Antimicrob Agents* 30: 366–8
- Singh R., Ray P., Das A., Sharma M. (2010) Penetration of antibiotics through Staphylococcus aureus and Staphylococcus epidermidis biofilms. J Antimicrob Chemother 65: 1955–8.
- Wongtrakoongate P., Tumapa S., Tungpradabkul S. (2012) Regulation of a quorum sensing system by stationary phase sigma factor RpoS and their co-regulation of target genes in Burkholderia pseudomallei. Microbiol Immunol 56: 281–94.
- Richau J.A., Leitao J.H., Sa-Correia I. (2000) Enzymes leading to the nucleotide sugar precursors for exopolysaccharide synthesis in *Burkholderia cepacia*. *Biochem Biophys Res Commun* 276: 71–6
- Osiriphun Y., Wongtrakoongate P., Sanongkiet S., Suriyaphol P., Thongboonkerd V., Tungpradabkul S. (2009) Identification and characterization of RpoS regulon and RpoS-dependent promoters in *Burkholderia pseudomallei*. *J Proteome Res* 8: 3118–31.
- Kiratisin P., Sanmee S. (2008) Roles and interactions of Burkholderia pseudomallei BpsIR quorum-sensing system determinants. J Bacteriol 190: 7291–7.
- Shrout J.D., Tolker-Nielsen T., Givskov M., Parsek M.R. (2011)
 The contribution of cell-cell signaling and motility to bacterial biofilm formation. MRS Bull Mater Res Society 36: 367–73.





Utilization of Whole-Cell MALDI-TOF Mass Spectrometry to Differentiate *Burkholderia pseudomallei* Wild-Type and Constructed Mutants

Suthamat Niyompanich^{1®}, Kitima Srisanga^{1®}, Janthima Jaresitthikunchai², Sittiruk Roytrakul², Sumalee Tungpradabkul¹*

- 1 Department of Biochemistry, Faculty of Science, Mahidol University, Bangkok, Thailand, 2 National Center for Genetic Engineering and Biotechnology (BIOTEC), Thailand Science Park, Pathum Thani, Thailand
- These authors contributed equally to this work.
- * pexcotung@gmail.com

Abstract

Whole-cell matrix-assisted laser desorption/ionization time-of-flight mass spectrometry (whole-cell MALDI-TOF MS) has been widely adopted as a useful technology in the identification and typing of microorganisms. This study employed the whole-cell MALDI-TOF MS to identify and differentiate wild-type and mutants containing constructed single gene mutations of Burkholderia pseudomallei, a pathogenic bacterium causing melioidosis disease in both humans and animals. Candidate biomarkers for the B. pseudomallei mutants, including rpoS, ppk, and bpsl isolates, were determined. Taxon-specific and clinical isolate-specific biomarkers of B. pseudomallei were consistently found and conserved across all average mass spectra. Cluster analysis of MALDI spectra of all isolates exhibited separate distribution. A total of twelve potential mass peaks discriminating between wild-type and mutant isolates were identified using ClinProTools analysis. Two peaks (m/z 2721 and 2748 Da) were specific for the rpoS isolate, three (m/z 3150, 3378, and 7994 Da) for ppk, and seven (m/z 3420, 3520, 3587, 3688, 4623, 4708, and 5450 Da) for bps/. Our findings demonstrated that the rapid, accurate, and reproducible mass profiling technology could have new implications in laboratory-based rapid differentiation of extensive libraries of genetically altered bacteria.

Introduction

The matrix-assisted laser desorption/ionization time-of-flight mass spectrometry (MALDI-TOF MS) approach is currently becoming a revolutionizing technology for use in the identification and typing of several diverse microorganisms, e.g., gram-positive and negative bacteria, yeast, and fungi [1–7]. This is a newly developed platform, which has been increasingly utilized in various microbiological applications, including routine clinical diagnosis, microbial





Citation: Niyompanich S, Srisanga K, Jaresitthikunchai J, Roytrakul S, Tungpradabkul S (2015) Utilization of Whole-Cell MALDI-TOF Mass Spectrometry to Differentiate *Burkholderia* pseudomallei Wild-Type and Constructed Mutants. PLoS ONE 10(12): e0144128. doi:10.1371/journal. pone.0144128

Editor: Yang Cai, University of New Orleans, UNITED STATES

Received: July 17, 2015

Accepted: November 14, 2015 **Published:** December 14, 2015

Copyright: © 2015 Niyompanich et al. This is an open access article distributed under the terms of the Creative Commons Attribution License, which permits unrestricted use, distribution, and reproduction in any medium, provided the original author and source are credited.

Data Availability Statement: All relevant data are within the paper.

Funding: Support was provided by the Thailand Research Fund, grant number BRG5680010 to ST and the Ph.D. scholarship from RGJ (the Royal Golden Jubilee) No. PHD/0341/2551 to SN.

Competing Interests: The authors have declared that no competing interests exist.



Abbreviations: MALDI-TOF MS, matrix-assisted laser desorption/ionization time-of-flight mass spectrometry.

systematics, environmental microbiology, epidemiological studies, and biodefense detection [8–11]. MALDI-TOF MS offers rapid, robust, and economic analysis in comparison to conventional phenotypic and molecular techniques, making it an attractive and desirable tool for rapid microbial examination [12, 13].

Whole-cell MALDI-TOF MS analysis requires simple steps in sample preparation without additional analyte extraction steps. There are two possible methods: 1) utilizes single colonies grown on culture media deposited directly on a MALDI target plate, then overlaid with a matrix solution; and 2) exploits the mixture of whole cells suspended in a matrix solution before being analyzed using a mass spectrometer [14]. Conceptually, mass spectral pattern profiles obtained from the whole-cell MALDI-TOF MS method encompass unique mass profiles for particular microbial species [15], enabling the discrimination of each microbial type. With the BioTyper-based identification process, the MALDI mass spectra are subsequently matched against the reference spectra entries in a database, rendering scores for the reliable identification of test isolates at genus, species, and subspecies levels [16, 17]. Currently, whole-cell MAL-DI-TOF MS is being increasingly adopted and evolved for detection of antibiotic resistance, recombinant proteins, and plasmid insertion in bacteria [18-23]. In Vibrio parahaemolyticus, the ability to differentiate the wild-type and mutant strains with single gene deletions, according to their unique mass spectra, has been reported using whole-cell MALDI-TOF MS [24]. Moreover, when combining it with sophisticated algorithms, this approach can generate potential biomarkers pertaining to each microbial type and strain [17]. This allows for a more advanced level of identification and classification among microorganisms.

B. pseudomallei is a pathogenic bacterium causing melioidosis disease in both humans and animals. It is endemic in Northeastern Thailand and Northern Australia, with the high mortality rates of approximately 40% and 20%, respectively [25, 26]. Moreover, B. pseudomallei has been classified by the Centers of Disease Control and Prevention (CDC) as a category B bioweapon agent [27]. Identification and characterization of B. pseudomallei isolates have been relied on various molecular methods, which were PCR-based or hybridization-based techniques, such as multilocus sequence typing (MLST), ribotyping, restriction fragment length polymorphism (RFLP), and microarray-based comparative genome hybridization (CGH) [28-31]. Although, these methods provide sufficient bacterial identification, they are time-consuming, labor intensive, and have high costs [32, 33]. MALDI-TOF has emerged as an alternative identification tool to rapidly and accurately detect B. pseudomallei in blood cultures of septicemic patients, and thus would be beneficial for medical diagnosis and prevention of melioidosis [34]. Additionally, MALDI-TOF MS has been applied for discovering of the potential taxonspecific and source-specific biomarkers for B. pseudomallei in different samples [35, 36]. A recent report from Cox et al. has further shown the utility of phage-amplification-based MAL-DI-TOF MS as a rapid tool in determining ceftazidime resistance in B. pseudomallei [37]. However, to the best of our knowledge, there have been no known reports of the use of whole-cell MALDI-TOF MS in the differentiation between B. pseudomallei wild-type and mutants derived from single gene mutations. With the availability of extensive libraries of genetically modified microorganisms in the laboratories, whole-cell MALDI-TOF MS could be utilized as a rapid laboratory-based technique to classify bioengineered bacteria. In the present study, four isolates, including one strain of wild-type PP844 and three constructed mutants (rpoS, ppk, and bpsI), were analyzed. The rpoS, ppk, and bpsI isolates were constructed by gene knockdowns in the respective location [38-40]. These isolates have been widely examined for their roles in oxidative stress response, quorum sensing regulation, and the pathogenesis of B. pseudomallei [38-42]. We assessed the applicability of the whole-cell MALDI-TOF MS for rapid identification and differentiation between the B. pseudomallei wild-type and mutants containing



constructed single gene mutations. We then investigated the specific biomarkers of each mutant isolate.

Materials and Methods

Bacterial isolates and growth conditions

The four bacterial strains utilized for MALDI-TOF MS in this study were the wild-type clinical isolate PP844, isolated from blood culture, and the three constructed rpoS, ppk, and bpsI mutants carrying gene disruption in rpoS, ppk, and bpsI genes, respectively. Gene disruption, using the pKNOCK-Tc^r suicide vector, was carried out in PP844 for the construction of rpoS and bpsI mutants and in NF10/38 for the ppk isolate. These mutants have been characterized with their gene disruptions by molecular biology methods as previously published [38–40]. Bacterial samples were kept in 80% glycerol and managed under BSL3 conditions. Each bacterial strain was recovered from storage at -80°C by culturing on Luria-Bertani (LB) agar. For the selection of mutants, tetracycline was supplemented into the medium with a final concentration of 60 μ g/mL. A single colony was picked and grown in LB broth with aerobic shaking at 37°C for 16 hours. All of the overnight-cultured bacteria were then inoculated into 0.1% inoculum and aerobically incubated at 37°C for 3 hours with agitation. Subsequently, the bacteria were serially diluted and grown on Ashdown's selective agar to ensure selection for growth of *B. pseudomallei* and incubated at 37°C for 7 days to obtain the colonies.

MALDI-TOF sample preparation

The microbial samples for MALDI-TOF analysis were prepared using previously described method [36]. In brief, the colonies which were grown on Ashdown's agar plate were transferred into 900 μ L of water and then deactivated with 300 μ L of ethanol. The pellet was collected by centrifugation and mixed with a matrix solution containing 10 mg sinapinic acid in 1 mL of 50% acetonitrile with 2.5% trifluoroacetic acid. Two microliters of bacterial extract, with concentration approximately 0.3–0.5 μ g/ μ L, were spotted on a MALDI steel target plate (MTP 384 ground steel plate, Bruker Daltonik, GmbH, Bremen, Germany) and were dried at room temperature. The *Escherichia coli* DH5 α was used as a positive control and the matrix solution without bacterial cells was used as a negative control. Twenty-four spots (n = 24) from each sample were deposited on a target plate for determination of experimental reproducibility, thus each isolate was repeatedly examined twenty-four times. After drying, the target plate was subjected to analysis in the MALDI-TOF instrument.

MS instrumentation

MALDI-TOF analysis was carried out in an Ultraflex III TOF/TOF mass spectrometer utilized with a 337 nm N_2 laser and was operated by flexControl software (Bruker Daltonik, GmbH, Bremen, Germany). The machine was run in the linear positive mode and mass spectra in the range of 2–20 kDa were collected. The following instrumental parameters were used: acceleration voltages of 25.00 and 23.45 kV for ion source 1 and ion source 2, respectively, with a lens voltage of 6.0 kV. External calibration was performed to determine mass peak accuracy using a ProteoMassTM peptide & protein MALDI-MS calibration kit (Sigma Aldrich, St. Louis, MO, United States) consisting of human ACTH fragment 18–39 (m/z 2465), bovine insulin oxidized B chain (m/z 3465), bovine insulin (m/z 5731), equine cytochrome c (m/z 12362), and equine apomyoglobin (m/z 16952). Each spectrum was compiled from 500 laser shots, with a 50 Hz laser.



Data acquisition and analysis

The twenty-four raw MALDI spectra of each isolate acquired from the mass spectrometer were subjected to spectral processing, including peak detection, smoothing, baseline subtraction, and recalibration using flexAnalysis 3.0 software (Bruker Daltonik, GmbH, Bremen, Germany). These spectra were used for pattern matching analysis to identify bacterial species using BioTyper 2.0 software (Bruker Daltonik, GmbH, Bremen, Germany) and for determining candidate biomarkers of each mutant using ClinProTools 2.2 software (Bruker Daltonik, GmbH, Bremen, Germany). A reference spectrum of the wild-type PP844 incorporated into BioTyper database was generated. Single MALDI mass spectra of all test isolates were subjected to the pattern matching analysis using BioTyper 2.0, with all peaks compared to the reference spectra in the database. The first ranked microorganism query (top hit) with a score in the log scale ranging from 0-3 was obtained and bacteria identified at the genus (a score between 1.7-1.89) and species levels (a score ≥ 1.9).

Determination of candidate biomarkers for each mutant was analyzed by ClinProTools 2.2. The software conducts data processing such as baseline subtraction, recalibration, and normalization to diminish measurement variations in the analysis, and data interpretation with statistical calculation included, allowing the generation of potential biomarkers from MALDI profiles [43]. Moreover, three major statistical tests, consisting of Anderson-Darling (AD), t-test/ANOVA (TTA), and Wilcoxon/Krustal-Wallis (W/KW) tests, have been incorporated into ClinProTools to appropriately analyze the data with normal or non-normal distribution. Data with a normal distribution are subjected to TTA test, while those of a non-normal distribution subjected to W/ KW test and AD test determines whether test data are based on normal distribution assumption (considering p-value of > 0.05 for normal distribution and of ≤ 0.05 for non-normal distribution). The setting parameters for spectra preparation in ClinProTools were: a resolution of 800 ppm, a mass range of 2000–20000 Da, a top hat baseline subtraction with 10% minimal baseline width, enabling null spectra exclusion, and recalibration with 500 ppm maximal peak shift and 30% match calibrant peaks. All MALDI spectra were normalized against total ion current (TIC). To identify candidate biomarkers of individual mutants, the average mass spectrum of each mutant was compared to that of wild-type PP844 (pair test). Thus, degree of freedom value of each analysis (2 sample classes) was 1. The average mass peak list of each pair test was acquired, after statistical analysis, based on the total average spectrum with a signal to noise threshold of 5.00, and mass peak intensities were used in the peak calculation process. The selected mass peaks, which exhibited p-values from AD test of ≤ 0.05 (see Table 1), were subsequently analyzed using W/KW test. Specific biomarkers for a given mutant were manually selected according to pvalues of W/KW statistics (p < 0.001) and exhibited > 2-fold differences in average peak intensity compared to wild-type. The "leave one out" mode was used for cross validation analysis using Quick Classifier (QC) model. The principal component analysis (PCA) created based on the Euclidian distance method and the unsupervised hierarchical clustering (dendrogram) constructed from PCA-derived data were used to examine the clustering of all isolates.

Results

Species identification of *Burkholderia pseudomallei*

Using BioTyper analysis, the positive control E. coli DH5 α was correctly identified with the identification score of 2.411. A set of twenty-four single spectra of the wild-type PP844 strain was constructed as the reference spectrum and incorporated into BioTyper database. Single MALDI spectra of all isolates acquired from flexAnalysis were subsequently subjected to bacterial identification analysis to achieve an identification score for each isolate. Scores acquired



Table 1. Candidate biomarkers of B. pseudomallei mutant isolates.

m/z value ^a	<i>p</i> -value from AD ^b test	p-value from W/KW test	Average peak intensity (arb.u.)				Standard deviation (S.D.)				Coefficient of variation (CV) ^c			
			PP844	rpoS	ppk	bpsl	PP844	rpoS	ppk	bpsl	PP844	rpoS	ppk	bpsl
2721	< 0.000001	< 0.000001	1.61	9.20	-	-	0.24	0.78	-	-	0.15	0.08	-	-
2748	< 0.000001	< 0.000001	1.09	5.32	-	-	0.17	0.40	-	-	0.16	0.08	-	-
3150	< 0.000001	< 0.000001	6.38	-	14.68	-	0.83	-	1.62	-	0.13	-	0.11	-
3378	< 0.000001	< 0.000001	8.38	-	20.00	-	0.72	-	1.86	-	0.09	-	0.09	-
7994	< 0.000001	< 0.000001	5.49	-	15.83	-	1.56	-	3.84	-	0.28	-	0.24	-
3420	< 0.000001	< 0.000001	3.19	-	-	14.25	0.34	-	-	2.10	0.11	-	-	0.15
3520	< 0.000001	< 0.000001	2.88	-	-	7.93	0.39	-	-	1.11	0.14	-	-	0.14
3587	< 0.000001	< 0.000001	3.15	-	-	10.50	0.33	-	-	1.04	0.10	-	-	0.10
3688	< 0.000001	< 0.000001	2.24	-	-	35.33	0.26	-	-	3.85	0.12	-	-	0.11
4623	< 0.000001	< 0.000001	1.80	-	-	4.37	0.16	-	-	0.30	0.09	-	-	0.07
4708	< 0.000001	< 0.000001	3.01	-	-	7.63	0.23	-	-	0.57	0.08	-	-	0.08
5450	< 0.000001	< 0.000001	1.00	-	-	4.23	0.19	-	-	0.30	0.19	-	-	0.07

^a All of the twelve selected biomarker ions exhibited significance at p < 0.001 on the basis of Wilcoxon/Krustal-Wallis (W/KW) statistics and had peak intensity differences > 2-fold. Twenty-four spots (n = 24) of each strain were analyzed for the experimental reproducibility. Degree of freedom for each pair test analysis (2 sample classes) was 1.

from BioTyper analysis ranging from logarithmic scale 0.00-3.00 indicate levels of microorganism identification as follows: (1) a score > 1.9 refers to a reliable identification at species level, (2) a score between 1.7–1.89 indicates a confident identification at genus level, and (3) a score < 1.7 denotes unreliable identification [12, 35]. Our wild-type and mutants possessing scores ranging from 2.43-2.81 were identified as B. pseudomallei at the species level, the scores obtained for wild-type, rpos, ppk, and bpsI isolates were 2.81, 2.54, 2.64, and 2.43, respectively. Karger et al. [35] have previously established five taxon-specific biomarkers, including m/z 4410, 5794, 6551, 7553, and 9713 Da, that are commonly found in mass profiles of B. pseudomallei using the whole-cell MALDI-TOF MS approach. These taxon-specific biomarkers were also shown to be conserved among environmental and clinical B. pseudomallei strains [36]. To examine whether the five prominent biomarkers were presented in our MALDI spectra, we determined these biomarkers in an average spectrum generated from twenty-four raw replicate spectra of each respective strain. It was observed that all of the average spectra in both the wildtype and mutant isolates exhibited high similarities in peak patterns, with differing peak intensities (Fig 1). All isolates used in this study were confirmed as B. pseudomallei by the identification scores obtained from BioTyper analysis and the existence of the five B. pseudomalleispecific biomarkers presented in our MALDI average spectra (appearing as vertical dashed lines in Fig 1). However, the observed bacterial morphology of all isolates cultured on Ashdown's selective agar illustrated distinct colony phenotypes (Fig 2), their components of ionized cell surface represented more reliable taxonomic identification as B. pseudomallei species based on whole-cell MALDI-TOF MS analysis.

Identification of clinical isolate-specific biomarkers

The two *B. pseudomallei*, PP844 and NF10/38, were clinical isolates used as parental strains for mutant construction. PP844 was isolated from the blood culture of a patient, admitted to

^b Anderson-Darling statistical test

^c For each m/z, coefficient of variation of a respective isolate was calculated from standard deviation (S.D.) divided by average peak intensity.



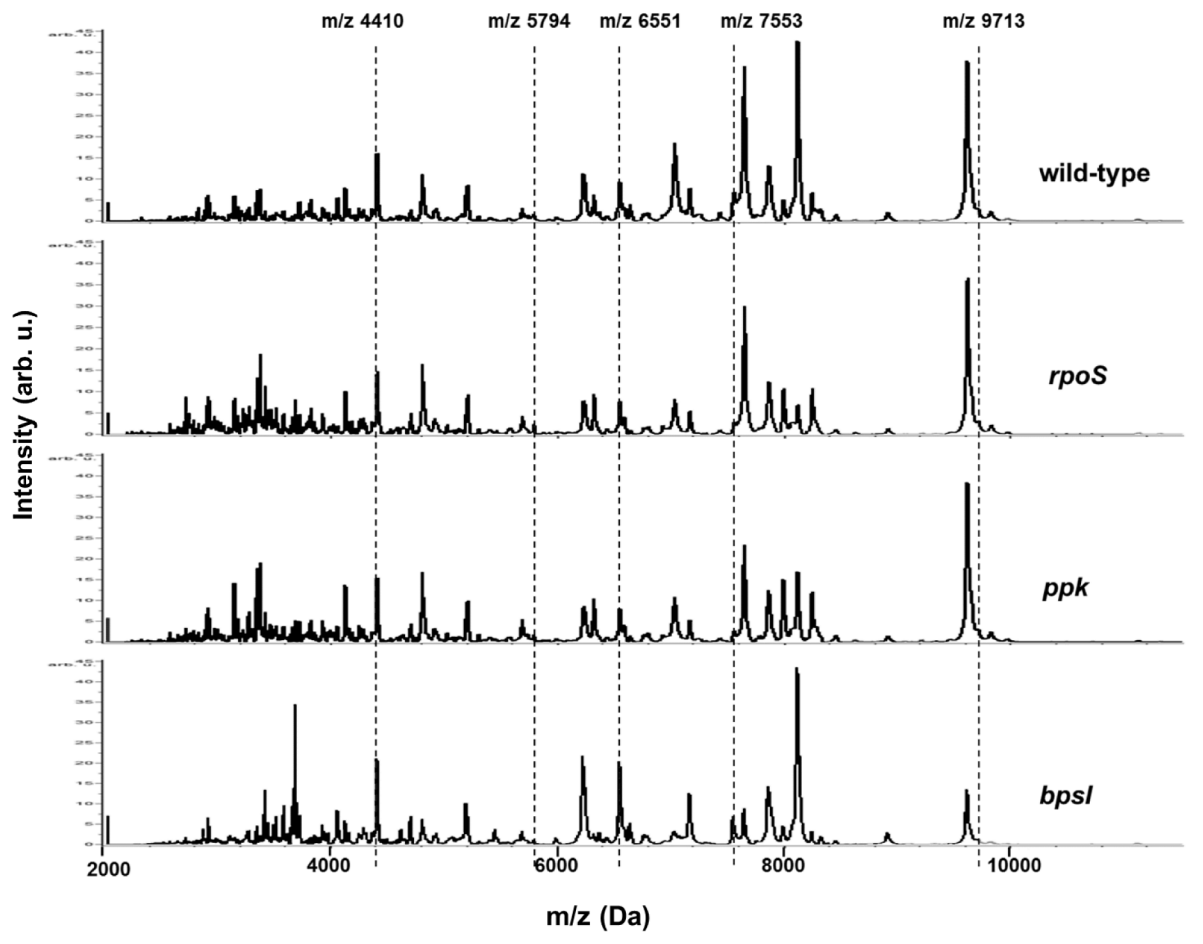


Fig 1. Taxon-specific biomarkers in *B. pseudomallei* average mass spectra. Five effective species-specific biomarkers, including m/z 4410, 5794, 6551, 7553, and 9713, were detected in all of the average mass spectra examined (the vertical dashed lines).

Srinagarind Hospital, Khon Kaen province, Thailand, where melioidosis is endemic. It was identified as *B. pseudomallei* based on its biochemical characteristics, colonial morphology on selective media, antibiotic sensitivity profiles, and reaction with polyclonal antibody [44]. NF10/38 was a blood culture isolate, obtained from the National Institute of Health, Ministry of Public Health, Thailand [45]. Target gene disruption was carried out in PP844 for the construction of *rpoS* and *bpsI* mutants and in NF10/38 for the *ppk* strain, as previously reported [38–40]. All bacterial isolates were kept as glycerol stocks for conducting experiments in laboratory and were cultivated on Ashdown's selective agar to affirm the absence of any microorganism contaminations. All laboratory operations were performed under BSL3 conditions. Our previous studies using ClinProTools software revealed that the four biomarkers specific to clinical isolates (m/z 3658, 6322, 7035, and 7984 Da) displayed significantly higher peak intensities in the clinical average spectrum than those of the environmental average spectrum in *B. pseudomallei* [36]. Each average MALDI spectrum obtained of both the wild-type and the three mutants contained the four typical clinical isolate-specific biomarkers (m/z 3658, 6322, 7035, and 7984 Da) as shown in Fig 3, supporting their clinical origin.



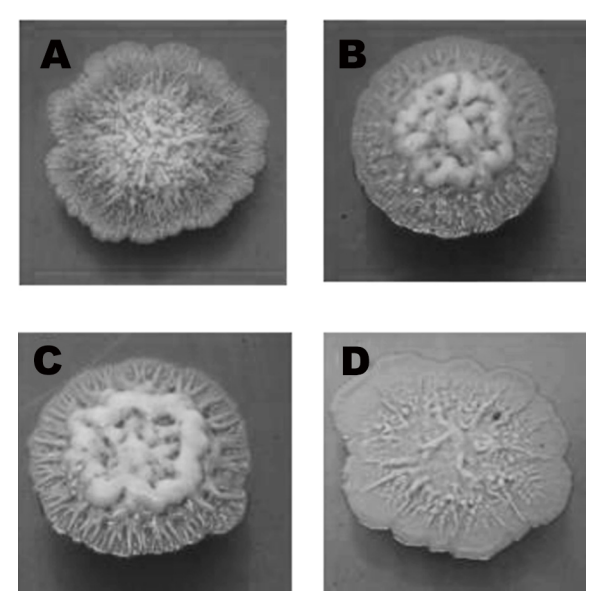


Fig 2. Colony morphology of *B. pseudomallei***.** Colony morphology of the strains was observed after incubation at 37°C for 7 days. The *rpoS* (B), *ppk* (C), and *bpsl* (D) mutants which contained each single gene mutation in *rpoS*, *ppk*, and *bpsl* genes, respectively, showed distinct morphology from the wild-type (A).

Cluster analysis

To determine whether MALDI profiles of each mutant with a single gene mutation were distributed in a distinct cluster, the total of single MALDI spectra of PP844, *rpoS*, *ppk*, and *bpsI* isolates were subjected to PCA and unsupervised hierarchical clustering analyses using Clin-ProTools. *E. coli* DH5α was used as an outgroup species in analyses. All isolates exhibited distinctly separate distribution, as illustrated by results of PCA score plot (Fig 4A). The unsupervised hierarchical clustering analysis derived from the PCA scores, resulting in a dendrogram (Fig 4B), revealed that PP844, *rpoS*, and *ppk* clustered in the same clade. In addition, the *rpoS* and *ppk* isolates were grouped closer and displayed the shortest distance among all the bacterial isolates tested. This indicated a high similarity in MALDI profiles between *rpoS* and *ppk*. It was observed that a clade of *bpsI* isolate showed a greater distribution from the others. Hence, based on this study, the whole-cell MALDI-TOF MS technique could be used to distinguish *B. pseudomallei* mutants containing single gene disruptions from the wild-type PP844.

Candidate biomarkers

Comparison between MALDI spectra of PP844, *rpoS*, *ppk*, and *bpsI* isolates revealed visually slight, but significant changes in mass intensities. To determine the biomarkers specific to each strain observed from the whole-cell MALDI-TOF MS analysis, the average mass spectrum of each of the three mutants was individually compared against that of the PP844 wild-type (pair test) using ClinProTools. We employed the statistical approach incorporated with ClinProTools to provide the average mass peak list of each pair test (signal to noise threshold of 5.00 in the mass range of 2–20 kDa). Subsequently all peaks were evaluated referring to fold differences of average peak intensities and the *p*-value from W/KW statistical calculation. The average peak intensity was calculated from peak intensity of the respective mutant isolate divided by that of the wild-type. As listed in Table 1 and displayed in Fig 5, the specific



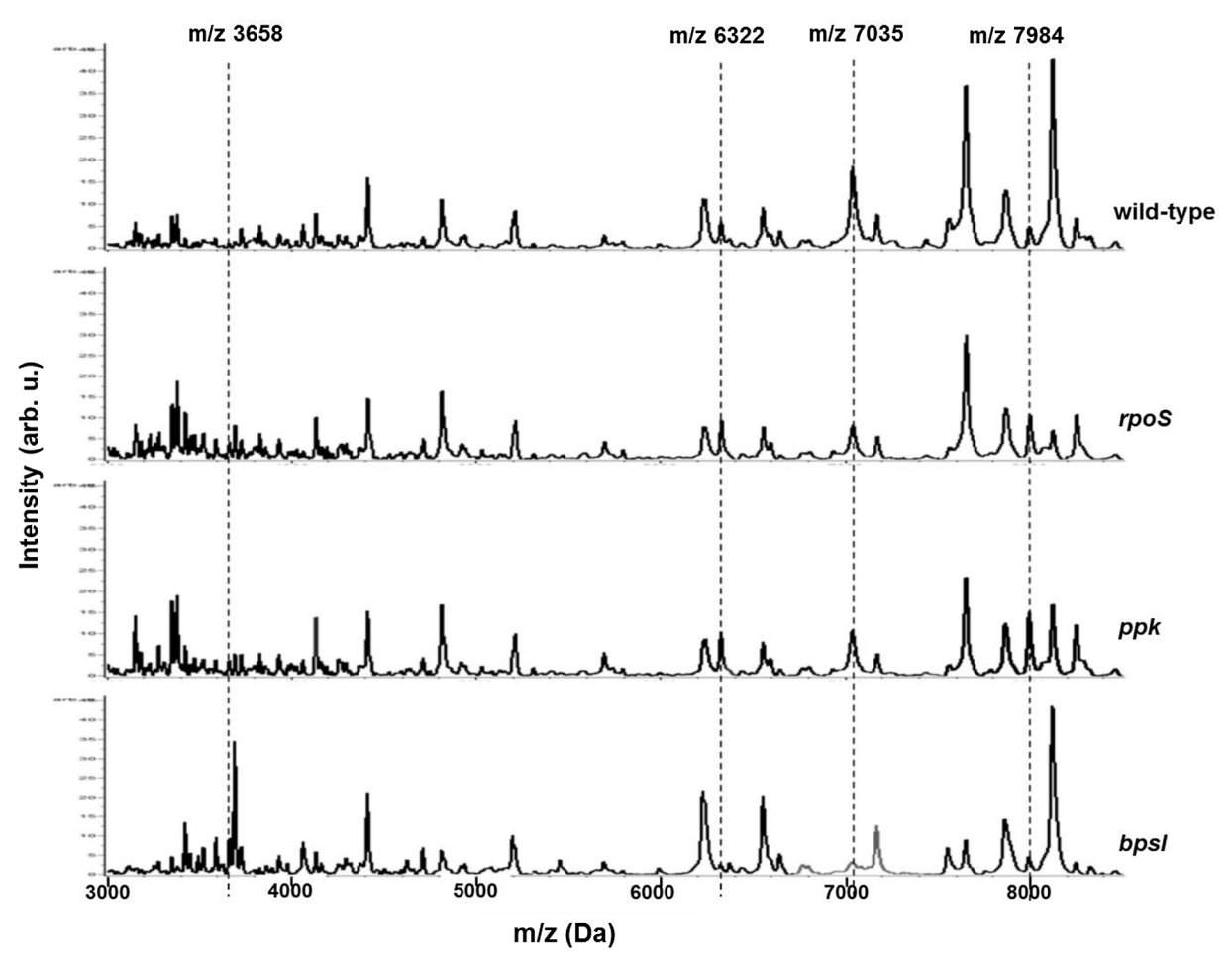
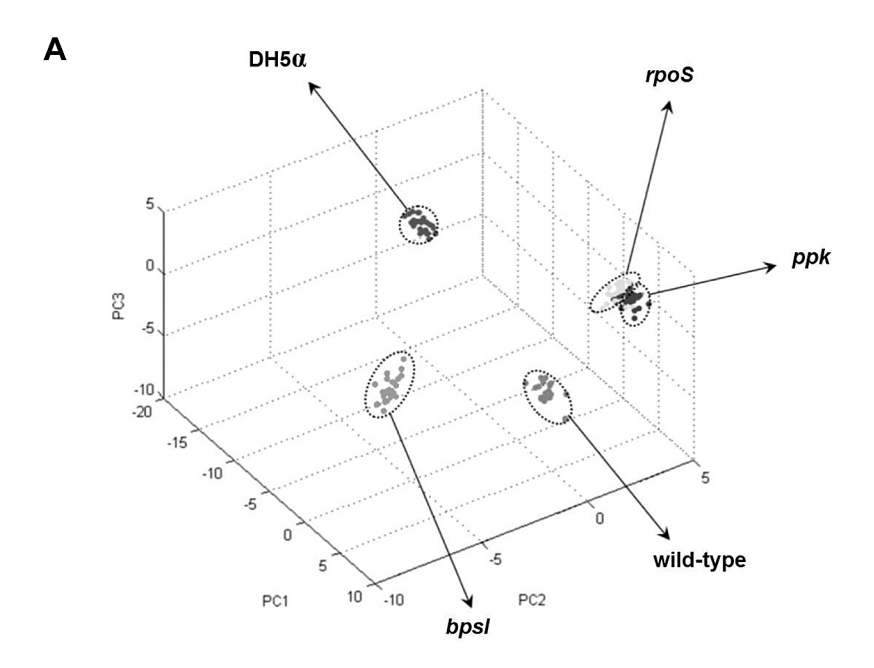


Fig 3. Clinical isolate-specific biomarkers in *B. pseudomallei* average mass spectra. All four biomarkers, including m/z 3658, 6322, 7035, and 7984 Da, were detected in all of the average mass spectra examined (the vertical dashed lines).

biomarkers for each mutant displayed significant differences (p < 0.001) and > 2-fold differences in average peak intensity. With these analyses, the mass peaks at m/z 2721 and 2748 Da were identified for the rpoS isolate, while the peaks at m/z 3150, 3378, and 7994 Da were specific for ppk. A total of seven mass peaks were defined for bpsI isolate, with a mass ranging from m/z 3000–6000, including m/z 3420, 3520, 3587, 3688, 4623, 4708, and 5450 Da. Moreover, Quick Classifier (QC) model, a univariate sorting algorithm that statistically calculates individual peak area, was used to evaluate cross validation of all data sets. A value of 100% was obtained, indicating high reliability of the model prediction and thus accurate classification of test isolates. In addition, the area under the ROC curve (AUC) value of individual mass peaks was determined, with each mass peak showed the AUC value of 1, indicating 100% sensitivity (all true positives were found) and 100% specificity (no false positives were found). However the same level of specificity and sensitivity might not be achieved if larger number of samples was examined. All together these mass peaks, unique to each isolate, could be potential biomarkers in order to facilitate the differentiation of the corresponding B. pseudomallei wild-type and mutants.





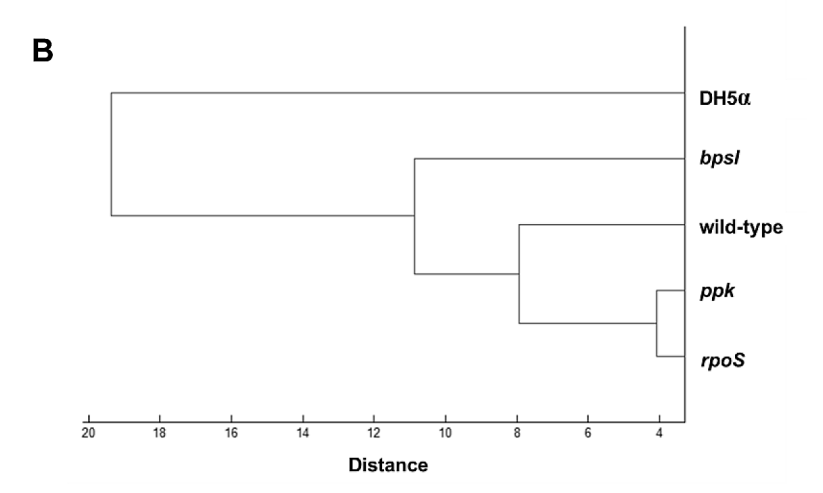


Fig 4. Cluster analysis of *B. pseudomallei* **wild-type and mutants.** (A) PCA score plot representing clusters of each isolate (dashed circles) illustrated separately distribution with the *rpoS* and *ppk* isolates producing a much closer cluster. (B) Dendrogram derived from PCA scores demonstrates that *B. pseudomallei* PP844, *rpoS*, and *ppk* clustered on the same clade, while a clade of *bpsI* showed a greater distance than others.

Discussion

In the present study, we have accomplished the accurate identification of *B. pseudomallei* wild-type and mutant isolates with scores ranging from 2.43–2.81 using BioTyper analysis. Five taxon-specific biomarkers previously determined among *B. pseudomallei* species, including m/z 4410, 5794, 6551, 7553, and 9713 Da [35], were investigated. These five prominent species-specific biomarkers were detected on the average spectra of the wild-type and mutants (Fig 1), which were confirmed as the *B. pseudomallei* species, in agreement with the results previously reported [35]. These results indicated the capacity of the whole-cell MALDI-TOF technique to consistently produce conserved and stable mass peaks in the examined bacterial species.



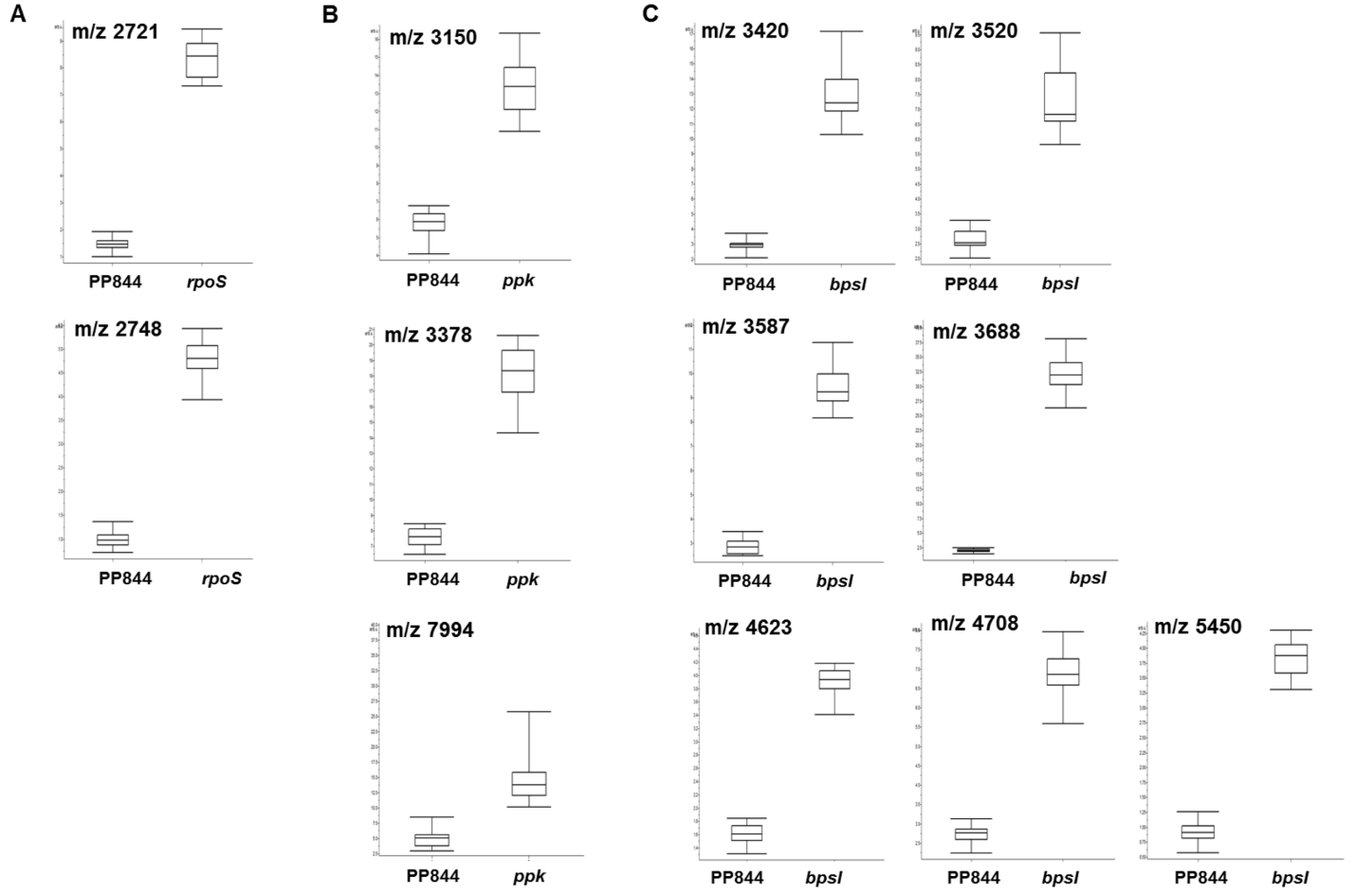


Fig 5. The box and whiskers plot of candidate biomarkers in *B. pseudomallei* mutants. All of the candidate biomarkers were selected from ClinProTools analysis on the basis of W/KW statistics with significance at p < 0.001 and exhibiting average peak intensity differences > 2-fold. The biomarkers at m/z 2721 and 2748 Da were identified for rpoS (A), m/z 3150, 3378, and 7994 Da for ppk (B), and m/z 3420, 3520, 3587, 3688, 4623, 4708, and 5450 Da for bpsl (C). The top and bottom whiskers indicate the maxima and minima values of mass peak intensity, respectively. The intersection line represents the median. In the box, a range below and upper the intersection line displays the 25%-quartiles and 75%-quartiles, respectively.

Moreover, as shown in Fig 2, these mutants, whose parent was clinical *B. pseudomallei* isolates, exhibited various different phenotypes that did not conform to those morphologies previously observed [46]. Nonetheless their MALDI profiles identified them as *B. pseudomallei* species. These results implied that MALDI profiles generated from desorbed components of bacterial cell surface were more reliable than identification based on colony morphology. However, it could also be possible that certain proteins affected by the mutated genes were responsible for the distinct colony appearances.

As displayed in Figs 1 and 3, the MALDI mass patterns for these wild-type and mutants were relatively similar, with nearly identical and differential peak intensities observed. Similar concentrations of each bacterial isolate (see Materials and Methods) were used in sample preparation, mass peaks could then be compared. Nearly identical peak intensities observed for isolates in each pair test could be referred as internal controls for comparison. Each sample displayed differential peak intensities at particular mass peaks, thus reflected different protein expressions. This could possibly be caused by gene knockdown in each mutant. The mutants examined in our study, including *rpoS*, *ppk*, and *bpsI*, have shown their roles involving the



regulation of stress responses, virulence, and pathogenicity of B. pseudomallei. RpoS is an alternative sigma factor encoded from the rpoS gene and plays a role in the stationary growth phase in response to carbon starvation and oxidative stress [38, 47], and could regulate apoptotic cell deaths in mouse macrophages [48]. The ppk gene is naturally conserved in all cell types and encodes a polyphosphate kinase enzyme to synthesize inorganic polyphosphates (poly P) [49]. Its role in B. pseudomallei is essential for the virulence properties, such as oxidative stress response, motilities, and biofilm formation [39]. The BpsI protein, encoded from the bpsI gene, regulates acyl-homoserine lactone (AHL) production and functions in the quorum sensing (QS) system [50], an important system involved in cell survival under oxidative conditions, as well as pathogenicity and production of virulence factors [40–42].

As shown in Fig 3, the clinical isolate-specific biomarkers appeared in all mass spectra of wild-type and mutants. Consequently, the *B. pseudomallei rpoS*, *ppk*, and *bpsI* isolates exhibited a clinical source manner whilst bearing target gene mutations, emphasizing their parental strains originated from the clinical source. These results accentuated that the whole-cell MAL-DI-TOF MS could reproducibly generate reliable conserved biomarkers. Thus, the ability to rapidly and accurately identify these mutants using the clinical isolate-specific biomarkers would be advantageous for tracking original source of isolates.

The results of the PCA and dendrogram clarified that all examined isolates were separately distributed, with *rpoS* and *ppk* clustered at a much closer distance (Fig 4A and 4B). It was notable that patterns of *rpoS* and *ppk* mass profiles contained a high degree of similarity but were not identical, reflecting disruptions of these two genes and the corresponding patterns in their altered protein expressions. Despite high similarity of their MALDI profiles, there is no known evidence concerning cross-talk regulation or correlation between *rpoS* and *ppk* in *B. pseudo-mallei*. Interestingly, *bpsI* further separated from the others, indicating different and unique ionized protein patterns. Other proteins associated with the QS system, in response to AHLs that play role in communication between bacteria and pathogenesis [40–42], might contribute to the mass profiles observed with the *bpsI* mutant strain. Hence, our results supported that the whole-cell MALDI-TOF MS technique could be a promising method to distinguish mutants with altered single gene mutations. Our conclusions are in agreement with Hazen et al [24], where whole-cell MALDI-TOF MS in *Vibrio parahaemolyticus* was used to differentiate the two mutant strains, *opaR* (quorum sensing regulator gene) and *mutS* (mismatch repair gene) bearing single gene deletions.

The use of sophisticated algorithms complementary with whole-cell MALDI TOF MS can also generate potential biomarkers specific for each isolate type or strain [17], thus providing greater identification and classification of microorganisms. In our study, biomarker analysis of MALDI profiles of all isolates, rigorously performed with data processing methods and statistical analysis such as those featured in ClinProTools to reduce bias and measurement variations (see Materials and Methods) resulted in accurate data interpretation. In addition, through TIC normalization in ClinProTools, all of the twelve biomarkers demonstrated especially low values of coefficient of variation (ranging from 0.07–0.28, Table 1) of each mass peaks, indicating sensitive and reliable data analysis in this study. For the first time, we obtained a total of twelve candidate biomarkers that could be specified for *rpoS* (m/z 2721 and 2748 Da), *ppk* (m/z 3150, 3378, and 7994 Da), and *bpsI* (m/z 3420, 3520, 3587, 3688, 4623, 4708, and 5450 Da). These mass peaks containing the AUC value of 1 could thus be potential biomarkers for the differentiation of the corresponding *B. pseudomallei* wild-type and mutants.

The whole-cell MALDI-TOF MS routinely detects mass peaks in the range of 2–20 kDa which are small-size protein molecules, reflecting ribosomal proteins, nucleic-acid binding proteins, and cold shock proteins [4, 51, 52]. An initial attempt to annotate the twelve biomarkers of the three mutant isolates using the Expasy TagIdent tool identified these mass peaks



corresponding to ribosomal proteins, cold shock-like proteins, and uncharacterized proteins (unreported data). Other small to midsize molecules might also be encompassed in mass spectra in addition to those detected proteins. MALDI-TOF/TOF MS and MALDI-TOF MS combined with the shotgun nanoLC-MS/MS analyses could be more straightforward approaches to identify the biomarkers on MALDI mass spectra [53–56].

Our study has extended the utilization of whole-cell MALDI-TOF MS for distinguishing between wild-type and mutants possessing altered single gene mutations. This whole-cell MALDI-TOF MS approach would benefit several laboratories that need to rapidly identify and classify extensive libraries of bacterial constructions based on MALDI mass profiles. Moreover, to enhance the distinction power of MALDI-TOF, the creation and expansion of a local database in each laboratory should be considered. This will allow for specific biomarker detection for more accurate identification and differentiation of microorganisms [8, 12, 15].

Conclusions

There are several advantages, compared to conventional approaches, offered by whole-cell MALDI-TOF MS making it a powerful tool in microbiological research. The distinctive spectral profiles generated from whole-cell MALDI-TOF MS is beneficial to species examination. In addition to the ability to identify and type microbial isolates at different taxonomic levels, there is an increasing utilization of this technology in the detection of antibiotic resistance, recombinant proteins, and plasmid insertion in bacteria. We demonstrated the efforts to use the whole-cell MALDI-TOF MS for distinguishing between *B. pseudomallei* wild-type and mutants, including PP844, *rpoS*, *ppk*, and *bpsI*, and further clarified the potential biomarkers that were specific to each isolate. These whole sets of biomarkers could thus be employed in the identification and differentiation of individual *B. pseudomallei*, in particular of mutant isolates.

Acknowledgments

We thank Dr. Kevin John Kirk from Faculty of Graduate Studies, Mahidol University, Thailand and Maria K. McClintock from Department of Chemical Engineering and Materials Science, University of Minnesota, United States, for proofreading the manuscript.

Author Contributions

Conceived and designed the experiments: ST. Performed the experiments: KS SN JJ. Analyzed the data: SN KS JJ SR ST. Contributed reagents/materials/analysis tools: JJ SR ST. Wrote the paper: SN SR ST.

References

- Rajakaruna L, Hallas G, Molenaar L, Dare D, Sutton H, Encheva V, et al. High throughput identification
 of clinical isolates of Staphylococcus aureus using MALDI-TOF-MS of intact cells. Infection, genetics
 and evolution: journal of molecular epidemiology and evolutionary genetics in infectious diseases.
 2009; 9(4):507–13. doi: 10.1016/j.meegid.2009.01.012 PMID: 19460316.
- Tanigawa K, Kawabata H, Watanabe K. Identification and typing of Lactococcus lactis by matrix-assisted laser desorption ionization-time of flight mass spectrometry. Applied and environmental microbiology. 2010; 76(12):4055–62. doi: 10.1128/AEM.02698-09 PMID: 20400559; PubMed Central PMCID: PMC2893499.
- Siegrist TJ, Anderson PD, Huen WH, Kleinheinz GT, McDermott CM, Sandrin TR. Discrimination and characterization of environmental strains of Escherichia coli by matrix-assisted laser desorption/ionization time-of-flight mass spectrometry (MALDI-TOF-MS). Journal of microbiological methods. 2007; 68 (3):554–62. doi: 10.1016/j.mimet.2006.10.012 PMID: 17184860.
- Dieckmann R, Helmuth R, Erhard M, Malorny B. Rapid classification and identification of salmonellae at the species and subspecies levels by whole-cell matrix-assisted laser desorption ionization-time of



- flight mass spectrometry. Applied and environmental microbiology. 2008; 74(24):7767–78. doi: 10. 1128/AEM.01402-08 PMID: 18952875; PubMed Central PMCID: PMC2607147.
- Marklein G, Josten M, Klanke U, Muller E, Horre R, Maier T, et al. Matrix-assisted laser desorption ionization-time of flight mass spectrometry for fast and reliable identification of clinical yeast isolates. Journal of clinical microbiology. 2009; 47(9):2912–7. doi: 10.1128/JCM.00389-09 PMID: 19571014; PubMed Central PMCID: PMC2738125.
- Clark AE, Kaleta EJ, Arora A, Wolk DM. Matrix-assisted laser desorption ionization-time of flight mass spectrometry: a fundamental shift in the routine practice of clinical microbiology. Clinical microbiology reviews. 2013; 26(3):547–603. doi: 10.1128/CMR.00072-12 PMID: 23824373; PubMed Central PMCID: PMC3719498.
- Mazzeo MF, Sorrentino A, Gaita M, Cacace G, Di Stasio M, Facchiano A, et al. Matrix-assisted laser desorption ionization-time of flight mass spectrometry for the discrimination of food-borne microorganisms. Applied and environmental microbiology. 2006; 72(2):1180–9. doi: 10.1128/AEM.72.2.1180– 1189.2006 PMID: 16461665; PubMed Central PMCID: PMC1392959.
- Welker M, Moore ER. Applications of whole-cell matrix-assisted laser-desorption/ionization time-offlight mass spectrometry in systematic microbiology. Systematic and applied microbiology. 2011; 34 (1):2–11. doi: 10.1016/j.syapm.2010.11.013 PMID: 21288677.
- Murray PR. Matrix-assisted laser desorption ionization time-of-flight mass spectrometry: usefulness for taxonomy and epidemiology. Clinical microbiology and infection: the official publication of the European Society of Clinical Microbiology and Infectious Diseases. 2010; 16(11):1626–30. doi: 10.1111/j.1469-0691.2010.03364.x PMID: 20825435.
- Demirev PA, Fenselau C. Mass spectrometry in biodefense. Journal of mass spectrometry: JMS. 2008; 43(11):1441–57. doi: 10.1002/jms.1474 PMID: 18720458.
- Fujinami Y, Kikkawa HS, Kurosaki Y, Sakurada K, Yoshino M, Yasuda J. Rapid discrimination of Legionella by matrix-assisted laser desorption ionization time-of-flight mass spectrometry. Microbiological research. 2011; 166(2):77–86. doi: 10.1016/j.micres.2010.02.005 PMID: 20347283.
- Seng P, Drancourt M, Gouriet F, La Scola B, Fournier PE, Rolain JM, et al. Ongoing revolution in bacteriology: routine identification of bacteria by matrix-assisted laser desorption ionization time-of-flight mass spectrometry. Clinical infectious diseases: an official publication of the Infectious Diseases Society of America. 2009; 49(4):543–51. doi: 10.1086/600885 PMID: 19583519.
- Carbonnelle E, Mesquita C, Bille E, Day N, Dauphin B, Beretti JL, et al. MALDI-TOF mass spectrometry tools for bacterial identification in clinical microbiology laboratory. Clinical biochemistry. 2011; 44 (1):104–9. doi: 10.1016/j.clinbiochem.2010.06.017 PMID: 20620134.
- Holland RD, Wilkes JG, Rafii F, Sutherland JB, Persons CC, Voorhees KJ, et al. Rapid identification of intact whole bacteria based on spectral patterns using matrix-assisted laser desorption/ionization with time-of-flight mass spectrometry. Rapid communications in mass spectrometry: RCM. 1996; 10 (10):1227–32. doi: 10.1002/(SICI)1097-0231(19960731)10:10<1227::AID-RCM659>3.0.CO;2–6 PMID: 8759332.
- Patel R. Matrix-assisted laser desorption ionization-time of flight mass spectrometry in clinical microbiology. Clinical infectious diseases: an official publication of the Infectious Diseases Society of America. 2013; 57(4):564–72. doi: 10.1093/cid/cit247 PMID: 23595835.
- Sauer S, Freiwald A, Maier T, Kube M, Reinhardt R, Kostrzewa M, et al. Classification and identification of bacteria by mass spectrometry and computational analysis. PloS one. 2008; 3(7):e2843. doi: 10. 1371/journal.pone.0002843 PMID: 18665227; PubMed Central PMCID: PMC2475672.
- Sandrin TR, Goldstein JE, Schumaker S. MALDI TOF MS profiling of bacteria at the strain level: a review. Mass spectrometry reviews. 2013; 32(3):188–217. doi: 10.1002/mas.21359 PMID: 22996584.
- Kostrzewa M, Sparbier K, Maier T, Schubert S. MALDI-TOF MS: an upcoming tool for rapid detection of antibiotic resistance in microorganisms. Proteomics Clinical applications. 2013; 7(11–12):767–78. doi: 10.1002/prca.201300042 PMID: 24123965.
- Nomura F. Proteome-based bacterial identification using matrix-assisted laser desorption ionizationtime of flight mass spectrometry (MALDI-TOF MS): A revolutionary shift in clinical diagnostic microbiology. Biochimica et biophysica acta. 2014. doi: 10.1016/j.bbapap.2014.10.022 PMID: 25448014.
- Lay JO Jr. MALDI-TOF mass spectrometry of bacteria. Mass spectrometry reviews. 2001; 20(4):172– 94. doi: 10.1002/mas.10003 PMID: 11835305.
- Russell SC, Edwards N, Fenselau C. Detection of plasmid insertion in Escherichia coli by MALDI-TOF mass spectrometry. Analytical chemistry. 2007; 79(14):5399–406. doi: 10.1021/ac0705061 PMID: 17579482.
- Camara JE, Hays FA. Discrimination between wild-type and ampicillin-resistant Escherichia coli by matrix-assisted laser desorption/ionization time-of-flight mass spectrometry. Analytical and bioanalytical chemistry. 2007; 389(5):1633–8. doi: 10.1007/s00216-007-1558-7 PMID: 17849103.



- Lartigue MF. Matrix-assisted laser desorption ionization time-of-flight mass spectrometry for bacterial strain characterization. Infection, genetics and evolution: journal of molecular epidemiology and evolutionary genetics in infectious diseases. 2013; 13:230–5. doi: 10.1016/j.meegid.2012.10.012 PMID: 23159555.
- 24. Hazen TH, Martinez RJ, Chen Y, Lafon PC, Garrett NM, Parsons MB, et al. Rapid identification of Vibrio parahaemolyticus by whole-cell matrix-assisted laser desorption ionization-time of flight mass spectrometry. Applied and environmental microbiology. 2009; 75(21):6745–56. doi: 10.1128/AEM.01171-09 PMID: 19749061; PubMed Central PMCID: PMC2772414.
- Wiersinga WJ, Currie BJ, Peacock SJ. Melioidosis. The New England journal of medicine. 2012; 367 (11):1035–44. doi: 10.1056/NEJMra1204699 PMID: 22970946.
- Lazar Adler NR, Govan B, Cullinane M, Harper M, Adler B, Boyce JD. The molecular and cellular basis
 of pathogenesis in melioidosis: how does Burkholderia pseudomallei cause disease? FEMS microbiology reviews. 2009; 33(6):1079–99. doi: 10.1111/j.1574-6976.2009.00189.x PMID: 19732156.
- Rotz LD, Khan AS, Lillibridge SR, Ostroff SM, Hughes JM. Public health assessment of potential biological terrorism agents. Emerging infectious diseases. 2002; 8(2):225–30. doi: 10.3201/eid0802.010164
 PMID: 11897082; PubMed Central PMCID: PMC2732458.
- Vesaratchavest M, Tumapa S, Day NP, Wuthiekanun V, Chierakul W, Holden MT, et al. Nonrandom distribution of Burkholderia pseudomallei clones in relation to geographical location and virulence. Journal of clinical microbiology. 2006; 44(7):2553–7. doi: 10.1128/JCM.00629-06 PMID: 16825379; PubMed Central PMCID: PMC1489466.
- Sermswan RW, Wongratanacheewin S, Trakulsomboon S, Thamlikitkul V. Ribotyping of Burkholderia pseudomallei from clinical and soil isolates in Thailand. Acta tropica. 2001; 80(3):237–44. PMID: 11700181.
- Winstanley C, Hales BA, Corkill JE, Gallagher MJ, Hart CA. Flagellin gene variation between clinical and environmental isolates of Burkholderia pseudomallei contrasts with the invariance among clinical isolates. Journal of medical microbiology. 1998; 47(8):689–94. doi: 10.1099/00222615-47-8-689 PMID: 9877189.
- Bartpho T, Wongsurawat T, Wongratanacheewin S, Talaat AM, Karoonuthaisiri N, Sermswan RW. Genomic islands as a marker to differentiate between clinical and environmental Burkholderia pseudomallei. PloS one. 2012; 7(6):e37762. doi: 10.1371/journal.pone.0037762 PMID: 22675491; PubMed Central PMCID: PMC3365882.
- Sauer S, Kliem M. Mass spectrometry tools for the classification and identification of bacteria. Nature reviews Microbiology. 2010; 8(1):74–82. doi: 10.1038/nrmicro2243 PMID: 20010952.
- Hsieh SY, Tseng CL, Lee YS, Kuo AJ, Sun CF, Lin YH, et al. Highly efficient classification and identification of human pathogenic bacteria by MALDI-TOF MS. Molecular & cellular proteomics: MCP. 2008; 7(2):448–56. doi: 10.1074/mcp.M700339-MCP200 PMID: 18045801.
- 34. Inglis TJ, Healy PE, Fremlin LJ, Golledge CL. Use of matrix-assisted laser desorption/ionization time-of-flight mass spectrometry analysis for rapid confirmation of Burkholderia pseudomallei in septicemic melioidosis. The American journal of tropical medicine and hygiene. 2012; 86(6):1039–42. doi: 10.4269/ajtmh.2012.11-0454 PMID: 22665614; PubMed Central PMCID: PMC3366518.
- 35. Karger A, Stock R, Ziller M, Elschner MC, Bettin B, Melzer F, et al. Rapid identification of Burkholderia mallei and Burkholderia pseudomallei by intact cell Matrix-assisted Laser Desorption/Ionisation mass spectrometric typing. BMC microbiology. 2012; 12:229. doi: 10.1186/1471-2180-12-229 PMID: 23046611; PubMed Central PMCID: PMC3534143.
- 36. Niyompanich S, Jaresitthikunchai J, Srisanga K, Roytrakul S, Tungpradabkul S. Source-identifying biomarker ions between environmental and clinical Burkholderia pseudomallei using whole-cell matrix-assisted laser desorption/ionization time-of-flight mass spectrometry (MALDI-TOF MS). PloS one. 2014; 9(6):e99160. doi: 10.1371/journal.pone.0099160 PMID: 24914956; PubMed Central PMCID: PMC4051666.
- Cox CR, Saichek NR, Schweizer HP, Voorhees KJ. Rapid identification and antibiotic resistance determination by bacteriophage amplification and MALDI-TOF MS. Bacteriophage. 2014; 4:e29011. doi: 10.4161/bact.29011 PMID: 25050191; PubMed Central PMCID: PMC4090906.
- Subsin B, Thomas MS, Katzenmeier G, Shaw JG, Tungpradabkul S, Kunakorn M. Role of the stationary growth phase sigma factor RpoS of Burkholderia pseudomallei in response to physiological stress conditions. Journal of bacteriology. 2003; 185(23):7008–14. PMID: 14617667; PubMed Central PMCID: PMC262693.
- 39. Tunpiboonsak S, Mongkolrob R, Kitudomsub K, Thanwatanaying P, Kiettipirodom W, Tungboontina Y, et al. Role of a Burkholderia pseudomallei polyphosphate kinase in an oxidative stress response, motilities, and biofilm formation. Journal of microbiology. 2010; 48(1):63–70. doi: 10.1007/s12275-010-9138-5 PMID: 20221731.



- Lumjiaktase P, Diggle SP, Loprasert S, Tungpradabkul S, Daykin M, Camara M, et al. Quorum sensing regulates dpsA and the oxidative stress response in Burkholderia pseudomallei. Microbiology. 2006; 152(Pt 12):3651–9. doi: 10.1099/mic.0.29226–0 PMID: 17159218.
- Ulrich RL, Deshazer D, Brueggemann EE, Hines HB, Oyston PC, Jeddeloh JA. Role of quorum sensing in the pathogenicity of Burkholderia pseudomallei. Journal of medical microbiology. 2004; 53(Pt 11):1053–64. PMID: 15496380.
- Valade E, Thibault FM, Gauthier YP, Palencia M, Popoff MY, Vidal DR. The Pmll-PmlR quorum-sensing system in Burkholderia pseudomallei plays a key role in virulence and modulates production of the MprA protease. Journal of bacteriology. 2004; 186(8):2288–94. PMID: <u>15060030</u>; PubMed Central PMCID: PMC412159.
- **43.** Ketterlinus R, Hsieh SY, Teng SH, Lee H, Pusch W. Fishing for biomarkers: analyzing mass spectrometry data with the new ClinProTools software. BioTechniques. 2005;Suppl: :37–40. PMID: 16528916.
- Utaisincharoen P, Anuntagool N, Limposuwan K, Chaisuriya P, Sirisinha S. Involvement of beta interferon in enhancing inducible nitric oxide synthase production and antimicrobial activity of Burkholderia pseudomallei-infected macrophages. Infection and immunity. 2003; 71(6):3053–7. PMID: <a href="https://doi.org/10.1051/j.ncharo.1051/j.nc
- 45. Tungpradabkul S, Wajanarogana S, Tunpiboonsak S, Panyim S. PCR-RFLP analysis of the flagellin sequences for identification of Burkholderia pseudomallei and Burkholderia cepacia from clinical isolates. Molecular and cellular probes. 1999; 13(2):99–105. doi: 10.1006/mcpr.1999.0221 PMID: 10208800.
- 46. Chantratita N, Wuthiekanun V, Boonbumrung K, Tiyawisutsri R, Vesaratchavest M, Limmathurotsakul D, et al. Biological relevance of colony morphology and phenotypic switching by Burkholderia pseudomallei. Journal of bacteriology. 2007; 189(3):807–17. doi: 10.1128/JB.01258-06 PMID: 17114252; PubMed Central PMCID: PMC1797308.
- Jangiam W, Loprasert S, Smith DR, Tungpradabkul S. Burkholderia pseudomallei RpoS regulates OxyR and the katG-dpsA operon under conditions of oxidative stress. Microbiology and immunology. 2010; 54(7):389–97. doi: 10.1111/j.1348-0421.2010.00230.x PMID: 20618685.
- Lengwehasatit I, Nuchtas A, Tungpradabkul S, Sirisinha S, Utaisincharoen P. Involvement of B. pseudomallei RpoS in apoptotic cell death in mouse macrophages. Microbial pathogenesis. 2008; 44 (3):238–45. doi: 10.1016/j.micpath.2007.08.017 PMID: 18022342.
- 49. Brown MR, Kornberg A. Inorganic polyphosphate in the origin and survival of species. Proceedings of the National Academy of Sciences of the United States of America. 2004; 101(46):16085–7. doi: 10. 1073/pnas.0406909101 PMID: 15520374; PubMed Central PMCID: PMC528972.
- Song Y, Xie C, Ong YM, Gan YH, Chua KL. The BpsIR quorum-sensing system of Burkholderia pseudomallei. Journal of bacteriology. 2005; 187(2):785–90. doi: 10.1128/JB.187.2.785–790.2005 PMID: 15629951; PubMed Central PMCID: PMC543524.
- Teramoto K, Sato H, Sun L, Torimura M, Tao H, Yoshikawa H, et al. Phylogenetic classification of Pseudomonas putida strains by MALDI-MS using ribosomal subunit proteins as biomarkers. Analytical chemistry. 2007; 79(22):8712–9. doi: 10.1021/ac701905r PMID: 17939647.
- Ryzhov V, Fenselau C. Characterization of the protein subset desorbed by MALDI from whole bacterial cells. Analytical chemistry. 2001; 73(4):746–50. PMID: <u>11248887</u>.
- Demirev PA, Feldman AB, Kowalski P, Lin JS. Top-down proteomics for rapid identification of intact microorganisms. Analytical chemistry. 2005; 77(22):7455–61. doi: 10.1021/ac051419g PMID: 16285700.
- 54. Christie-Oleza JA, Pina-Villalonga JM, Guerin P, Miotello G, Bosch R, Nogales B, et al. Shotgun nanoLC-MS/MS proteogenomics to document MALDI-TOF biomarkers for screening new members of the Ruegeria genus. Environmental microbiology. 2013; 15(1):133–47. doi: 10.1111/j.1462-2920.2012.02812.x PMID: 22712501.
- Suarez S, Ferroni A, Lotz A, Jolley KA, Guerin P, Leto J, et al. Ribosomal proteins as biomarkers for bacterial identification by mass spectrometry in the clinical microbiology laboratory. Journal of microbiological methods. 2013; 94(3):390–6. doi: 10.1016/j.mimet.2013.07.021 PMID: 23916798; PubMed Central PMCID: PMC3980635.
- Durighello E, Bellanger L, Ezan E, Armengaud J. Proteogenomic biomarkers for identification of Francisella species and subspecies by matrix-assisted laser desorption ionization-time-of-flight mass spectrometry. Analytical chemistry. 2014; 86(19):9394–8. doi: 10.1021/ac501840g PMID: 25215633.



doi: 10.1093/femsle/fnw161

Advance Access Publication Date: 19 June 2016 Research Letter

RESEARCH LETTER - Pathogens & Pathogenicity

Burkholderia pseudomallei rpoS mediates iNOS suppression in human hepatocyte (HC04) cells

Sucharat Sanongkiet 1,† , Saranyoo Ponnikorn 3,† , Rachanee Udomsangpetch 2 and Sumalee Tungpradabkul 1,*

¹Department of Biochemistry, Faculty of Science, Mahidol University, Bangkok 10400, Thailand, ²Center for Innovation Development and Technology Transfer, Faculty of Medical Technology, Mahidol University, Salaya, Nakhon Pathom 73170, Thailand and ³Chulabhorn International College of Medicine, Thammasart University, Rangsit campus, Pathumthani 12120, Thailand

*Corresponding author: Department of Biochemistry, Faculty of Science, Mahidol University, 272 Rama VI Road, Ratchathewi, Bangkok 10400, Thailand. Tel: +66-2-201-5372; Fax: +66-2-354-7174; E-mail: pexcotung@gmail.com

One sentence summary: This study investigated the induction of nitric oxide synthase (iNOS) in human hepatocyte cells (HC-04) infected with wild-type Burkholderia pseudomallei or an rpoS mutant. RpoS was implicated in the ability to suppress iNOS induction and with the induction of autophagy, indicating that it plays an important role in B. pseudomallei interactions with liver cells.

Editor: Craig Winstanley

ABSTRACT

Burkholderia pseudomallei is an intracellular Gram-negative bacterial pathogen and the causative agent of melioidosis, a widespread disease in Southeast Asia. Reactive nitrogen, in an intermediate form of nitric oxide (NO), is one of the first lines of defense used by host cells to eliminate intracellular pathogens, through the stimulation of inducible nitric oxide synthase (iNOS). Studies in phagocytotic cells have shown that the iNOS response is muted in B. pseudomallei infection, and implicated the rpoS sigma factor as a key regulatory factor mediating suppression. The liver is a main visceral organ affected by B. pseudomallei, and there is little knowledge about the interaction of liver cells and B. pseudomallei. This study investigated the induction of iNOS, as well as autophagic flux and light-chain 3 (LC3) localization in human liver (HC04) cells in response to infection with B. pseudomallei and its rpoS deficient mutant. Results showed that the rpoS mutant was unable to suppress iNOS induction and that the mutant showed less induction of autophagy and lower co-localization with LC3, and this was coupled with a lower intracellular growth rate. Combining these results suggest that B. pseudomallei rpoS is an important factor in establishing infection in liver cells.

Keywords: autophagy; Burkholderia pseudomallei; hepatocyte; inducible nitric oxide synthase (iNOS); melioidosis; RpoS

INTRODUCTION

The intracellular Gram-negative bacterium Burkholderia pseudomallei is the causative agent of melioidosis (Woods et al. 1999; White 2003; Cheng and Currie 2005), a tropical disease that is present throughout Southeast Asia (Woods et al. 1999; White 2003; Cheng and Currie 2005). Clinical symptoms of infection are

commonly characterized by pneumonia and multiple abscesses, which are mostly found at bacteria dissemination sites such as the lungs, liver and spleen (Cheng and Currie 2005), with the liver being implicated as a primary target for B. pseudomallei (Ben et al. 2004; Lee et al. 2006; Pal et al. 2014). The liver is a critical organ that plays an important role in maintaining homeostasis (Parker and Picut 2005) and is comprised of several cell types

[†]These authors contributed equally to this work.

including hepatocytes, which can generate and secrete inflammatory cytokines and chemokines in response to bacterial infections (Parker and Picut 2005).

The rpoS gene of B. pseudomallei encodes for the important transcription factor, sigma S, which plays a role in transcriptional regulation and which responds during stress conditions (Lange and Hengge-Aronis 1991; Hengge-Aronis et al. 1993; Hengge-Aronis 2000; Osiriphun et al. 2009). Notably, it has been reported that the RpoS of B. pseudomallei regulates many factors involved in pathogenesis such as multinucleated giant cell formation and the induction of apoptosis in the RAW264.7 murine macrophage cell line (Utaisincharoen et al. 2006; Lengwehasatit et al. 2008).

As previously reported, B. pseudomallei can interfere with the induction of nitric oxide synthase (iNOS) expression, which is involved in the elimination of intracellular bacteria via the reactive nitrogen intermediate nitric oxide (NO) in the RAW264.7 murine macrophage cell line (Utaisincharoen et al. 2001, 2003). However, a recent publication by Bast et al. (2011) showed that iNOS-derived NO might not be the main mechanism that eliminates the bacteria in human hepatocytes. Besides iNOS-derived NO production, the induction of autophagy has been associated with the elimination of intracellular pathogens (Campoy and Colombo 2009; Gomes and Dikic 2014).

Autophagy is the catabolic pathway which cells use to degrade unnecessary or dysfunctional cellular components through the action of lysosomes (Mizushima 2007; Glick, Barth and Macleod 2010). Moreover, it also acts as an antimicrobial response found in many cell types (Campoy and Colombo 2009; Gomes and Dikic 2014). Autophagy has been reported as a mechanism that is used to eliminate several bacteria such as Mycobacterium tuberculosis and Group A Streptococcus (Campoy and Colombo 2009; Mostowy and Cossart 2012). Recently, several studies have reported that the LC3 (light-chain 3)-associated phagosome helps in the elimination of B. pseudomallei from infected mouse macrophages (Gong et al. 2011; Randow, MacMicking and James 2013; Romao and Münz 2014). However, any relationship between iNOS expression and the stimulation of autophagy in host cells infected with B. pseudomallei has not been shown.

In this study, HC04 cells were used to determine any relationship between iNOS expression and the induction of autophagy as a consequence of infection with B. pseudomallei PP844, a wildtype strain, and an rpoS-deficient mutant strain. Evidence was obtained at both the transcriptional and the translational levels, and showed an inverse correlation between expression of iNOS and the induction of autophagy in B. pseudomallei-infected HC04

MATERIALS AND METHODS

Cells and culture conditions

The human hepatocyte cell line HC04, which was established and characterized by Sattabongkot et al. (2006), was maintained in equal volumes of DMEM and Ham's F-12 media (Gibco, ThermoFisher Scientific, Waltham, MA, USA) supplemented with 10% fetal bovine serum (Gibco) and incubated in a 37°C-humidified incubator in a 5% CO₂ atmosphere.

Bacterial strains

Burkholderia pseudomallei PP844 was originally isolated from a melioidosis patient at Srinagarind Hospital, Khon Kaen, Thailand (Wuthiekanun et al. 1996; Anuntagool et al. 1998). The B. pseudomallei rpoS mutant strain used in this study was originally constructed and verified by Subsin et al. (2003). Escherichia coli B was purchased from Coli Genetic Stock Center (CGSC, Yale University, CT, USA).

Infection

The HC04 cell line was infected at an interested multiplicity of infection (MOI) following a previously established standard methodology (Utaisincharoen et al. 2001). Briefly, a total of 5 \times 10⁵ cells were seeded into wells of a 6-well plate and incubated overnight under standard conditions, after which cells were counted before co-culture with bacteria at MOI 10 or 100 and incubation for the times specified. Mock infections (no bacteria) were undertaken in parallel.

Evaluation of intracellular survival of Burkholderia pseudomallei

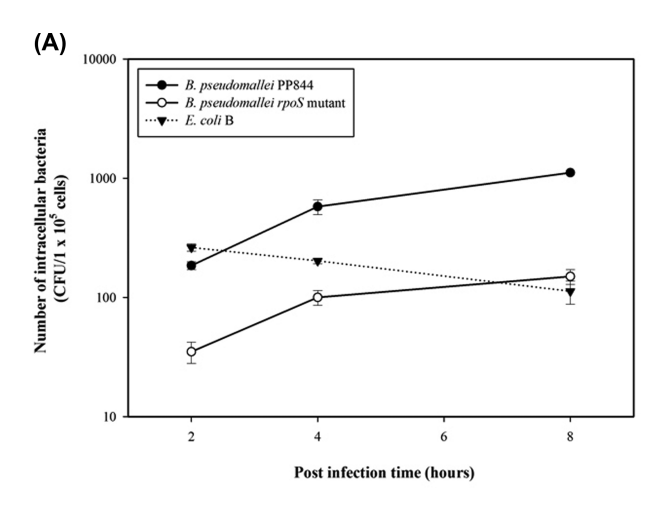
Burkholderia pseudomallei-infected HC04 cells were pelleted by centrifugation at 130 \times g and lysed with 0.1% TritonX-100 (Sigma-Aldrich, St. Louis, MO, USA) in PBS pH 7.4. Ten-fold of serial dilution were undertaken and the number of bacteria was determined as colony forming units at each time point post infection using the drop plate method. The colony forming unit (CFU) calculations were determined using the standard method (Herigstad, Hamilton and Heersink 2001).

Immunofluorescence analysis

Burkholderia pseudomallei-infected and mock-infected HC04 cells were incubated with 4% paraformaldehyde for 10 min and permeabilized with 0.3% TritonX-100 in 1× PBS pH 7.4. After washing with $1 \times PBS$ pH 7.4, the cells were incubated with a 1:1000 dilution of a rabbit anti-NOS2 polyclonal antibody (sc651; Santa Cruz Biotechnology, Inc. Dallas, TX, USA) or a 1:500 dilution of a rabbit anti-LC3 polyclonal antibody (2775S; Cell Signaling Technology, Danvers, MA, USA) as appropriate for 1 h. Slides were subsequently incubated with a 1:500 dilution of a goat antirabbit IgG, conjugated with Alexa fluor@488 (A11008; Invitrogen, ThermoFisher Scientific, Waltham, MA, USA) and were additionally stained with DAPI (4',6-diamidino-2-phenylindole) (D1306; Invitrogen, ThermoFisher Scientific) to detect bacteria under an Olympus FV10i confocal microscope.

RNA extraction and gene expression

Total RNA was extracted from B. pseudomallei-infected and mockinfected HC04 cells using TRIzol® reagent (Invitrogen, ThermoFisher Scientific) and was subsequently treated with DNaseI (Promega, Madison, WI, USA). The cDNA was synthesized using gene-specific reverse primers and Moloney Murine Leukemia Virus (M-MLV) reverse transcriptase (Promega). The sequences of iNOS primers are (forward) 5'-ATGCCAGATGGCAGCATCAGA-3' and (reverse) 5'-ATCTCCTCCAGGATGTTGTA-3'. The sequences of β -actin primer are (forward) 5'-CTCTTCCAGCCTTCCT-3' and (reverse) 5'-AGCACTGTGTTGGCGTACAG-3'. The total cDNA of each sample were used to quantitate the levels of gene expression using KAPA SYBR FAST qPCR Kit (Kapabiosystems Co.). The expression of iNOS and β -actin was analyzed using the qPCR_Mx3000P software (Agilent Technologies, CA, USA).



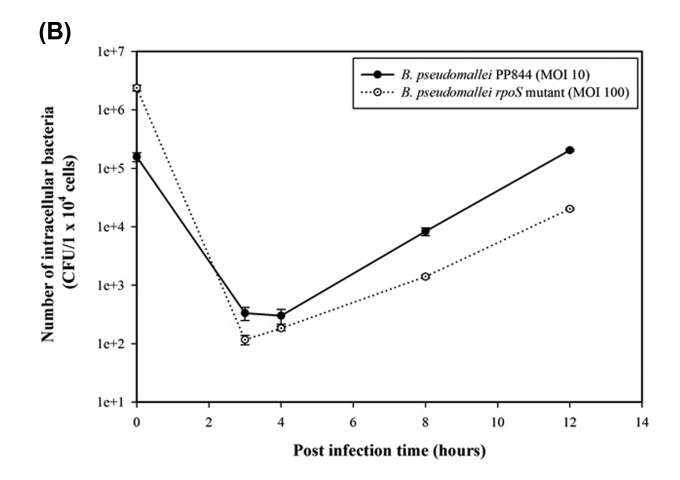


Figure 1. The survivability of B. pseudomallei PP844 and its rpoS mutant in HC04 cell. (A) The intracellular replication of B. pseudomallei PP844, B. pseudomallei rpoS mutant and E. coli B in HC04 cells starting with the same MOI 10 at 2, 4 and 8 h.p.i. The number of intracellular bacteria was determined using the drop plate technique and calculated by using a CFU method. Data are Means ± SEMs from experiments carried out in duplicate. (B) The intracellular replication of B. pseudomallei PP844 (MOI 10) and B. pseudomallei rpoS mutant (MOI100) in HC04 cells. The number of intracellular bacteria was determined using the drop plate technique and calculated by using a CFU method. Data are Means \pm SEMs from experiments carried out in duplicate.

Table 1. The representative of data from Fig. 1B.

B. pseudomallei strains Post infection time (hours)	PP844 (wild type) (CFU)	rpoS mutant (CFU)	P-value
0	156 666 ± 26 870	2366 667 ± 268 701	ND
3	333 ± 85	117 ± 21	*
4	300 ± 85	183 ± 17	*
8	8333 ± 1273	1400 ± 85	0.019
12	203 333 ± 8485	20 167 ± 778	< 0.001

ND means not determined.

Asterisk (*) means there is no significant different.

Autophagic flux analysis

HC04 cells were either not treated or treated with 125 nM bafilomycin A1 for 2 h before mock infection or infection with B. pseudomallei at MOI 10. Cells and bacteria were co-cultured under standard conditions for the times indicated after which cells were washed with 1x PBS pH 7.4, and total proteins extracted. The expression levels of LC3-II and Glyceraldehyde-3-Phosphate Dehydrogenase (GAPDH) were determined by western blotting using a rabbit anti-LC3 polyclonal antibody (2775S; Cell Signaling Technology) and a mouse anti-GAPDH monoclonal antibody (611463; BD Pharmacia, San Jose, CA, USA) followed by a Horseradish peroxidase (HRP)-conjugated goat antirabbit IgG antibody (sc2004; Santa Cruz Biotechnology, Inc.) and a HRP-conjugated goat anti-mouse IgG antibody (sc2005; Santa Cruz Biotechnology, Inc.). Signal was observed using Luminata Forte Western HRP substrate (WBLUF0100; Merck Millipore, Darmstadt, Germany). Band intensities were quantitated using the ImageJ software.

Statistical analysis

Graphs, means and standard deviations were calculated using SigmaPlot 11.0 (Informer Technologies, Inc.). Statistical analyses were determined by one-way Analysis of Variance (ANOVA) using SigmaPlot 11.0 (Informer Technologies, Inc.). A P-value ≤0.05 was considered statistically significant.

RESULTS

The intracellular survival of Burkholderia pseudomallei in HC04 cells

While it has been established that Burkholderia pseudomallei PP844 and its rpoS mutant do not show differences in growth rate when grown in Luria-Bertani (LB) medium (Subsin et al. 2003), we initially sought to determine whether there were differences in intracellular survival in liver cells. HC04 cells were therefore infected with either B. pseudomallei PP844, its rpoS mutant or Escherichia coli B and at selected times post infection the intracellular bacterial numbers determined by the drop plate method with results expressed in terms of CFUs of the intracellular bacteria (Herigstad, Hamilton and Heersink 2001). Results showed that B. pseudomallei PP844 produced significantly higher levels of intracellular bacteria than the rpoS mutant strain at all time points examined (Fig. 1A), suggesting that RpoS plays a role in the invasion and/or intracellular survival of B. pseudomallei.

To confidently conclude whether the rpoS gene influence on the intracellular survival of B. pseudomallei inside the HC04 cells, the increasing MOI of the rpoS-deficient B. pseudomallei was performed at MOI 100 to properly assess the ability of bacteria replication. Results showed that B. pseudomallei rpoS mutant still exhibited lower level of intracellular replication than its parental strain (Fig. 1B) (Table 1), which indicated that rpoS influence on

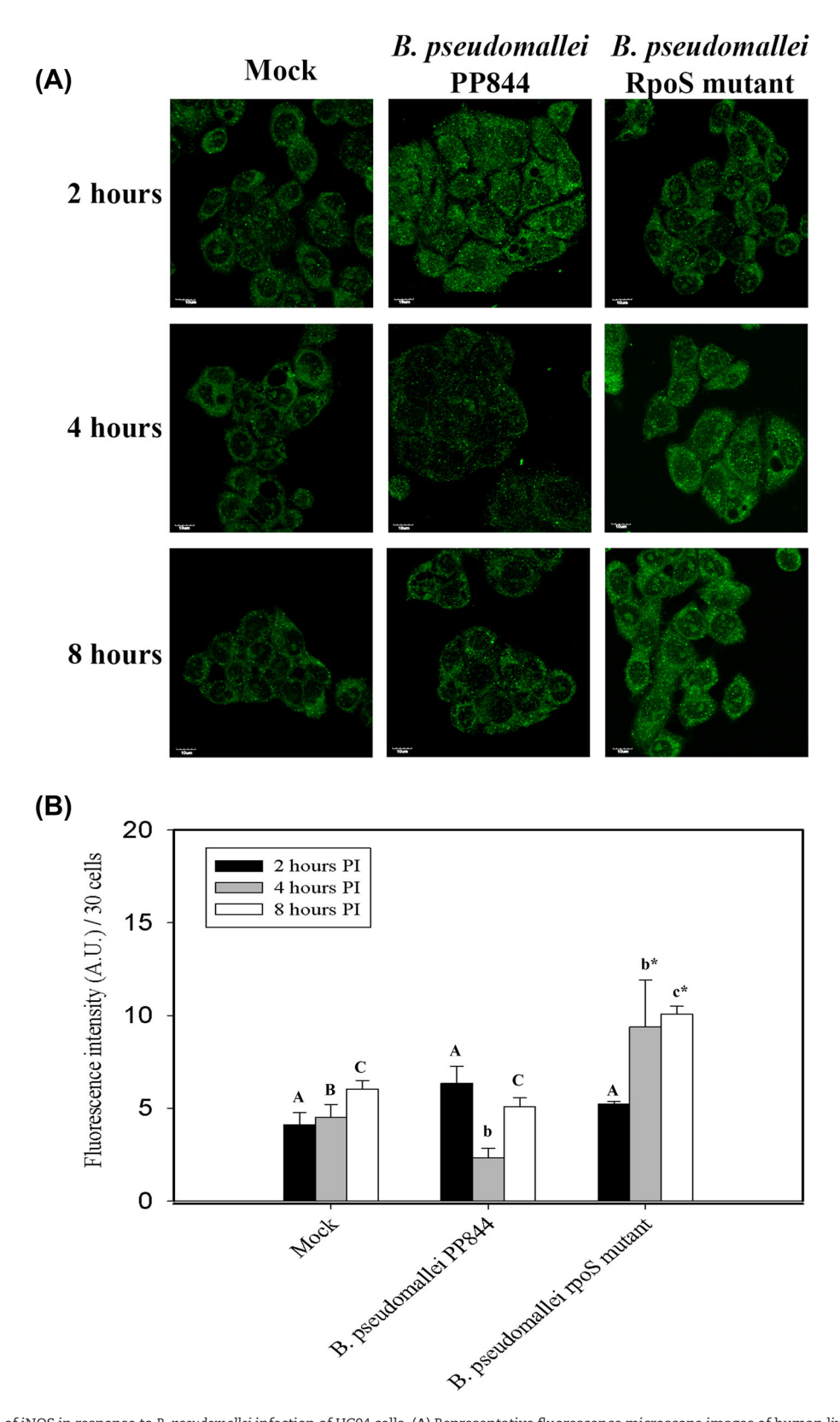


Figure 2. Expression of iNOS in response to B. pseudomallei infection of HC04 cells. (A) Representative fluorescence microscope images of human liver HC04 cells mock infected or infected with B. pseudomallei or its rpoS mutant at MOI 10. Images were captured at 2, 4 and 8 h.p.i. The scale bar in each panel is 10 μ m. (B) Measurement of fluorescence intensity was undertaken using ImageJ software. Statistical analyses were determined using SigmaPlot 11.0 one-way ANOVA. Lower case letters indicate a significant difference from the corresponding upper case letters (P-value <0.05). Lower case letters with a star indicate that rpoS mutant was statistically different from wild type.

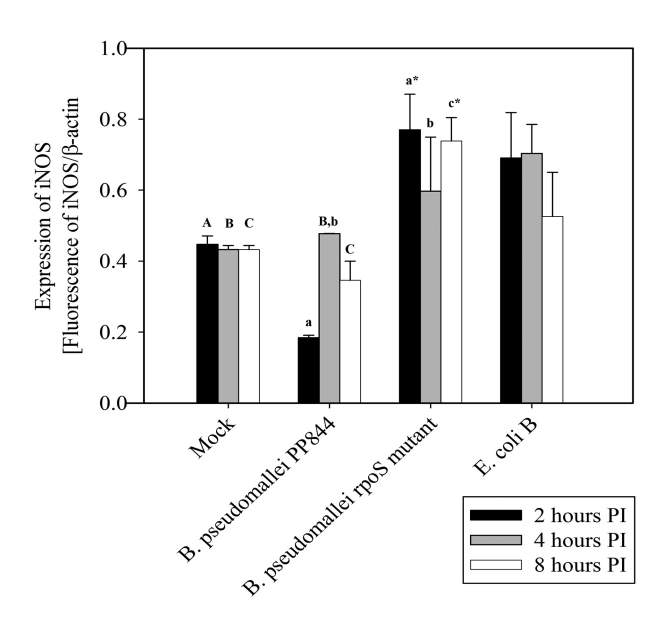


Figure 3. Quantification of iNOS expression. Human liver HC04 cells were mock infected or infected with B. pseudomallei or its rpoS mutant or E. coli B at MOI 10 and at 2, 4 and 8 h.p.i. RNA was extracted and expression of iNOS determined by qRT-PCR. The level of iNOS expression was normalized against the expression of β -actin. Statistical analyses were undertaken using SigmaPlot 11.0 one-way ANOVA. Lower case letters indicate a significant difference from the corresponding upper case letters (P-value < 0.05). Lower case letters with a star indicate that the rpoS mutant was statistically different from wild type.

the intracellular survivability of B. pseudomallei both invasion and replication inside the cell.

Expression of iNOS in HC04 cells after infection with Burkholderia pseudomallei

To investigate the expression of iNOS in response to infection, HC04 cells were mock infected or infected with B. pseudomallei PP844 and its rpoS mutant under standard conditions and at appropriate time points, cells were examined under a confocal microscope after staining with appropriate antibodies. Results showed the clear induction of iNOS starting from 4 h post infection (h.p.i.) in response to B. pseudomallei infection of the rpoS mutant, but not by the parental PP844 strain (Fig. 2A and B).

To confirm this result, levels of iNOS mRNA expression were investigated using quantitative RT-PCR (qRT-PCR). HC04 cells were therefore mock infected or infected with B. pseudomallei PP844 and its rpoS mutant under standard conditions, in parallel with infection with E. coli B which is known to induce iNOS expression (Titheradge 1997) as a positive control. Results showed that iNOS mRNA expression was significantly higher in cells infected with the rpoS mutant at all time points examined compared to mock, and higher at 2 and 8 h.p.i compared to the parental PP844 strain. At 4 h.p.i, expression of iNOS in response to rpoS mutant infection was increased as compared to the parental strain, but this did not reach statistical significance. Levels of iNOS expression in the rpoS mutant infection were not statistically different from the levels of iNOS expression seen in response to infection with E. coli B (Fig. 3). Interestingly, a significant inhibition of iNOS expression was seen at 2 h.p.i after infection by the parental B. pseudomallei PP844 strain (Fig. 3). Importantly, the results were consistent with the results of the immunofluorescence assay, although increased expression of the iNOS message was seen somewhat earlier than the concomitant

increase in protein expression in B. pseudomallei rpoS mutant infection. However, these results are consistent with previous reports that RpoS is involved in inhibition of iNOS expression in response to infection by B. pseudomallei (Utaisincharoen et al. 2006).

Autophagic flux analysis

To determine whether the level of iNOS expression might be related to the induction of autophagy, the expression of the microtubule-associated protein light-chain 3 (LC3), a key autophagy-related protein (Tanida, Ueno and Kominami 2004), was determined and used to calculate the autophagic flux. After infecting HC04 cells in the presence or absence of bafilomycin A1 to inhibit fusion between autophagosomes and lysosomes (Yamamoto et al. 1998), total proteins were collected at 2, 4 and 8 h.p.i and the levels of LC3-II determined by western blotting. The expression of GAPDH was additionally determined as an internal control to normalize the LC3 expression.

Results (Fig. 4) indicated that at 2 h.p.i. B. pseudomallei PP844 showed increased autophagic flux as compared to the rpoS mutant, while at 4 and 8 h.p.i. the autophagic flux in B. pseudomallei PP844-infected cells was slightly higher than in cells infected by the rpoS mutant. A comparison with the results for iNOS expression suggests that the suppression of iNOS might be associated with the induction of autophagy in the host cell.

Co-localization of LC3 and Burkholderia pseudomallei

The previous results showed decreased autophagic flux in the rpoS mutant as compared to B. pseudomallei PP844. To further investigate this, the expression of LC3 was examined by confocal microscopy, and cells were counterstained with DAPI to allow visualization of the nucleus and the bacterial genome. Results (Fig. 5) showed a markedly high level of expression of LC3 in B. pseudomallei PP844 as compared to the rpoS mutant, and moreover analysis of co-localization between LC3 and the bacterial genome at 4 h.p.i. showed a significantly higher colocalization between B. pseudomallei PP844 and LC3 than between the rpoS mutant and LC3 (Fig. 5). By 8 h.p.i., the co-localization between the bacterial genome and LC3 was still higher for B. pseudomallei PP844 than for the rpoS mutant, although this was no longer statistically significant.

DISCUSSION

Previous studies have implicated the liver as one of the visceral organs infected by Burkholderia pseudomallei, resulting in the formation of abscesses and contributing to the pathology of melioidosis (Ben et al. 2004; Lee et al. 2006; Pal et al. 2014). However, the interaction between B. pseudomallei and liver cells remains poorly characterized. To better understand the pathophysiology of liver cells under B. pseudomallei infection, this study used the human hepatocyte HC04 cell line which has previously been shown to be an appropriate model cell line for liver cell pathogens (Sattabongkot et al. 2006).

The rpoS gene encodes the alternative RNA polymerase sigma factor, and previous studies have implicated RpoS as a global regulatory factor induced in response to a variety of cellular stresses conditions (Lange and Hengge-Aronis 1991; Hengge-Aronis et al. 1993; Hengge-Aronis 2000; Osiriphun et al. 2009). In B. pseudomallei, it has been shown that lack of rpoS does not affect bacterial growth in LB medium (Subsin et al. 2003). As shown in the result, B. pseudomallei parental strain exhibited higher invasive ability into HC04 than the rpoS-deficient

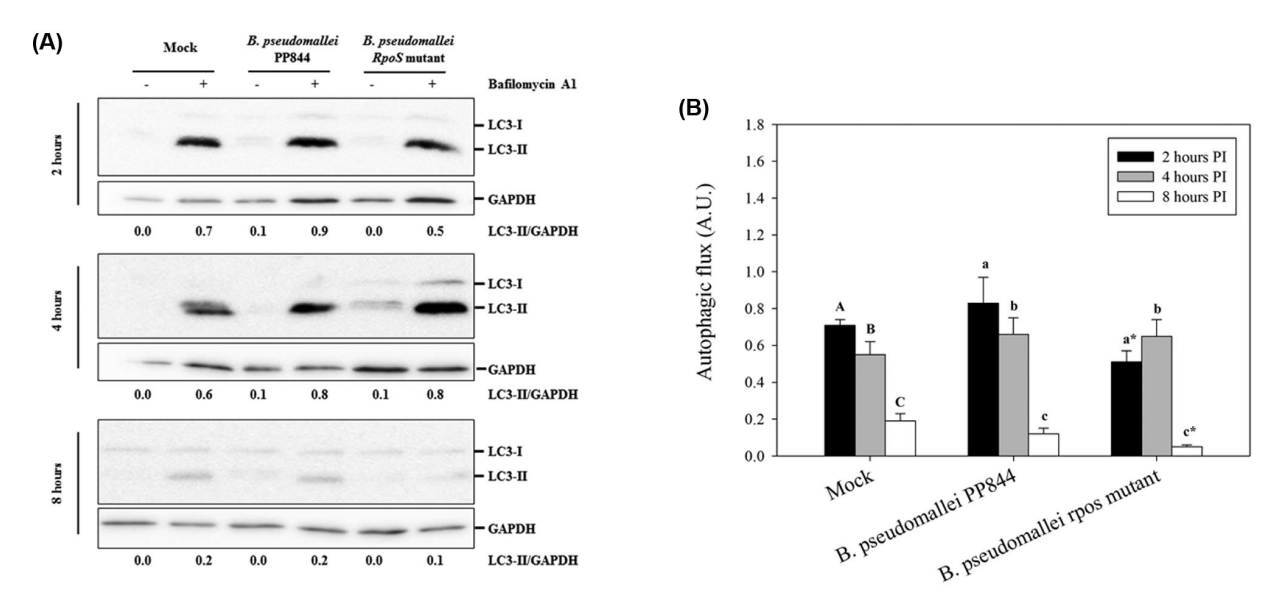


Figure 4. Assessment of autophagic flux in HC04 cells. (A) Human liver HC04 cells were mock infected or infected with B. pseudomallei or its rpoS mutant at MOI 10 in the presence or absence of bafilomycin A1 and at 2, 4 and 8 h.p.i. expression of LC3-I (14kDa) and II (16kDa) determined by western blotting. GAPDH were used as a loading control for each condition. The intensity of LC3-II and GAPDH were determined using ImageJ software and the numbers below the blots show the ratio between LC3-II and GAPDH. (B) The plot of autophagic flux in HC04 cells as determined from A. Statistical analyses were undertaken using SigmaPlot 11.0 one-way ANOVA. Lower case letters indicate a significant difference from the corresponding upper case letters (P-value <0.05). Lower case letters with a star indicate that the rpoS mutant was statistically different from wild type.

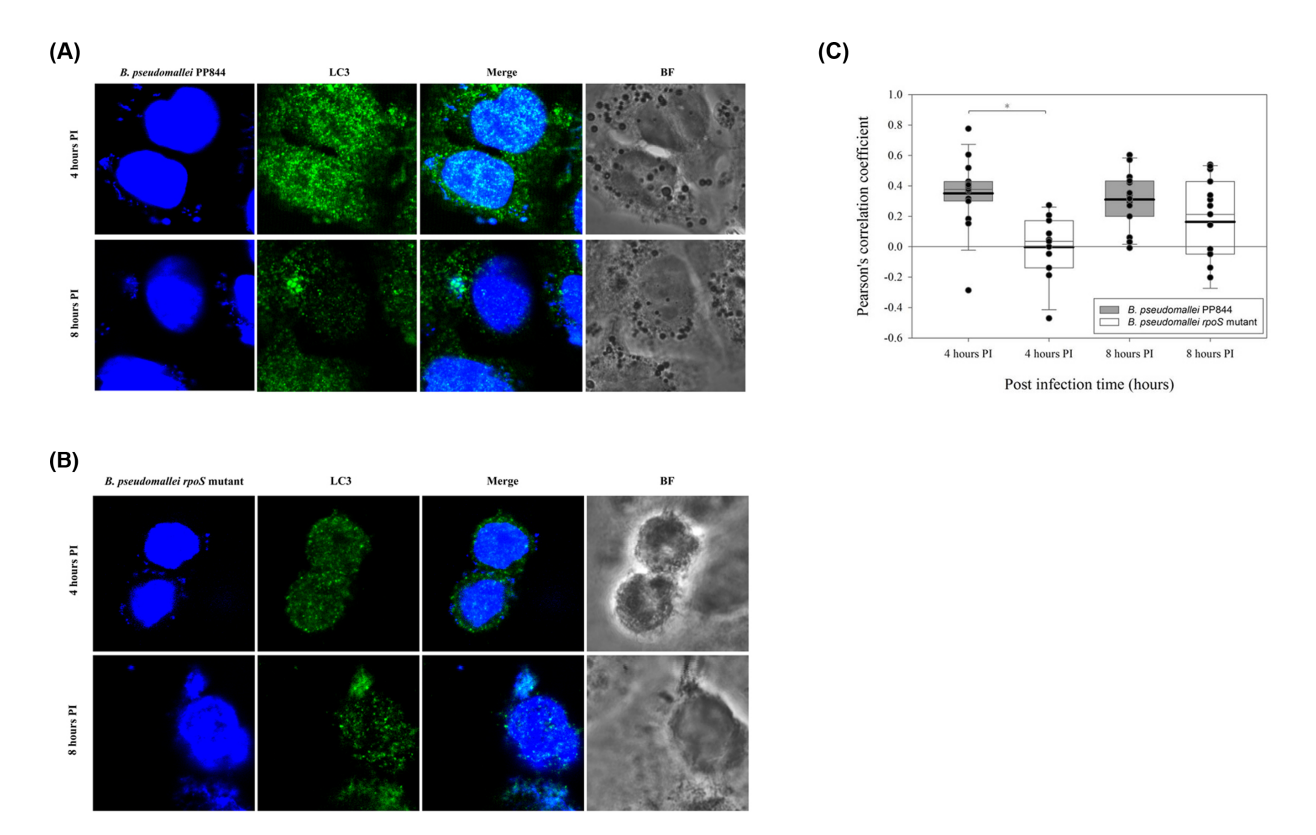


Figure 5. Co-localization of B. pseudomallei and LC3 in HC04 cells. Human liver HC04 cells were mock infected or infected with (A) B. pseudomallei or (B) its rpoS mutant at MOI 10 and at 4 and 8 h.p.i. examined for LC3 expression using an Alexa Fluor 488 antibody (green) and the presence of bacteria through DAPI (blue) staining and examination under a fluorescent microscope. (C) Pearson's correlation coefficients (PCC) for LC3 and bacteria (extra nuclei DAPI signal) were determined using the ImageJ software with the Pearson-spearman correlation (PSC) co-localization plug-in. PCC values for each condition are shown in a box chart which shows the mean (black line) and median (gray line) values. The lower and the upper borders of the box are 5th and 95th percentiles, respectively.

strain (Fig. 1A). Moreover, the results in Fig. 1B and Table 1 show that B. pseudomallei deficient rpoS gene markedly reduced numbers of bacteria in liver cells, suggesting that rpoS plays a role in the intracellular survival of B. pseudomallei PP844 (Fig. 1B and Table 1).

The exact mechanism by which the pathogen survives the intracellular environment is still unclear. However, Escherichia coli DpsA has been studied, and it has been suggested that DpsA acts as a regulator of the cell-cycle check point during oxidative stress to reduce cell growth, providing an opportunity for repairing oxidative DNA damage (Chodavarapu et al. 2008). Consistent with the role of B. pseudomallei DpsA in enhancing intracellular survival, a decreased level of dpsA expression in the rpoS-mutant strain under oxidative stress results in a reduced intracellular survival (Jangiam et al. 2010; Al-Maleki et al. 2014).

Host cells have a number of innate immune responses to suppress or eliminate invading pathogens, and the pathogens adapt to suppress or subvert these responses, allowing their survival and replication. Inducible nitric oxide synthase (iNOS) is one such system (Bogdan 2015) and previous studies in the mouse macrophage RAW264.7 cell line showed early suppression of iNOS by B. pseudomallei (Utaisincharoen et al. 2001), a result consistent with our present study in liver cells. Markedly however, suppression of iNOS expression was limited to B. pseudomallei PP844 and the rpoS mutant showed no inhibition of iNOS expression. Indeed, robust induction of iNOS expression was observed in the rpoS mutant, consistent with the levels of induction of iNOS expression seen with the control E. coli B infection.

Autophagy is a cellular degradation pathway that delivers sequestered cytoplasmic constituents such as damaged cell organelles to lysosomes for degradation and the subsequent recycling of cellular constituents (Klionsky and Emr 2000). However, autophagy has additionally been shown to be an essential component of the host response to a number of different pathogens (Levine 2005). Previous studies in RAW264.7 cells have shown that activation of autophagy could decrease the intracellular survival of B. pseudomallei, and the secreted protein BopA was suggested to be the factor mediating B. pseudomallei escape from autophagy (Cullinane et al. 2008). As shown here, there was an increase in autophagic flux in response to infection of liver cells with B. pseudomallei PP844, but not with the rpoS mutant (Fig. 4A and B).

The link between iNOS and autophagy is somewhat contradictory. In macrophages, stimulation of iNOS-derived NO by Lipopolysaccharide (LPS) leads to a triggering of autophagy via MAPK/NF-κB/iNOS signaling (Han et al. 2013), whereas in Hela cells it was shown that inhibition of iNOS increased autophagic flux (Sarkar et al. 2011). Our results suggest that the rpoS mutant which induces a strong induction of iNOS blocks increased autophagic flux seen with B. pseudomallei PP844.

Several studies have reported the co-localization of LC3 and B. pseudomallei containing phagosomes and it is suggested that the autophagic machinery is recruited to B. pseudomallei containing phagosomes through the action of the B. pseudomallei Bsa type III secretion system (D'Cruze et al. 2011; Gong et al. 2011; Rinchai et al. 2015). However, as observed here, co-localization of LC3 and B. pseudomallei was significantly reduced in early infection in the rpoS mutant as compared to B. pseudomallei PP844. Interestingly, the hydrophobic affinity chromatography technique which was used to investigate the interaction between LC3 and bacterial protein found that there is some bacterial protein that interacts with LC3 and it is under the RpoS regulation (Joompa, pers. comm.). This supports our finding in Figs 4 and 5. Collectively our results show an inverse relationship between iNOS expression and autophagy, and show that rpoS is pivotal in suppressing the host cell induction of iNOS in response to B. pseudomallei in liver cells.

ACKNOWLEDGEMENTS

We would like to thank the Yoshimori laboratory at the Department of Genetics, Osaka University Graduate School of Medicine for providing the reagents and equipment used in this study. Thanks to Prof. Duncan R. Smith at the Institute of Molecular Biosciences and Center for Emerging and Neglected Infectious Disease, Mahidol University for comments about the experiment and language editing.

FUNDING

This work was supported by the Thailand Research Fund [BRG5680010]. SP was supported by Thailand Research Fund and Thammasat University [TRG5780195]. SS was supported by the Development and Promotion of Science and Technology Talents project (DPST) [04/2548].

Conflict of interest. None declared.

REFERENCES

- Al-Maleki AR, Mariappan V, Vellasamy KM et al. Enhanced intracellular survival and epithelial cell adherence abilities of Burkholderia pseudomallei morphotypes are dependent on differential expression of virulence-associated proteins during mid-logarithmic growth phase. J Proteomics 2014;106: 205-20.
- Anuntagool N, Intachote P, Wuthiekanun V et al. Lipopolysaccharide from nonvirulent Ara+ Burkholderia pseudomallei isolates is immunologically indistinguishable from Lipopolysaccharide from virulent ara-clinical isolates. Clin Diagn Lab Immun 1998;5:225-9.
- Bast A, Schmidt IHE, Brauner P et al. Defense mechanisms of hepatocytes against Burkholderia pseudomallei. Front Microbiol 2011;2:277.
- Ben R-J, Tsai Y-Y, Chen J-C et al. Non-septicemic Burkholderia pseudomallei liver abscess in a young man. J Microbiol Immunol 2004;37:254-7.
- Bogdan C. Nitric oxide synthase in innate and adaptive immunity: an update. Trends Immunol 2015;36:161-78.
- Campoy E, Colombo MI. Autophagy in intracellular bacterial infection. BBA-Mol Cell Res 2009;1793:1465-77.
- Cheng AC, Currie BJ. Melioidosis: epidemiology, pathophysiology, and management. Clin Microbiol Rev 2005;18: 383-416.
- Chodavarapu S, Gomez R, Vicente M et al. Escherichia coli Dps interacts with DnaA protein to impede initiation: a model of adaptive mutation. Mol Microbiol 2008;67:1331-46.
- Cullinane M, Gong L, Li X et al. Stimulation of autophagy suppresses the intracellular survival of Burkholderia pseudomallei in mammalian cell lines. Autophagy 2008;4:744-53.
- D'Cruze T, Gong L, Treerat P et al. Role for the Burkholderia pseudomallei type three secretion system cluster 1 bpscN gene in virulence. Infect Immun 2011;79:3659-64.
- Glick D, Barth S, Macleod KF. Autophagy: cellular and molecular mechanisms. J Pathol 2010;221:3-12.
- Gomes LC, Dikic I. Autophagy in antimicrobial immunity. Mol Cell 2014;54:224-33.

- Gong L, Cullinane M, Treerat P et al. The Burkholderia pseudomallei type III secretion system and BopA are required for evasion of LC3-associated phagocytosis. PLoS One 2011;6:e17852.
- Hengge-Aronis R. A role for the sigma S subunit of RNA polymerase in the regulation of bacterial virulence. Adv Exp Med Biol 2000;485:85-93.
- Hengge-Aronis R, Lange R, Henneberg N et al. Osmotic regulation of rpoS-dependent genes in Escherichia coli. J Bacteriol 1993;175:259-65.
- Herigstad B, Hamilton M, Heersink J. How to optimize the drop plate method for enumerating bacteria? J Microbiol Meth 2001;44:121-9.
- Han H-E, Kim T-K, Son H-J et al. Activation of Autophagy Pathway Suppresses the Expression of iNOS, IL6 and Cell Death of LPS-Stimulated Microglia Cells. Biomol Ther (Seoul) 2013;21:21-8.
- Jangiam W, Loprasert S, Smith DR et al. Burkholderia pseudomallei RpoS regulates OxyR and the katG-dpsA operon under conditions of oxidative stress. Microbiol Immunol 2010;54:
- Klionsky DJ, Emr SD. Autophagy as a regulated pathway of cellular degradation. Science 2000;290:1717-21.
- Lange R, Hengge-Aronis R. Identification of a central regulator of stationary-phase gene expression in Escherichia coli. Mol Microbiol 1991;5:49-59.
- Lee Y-L, Lee SS-J, Tsai H-C et al. Pyogenic liver abscess caused by Burkholderia pseudomallei in Taiwan. J Formos Med Assoc 2006;105:689-93.
- Lengwehasatit I, Nuchtas A, Tungpradabkul S et al. Involvement of B. pseudomallei RpoS in apoptotic cell death in mouse macrophages. Microb Pathogenesis 2008;44:238-45.
- Levine B. Eating oneself and uninvited guests: autophagyrelated pathways in cellular defense. Cell 2005;120:159-62.
- Mizushima N. Autophagy: process and function. Gene Dev 2007;21:2861-73.
- Mostowy S, Cossart P. Bacterial autophagy: restriction or promotion of bacterial replication? Trends Cell Biol 2012;22:283-91.
- Osiriphun Y, Wongtrakoongate P, Sanongkiet S et al. Identification and characterization of RpoS regulon and RpoSdependent promoters in Burkholderia pseudomallei. J Proteome Res 2009;8:3118-31.
- Pal P, Ray S, Moulick A et al. Liver abscess caused by Burkholderia pseudomallei in a young man: a case report and review of literature. World J Clin Cases 2014;2:604-7.
- Parker GA, Picut CA. Liver immunobiology. Toxicol Pathol 2005;33:52-62.
- Randow F, MacMicking JD, James LC. Cellular self-defense: how cell-autonomous immunity protects against pathogens. Science 2013;340:701-6.

- Rinchai D, Riyapa D, Buddhisa S et al. Macroautophagy is essential for killing of intracellular Burkholderia pseudomallei in human neutrophils. Autophagy 2015;11:748-55.
- Romao S, Münz C. LC3-associated phagocytosis. Autophagy 2014;10:526-8.
- Sarkar S, Korolchuk VI, Renna M et al. Complex inhibitory effects of nitric oxide on autophagy. Mol Cell 2011;43:19-32.
- Sattabongkot J, Yimamnuaychoke N, Leelaudomlipi S et al. Establishment of a human hepatocyte line that supports in vitro development of the exo-erythrocytic stages of the malaria parasites Plasmodium falciparum and P. vivax. Am J Trop Med Hya 2006;74:708-15.
- Subsin B, Thomas MS, Katzenmeier G et al. Role of the stationary growth phase sigma factor RpoS of Burkholderia pseudomallei in response to physiological stress conditions. J Bacteriol 2003;185:7008-14.
- Tanida I, Ueno T, Kominami E. LC3 conjugation system in mammalian autophagy. Int J Biochem Cell B 2004;36: 2503-18.
- Titheradge MA. Nitric Oxide Protocols, Vol. 100. New Jersey: Humana Press, 1997.
- Utaisincharoen P, Anuntagool N, Limposuwan K et al. Involvement of beta interferon in enhancing inducible nitric oxide synthase production and antimicrobial activity of Burkholderia pseudomallei-infected macrophages. Infect Immun 2003;71:3053-7.
- Utaisincharoen P, Arjcharoen S, Limposuwan K et al. Burkholderia pseudomallei RpoS regulates multinucleated giant cell formation and inducible nitric oxide synthase expression in mouse macrophage cell line (RAW 264.7). Microb Pathogenesis 2006;40:184-9.
- Utaisincharoen P, Tangthawornchaikul N, Kespichayawattana W et al. Burkholderia pseudomallei interferes with inducible nitric oxide synthase (iNOS) production: a possible mechanism of evading macrophage killing. Microbiol Immunol 2001;45:307-
- White NJ. Melioidosis. Lancet 2003;361:1715-22.
- Woods DE, DeShazer D, Moore RA et al. Current studies on the pathogenesis of melioidosis. Microbes Infect 1999;1:
- Wuthiekanun V, Smith MD, Dance DA et al. Biochemical characteristics of clinical and environmental isolates of Burkholderia pseudomallei. J Med Microbiol 1996;45:408-12.
- Yamamoto A, Tagawa Y, Yoshimori T et al. Bafilomycin A1 prevents maturation of autophagic vacuoles by inhibiting fusion between autophagosomes and lysosomes in rat hepatoma cell line, H-4-II-E cells. Cell Struct Funct 1998;23: